Universitatea
Transilvania
din Braşov

HABILITATION THESIS

Title:

Frontier Developments in Continuum Mechanics and Nonlinear Dynamics: Theories, Methods, and Applications

Domain: Mathematics

Author: Assoc. Prof. Dr. Olivia Ana FLOREA
University: Transilvania University of Braşov

Braşov, 2024

Contents

(A) Rezumat

Teza de față reprezintă o explorare cuprinzătoare a unor subiecte avansate în mecanica mediilor continue, analiza numerică și aplicațiile acestora în știința materialelor și chimie. Este structurată în trei capitole principale, fiecare aprofundând domenii specifice de cercetare care se bazează pe munca anterioară și contribuțiile autorului în acest domeniu.

Primul capitol se concentrează pe cercetările autorului în mecanica mediilor continue, în special pe materialele termoelastice cu structuri de dublă porozitate. Acest capitol reprezintă o extensie a tezei de doctorat a autorului în Matematică, finalizată în 2019, și prezintă progrese semnificative în înțelegerea interacțiunilor complexe dintre comportamentele termice și mecanice în materialele cu dublă porozitate. Capitolul este împărțit în trei secțiuni, fiecare evidențiind cercetări publicate în reviste de renume precum Continuum Mechanics and Thermodynamics și Analele Științifice ale Universității Ovidius. Studiile prezentate în acest capitol explorează diverse cadre teoretice, inclusiv relația de reciprocitate a lui Betti, teoria termoelasticității Moore–Gibson–Thompson (MGT) și termoelasticitatea Green-Lindsay, aplicate materialelor cu dublă porozitate. Aceste cadre sunt esențiale pentru abordarea stabilității, unicității și răspunsurilor dinamice ale acestor materiale, cu implicații pentru utilizarea lor în inginerie și tehnologie, în special în medii supuse stresurilor termice și mecanice extreme.

Al doilea capitol își schimbă focusul către analiza numerică a sistemelor dinamice, utilizând metode precum calculul fracționat numeric. Acest capitol se bazează pe teza de doctorat a autorului în Inginerie Mecanică, finalizată în 2010, și demonstrează aplicarea acestor metode numerice în rezolvarea sistemelor complexe care sunt dificil de abordat analitic. Capitolul este împărțit în patru secțiuni, cu cercetări publicate în reviste precum Dynamic Systems and Applications și Analele Științifice ale Universității Ovidius. Studiile acoperă o gamă largă de subiecte, inclusiv dinamica unui sistem cu pendul dublu, mișcarea unei bile grele pe un fir rotativ și abordarea numerică a rezolvării ecuației telegrafistului. Rezultatele obținute din aceste studii subliniază puterea metodelor numerice în captarea

comportamentelor complexe ale sistemelor dinamice, cum ar fi mișcarea haotică și oscilațiile periodice, care sunt adesea dificil de prezis folosind abordări analitice tradiționale.

Al treilea capitol aplică descoperirile din studiul sistemelor dinamice în domeniul chimiei, în special în analiza materialelor poroase și a aplicațiilor acestora în procesele de combustie. Prima secțiune a acestui capitol prezintă cercetări asupra comportamentului haotic al nanoparticulelor de Titanat de Bariu, publicate în Physics Letters A, care extind cadrul hamiltonian pentru a dezvălui dinamica vibrațională complexă a acestor nanoparticule în anumite condiții. Acest studiu se bazează pe lucrările anterioare ale lui Koo și Lee, care au explorat ferroelectricitatea și antiferromagnetismul în materiale multiferroice. A doua secțiune investighează porozitatea brichetelor din deșeuri de lemn și impactul acesteia asupra combustiei, publicată în Waste and Biomass Valorization. Această cercetare introduce metode noi de evaluare a porozității brichetelor, oferind noi perspective asupra proceselor de transfer de căldură și masă în aceste materiale și extinzând modelele existente de porozitate la o nouă aplicație.

Fiecare capitol al tezei nu doar că se bazează pe munca anterioară a autorului, dar face și contribuții semnificative în domeniile respective. Cercetarea prezentată în primul capitol avansează înțelegerea teoretică a materialelor termoelastice cu dublă porozitate, oferind noi instrumente pentru analizarea și proiectarea materialelor destinate mediilor supuse stresului ridicat. Al doilea capitol demonstrează eficacitatea metodelor numerice în explorarea sistemelor dinamice complexe, oferind soluții practice pentru probleme care sunt altfel greu de rezolvat analitic. În final, al treilea capitol evidențiază aplicarea acestor tehnici matematice și numerice avansate în probleme din lumea reală, cum ar fi dinamica haotică a nanoparticulelor și optimizarea proceselor de combustie în materiale poroase.

În ansamblu, această teză subliniază importanța combinării cadrelor teoretice riguroase cu metode numerice puternice pentru a aborda probleme complexe în știința materialelor, ingineria mecanică și chimie. Rezultatele obținute din diversele studii nu doar că avansează cunoașterea în aceste domenii, dar oferă și perspective practice care ar putea informa dezvoltarea de noi tehnologii și materiale. Simulările și analizele realizate folosind instrumente precum MATLAB și Maple demonstrează în continuare utilitatea acestor metode atât în cercetarea academică, cât și în contextul aplicat al ingineriei.

(A-i) Summary

The present thesis is a comprehensive exploration of advanced topics in continuum mechanics, numerical analysis, and their applications in material science and chemistry. It is structured into three main chapters, each delving into specific areas of research that build upon the author's previous work and contributions to the field.

The first chapter focuses on the author's research in continuum mechanics, specifically on thermoelastic materials with double porosity structures. This chapter is an extension of the author's PhD thesis in Mathematics, completed in 2019, and presents significant advancements in understanding the complex interactions between thermal and mechanical behaviors in materials with double porosity. The chapter is divided into three sections, each highlighting research published in reputable journals such as Continuum Mechanics and Thermodynamics and Scientific Annals of Ovidius University. The studies presented in this chapter explore various theoretical frameworks, including Betti's reciprocity relation, Moore–Gibson–Thompson (MGT) thermoelasticity theory, and Green-Lindsay thermoelasticity, applied to double porous materials. These frameworks are essential for addressing the stability, uniqueness, and dynamic responses of these materials, with implications for their use in engineering and technology, particularly in environments subjected to extreme thermal and mechanical stresses.

The second chapter shifts focus to the numerical analysis of dynamical systems, employing methods such as numerical fractional calculus. This chapter builds on the author's PhD thesis in Mechanical Engineering, completed in 2010, and demonstrates the application of these numerical methods in solving complex systems that are difficult to address analytically. The chapter is divided into four sections, with research published in journals like Dynamic Systems and Applications and Scientific Annals of Ovidius University. The studies cover a wide range of topics, including the dynamics of a double pendulum system, the motion of a heavy ball on a rotating wire, and the numerical approach to solving the telegrapher equation. The results obtained from these studies underscore the power of

numerical methods in capturing the intricate behaviors of dynamical systems, such as chaotic motion and periodic oscillations, which are often challenging to predict using traditional analytical approaches.

The third chapter applies the findings from the study of dynamical systems to the field of chemistry, particularly in the analysis of porous materials and their applications in combustion processes. The first section of this chapter presents research on the chaotic behavior of Barium Titanate nanoparticles, published in Physics Letters A, which extends the Hamiltonian framework to reveal the complex vibrational dynamics of these nanoparticles under certain conditions. This study builds on previous work by Koo and Lee, who explored ferroelectricity and antiferromagnetism in multiferroic materials. The second section investigates the porosity of waste wood briquettes and its impact on combustion, published in Waste and Biomass Valorization. This research introduces novel methods for assessing briquette porosity, offering new insights into heat and mass transfer processes in these materials and extending existing porosity models to a new application.

Each chapter of the thesis not only builds on the author's previous work but also makes significant contributions to their respective fields. The research presented in the first chapter advances the theoretical understanding of thermoelastic materials with double porosity, providing new tools for analyzing and designing materials for high-stress environments. The second chapter demonstrates the effectiveness of numerical methods in exploring complex dynamical systems, offering practical solutions for problems that are otherwise analytically intractable. Finally, the third chapter showcases the application of these advanced mathematical and numerical techniques in real-world problems, such as the chaotic dynamics of nanoparticles and the optimization of combustion processes in porous materials.

Overall, this thesis highlights the importance of combining rigorous theoretical frameworks with powerful numerical methods to tackle complex problems in material science, mechanical engineering, and chemistry. The results obtained from the various studies not only advance the state of knowledge in these fields but also provide practical insights that could inform the development of new technologies and materials. The simulations and analyses conducted using tools like MATLAB and Maple further demonstrate the utility of these methods in both academic research and applied engineering contexts.

(B) Scientific and professional achievements and the evolution and development plans for career development

(B-i) Scientific and professional achievements

Introduction

The present thesis is structured in three parts as follows.

The first chapter contains the results of the author in the continuum mechanics field, more exactly are approaching the thermoelastic materials with double porosity structure. This chapter is a continuation of the PhD Thesis obtained in Mathematics domain in 2019. This chapter contains three sections that present the main published research in journals as Continuum Mechanics and Thermodynamics and Scientific Analls of Ovidius University.

The second chapter contains approaching of the numerical analysis of dynamical systems using different numerical methods as numerical fractional calculus. Numerical analysis was realized in different mathematical softwares as Maple or Matlab including the Simulink environment. This chapter represents a continuation of the PhD Thesis obtained in Mechanical Engineering domain in 2010. This chapter contains four sections that present the main published reserach in journals as Dynamic Systems and Applications, Scientific Analls of Ovidius University, etc.

The third chapter of the presented thesis contains the applications of the dynamical systems in chemistry highlight in the first section with a result published in Physics Letters A and an application of porous materials in the combustion analysys, result published in Waste and Biomass Valorization Journal.

In the realm of advanced material science, the study of thermoelastic materials with double porosity is a groundbreaking field that explores the unique interaction between thermal and mechanical behaviors in complex structures. The research by Emin, Florea, and Crăciun published in [Emin(2020)] presented in Section 1.1. delves into the theoretical framework underlying these materials, presenting novel insights and solutions for anisotropic thermoelastic bodies. By employing Betti's reciprocity relation, the authors establish important uniqueness results, offering a new understanding of the stability and behavior of these complex materials. This work not only advances our theoretical comprehension but also paves the way for practical applications in engineering and technology, where the control of thermal and mechanical properties is paramount.

The section 1.2 contains the study of Florea and Bobe [Florea(2021a)] which is particularly important for its application of the Moore–Gibson–Thompson (MGT) thermoelasticity theory to double porous materials. The MGT framework is a sophisticated technique that extends classical thermoelastic models by incorporating finite thermal wave speeds, which is crucial for accurately capturing the thermal and mechanical responses in advanced materials. By applying the MGT theory to materials with dual porosity, the authors provide deeper insights into the complex interactions between thermal and mechanical fields, making their research highly relevant for the development of materials used in extreme conditions, such as those found in geothermal and aerospace engineering.

The section 1.3. contains a study by Emin and Florea, published in [Emin(2023)] delves into the application of Green-Lindsay thermoelasticity to double porous materials, providing significant advancements in the field of material science. The authors present their key findings, including a Betti-type result that establishes a crucial reciprocity relation between two systems of external loadings. This relation is particularly valuable for proving the uniqueness of solutions in mixed initial-boundary value problems involving double porous materials. By utilizing the Green-Lindsay function alongside Biot's energy function, the study offers a robust framework for addressing complex thermoelastic challenges, with implications for the design and optimization of materials used in demanding environments, such as aerospace and civil engineering.

The section 2.1. contains a study on the fractional features of a double pendulum system, published in Dynamic Systems and Applications, (2020) that provides a detailed exploration of the application of fractional calculus to the dynamics of a double pendulum. The authors offer a concise overview of fractional calculus and present the classical description of a double pendulum, including the classical Euler-Lagrange equations (CELE). It is introduced the fractional Euler-Lagrange equations (FELE) and the corresponding system of fractional Hamiltonian equations for the double pendulum, utilizing Caputo's derivatives to extend the classical framework. The authors numerically implement the nonlinear fractional system of differential equations using the Euler technique to discretize the convolution integrals. The study analyzes the behavior of the double pendulum for different values of fractional derivatives using Maple software, revealing how fractional dynamics can significantly alter the system's behavior, providing new insights into the complex motion of double pendulum systems.

The section 2.2 presents the results obtained in the study of the motion of a heavy ball sliding on a rotating wire, published in the Bulletin of the Transilvania

University of Brașov (2020). It highlights the effectiveness of numerical techniques in solving complex differential equations that often lack straightforward analytical solutions. The study provides a physical description of the system where the Euler-Lagrange equation governing the motion is derived. The authors detail the numerical methods employed and present the results of their simulations, accompanied by a thorough discussion. These simulations offer valuable insights into the dynamics of the system, demonstrating how numerical approaches can be utilized to explore the intricate behavior of a heavy ball sliding on a rotating wire, a problem that is challenging to solve analytically.

The section 2.3. presents the study of numerical approach for telegraph equation, published in Acta Technica Napocensis (2020) focused on the well-known second-order partial differential equation known equation, which models current and voltage in transmission media and finds applications in fields such as random walk, signal analysis, and wave propagation. It is solved the boundary value problem of the telegrapher equation analytically using Fourier series, providing an exact solution framework. The study explores numerical solutions for the telegrapher equation under various initial and boundary conditions, offering insights into the behavior of the system across different scenarios and demonstrating the versatility of numerical methods in solving complex differential equations.

The study Numerical Aspects of Two Coupled Harmonic Oscillators, published in An. Șt. Univ. Ovidius Constanța (2020), is presented in section 2.4. and it provides a thorough analysis of the dynamics of coupled harmonic oscillators. The authors present a detailed system description, deriving the Euler-Lagrange equations from the Lagrange equation, which forms the basis for the analysis. The mathematical solution to these equations is obtained using the Laplace transform. The focus shifts to numerical techniques, where the authors explore two specific cases—anti-symmetric and mixed symmetric configurations—demonstrating how these numerical methods can effectively capture the behavior of coupled oscillators under different conditions. This study highlights the power of combining analytical and numerical approaches to gain deeper insights into complex oscillatory systems.

The section 3.1. contains the results on the study *Microscopic Hamiltonian and chaotic behavior for Barium Titanate nanoparticles revealed by photonic tunneling model*,published in Physics Letters A (2023). The authors extend the Hamiltonian framework derived from the photonic tunneling model initially proposed by Je Huan Koo and Kwang-Sei Lee, who explored ferroelectricity and antiferromagnetism in multiferroic materials. Koo and Lee previously employed the second quantization formalism to calculate impulsive polarization in ferroelectrics, uncovering various

nonlinear behaviors in these complex media. Building on this foundation, the present study investigates the potential for complex chaotic vibrations in Barium Titanate nanoparticles by deriving semiquantal dynamics through the Ehrenfest theorem, revealing the intricate dynamics of these nanoparticles under certain conditions.

The section 3.2. presents the study on *Indirect Evaluation of the Porosity of Waste Wood Briquettes by Assessing Their Surface Quality*, published in Waste and Biomass Valorization (2021). They are investigated the relationships between key properties of wood briquettes, specifically focusing on the correlations between porosity and density, surface roughness parameters and density, as well as surface roughness and porosity. The study utilizes three different methods to determine porosity and density, offering a comprehensive analysis. A significant contribution of this research is the extension of porosity models, originally developed for wood, to wood briquettes, a novel application that has not been previously reported. Notably, the study introduces the wet porosity model for briquettes, which shows potential for enhancing combustion analysis and improving our understanding of heat and mass transfer processes in these materials.

Chapter 1

Advanced Theoretical Insights in Thermoelasticity of Double Porous Materials

1.1 Some uniqueness results for thermoelastic materials with double porosity structure

The applications of double porosity materials spread accross a wide range of domains e.g. civil engineering, geotechnics [Berryman(2000)], [Khalili(2003)], biomechanics [Cowin(1999)]. First mathematical model of a thermoelastic material with double porosity structure was studied by Barenblatt [Barenblatt(1960a)], [Barenblatt(1960b)]. Straughan in [Straughan(2013)] expressed the connection between the two porosities of a material referring to the pores of the body and the cracks of the skeleton.

Based on the results obtained by Biot [Biot(1941)] for the materials with single porosity and by Barenblatt & co [Barenblatt(1960a)] for the bodies with double porosity, Wilson and Aifantis [Wilson(1982)] have continued the research in the field of deformable bodies with double porosity.

The uniqueness, reciprocity and variational theorems for the basic equations that govern the elastic materials with voids were proved by Ieşan [Ieşan(1985)] and in [Ieşan(1986)] Ieşan included the thermal effect for such media. Based on the Nunziato-Cowin theory for materials with voids [Cowin(1983)], Ieşan and Quintanilla in [Ieşan(2014)] developed a nonlinear theory for thermoelastic bodies with double porosity.

The dynamical problems for the theory of elasticity, viscoelasticity and

thermoelasticity for bodies with double porosity were studied in many papers [Svanadze(2005)], [Svanadze(2010)], [Svanadze(2012)], [Svanadze(2014a)], [Svanadze(2015)], [Svanadze(2016)], [Svanadze(2017)]. In [Svanadze(2014b)], Svanadze obtained some theorems for the isotropic materials with double porosity structure. Straughan studied the stability and uniqueness for the materials with double porosity by introducing a novel functional in order to obtain Holder stability estimates [Straughan(2013)]. Kansal in [Kansal(2018)] obtained uniqueness and reciprocity theorems for anisotropic materials with double porosity based on the Lord-Shuman model [Lord(1967)]. Mixed problem with initial and boundary conditions, in the context of thermoelasticity of dipolar bodies were recently studied in [Marin(2020c)], [Marin(2020d)].

Uniqueness results for a mixed initial boundary problem for dipolar thermoelastic bodies were studied by Marin and Craciun in [Marin(2017c)] and for the microstretch thermoealstic materials were investigated in [Marin(2017b)]. The uniqueness theorems for the classical solutions of the boundary value problems of steady vibrations in case of isotropic porous solids are proved in [Svanadze(2020)]. Existence and uniqueness of solutions for thermoelastic materials with two porosities in the case of one dimensional theory was studied by Bazarra and co in [Bazarra(2019b)].

The continuous dependence by means of some estimate regarding the gradient of deformations and the gradient of the function that describes the evolution of the voids is presented in [Marin(2020e)]. In [Barbu(2020)] was investigated an overdetermined problem for a general class of anisotropic equations on a cylindrical domain. Some estimates regarding the behavior of solutions for a mixed problem in the context of a semi-infinite cylinder composed of two sub-cylinders with an interface at the common boundary were proved in [Marin(2019)].

The mixed initial boundary value problem for a thermoelastic body with double porosity structure was studied by Emin, Crăciun & Florea, in [Emin(2020)]. There are obtained the uniqueness theorems based on the Betti type reciprocity relation that establishes a connection between two systems of external loadings and the solution of those loadings.

1.1.1 Basic equations

Let us consider a material with two porosities. In (1.1.1) are presented the equations that model this type of thermoelastic structure:

$$\begin{aligned} \rho\ddot{u}_i &= t_{ji,j} + \rho F_i, \\ \kappa_1\ddot{\varphi} &= \sigma_{j,j} + p + \rho M, \\ \kappa_2\ddot{\psi} &= \tau_{j,j} + r + \rho N, \end{aligned} \tag{1.1.1}$$

In the above equations we noted the density of material by ρ and the displacement by u_i, the equilibrated inertia coefficients are κ_1, κ_2 and the volume fraction fields φ, ψ, that are considered in the reference configuration. The vectors of the equilibrated stress are σ_j, τ_j and respectively the stress tensors at the body's surface ∂B are t_{ij}. On the body act some forces that are further mentioned: p, r are the intrinsic forces, F_i are the direct forces, M is the extrinsic forces that act on the pores, N is the extrinsic forces that act on the cracks.

Further we express the energy's equation:

$$\rho T_0\dot{\eta} = q_{j,j} + \varrho\delta, \tag{1.1.2}$$

In the reference configuration the body has a constant absolute temperature T_0, the entropy is noted by η, and q_j, δ are the heat flux and the heat supply considered per unit mass and unit time, respectively.

The stress tensors of components t_{ij}, τ_i, σ_i, the intrinsic forces p, r, the specific entropy η, the heat conduction vector of components q_i are defined through the constitutive equations in the linear theory for centrosymmetric materials that follows, [Florea(2019b)]:

$$\begin{aligned} t_{ij} &= C_{ijkl}u_{k,l} + B_{ij}\varphi + D_{ij}\psi - \beta_{ij}\theta, \\ \sigma_i &= \alpha_{ij}\varphi_{,j} + b_{ij}\psi_{,j}, \\ \tau_i &= b_{ij}\varphi_{,j} + \gamma_{ij}\psi_{,j}, \\ p &= -B_{ij}u_{i,j} - \alpha_1\varphi - \alpha_3\psi + \gamma_1\theta, \\ r &= -D_{ij}u_{i,j} - \alpha_3\varphi - \alpha_2\psi + \gamma_2\theta, \\ \rho\eta &= \beta_{ij}u_{i,j} + \gamma_1\varphi + \gamma_2\psi + a\theta, \\ q_i &= K_{ij}\theta_{,j}, \end{aligned} \tag{1.1.3}$$

In the above constitutive equations we have the terms: elasticity tensor is noted by C_{ijkl}, the tensor of thermal dilatation is β_{ij}, the heat conductivity tensor is K_{ij} and θ is the temperature measured from the reference temperature $\mathcal{T}_0$. In the theory of the bodies with double porosity structure there are some typical functions that in our constitutive equations are noted by: B_{ij}, D_{ij}, α_{ij}, b_{ij}, γ_{ij}, α_1, α_2, α_3, γ_1, γ_2, a.

Taking into account the motion's equations (1.1.1) and the energy's equation (1.1.2) and replacing them into the constitutive equations, we further obtain:

$$\begin{aligned}
\rho\ddot{u}_i &= \left(C_{jikl}u_{k,l} + B_{ji}\varphi + D_{ji}\psi - \beta_{ji}\theta\right)_{,j} + \rho F_i,\\
\kappa_1\ddot{\varphi} &= \left(\alpha_{ij}\varphi_{,i} + b_{ij}\psi_{,i}\right)_{,j} - B_{ij}u_{i,j} - \alpha_1\varphi - \alpha_3\psi + \gamma_1\theta + \rho M,\\
\kappa_2\ddot{\psi} &= \left(b_{ij}\varphi_{,i} + \gamma_{ij}\psi_{,i}\right)_{,j} - D_{ij}u_{i,j} - \alpha_3\varphi - \alpha_2\psi + \gamma_2\theta + \rho N,\\
aT_0\dot{\theta} &= -T_0(\beta_{ij}\dot{u}_{i,j} + \gamma_1\dot{\varphi} + \gamma_2\dot{\psi}) + (K_{ij}\theta_{,j})_{,j} + \rho\delta.
\end{aligned} \tag{1.1.4}$$

The constitutive coefficients are symmetric and they satisfy the next relations:

$$\begin{aligned}
C_{ijkl} = C_{ijlk} = C_{klij};\quad \alpha_{ij} = \alpha_{ji};\quad \beta_{ij} = \beta_{ji};\\
\gamma_{ij} = \gamma_{ji};\quad B_{ij} = B_{ji};\quad D_{ij} = D_{ji};\quad K_{ij} = K_{ji}.
\end{aligned} \tag{1.1.5}$$

The entropy inequality implies:

$$K_{ij}\theta_i\theta_j \geq 0. \tag{1.1.6}$$

We consider the not null initial conditions:

$$\begin{aligned}
u_i(x_0,0) = u_i^0(x_0),\ \dot{u}_i(x_0,0) = v_i^0(x_0),\ \varphi(x_0,0) = \varphi_0(x_0),\ \dot{\varphi}(x_0,0) = \tilde{\varphi}_0(x_0),\\
\psi(x_0,0) = \psi_0(x_0),\ \dot{\psi}(x_0,0) = \tilde{\psi}_0(x_0),\ \eta(x_0,0) = \eta_0(x_0),
\end{aligned} \tag{1.1.7}$$

where $x_0 \in \bar{B}$.

We consider that the surface ∂B has the subsets $\partial B_1, \partial B_2, \partial B_3, \partial B_4$ and their complements $\partial B_1^c, \partial B_2^c, \partial B_3^c, \partial B_4^c$. They are satisfying the following conditions:

$$\partial B_i \cup \partial B_i^c = \partial B,\quad \partial B_i \cap \partial B_i^c = \Phi,\ \text{where } i = \overline{1,4}.$$

The boundary conditions are given by the relations that follow:

$$\begin{aligned}
u_i = u_i^b \quad &\text{on} \quad \partial B_1 \times [0,\infty), \quad t_i = t_i^b \quad \text{on} \quad \partial B_1^c \times [0,\infty),\\
\varphi = \varphi^b \quad &\text{on} \quad \partial B_2 \times [0,\infty), \quad \lambda = \lambda^b \quad \text{on} \quad \partial B_2^c \times [0,\infty),\\
\psi = \psi^b \quad &\text{on} \quad \partial B_3 \times [0,\infty), \quad m = \omega^b \quad \text{on} \quad \partial B_3^c \times [0,\infty),\\
\theta = \theta^b \quad &\text{on} \quad \partial B_4 \times [0,\infty), \quad \nu = \Omega^b \quad \text{on} \quad \partial B_4^c \times [0,\infty),
\end{aligned} \tag{1.1.8}$$

where t_i represent the components of surface traction, α, β represent the components of surface couple and Q represents the heat flux, and they can be expressed as follows:

$$t_i = t_{ij}n_j,\quad \lambda = \sigma_i n_i,\quad m = \tau_i n_i,\quad \nu = q_i n_i. \tag{1.1.8'}$$

In (1.1.7) u_i^0, v_i^0, φ_0, $\tilde{\varphi}_0$, ψ_0, $\tilde{\psi}_0$, η_0 are set down functions and in (1.1.8) u_i^b, t_i^b, φ^b, λ^b, ψ^b, ma^b, θ^b, Ω^b are given functions.

The ordered array $(u_i, \varphi, \psi, \theta)$ is a solution for the mixed boundary value problem of a thermoelastic material with double porosity in the cylinder $\Omega_0 = B \times [0, \infty)$. This solution fulfills the differential equations in the system (1.1.4) for all $(x, \xi) \in \Omega_0$, the initial conditions (1.1.7) and the boundary conditions (1.1.8).

We consider the following assumptions to be valid:

1) the constitutive coefficients, the density ρ, the coefficients of inertia κ_1, κ_2 and the prescribed functions in the initial conditions (1.1.7) are functions that are continuous on $\bar{B}$;

2) the body forces F_i, the extrinsic forces M, N and the heat supply h are functions that are continuous on the cylinder $\Omega_0 = B \times [0, \infty)$;

3) $u_i^b, \varphi^b, \psi^b, \theta^b$ are functions that are continuous in their domains of definition;

4) t_i^b, λ^b, ω^b, Ω^b are functions that are continuous in time and piecewise regular in their domains of definition.

1.1.2 Main results

Theorem 1.1.1. *Let us consider the following functions:*

$$\begin{aligned} X(\xi) = & \int_B [\rho \dot{u}_i(\xi)\dot{u}_i(\xi) + \kappa_1 \dot{\varphi}(\xi)\dot{\varphi}(\xi) + \kappa_2 \dot{\psi}(\xi)\dot{\psi}(\xi)]\, dV, \\ Y(\xi) = & \int_B [C_{ijkl} u_{k,l}(\xi) u_{i,j}(\xi) + 2B_{ij} u_{i,j}(\xi)\varphi(\xi) + 2D_{ij} u_{i,j}(\xi)\psi(\xi) \\ & + \alpha_{ij}\varphi_{,i}(\xi)\varphi_{,j}(\xi) + 2b_{ij}\varphi_{,i}(\xi)\psi_{,j}(\xi) + \gamma_{ij}\psi_{,i}(\xi)\psi_{,j}(\xi) \\ & + \alpha_1 \varphi^2(\xi) + \alpha_2 \psi^2(\xi) + 2\alpha_3 \varphi(\xi)\psi(\xi) + a\theta^2(\xi)]\, dV. \end{aligned} \tag{1.1.9}$$

The below identity is satisfied by the considered functions X and Y:

$$\begin{aligned} & Y(\xi) - X(\xi) = \\ & = \int_B \{C_{ijkl} u_{i,j}(0) u_{k,l}(2\xi) + B_{ij}[u_{i,j}(0)\varphi(2\xi) + u_{i,j}(2\xi)\varphi(0)] \\ & \quad + D_{ij}[u_{i,j}(0)\psi(2\xi) + u_{i,j}(2\xi)\psi(0)] + \alpha_{ij}\varphi_{,i}(0)\varphi_{,j}(2\xi) \\ & \quad + b_{ij}[\varphi_{,i}(0)\psi_{,j}(2\xi) + \varphi_{,i}(2\xi)\psi_{,j}(0)] + \gamma_{ij}\psi_{,i}(0)\psi_{,j}(2\xi) \\ & \quad + \alpha_1 \varphi(0)\varphi(2\xi) + \alpha_2 \psi(0)\psi(2\xi) + \alpha_3[\varphi(0)\psi(2\xi) + \\ & \quad + \varphi(2\xi)\psi(0)] + a\theta(0)\theta(2\xi)\ \}\ dV \end{aligned} \tag{1.1.10}$$

$$
\begin{aligned}
&-\int_0^{\xi}\int_{\partial B}[t_i(\xi-\zeta)\dot{u}_j(\xi+\zeta)+\lambda(\xi-\zeta)\dot{\varphi}(\xi+\zeta)+m(\xi-\zeta)\dot{\psi}(\xi+\zeta)-\\
&\qquad -\tfrac{1}{\rho T_0}\nu(\xi-\zeta)\theta(\xi+\zeta)]\,dA\,d\xi\\
&+\int_0^{\xi}\int_{\partial B}[t_i(\xi+\zeta)\dot{u}_j(\xi-\zeta)+\lambda(\xi+\zeta)\dot{\varphi}(\xi-\zeta)+m(\xi+\zeta)\dot{\psi}(\xi-\zeta)-\\
&\qquad \tfrac{1}{\rho T_0}\nu(\xi+\zeta)\theta(\xi-\zeta)]\,dA\,d\xi\\
&-\int_0^{\xi}\int_{B}[\rho F_i(\xi-\zeta)\dot{u}_j(\xi+\zeta)+\rho M(\xi-\zeta)\dot{\varphi}(\xi+\zeta)+\rho N(\xi-\zeta)\dot{\psi}(\xi+\zeta)-\\
&-\qquad \tfrac{1}{T_0}\delta(\xi-\zeta)\theta(\xi+\zeta)]\,dV\,d\xi\\
&+\int_0^{\xi}\int_{B}[\rho F_i(\xi+\zeta)\dot{u}_j(\xi-\zeta)+\rho M(\xi+\zeta)\dot{\varphi}(\xi-\zeta)+\rho N(\xi+\zeta)\dot{\psi}(\xi-\zeta)-\\
&\qquad -\tfrac{1}{T_0}\delta(\xi+\zeta)\theta(\xi-\zeta)]\,dV\,d\xi,
\end{aligned}
\tag{1.1.11}
$$

where $\xi\in[0,\infty)$.

Proof. To be able to prove the theorem we shall introduce the following function:

$$
\begin{aligned}
W(a,b)=t_{ij}(a)\dot{u}_{i,j}(b)+\sigma_i(a)\dot{\varphi}_{,i}(b)+\tau_i(a)\dot{\psi}_{,i}(b)\\
+\theta(a)\dot{\eta}(b)-p(a)\dot{\varphi}(b)-r(a)\dot{\psi}(b).
\end{aligned}
\tag{1.1.12}
$$

Replacing $a\leftrightarrow\xi-\zeta$ and $b\leftrightarrow\xi+\zeta$ and given the constitutive equations, is obtained:

$$
\begin{aligned}
W(\xi-\zeta,\xi+\zeta)=[t_{ij}(\xi-\zeta)\dot{u}_j(\xi+\zeta)+\sigma_i(\xi-\zeta)\dot{\varphi}(\xi+\zeta)\\
+\tau_i(\xi-\zeta)\dot{\psi}(\xi+\zeta)+\tfrac{1}{\rho T_0}\theta(\xi-\zeta)q_i(\xi+\zeta)]_{,i}+\rho F_i(\xi-\zeta)\dot{u}_j(\xi+\zeta)\\
+\rho M(\xi-\zeta)\dot{\varphi}(\xi+\zeta)+\rho N(\xi-\zeta)\dot{\psi}(\xi+\zeta)+\tfrac{1}{T_0}\theta(\xi-\zeta)\delta(\xi+\zeta)\\
-\tfrac{K_{ij}}{\rho T_0}q_{,i}(\xi-\zeta)q_{,j}(\xi+\zeta)+\tfrac{d}{d\xi}[\rho\dot{u}_i(\xi-\zeta)\dot{u}_j(\xi+\zeta)]\\
-\rho\dot{u}_i(\xi-\zeta)\ddot{u}_j(\xi+\zeta)+\tfrac{d}{d\xi}[\kappa_1\dot{\varphi}(\xi-\zeta)\dot{\varphi}(\xi+\zeta)]\\
-\kappa_1\dot{\varphi}(\xi-\zeta)\ddot{\varphi}(\xi+\zeta)+\tfrac{d}{d\xi}[\kappa_2\dot{\psi}(\xi-\zeta)\dot{\psi}(\xi+\zeta)]\\
-\kappa_2\dot{\psi}(\xi-\zeta)\ddot{\psi}(\xi+\zeta).
\end{aligned}
\tag{1.1.13}
$$

Replacing $a\leftrightarrow\xi+\zeta$ and $b\leftrightarrow\xi-\zeta$ and and given the constitutive equations, is obtained:

$$
\begin{aligned}
W(\xi+\zeta,\xi-\zeta)=[t_{ij}(\xi+\zeta)\dot{u}_j(\xi-\zeta)+\sigma_i(\xi+\zeta)\dot{\varphi}(\xi-\zeta)\\
+\tau_i(\xi+\zeta)\dot{\psi}(\xi-\zeta)+\tfrac{1}{\rho T_0}\theta(\xi+\zeta)q_i(\xi-\zeta)]_{,i}+\rho F_i(\xi+\zeta)\dot{u}_j(\xi-\zeta)\\
+\rho M(\xi+\zeta)\dot{\varphi}(\xi-\zeta)+\rho N(\xi+\zeta)\dot{\psi}(\xi-\zeta)+\tfrac{1}{T_0}\theta(\xi+\zeta)\delta(\xi-\zeta)\\
-\tfrac{K_{ij}}{\rho T_0}q_{,i}(\xi+\zeta)q,j(\xi-\zeta)+\tfrac{d}{d\xi}[\rho\dot{u}_i(\xi+\zeta)\dot{u}_j(\xi-\zeta)]\\
-\rho\dot{u}_i(\xi+\zeta)\ddot{u}_j(\xi-\zeta)+\tfrac{d}{d\xi}[\kappa_1\dot{\varphi}(\xi+\zeta)\dot{\varphi}(\xi-\zeta)]\\
-\kappa_1\dot{\varphi}(\xi+\zeta)\ddot{\varphi}(\xi-\zeta)+\tfrac{d}{d\xi}[\kappa_2\dot{\psi}(\xi+\zeta)\dot{\psi}(\xi-\zeta)]\\
-\kappa_2\dot{\psi}(\xi+\zeta)\ddot{\psi}(\xi-\zeta).
\end{aligned}
\tag{1.1.14}
$$

From (1.1.13) and (1.1.14) we obtain:

$$\begin{aligned}
W(\xi-\zeta,\xi+\zeta)-W(\xi+\zeta,\xi-\zeta)=[t_{ij}(\xi-\zeta)\dot{u}_j(\xi+\zeta)\\
+\sigma_i(\xi-\zeta)\dot{\varphi}(\xi+\zeta)+\tau_i(\xi-\zeta)\dot{\psi}(\xi+\zeta)+\tfrac{1}{\rho T_0}\theta(\xi-\zeta)q_i(\xi+\zeta)\\
-t_{ij}(\xi+\zeta)\dot{u}_j(\xi-\zeta)-\sigma_i(\xi+\zeta)\dot{\varphi}(\xi-\zeta)-\tau_i(\xi+\zeta)\dot{\psi}(\xi-\zeta)\\
-\tfrac{1}{\rho T_0}\theta(\xi+\zeta)q_i(\xi-\zeta)]_{,i}+\rho F_i(\xi-\zeta)\dot{u}_j(\xi+\zeta)-\rho F_i(\xi+\zeta)\dot{u}_j(\xi-\zeta)\\
+\rho M(\xi-\zeta)\dot{\varphi}(\xi+\zeta)-\rho M(\xi+\zeta)\dot{\varphi}(\xi-\zeta)+\rho N(\xi-\zeta)\dot{\psi}(\xi+\zeta)\\
-\rho N(\xi+\zeta)\dot{\psi}(\xi-\zeta)+\tfrac{1}{T_0}\theta(\xi-\zeta)\delta(\xi+\zeta)-\tfrac{1}{T_0}\theta(\xi+\zeta)h(\xi-\zeta)\\
-\rho\dot{u}_i(\xi-\zeta)\ddot{u}_j(\xi+\zeta)+\rho\dot{u}_i(\xi+\zeta)\ddot{u}_j(\xi-\zeta)\\
-\kappa_1\dot{\varphi}(\xi-\zeta)\ddot{\varphi}(\xi+\zeta)+\kappa_1\dot{\varphi}(\xi+\zeta)\ddot{\varphi}(\xi-\zeta)\\
-\kappa_2\dot{\psi}(\xi-\zeta)\ddot{\psi}(\xi+\zeta)+\kappa_2\dot{\psi}(\xi+\zeta)\ddot{\psi}(\xi-\zeta).
\end{aligned}\tag{1.1.15}$$

By integration the identity (1.1.15) on the domain B and using the divergence theorem we obtain:

$$\begin{aligned}
\int\limits_B (W(\xi-\zeta,\xi+\zeta)-W(\xi+\zeta,\xi-\zeta))\,dV=\\
=\int\limits_{\partial B}[t_i(\xi-\zeta)\dot{u}_j(\xi+\zeta)+\lambda(\xi-\zeta)\dot{\varphi}(\xi+\zeta)+m(\xi-\zeta)\dot{\psi}(\xi+\zeta)-\\
-\tfrac{1}{\rho T_0}\nu(\xi-\zeta)\theta(\xi+\zeta)]\,dA\\
-\int\limits_{\partial B}[t_i(\xi+\zeta)\dot{u}_j(\xi-\zeta)+\lambda(\xi+\zeta)\dot{\varphi}(\xi-\zeta)+m(\xi+\zeta)\dot{\psi}(\xi-\zeta)-\\
-\tfrac{1}{\rho T_0}\nu(\xi+\zeta)\theta(\xi-\zeta)]\,dA\\
+\int\limits_B[\rho F_i(\xi-\zeta)\dot{u}_j(\xi+\zeta)+\rho M(\xi-\zeta)\dot{\varphi}(\xi+\zeta)+\rho N(\xi-\zeta)\dot{\psi}(\xi+\zeta)-\\
-\tfrac{1}{T_0}\delta(\xi-\zeta)\theta(\xi+\zeta)]\,dV\\
-\int\limits_B[\rho F_i(\xi+\zeta)\dot{u}_j(\xi-\zeta)+\rho M(\xi+\zeta)\dot{\varphi}(\xi-\zeta)+\rho N(\xi+\zeta)\dot{\psi}(\xi-\zeta)-\\
-\tfrac{1}{T_0}\delta(\xi+\zeta)\theta(\xi-\zeta)]\,dV\\
+\int\limits_B\tfrac{d}{d\xi}[\rho\dot{u}_i(\xi-\zeta)\dot{u}_i(\xi+\zeta)+\kappa_1\dot{\varphi}(\xi-\zeta)\dot{\varphi}(\xi+\zeta)+\\
+\kappa_2\dot{\psi}(\xi-\zeta)\dot{\psi}(\xi+\zeta)]\,dV.
\end{aligned}\tag{1.1.16}$$

Returning to (1.1.13) we obtain the following identity:

$$\begin{aligned}
W(\xi-\zeta,\xi+\zeta)-W(\xi+\zeta,\xi-\zeta)=\\
=\tfrac{d}{d\xi}[C_{ijkl}u_{i,j}(\xi-\zeta)u_{k,l}(\xi+\zeta)+B_{ij}u_{i,j}(\xi-\zeta)\varphi(\xi+\zeta)+\\
+B_{ij}\varphi(\xi-\zeta)u_{i,j}(\xi+\zeta)+D_{ij}\psi(\xi+\zeta)u_{i,j}(\xi-\zeta)+D_{ij}u_{i,j}(\xi+\zeta)\psi(\xi-\zeta)\\
+\alpha_{ij}\varphi_{,i}(\xi-\zeta)\varphi_{,j}(\xi+\zeta)+b_{ij}\varphi_{,i}(\xi-\zeta)\psi_{,j}(\xi+\zeta)+b_{ij}\psi_{,i}(\xi-\zeta)\varphi_{,j}(\xi+\zeta)+\\
+\gamma_{ij}\psi_{,i}(\xi-\zeta)\psi_{,j}(\xi+\zeta)+a\theta(\xi-\zeta)\theta(\xi+\zeta)+\alpha_1\varphi(\xi-\zeta)\varphi(\xi+\zeta)+\\
+\alpha_2\psi(\xi-\zeta)\psi(\xi+\zeta)+\alpha_3\varphi(\xi-\zeta)\psi(\xi+\zeta)+\alpha_3\psi(\xi-\zeta)\varphi(\xi+\zeta)].
\end{aligned}\tag{1.1.17}$$

We integrate (1.1.17) on the domain B taking into account (1.1.16), we have:

$$\begin{aligned}
\int_B \tfrac{d}{d\xi}[C_{ijkl}u_{i,j}(\xi-\zeta)u_{k,l}(\xi+\zeta) &+ B_{ij}u_{i,j}(\xi-\zeta)\varphi(\xi+\zeta)+\\
+B_{ij}\varphi(\xi-\zeta)u_{i,j}(\xi+\zeta) &+ D_{ij}\psi(\xi+\zeta)u_{i,j}(\xi-\zeta)+\\
+D_{ij}u_{i,j}(\xi+\zeta)\psi(\xi-\zeta) &+ \alpha_{ij}\varphi_{,i}(\xi-\zeta)\varphi_{,j}(\xi+\zeta)+\\
+b_{ij}\varphi_{,i}(\xi-\zeta)\psi_{,j}(\xi+\zeta)+ &+b_{ij}\psi_{,i}(\xi-\zeta)\varphi_{,j}(\xi+\zeta)+\\
+\gamma_{ij}\psi_{,i}(\xi-\zeta)\psi_{,j}(\xi+\zeta)&+a\theta(\xi-\zeta)\theta(\xi+\zeta)\\
+\alpha_1\varphi(\xi-\zeta)\varphi(\xi+\zeta)&+\alpha_2\psi(\xi-\zeta)\psi(\xi+\zeta)\\
+\alpha_3\varphi(\xi-\zeta)\psi(\xi+\zeta)+&+\alpha_3\psi(\xi-\zeta)\varphi(\xi+\zeta)]\,dV\\
=\int_{\partial B}[t_i(\xi-\zeta)\dot{u}_j(\xi+\zeta)&+\lambda(\xi-\zeta)\dot{\varphi}(\xi+\zeta)+m(\xi-\zeta)\dot{\psi}(\xi+\zeta)-\\
-\tfrac{1}{\rho T_0}\nu(\xi-\zeta)\theta(\xi+\zeta)]\,dA&\\
-\int_{\partial B}[t_i(\xi+\zeta)\dot{u}_j(\xi-\zeta)&+\lambda(\xi+\zeta)\dot{\varphi}(\xi-\zeta)+m(\xi+\zeta)\dot{\psi}(\xi-\zeta)-\\
-\tfrac{1}{\rho T_0}\nu(\xi+\zeta)\theta(\xi-\zeta)]\,dA&\\
+\int_B[\rho F_i(\xi-\zeta)\dot{u}_j(\xi+\zeta)&+\rho M(\xi-\zeta)\dot{\varphi}(\xi+\zeta)+\rho N(\xi-\zeta)\dot{\psi}(\xi+\zeta)-\\
-\tfrac{1}{T_0}\delta(\xi-\zeta)\theta(\xi+\zeta)]\,dV&\\
-\int_B[\rho F_i(\xi+\zeta)\dot{u}_j(\xi-\zeta)&+\rho M(\xi+\zeta)\dot{\varphi}(\xi-\zeta)+\rho N(\xi+\zeta)\dot{\psi}(\xi-\zeta)-\\
-\tfrac{1}{T_0}\delta(\xi+\zeta)\theta(\xi-\zeta)]\,dV&\\
+\int_B\tfrac{d}{d\xi}[\rho\dot{u}_i(\xi-\zeta)\dot{u}_i(\xi+\zeta)&+\kappa_1\dot{\varphi}(\xi-\zeta)\dot{\varphi}(\xi+\zeta)+\\
+\kappa_2\dot{\psi}(\xi-\zeta)\dot{\psi}(\xi+\zeta)]\,dV.&
\end{aligned} \tag{1.1.18}$$

Further we integrate (1.1.18) on the range $[0,\xi]$ with respect to ζ and the theorem Th[1.1.1] result is obtained.

□

Theorem 1.1.2. *For $\forall\xi\in[0,\infty)$ the defined functions from* (1.1.9) *satisfy the following relations:*

$$\begin{aligned}
Y(\xi)&=\tfrac{1}{2}[X(0)+Y(0)]+\\
+\tfrac{1}{2}\int_B[C_{ijkl}u_{i,j}(0)u_{k,l}(2\xi)&+B_{ij}[u_{i,j}(0)\varphi(2\xi)+u_{i,j}(2\xi)\varphi(0)]+\\
+D_{ij}[u_{i,j}(0)\psi(2\xi)&+u_{i,j}(2\xi)\psi(0)]+\alpha_{ij}\varphi_{,i}(0)\varphi_{,j}(2\xi)+\\
+b_{ij}[\varphi_{,i}(0)\psi_{,j}(2\xi)&+\varphi_{,i}(2\xi)\psi_{,j}(0)]+\gamma_{ij}\psi_{,i}(0)\psi_{,j}(2\xi)+
\end{aligned} \tag{1.1.19}$$

$$+\alpha_1\varphi(0)\varphi(2\xi)+\alpha_2\psi(0)\psi(2\xi)+\alpha_3[\varphi(0)\psi(2\xi)+\varphi(2\xi)\psi(0)]+$$
$$+a\theta(0)\theta(2\xi)]\ dV$$
$$-\tfrac{1}{2}\int_0^\xi\int_{\partial B}[t_i(\xi-\zeta)\dot{u}_j(\xi+\zeta)+\lambda(\xi-\zeta)\dot{\varphi}(\xi+\zeta)+m(\xi-\zeta)\dot{\psi}(\xi+\zeta)-$$
$$-\tfrac{1}{\rho T_0}\nu(\xi-\zeta)\theta(\xi+\zeta)]\ dA\ d\zeta$$
$$+\tfrac{1}{2}\int_0^\xi\int_{\partial B}[t_i(\xi+\zeta)\dot{u}_j(\xi-\zeta)+\lambda(\xi+\zeta)\dot{\varphi}(\xi-\zeta)+m(\xi+\zeta)\dot{\psi}(\xi-\zeta)-$$
$$-\tfrac{1}{\rho T_0}\nu(\xi+\zeta)\theta(\xi-\zeta)]\ dA\ d\zeta$$
$$-\tfrac{1}{2}\int_0^\xi\int_B[\rho F_i(\xi-\zeta)\dot{u}_j(\xi+\zeta)+\rho M(\xi-\zeta)\dot{\varphi}(\xi+\zeta)+\rho N(\xi-\zeta)\dot{\psi}(\xi+\zeta)-$$
$$-\tfrac{1}{T_0}\delta(\xi-\zeta)\theta(\xi+\zeta)]\ dV\ d\zeta$$
$$+\tfrac{1}{2}\int_0^\xi\int_B[\rho F_i(\xi+\zeta)\dot{u}_j(\xi-\zeta)+\rho M(\xi+\zeta)\dot{\varphi}(\xi-\zeta)+\rho N(\xi+\zeta)\dot{\psi}(\xi-\zeta)-$$
$$-\tfrac{1}{T_0}\delta(\xi+\zeta)\theta(\xi-\zeta)]\ dV\ d\zeta$$
$$+\int_0^\xi\int_{\partial B}[t_i(\xi)\dot{u}_j(\xi)+\lambda(\xi)\dot{\varphi}(\xi)+m(\xi)\dot{\psi}(\xi)-\tfrac{1}{\rho T_0}\nu(\xi)\theta(\xi)]\ dA\ d\zeta$$
$$+\int_0^\xi\int_B[\rho F_i(\xi)\dot{u}_j(\xi)+\rho M(\xi)\dot{\varphi}(\xi)+\rho N(\xi)\dot{\psi}(\xi)-\tfrac{1}{T_0}\delta(\xi)\theta(\xi)]\ dV\ d\zeta$$
$$-\int_0^\xi\int_B\tfrac{K_{ij}}{\rho T_0}\theta_{,i}(\xi)\theta_{,j}(\xi)\ dV\ d\zeta,$$

$$X(\xi)=\tfrac{1}{2}[X(0)+Y(0)]-$$
$$-\tfrac{1}{2}\int_B[C_{ijkl}u_{i,j}(0)u_{k,l}(2\xi)+B_{ij}[u_{i,j}(0)\varphi(2\xi)+u_{i,j}(2\xi)\varphi(0)]$$
$$+D_{ij}[u_{i,j}(0)\psi(2\xi)+u_{i,j}(2\xi)\psi(0)]+\alpha_{ij}\varphi_{,i}(0)\varphi_{,j}(2\xi)+$$
$$+b_{ij}[\varphi_{,i}(0)\psi_{,j}(2\xi)+\varphi_{,i}(2\xi)\psi_{,j}(0)]+\gamma_{ij}\psi,i(0)\psi,j(2\xi)+$$
$$+\alpha_1\varphi(0)\varphi(2\xi)+\alpha_2\psi(0)\psi(2\xi)+\alpha_3[\varphi(0)\psi(2\xi)+\varphi(2\xi)\psi(0)]$$
$$+a\theta(0)\theta(2\xi)]\ dV$$
$$+\tfrac{1}{2}\int_0^\xi\int_{\partial B}[t_i(\xi-\zeta)\dot{u}_j(\xi+\zeta)+\lambda(\xi-\zeta)\dot{\varphi}(\xi+\zeta)+m(\xi-\zeta)\dot{\psi}(\xi+\zeta)-$$
$$-\tfrac{1}{\rho T_0}\nu(\xi-\zeta)\theta(\xi+\zeta)]\ dA\ d\zeta- \tag{1.1.20}$$

$$
\begin{aligned}
&-\tfrac{1}{2}\int_0^{\xi}\int_{\partial B}[t_i(\xi+\zeta)\dot{u}_j(\xi-\zeta)+\lambda(\xi+\zeta)\dot{\varphi}(\xi-\zeta)+m(\xi+\zeta)\dot{\psi}(\xi-\zeta)-\\
&\qquad-\tfrac{1}{\rho T_0}\nu(\xi+\zeta)\theta(\xi-\zeta)]\,dA\,d\zeta\\
&+\tfrac{1}{2}\int_0^{\xi}\int_{B}[\rho F_i(\xi-\zeta)\dot{u}_j(\xi+\zeta)+\rho M(\xi-\zeta)\dot{\varphi}(\xi+\zeta)+\rho N(\xi-\zeta)\dot{\psi}(\xi+\zeta)-\\
&\qquad-\tfrac{1}{T_0}\delta(\xi-\zeta)\theta(\xi+\zeta)]\,dV\,d\zeta\\
&-\tfrac{1}{2}\int_0^{\xi}\int_{B}[\rho F_i(\xi+\zeta)\dot{u}_j(\xi-\zeta)+\rho M(\xi+\zeta)\dot{\varphi}(\xi-\zeta)+\rho N(\xi+\zeta)\dot{\psi}(\xi-\zeta)-\\
&\qquad-\tfrac{1}{T_0}\delta(\xi+\zeta)\theta(\xi-\zeta)]\,dV\,d\zeta\\
&+\int_0^{\xi}\int_{\partial B}[t_i(\xi)\dot{u}_j(\xi)+\lambda(\xi)\dot{\varphi}(\xi)+m(\xi)\dot{\psi}(\xi)-\tfrac{1}{\rho T_0}\nu(\xi)\theta(\xi)]\,dA\,d\zeta\\
&+\int_0^{\xi}\int_{B}[\rho F_i(\xi)\dot{u}_j(\xi)+\rho M(\xi)\dot{\varphi}(\xi)+\rho N(\xi)\dot{\psi}(\xi)-\tfrac{1}{T_0}\delta(\xi)\theta(\xi)]\,dV\,d\zeta\\
&-\int_0^{\xi}\int_{B}\tfrac{K_{ij}}{\rho T_0}\theta_{,i}(\xi)\theta_{,j}(\xi)\,dV\,d\zeta,
\end{aligned}
$$

Proof. We consider the relations (1.1.12) and (1.1.14) in which $a=\xi, b=\xi$ and if we take into consideration the constitutive equations (1.1.3), then the function $W(\xi,\xi)$ has the following structure:

$$
\begin{aligned}
W(\xi,\xi)=&C_{ijkl}u_{i,j}(\xi)\dot{u}_{k,l}(\xi)+B_{ij}[\dot{u}_{i,j}(\xi)\varphi(\xi)+u_{i,j}(\xi)\dot{\varphi}(\xi)]+\\
&+D_{ij}[\dot{u}_{i,j}(\xi)\psi(\xi)+u_{i,j}(\xi)\dot{\psi}(\xi)]+\alpha_{ij}\dot{\varphi}_{,i}(\xi)\varphi_{,j}(\xi)+\\
&+b_{ij}[\dot{\varphi}_{,i}(\xi)\psi_{,j}(\xi)+\dot{\psi}_{,i}(\xi)\varphi_{,j}(\xi)]+\gamma_{ij}\dot{\psi}_{,i}(\xi)\psi_{,j}(\xi)+\\
&+a\theta(\xi)\dot{\theta}(\xi)+\alpha_1\varphi(\xi)\dot{\varphi}(\xi)+\alpha_2\psi(\xi)\dot{\psi}(\xi)+\\
&+\alpha_3[\dot{\varphi}(\xi)\psi(\xi)+\dot{\psi}(\xi)\varphi(\xi)].
\end{aligned}
\tag{1.1.21}
$$

We observe that if we derive (1.1.9) in relation to ξ we have:

$$
\begin{aligned}
\dot{X}(\xi)=&\int_B[\rho\ddot{u}_i(\xi)\dot{u}_i(\xi)+\rho\dot{u}_i(\xi)\ddot{u}_i(\xi)+\kappa_1\ddot{\varphi}(\xi)\dot{\varphi}(\xi)+\\
&+\kappa_1\dot{\varphi}(\xi)\ddot{\varphi}(\xi)+\kappa_2\ddot{\psi}(\xi)\dot{\psi}(\xi)+\kappa_2\dot{\psi}(\xi)\ddot{\psi}(\xi)]\,dV\\
=&\,2\int_B[\rho\dot{u}_i(\xi)\ddot{u}_i(\xi)+\kappa_1\dot{\varphi}(\xi)\ddot{\varphi}(\xi)+\kappa_2\dot{\psi}(\xi)\ddot{\psi}(\xi)]\,dV,
\end{aligned}
$$

$$
\begin{aligned}
\dot{Y}(\xi)=&\int_B[C_{ijkl}\dot{u}_{i,j}(\xi)u_{k,l}(\xi)+C_{ijkl}u_{i,j}(\xi)\dot{u}_{k,l}(\xi)+2B_{ij}[\dot{u}_{i,j}(\xi)\varphi(\xi)\\
&+u_{i,j}(\xi)\dot{\varphi}(\xi)]+2D_{ij}[\dot{u}_{i,j}(\xi)\psi(\xi)+u_{i,j}(\xi)\dot{\psi}(\xi)]\\
&+\alpha_{ij}[\dot{\varphi}_{,i}(\xi)\varphi_{,j}(\xi)+\varphi_{,i}(\xi)\dot{\varphi}_{,j}(\xi)]+2b_{ij}[\dot{\varphi}_{,i}(\xi)\psi_{,j}(\xi)\\
&+\varphi_{,i}(\xi)\dot{\psi}_{,j}(\xi)]+\gamma_{ij}[\dot{\psi}_{,i}(\xi)\psi_{,j}(\xi)+\psi_{,i}(\xi)\dot{\psi}_{,j}(\xi)]\\
&+2\alpha_1\varphi(\xi)\dot{\varphi}(\xi)+2\alpha_2\psi(\xi)\dot{\psi}(\xi)+2\alpha_3[\dot{\varphi}(\xi)\psi(\xi)+\varphi(\xi)\dot{\psi}(\xi)]+2a\theta(\xi)\dot{\theta}(\xi)]\,dV\\
=&\int_B 2W(\xi,\xi)\,dV.
\end{aligned}
$$

Integrating on the domain B and considering the divergence theorem the following relation is deduced:

$$\begin{aligned}\dot{X}(\xi)+\dot{Y}(\xi)=2\int\limits_{\partial B}[t_i(\xi)u_j(\xi)+\lambda(\xi)\dot{\varphi}(\xi)+m(\xi)\dot{\psi}(\xi)\\ -\tfrac{1}{\rho T_0}\nu(\xi)\theta(\xi)]\,dA+\\ 2\int\limits_B[\rho F_i(\xi)\dot{u}_i(\xi)+\rho M(\xi)\dot{\varphi}(\xi)+\rho N(\xi)\dot{\psi}(\xi)\\ +\tfrac{1}{T_0}\theta(\xi)\delta(\xi)]\,dV-2\int\limits_B\tfrac{K_{ij}}{\rho T_0}\theta_{,i}(\xi)\theta_{,j}(\xi)\,dV\end{aligned}\tag{1.1.22}$$

After the integration of the relation (1.1.22) on $[0,\xi]$ we derive:

$$\begin{aligned}X(\xi)-X(0)+Y(\xi)-Y(0)=\\ =2\int\limits_0^\xi\int\limits_{\partial B}[t_i(\xi)u_j(\xi)+\lambda(\xi)\dot{\varphi}(\xi)+m(\xi)\dot{\psi}(\xi)-\tfrac{1}{\rho T_0}\nu(\xi)\theta(\xi)]\,dA\,d\zeta\\ +2\int\limits_0^\xi\int\limits_B[\rho F_i(\xi)\dot{u}_i(\xi)+\rho M(\xi)\dot{\varphi}(\xi)+\rho N(\xi)\dot{\psi}(\xi)+\tfrac{1}{T_0}\theta(\xi)\delta(\xi)]\,dV\,d\zeta\\ -2\int\limits_0^\xi\int\limits_B\tfrac{K_{ij}}{\rho T_0}\theta_{,i}(\xi)\theta_{,j}(\xi)\,dV\,d\zeta.\end{aligned}\tag{1.1.23}$$

We will solve the system of equations (1.1.10) and (1.1.23) and we obtain $Y(\xi)$ and $X(\xi)$ which are the relations of theorem Th[1.1.2]. Thus, by summing, we obtain $Y(\xi)$ from formula (1.1.19) and by subtraction, we obtain $X(\xi)$ from formula (1.1.20). □

Theorems Th[1.1.1] and Th[1.1.2] allow us to obtain the following uniqueness theorem:

Theorem 1.1.3. *If the assumptions* (1.1.1) - (1.1.5) *are fulfilled then the mixed problem for thermoelastic bodies with double porosity* (1.1.4) *accompanied by the initial conditions* (1.1.7) *and the boundary conditions* (1.1.8) *admits a unique solution.*

Proof. We will proof the theorem by contradiction. We consider that the proposed mixed problem admit two different solutions: $u_i^{(k)}$, $\varphi^{(k)}$, $\psi^{(k)}$, $\theta^{(k)}$, $t_{ij}^{(k)}$, $\sigma_i^{(k)}$, $\tau_i^{(k)}$, $p^{(k)}$, $r^{(k)}$, $\eta^{(k)}$, $q_i^{(k)}$, $k=1,2$. The difference between the two considered solutions will be noted by: $\hat{u}_i$, $\hat{\varphi}$, $\hat{\psi}$, $\hat{\theta}$, $\hat{t}_{ij}$, $\hat{\sigma}_i$, $\hat{\tau}_i$, $\hat{p}$, $\hat{r}$, $\hat{\eta}$, $\hat{q}_i$. Due to the linearity, the difference between the two solutions is also a solution of the problem corresponding to the null initial conditions and the null boundary conditions.

Considering the null boundary conditions, the expression of the function $X(\xi)$ from (1.1.20) becomes:

$$X(\xi)=-\int\limits_0^\xi\int\limits_B\frac{K_{ij}}{\rho T_0}\hat{\theta}_{,i}(\xi)\hat{\theta}_{,j}(\xi)\,dV\,d\zeta.\tag{1.1.24}$$

Considering the expression of $X(\xi)$ in (1.1.9) and from (1.1.24) we obtain

$$\begin{aligned}\int\limits_B [\rho\hat{\dot{u}}_i(\xi)\hat{u}_i(\xi) + \kappa_1\hat{\dot{\varphi}}(\xi)\hat{\varphi}(\xi) + \kappa_2\hat{\dot{\psi}}(\xi)\hat{\psi}(\xi)] \\ + \tfrac{1}{\rho T_0}\int\limits_0^\xi\int\limits_B K_{ij}\hat{\theta}_{,i}(\xi)\hat{\theta}_{,j}(\xi)\, dV\, d\zeta = 0,\end{aligned} \tag{1.1.25}$$

where $\xi \in [0,\infty)$.

Due to the fact that $a > 0$, κ_1, κ_2 are positive definite tensors and K_{ij} is a positive semi-definite tensor, considering (1.1.25) we derive:

$$\hat{\dot{u}}_i(x,\xi) = 0, \quad \hat{\dot{\varphi}}(x,\xi) = 0, \quad \hat{\dot{\psi}}(x,\xi) = 0, \quad \forall (x,\xi) \in B \times [0,\infty), \tag{1.1.26}$$

respectively,

$$\int\limits_0^\xi\int\limits_B K_{ij}\hat{\theta}_{,i}(\xi)\hat{\theta}_{,j}(\xi)\, dV\, d\zeta = 0, \quad \forall \xi \in [0,\infty). \tag{1.1.27}$$

Taking into account the null initial conditions for the difference between the two solutions, and considering (1.1.26) we obtain:

$$\hat{u}_i(x,\xi) = 0, \quad \hat{\varphi}(x,\xi) = 0, \quad \hat{\psi}(x,\xi) = 0, \quad \forall (x,\xi) \in B \times [0,\infty). \tag{1.1.28}$$

If we now consider the null boundary conditions, then the expression of $Y(\xi)$ in (1.1.19) becomes:

$$Y(\xi) = -\int\limits_0^\xi\int\limits_B \frac{K_{ij}}{\rho T_0}\hat{\theta}_{,i}(\xi)\hat{\theta}_{,j}(\xi)\, dV\, d\zeta. \tag{1.1.29}$$

From the expression of $Y(\xi)$ in (1.1.9), taking into account (1.1.28) and (1.1.29), we obtain:

$$\int\limits_B a\hat{\theta}^2(\xi)\, dV = -\int\limits_0^\xi\int\limits_B \frac{K_{ij}}{\rho T_0}\hat{\theta}_{,i}(\xi)\hat{\theta}_{,j}(\xi)\, dV\, d\zeta.$$

Considering (1.1.27) we obtain:

$$\int\limits_B a\hat{\theta}^2(\xi)\, dV = 0. \tag{1.1.30}$$

Due to the fact that $a > 0$, the relation (1.1.30) leads to:

$$\hat{\theta}(x,\xi) = 0, \quad (x,\xi) \in B \times [0,\infty). \tag{1.1.31}$$

In conclusion, due to the fact that the difference of the two considered solutions is null, (1.1.28) and (1.1.31) lead to the fact that the considered problem has a unique solution. □

The basis of the following uniqueness theorem is given by the proof of the following Betti's type reciprocity relation that is in fact a relation between two systems of external loads and the solutions corresponding to these loads.

We now introduce the functions f and g defined on the cylinder $\Omega_0 = B \times [0, \infty)$, that are continuous in time and whose convolution product is defined by the relation:

$$(f * g)(x, \xi) = \int_0^\xi f(x, \xi - \zeta) g(\xi, \zeta)\, d\zeta. \tag{1.1.32}$$

Integrating the energy equation (1.1.2) we obtain:

$$\rho T_0 \eta - \rho T_0 \eta_0 = \int_0^\xi q_{j,j}(x, \zeta)\, d\zeta + \rho \int_0^\xi \delta(x, \zeta)\, d\zeta. \tag{1.1.33}$$

If in the convolution product (1.1.32) we consider that the function f is the identity function $f = 1$ then we have the following notation:

$$g_*(x, \xi) = \int_0^\xi 1 \cdot g(\xi, \zeta)\, d\zeta = 1 * g(\xi, \zeta).$$

Using the notation above we have:

$$q_{*j,j} = \int_0^\xi q_{j,j}(x, \zeta)\, d\zeta; \quad \delta_* = \int_0^\xi h(x, \zeta)\, d\zeta. \tag{1.1.34}$$

Therefore the energy equation (1.1.2) can also be written as follows:

$$\eta = \frac{1}{\rho T_0}(q_{*j,j} + \omega), \tag{1.1.35}$$

where $\omega = \rho \delta_* + \rho T_0 \eta_0$.

Let us consider two systems of loads marked by $H^{(a)}$, where $a = 1, 2$:

$$\begin{aligned} H^{(a)} = \{&F_i^{(a)}, \omega^{(a)}, N^{(a)}, \delta^{(a)}, u_i^{*(a)}, t_i^{*(a)}, \varphi^{*(a)}, \lambda^{*(a)}, \psi^{*(a)}, \\ &\omega^{*(a)}, \theta^{*(a)}, \Omega^{*(a)}, u_i^{0(a)}, v_i^{0(a)}, \varphi_0^{(a)}, \tilde{\varphi}_0^{(a)}, \psi_0^{(a)}, \tilde{\psi}_0^{(a)}, \eta_0^{(a)}\}, \end{aligned} \tag{1.1.36}$$

respectively the set of corresponding solutions $S^{(a)}$, where $a = 1, 2$:

$$S^{(a)} = \{u_i^{(a)}, \varphi^{(a)}, \psi^{(a)}, \theta^{(a)}, t_{ij}^{(a)}, \sigma_i^{(a)}, \tau_i^{(a)}, q_i^{(a)}, r^{(a)}, p^{(a)}\}, \tag{1.1.37}$$

where: $t_i^{(a)} = t_{ij}^{(a)} n_j$, $\lambda^{(a)} = \sigma_i^{(a)} n_i$, $\omega^{(a)} = \tau_i^{(a)} n_i$, $\Omega^{(a)} = q_i^{(a)} n_i$. Let us consider the function:

$$\begin{aligned} \mathcal{F}_{ab}(\xi, \zeta) = &t_{ij}^{(a)}(\xi) u_{i,j}^{(b)}(\zeta) + \sigma_i^{(a)}(\xi) \varphi_{,i}^{(b)}(\zeta) + \tau_i^{(a)}(\xi) \psi_{,i}^{(b)}(\zeta) \\ &- p^{(a)}(\xi) \varphi^{(b)}(\zeta) - r^{(a)}(\xi) \psi^{(b)}(\zeta) - \eta^{(a)}(\xi) \theta^{(b)}(\zeta). \end{aligned} \tag{1.1.38}$$

We introduce the constitutive equations (1.1.3) in (1.1.38) and we obtain:

$$\begin{aligned}\mathcal{F}_{ab}(\xi,\zeta)=C_{ijkl}u^{(a)}_{k,l}(\xi)u^{(b)}_{i,j}(\zeta)+B_{ij}[\varphi^{(a)}(\xi)u^{(b)}_{i,j}(\zeta)+u^{(a)}_{i,j}(\xi)\varphi^{(b)}(\zeta)]\\ +D_{ij}[\psi^{(a)}(\xi)u^{(b)}_{i,j}(\zeta)+u^{(a)}_{i,j}(\xi)\psi^{(b)}(\zeta)]-\beta_{ij}[\theta^{(a)}(\xi)u^{(b)}_{i,j}(\zeta)+u^{(a)}_{i,j}(\xi)\theta^{(b)}(\zeta)]\\ +\alpha_{ij}\varphi^{(a)}_{,j}(\xi)\varphi^{(b)}_{,i}(\zeta)+b_{ij}[\psi^{(a)}_{,j}(\xi)\varphi^{(b)}_{,i}(\zeta)+\varphi^{(a)}_{,j}(\zeta)\psi^{(b)}_{,i}(\zeta)]\\ +\gamma_{ij}\psi^{(a)}_{,j}(\xi)\psi^{(b)}_{,i}(\zeta)+\alpha_1\varphi^{(a)}(\xi)\varphi^{(b)}(\zeta)+\alpha_2\psi^{(a)}(\xi)\psi^{(b)}(\zeta)\\ +\alpha_3[\varphi^{(a)}(\xi)\psi^{(b)}(\zeta)+\psi^{(a)}(\xi)\varphi^{(b)}(\zeta)]-\gamma_1[\theta^{(a)}(\xi)\varphi^{(b)}(\zeta)+\varphi^{(a)}(\xi)\theta^{(b)}(\zeta)]\\ -\gamma_2[\theta^{(a)}(\xi)\psi^{(b)}(\zeta)+\psi^{(a)}(\xi)\theta^{(b)}(\zeta)]-a\theta^{(a)}(\xi)\theta^{(b)}(\zeta).\end{aligned}\tag{1.1.39}$$

Taking into account the symmetry relations (1.1.5) we observe that the commutative takes place:

$$\mathcal{F}_{ab}(\xi,\zeta)=\mathcal{F}_{ba}(\zeta,\xi).\tag{1.1.40}$$

We observe that:

$$\begin{aligned}&(t^{(a)}_{ij}(\xi)u^{(b)}_{j}(\zeta)+\sigma^{(a)}_{i}(\xi)\varphi^{(b)}(\zeta)+\tau^{(a)}_{i}(\xi)\psi^{(b)}(\zeta))_{,i}=\\ &=t^{(a)}_{ij,i}(\xi)u^{(b)}_{j}(\zeta)+t^{(a)}_{ij}(\xi)u^{(b)}_{j,i}(\zeta)+\sigma^{(a)}_{i,i}(\xi)\varphi^{(b)}(\zeta)+\sigma^{(a)}_{i}(\xi)\varphi^{(b)}_{,i}(\zeta)\\ &+\tau^{(a)}_{i,i}(\xi)\psi^{(b)}(\zeta)+\tau^{(a)}_{i}(\xi)\psi^{(b)}_{,i}(\zeta).\end{aligned}$$

Using the equations of motion (1.1.1) the above relation leads us to:

$$\begin{aligned}t^{(a)}_{ij}(\xi)u^{(b)}_{j,i}(\zeta)+\sigma^{(a)}_{i}(\xi)\varphi^{(b)}_{,i}(\zeta)+\tau^{(a)}_{i}(\xi)\psi^{(b)}_{,i}(\zeta)=\\ (t^{(a)}_{ij}(\xi)u^{(b)}_{j}(\zeta)+\sigma^{(a)}_{i}(\xi)\varphi^{(b)}(\zeta)+\tau^{(a)}_{i}(\xi)\psi^{(b)}(\zeta))_{,i}-(\rho\ddot{u}^{(a)}_{i}(\xi)-\\ -\rho F^{(a)}_{i}(\xi))u^{(b)}_{j}(\zeta)-(\kappa_1\ddot{\varphi}^{(a)}(\xi)-p^{(a)}(\xi)-\rho\omega^{(a)}(\xi))\varphi^{(b)}(\zeta)\\ -(\kappa_2\ddot{\psi}^{(a)}(\xi)-r^{(a)}(\xi)-\rho N^{(a)}(\xi))\psi^{(b)}(\zeta).\end{aligned}\tag{1.1.41}$$

We use the energy equation written as in (1.1.2) and we have:

$$\begin{aligned}\eta^{(a)}(\xi)\theta^{(b)}(\zeta)=\tfrac{1}{\rho T_0}(q^{(a)}_{*i}(\xi)\theta^{(b)}(\zeta))_{,i}+\tfrac{1}{\rho T_0}\omega^{(a)}(\xi)\theta^{(b)}(\zeta)\\ -\tfrac{1}{\rho T_0}q^{(a)}_{*i}(\xi)\theta^{(b)}_{,i}(\zeta).\end{aligned}\tag{1.1.42}$$

Substituting (1.1.41) and (1.1.42) in (1.1.38) we obtain:

$$\begin{aligned}\mathcal{F}_{ab}(\xi,\zeta)=(t^{(a)}_{ij}(\xi)u^{(b)}_{j}(\zeta)+\sigma^{(a)}_{i}(\xi)\varphi^{(b)}(\zeta)+\tau^{(a)}_{i}(\xi)\psi^{(b)}(\zeta)\\ -\tfrac{1}{\rho T_0}Q^{(a)}_{*i}(\xi)\theta^{(b)}(\zeta))_{,i}-(\rho\ddot{u}^{(a)}_{i}(\xi)-\rho F^{(a)}_{i}(\xi))u^{(b)}_{i}(\zeta)\\ -(\kappa_1\ddot{\varphi}^{(a)}(\xi)-\rho\omega^{(a)}(\xi))\varphi^{(b)}(\zeta)-(\kappa_2\ddot{\psi}^{(a)}(\xi)-\rho N^{(a)}(\xi))\psi^{(b)}(\zeta)\\ -\tfrac{1}{\rho T_0}\omega^{(a)}(\xi)\theta^{(b)}(\zeta)+\tfrac{1}{\rho T_0}q^{(a)}_{*i}(\xi)\theta^{(b)}_{,i}(\zeta).\end{aligned}\tag{1.1.43}$$

We integrate the previous relation on the domain B and using the divergence theorem

and take into account (1.1.8'). We have:

$$\begin{aligned}
&\int\limits_B [t_{ij}^{(a)}(\xi)u_i^{(b)}(\zeta)+\sigma_i^{(a)}(\xi)\varphi^{(b)}(\zeta)+\tau_i^{(a)}(\xi)\psi^{(b)}(\zeta)\\
&\qquad -\tfrac{1}{\rho T_0}q_{*i}^{(a)}(\xi)\theta^{(b)}(\zeta)]_{,i}\,dV=\\
&=\int\limits_{\partial B}[t_{ij}^{(a)}(\xi)u_i^{(b)}(\zeta)n_i+\sigma_i^{(a)}(\xi)\varphi^{(b)}(\zeta)n_i+\tau_i^{(a)}(\xi)\psi^{(b)}(\zeta)n_i\\
&\qquad -\tfrac{1}{\rho T_0}q_{*i}^{(a)}(\xi)\theta^{(b)}(\zeta)n_i]\,dA=\\
&=\int\limits_{\partial B}[t_i^{(a)}(\xi)u_i^{(b)}(\zeta)+\alpha^{(a)}(\xi)\varphi^{(b)}(\zeta)+\beta^{(a)}(\xi)\psi^{(b)}(\zeta)\\
&\qquad -\tfrac{1}{\rho T_0}q_{*}^{(a)}(\xi)\theta^{(b)}(\zeta)]\,dA.
\end{aligned}\tag{1.1.44}$$

Based on the previous relations we can express the following result:

Lemma 1.1.1. *For the function:*

$$\begin{aligned}
\mathcal{F}_{ab}(\xi,\zeta)=&\int\limits_B[\rho F_i^{(a)}(\xi)u_i^{(b)}(\zeta)+\rho\omega^{(a)}(\xi)\varphi^{(b)}(\zeta)+\rho N^{(a)}(\xi)\psi^{(b)}(\zeta)\\
&\qquad -\tfrac{1}{\rho T_0}\omega^{(a)}(\xi)\theta^{(b)}(\zeta)]\,dV\\
&-\int\limits_B[\rho\ddot{u}_i^{(a)}(\xi)u_i^{(b)}(\zeta)+\kappa_1\ddot{\varphi}^{(a)}(\xi)\varphi^{(b)}(\zeta)+\kappa_2\ddot{\psi}^{(a)}(\xi)\psi^{(b)}(\zeta)]\,dV\\
&\qquad +\tfrac{1}{\rho T_0}\int\limits_B Q_{*i}^{(a)}(\xi)\theta_{,i}^{(b)}(\zeta)\,dV\\
&+\int\limits_{\partial B}[t_i^{(a)}(\xi)u_i^{(b)}(\zeta)+\lambda^{(a)}(\xi)\varphi^{(b)}(\zeta)+\omega^{(a)}(\xi)\psi^{(b)}(\zeta)\\
&\qquad -\tfrac{1}{\rho T_0}q_{*}^{(a)}(\xi)\theta^{(b)}(\zeta)]\,dA.
\end{aligned}\tag{1.1.45}$$

the following commutative relation takes place:

$$\mathcal{F}_{ab}(\xi,\zeta)=\mathcal{F}_{ba}(\zeta,\xi),\quad \forall\xi,\zeta\in[0,\infty),\quad a,b=1,2.\tag{1.1.46}$$

The result of this lemma will be used in the following reciprocity theorem:

Theorem 1.1.4. *Let us consider the systems of loads* (1.1.36) *and the solutions corresponding to these loads* (1.1.37)*. Then the following relation of reciprocity occurs:*

$$\begin{aligned}
&\int\limits_B[F_i^{(1)}*u_i^{(2)}+\omega^{(1)}*\varphi^{(2)}+N^{(1)}*\psi^{(2)}-\tfrac{1}{\rho T_0}\xi*\omega^{(1)}*\theta^{(2)}]\,dV\\
&+\int\limits_{\partial B}[\xi*(t_i^{(1)}*u_i^{(2)}+\lambda^{(1)}*\varphi^{(2)}+\omega^{(1)}*\psi^{(2)}-\tfrac{1}{\rho T_0}\Omega^{(1)}*\theta^{(2)})]\,dA\\
&=\int\limits_B[F_i^{(2)}*u_i^{(1)}+\omega^{(2)}*\varphi^{(1)}+N^{(2)}*\psi^{(1)}-\tfrac{1}{\rho T_0}\xi*\omega^{(2)}*\theta^{(1)}]\,dV\\
&+\int\limits_{\partial B}[\xi*(t_i^{(2)}*u_i^{(1)}+\lambda^{(2)}*\varphi^{(1)}+\omega^{(2)}*\psi^{(1)}-\tfrac{1}{\rho T_0}\Omega^{(2)}*\theta^{(1)})]\,dA,
\end{aligned}\tag{1.1.47}$$

where:

$$\begin{aligned}
\mathbf{F}_i^{(a)}&=\rho\xi*F_i^{(a)}+\rho u_i^{0(a)}+\rho\xi v_i^{0(a)},\\
\omega^{(a)}&=\rho\xi*\omega^{(a)}+\kappa_1\varphi_0^{(a)}+\kappa_1\xi\tilde{\varphi}_0^{(a)},\\
\mathbf{N}^{(a)}&=\rho\xi*N^{(a)}+\kappa_2\psi_0^{(a)}+\kappa_2\xi\tilde{\psi}_0^{(a)}.
\end{aligned}$$

Proof. In the commutativity relation (1.1.46) we perform the change of variables $\xi = s$ and $\zeta = \xi - s$:

$$\mathcal{F}_{ab}(s, \xi - s) = \mathcal{F}_{ba}(\xi - s, s). \tag{1.1.48}$$

We consider the symmetry relations (1.1.5) and we obtain:

$$\begin{aligned}
&\mathcal{F}_{ab}(s, \xi - s) = \\
&\quad = \int\limits_B [\rho F_i^{(a)}(s) u_i^{(b)}(\xi - s) + \rho\omega^{(a)}(s)\varphi^{(b)}(\xi - s) + \rho N^{(a)}(s)\psi^{(b)}(\xi - s) \\
&\qquad - \tfrac{1}{\rho T_0}\omega^{(a)}(s)\theta^{(b)}(\xi - s)]\, dV \\
&\quad - \int\limits_B [\rho \ddot{u}_i^{(a)}(s) u_i^{(b)}(\xi - s) + \kappa_1 \ddot{\varphi}^{(a)}(s)\varphi^{(b)}(\xi - s) + \kappa_2 \ddot{\psi}^{(a)}(s)\psi^{(b)}(\xi - s)]\, dV \\
&\qquad + \tfrac{1}{\rho T_0} \int\limits_B q_{*i}^{(a)}(s)\theta_{,i}^{(b)}(\xi - s)\, dV \\
&\quad + \int\limits_{\partial B} [t_i^{(a)}(s) u_i^{(b)}(\xi - s) + \lambda^{(a)}(s)\varphi^{(b)}(\xi - s) + \omega^{(a)}(s)\psi^{(b)}(\xi - s) \\
&\qquad - \tfrac{1}{\rho T_0}\Omega_*^{(a)}(s)\theta^{(b)}(\xi - s)]\, dA.
\end{aligned}$$

If we apply the integration on $[0, \xi]$ we notice that we have convolution products and taking into account (1.1.34) we obtain:

$$\begin{aligned}
\int\limits_0^\xi \mathcal{F}_{ab}(s, \xi - s)\, ds = \int\limits_B [\rho F_i^{(a)} * u_i^{(b)} + \rho\omega^{(a)} * \varphi^{(b)} + \rho N^{(a)} * \psi^{(b)} \\
- \tfrac{1}{\rho T_0}\omega^{(a)} * \theta^{(b)}]\, dV \\
- \int\limits_B [\rho \ddot{u}_i^{(a)} * u_i^{(b)} + \kappa_1 \ddot{\varphi}^{(a)} * \varphi^{(b)} + \kappa_2 \ddot{\psi}^{(a)} * \psi^{(b)}]\, dV \\
+ \tfrac{1}{\rho T_0} \int\limits_B (1 * q_i^{(a)} * \theta_{,i}^{(b)}) \\
+ \int\limits_{\partial B} [t_i^{(a)} * u_i^{(b)} + \lambda^{(a)} * \varphi^{(b)} + \omega^{(a)} * \psi^{(b)} - \tfrac{1}{\rho T_0} 1 * \Omega^{(a)} * \theta^{(b)}]\, dA.
\end{aligned} \tag{1.1.49}$$

Taking into account (1.1.49), the relation (1.1.48) leads to:

$$\begin{aligned}
\int\limits_B [\rho F_i^{(1)} * u_i^{(2)} + \rho\omega^{(1)} * \varphi^{(2)} + \rho N^{(1)} * \psi^{(2)} \\
- \tfrac{1}{\rho T_0}\omega^{(1)} * \theta^{(2)}]\, dV \\
- \int\limits_B [\rho \ddot{u}_i^{(1)} * u_i^{(2)} + \kappa_1 \ddot{\varphi}^{(1)} * \varphi^{(2)} + \kappa_2 \ddot{\psi}^{(1)} * \psi^{(2)}]\, dV \\
+ \tfrac{1}{\rho T_0} \int\limits_B (1 * q_i^{(1)} * \theta_{,i}^{(2)})\, dV \\
+ \int\limits_{\partial B} [t_i^{(1)} * u_i^{(2)} + \lambda^{(1)} * \varphi^{(2)} + \omega^{(1)} * \psi^{(2)} - \tfrac{1}{\rho T_0} 1 * \Omega^{(1)} * \theta^{(2)}]\, dA = \\
= \int\limits_B [\rho F_i^{(2)} * u_i^{(1)} + \rho\omega^{(2)} * \varphi^{(1)} + \rho N^{(2)} * \psi^{(1)} \\
- \tfrac{1}{\rho T_0}\omega^{(2)} * \theta^{(1)}]\, dV \\
- \int\limits_B [\rho \ddot{u}_i^{(2)} * u_i^{(1)} + \kappa_1 \ddot{\varphi}^{(2)} * \varphi^{(1)} + \kappa_2 \ddot{\psi}^{(2)} * \psi^{(1)}]\, dV \\
+ \tfrac{1}{\rho T_0} \int\limits_B (1 * q_i^{(2)} * \theta_{,i}^{(1)})\, dV \\
+ \int\limits_{\partial B} [t_i^{(2)} * u_i^{(1)} + \lambda^{(2)} * \varphi^{(1)} + \omega^{(2)} * \psi^{(1)} - \tfrac{1}{\rho T_0} 1 * \Omega^{(2)} * \theta^{(1)}]\, dA.
\end{aligned} \tag{1.1.50}$$

We consider the function $g(\xi)=\xi$ and we apply the product of convolution between $g(\xi)$ and the relation (1.1.50) which leads to obtaining the quantity:

$$\begin{aligned}\mathcal{M}=\int\limits_B[&\rho\xi*F_i^{(a)}*u_i^{(b)}+\rho\xi*\omega^{(a)}*\varphi^{(b)}+\rho\xi*N^{(a)}*\psi^{(b)}\\&-\tfrac{1}{\rho T_0}\xi*\omega^{(a)}*\theta^{(b)}]\,dV\\-\int\limits_B[&\rho\xi*\ddot{u}_i^{(a)}*u_i^{(b)}+\kappa_1\xi*\ddot{\varphi}^{(a)}*\varphi^{(b)}+\kappa_2\xi*\ddot{\psi}^{(a)}*\psi^{(b)}]\,dV\\&+\tfrac{1}{\rho T_0}\int\limits_B(\xi*1*q_i^{(a)}*\theta_{,i}^{(b)})\,dV\\+\int\limits_{\partial B}[&\xi*t_i^{(a)}*u_i^{(b)}+\xi*\lambda^{(a)}*\varphi^{(b)}+\xi*\omega^{(a)}*\psi^{(b)}-\\&\tfrac{1}{\rho T_0}\xi*1*\Omega^{(a)}*\theta^{(b)}]\,dA.\end{aligned}$$

The convolution product is:

$$(f*g)(\xi)=\int\limits_0^{\xi}f(\xi)g(\xi-\zeta)\,d\zeta,$$

therefore we may write the following calculus:

$$\begin{aligned}\xi*\ddot{g}=\int\limits_0^{\xi}\zeta\ddot{g}(\xi-\zeta)\,d\zeta&=-\zeta\dot{g}(\xi-\zeta)|_0^{\xi}+\int\limits_0^{\xi}g'(\xi-\zeta)\,d\zeta-\xi\dot{g}(0)-g(\xi-\zeta)|_0^{\xi}\\&=-\xi\dot{g}(0)-g(0)+g(\xi).\end{aligned}$$

Based on the above demonstration we conclude that:

$$\begin{aligned}\xi*\ddot{u}_i^{(a)}=u_i^{(a)}-u_i^{(a)}(0)-\xi\dot{u}_i^{(a)}(0)&=u_i^{(a)}-u_i^{0(a)}-\xi v_i^{0(a)},\\\xi*\ddot{\varphi}^{(a)}&=\varphi^{(a)}-\varphi_0^{(a)}-\xi\tilde{\varphi}_0^{(a)},\\\xi*\ddot{\psi}^{(a)}&=\psi^{(a)}-\psi_0^{(a)}-\xi\tilde{\psi}_0^{(a)}.\end{aligned}$$

Replacing in (1.1.50) the reciprocity relation (1.1.47) is obtained:

$$\begin{aligned}\int\limits_B[&\rho\xi*F_i^{(1)}*u_i^{(2)}+\rho\xi*\omega^{(1)}*\varphi^{(2)}+\rho\xi*N^{(1)}*\psi^{(2)}-\tfrac{1}{\rho T_0}\xi*\omega^{(1)}*\theta^{(2)}\\&-\rho u_i^{(1)}*u_i^{(2)}+\rho u_i^{0(1)}*u_i^{(2)}+\rho\xi v_i^{0(1)}*u_i^{(2)}\\&-\kappa_1\varphi^{(1)}*\varphi^{(2)}+\kappa_1\varphi_0^{(1)}*\varphi^{(2)}+\kappa_1\xi\tilde{\varphi}_0^{(1)}*\varphi^{(2)}\\&-\kappa_2\psi^{(1)}*\psi^{(2)}+\kappa_2\psi_0^{(1)}*\psi^{(2)}+\kappa_2\xi\tilde{\psi}_0^{(1)}*\psi^{(2)}+\tfrac{1}{\rho T_0}\xi*q_i^{(1)}*\theta_{,i}^{(2)}]\,dV\\&+\int\limits_{\partial B}\xi*[t_i^{(1)}*u_i^{(2)}+\lambda^{(1)}*\varphi^{(2)}+\omega^{(1)}*\psi^{(2)}-\tfrac{1}{\rho T_0}\Omega^{(1)}*\theta^{(2)}]\,dA=\\=\int\limits_B[&\rho\xi*F_i^{(2)}*u_i^{(1)}+\rho\xi*\omega^{(2)}*\varphi^{(1)}+\rho\xi*N^{(2)}*\psi^{(1)}-\tfrac{1}{\rho T_0}\xi*\omega^{(2)}*\theta^{(1)}\\&-\rho u_i^{(2)}*u_i^{(1)}+\rho u_i^{0(2)}*u_i^{(1)}+\rho\xi v_i^{0(2)}*u_i^{(1)}\\&-\kappa_1\varphi^{(2)}*\varphi^{(1)}+\kappa_1\varphi_0^{(2)}*\varphi^{(1)}+\kappa_1\xi\tilde{\varphi}_0^{(2)}*\varphi^{(1)}\\&-\kappa_2\psi^{(2)}*\psi^{(1)}+\kappa_2\psi_0^{(2)}*\psi^{(1)}+\kappa_2\xi\tilde{\psi}_0^{(2)}*\psi^{(1)}+\tfrac{1}{\rho T_0}\xi*q_i^{(2)}*\theta_{,i}^{(1)}]\,dV\\&+\int\limits_{\partial B}\xi*[t_i^{(2)}*u_i^{(1)}+\lambda^{(2)}*\varphi^{(1)}+\omega^{(2)}*\psi^{(1)}-\tfrac{1}{\rho T_0}\Omega^{(2)}*\theta^{(1)}]\,dA,\end{aligned}$$

which is equivalent to:

$$\begin{aligned}
&\int_B [(\rho\xi * F_i^{(1)} + \rho u_i^{0(1)} + \rho\xi v_i^{0(1)}) * u_i^{(2)} + (\rho\xi * \omega^{(1)} + \kappa_1\varphi_0^{(1)} + \kappa_1\xi\tilde{\varphi}_0^{(1)}) * \varphi^{(2)} \\
&\qquad + (\rho\xi * N^{(1)} + \kappa_2\psi_0^{(1)} + \kappa_2\xi\tilde{\psi}_0^{(1)}) * \psi^{(2)} - \tfrac{1}{\rho T_0}\xi * \omega^{(1)} * \theta^{(2)}]\, dV \\
&\qquad + \int_{\partial B} \xi * [t_i^{(1)} * u_i^{(2)} + \lambda^{(1)} * \varphi^{(2)} + \omega^{(1)} * \psi^{(2)} - \tfrac{1}{\rho T_0}\Omega^{(1)} * \theta^{(2)}]\, dA = \\
&= \int_B [(\rho\xi * F_i^{(2)} + \rho u_i^{0(2)} + \rho\xi v_i^{0(2)}) * u_i^{(1)} + (\rho\xi * \omega^{(2)} + \kappa_1\varphi_0^{(2)} + \kappa_1 t\tilde{\varphi}_0^{(2)}) * \varphi^{(1)} \\
&\qquad + (\rho\xi * N^{(2)} + \kappa_2\psi_0^{(2)} + \kappa_2\xi\tilde{\psi}_0^{(2)}) * \psi^{(1)} - \tfrac{1}{\rho T_0}\xi * \omega^{(2)} * \theta^{(1)}]\, dV \\
&\qquad + \int_{\partial B} \xi * [t_i^{(2)} * u_i^{(1)} + \lambda^{(2)} * \varphi^{(1)} + \omega^{(2)} * \psi^{(1)} - \tfrac{1}{\rho T_0}\Omega^{(2)} * \theta^{(1)}]\, dA.
\end{aligned}$$

Hence, the result of the theorem Th[1.1.4] is obtained. □

We will further consider $a = b = 1$. In relation (1.1.46) we will make the variable changes $\xi \to \xi + \zeta$, $\zeta \to \xi - \zeta$, which leads to:

$$F_{11}(\xi + \zeta, \xi - \zeta) = F_{11}(\xi - \zeta, \xi + \zeta). \tag{1.1.51}$$

Integrating the left member of the function from (1.1.51) on the interval $[0, \xi]$:

$$\begin{aligned}
&\int_0^\xi F_{11}(\xi + \zeta, \xi - \zeta)\, d\zeta = \\
&= \int_0^\xi \int_B [\rho F_i(\xi + \zeta) u_i(\xi - \zeta) + \rho M(\xi + \zeta)\varphi(\xi - \zeta) + \rho N(\xi + \zeta)\psi(\xi - \zeta) \\
&\qquad - \tfrac{1}{\rho T_0}\omega(\xi + \zeta)\theta(\xi - \zeta)]\, dV\, d\zeta \\
&- \int_0^\xi \int_B [\rho\ddot{u}_i(\xi + \zeta) u_i(\xi - \zeta) + \kappa_1\ddot{\varphi}(\xi + \zeta)\varphi(\xi - \zeta) + \kappa_2\ddot{\psi}(\xi + \zeta)\psi(\xi - \zeta)]\, dV\, d\zeta \\
&\qquad + \tfrac{1}{\rho T_0}\int_0^\xi \int_B q_{*i}(\xi + \zeta)\theta_{,j}(\xi - \zeta)\, dV\, d\zeta \\
&\qquad + \int_0^\xi \int_{\partial B} [t_i(\xi + \zeta) u_i(\xi - \zeta) + \lambda(\xi + \zeta)\varphi(\xi - \zeta) + m(\xi + \zeta)\psi(\xi - \zeta) \\
&\qquad - \tfrac{1}{\rho T_0}\Omega_*(\xi + \zeta)\theta(\xi - \zeta)]\, dA\, d\zeta.
\end{aligned} \tag{1.1.52}$$

Using the integration by parts we obtain:

$$\begin{aligned}
&\int_0^\xi \ddot{u}_i(\xi + \zeta) u_i(\xi - \zeta) d\zeta = \\
&= u_i(\xi - \zeta)\dot{u}_i(\xi + \zeta)|_0^\xi + \int_0^\xi \dot{u}_i(\xi + \zeta)\dot{u}_i(\xi - \zeta) d\zeta = \\
&= u_i(0)\dot{u}_i(2\xi) - u_i(\xi)\dot{u}_i(\xi) + \int_0^\xi \dot{u}_i(\xi + \zeta)\dot{u}_i(\xi - \zeta) d\zeta.
\end{aligned}$$

Analogically:

$$\int_0^\xi \ddot{\varphi}(\xi+\zeta)\varphi(\xi-\zeta)d\zeta = \varphi(0)\dot{\varphi}(2\xi) - \varphi(\xi)\dot{\varphi}(\xi) + \int_0^\xi \dot{\varphi}(\xi+\zeta)\dot{\varphi}(\xi-\zeta)d\zeta,$$
$$\int_0^\xi \ddot{\psi}(\xi+\zeta)\psi(\xi-\zeta)d\zeta = \psi(0)\dot{\psi}(2\xi) - \psi(\xi)\dot{\psi}(\xi) + \int_0^\xi \dot{\psi}(\xi+\zeta)\dot{\psi}(\xi-\zeta)d\zeta.$$

Consequently it is obtained the following relation:

$$\begin{aligned}
&\int_0^\xi F_{11}(\xi+\zeta,\xi-\zeta)\,d\zeta = \\
&= \int_0^\xi \int_B [\rho F_i(\xi+\zeta)u_i(\xi-\zeta) + \rho M(\xi+\zeta)\varphi(\xi-\zeta) + \rho N(\xi+\zeta)\psi(\xi-\zeta) \\
&\qquad -\tfrac{1}{\rho T_0}\omega(\xi+\zeta)\theta(\xi-\zeta)]\,dV\,d\zeta \\
&\quad + \int_0^\xi \int_{\partial B} [t_i(\xi+\zeta)u_i(\xi-\zeta) + \lambda(\xi+\zeta)\varphi(\xi-\zeta) + m(\xi+\zeta)\psi(\xi-\zeta) \\
&\qquad -\tfrac{1}{\rho T_0}\Omega_*(\xi+\zeta)\theta(\xi-\zeta)]\,dA\,d\zeta \\
&\qquad -\tfrac{1}{\rho T_0}\int_0^\xi \int_B K_{ij}\theta_{*,i}(\xi+\zeta)\theta_{,j}(\xi-\zeta)\,dV\,d\zeta \\
&\quad -\rho\int_B (u_i(0)\dot{u}_i(2\xi) - u_i(\xi)\dot{u}_i(\xi) + \int_0^\xi \dot{u}_i(\xi+\zeta)\dot{u}_i(\xi-\zeta)d\zeta)\,dV \\
&\quad -\kappa_1\int_B (\varphi(0)\dot{\varphi}(2\xi) - \varphi(\xi)\dot{\varphi}(\xi) + \int_0^\xi \dot{\varphi}(\xi+\zeta)\dot{\varphi}(\xi-\zeta)d\zeta)\,dV \\
&\quad -\kappa_2\int_B (\psi(0)\dot{\psi}(2\xi) - \psi(\xi)\dot{\psi}(\xi) + \int_0^\xi \dot{\psi}(\xi+\zeta)\dot{\psi}(\xi-\zeta)d\zeta)\,dV.
\end{aligned} \tag{1.1.53}$$

We proceed analogously for the right member from (1.1.51) integrating the function on the interval $[0,\xi]$:

$$\begin{aligned}
&\int_0^\xi F_{11}(\xi-\zeta,\xi+\zeta)\,d\zeta = \\
&= \int_0^\xi \int_B [\rho F_i(\xi-\zeta)u_i(\xi+\zeta) + \rho M(\xi-\zeta)\varphi(\xi+\zeta) + \rho N(\xi-\zeta)\psi(\xi+\zeta) \\
&\qquad -\tfrac{1}{\rho T_0}\omega(\xi-\zeta)\theta(\xi+\zeta)]\,dV\,d\zeta \\
&\quad -\int_0^\xi \int_B [\rho\ddot{u}_i(\xi-\zeta)u_i(\xi+\zeta) + \kappa_1\ddot{\varphi}(\xi-\zeta)\varphi(\xi+\zeta) + \kappa_2\ddot{\psi}(\xi-\zeta)\psi(\xi+\zeta)]\,dV\,d\zeta \\
&\qquad +\tfrac{1}{\rho T_0}\int_0^\xi \int_B q_{*i}(\xi-\zeta)\theta_{,j}(\xi+\zeta)\,dV\,d\zeta \\
&\quad + \int_0^\xi \int_{\partial B} [t_i(\xi-\zeta)u_i(\xi+\zeta) + \lambda(\xi-\zeta)\varphi(\xi+\zeta) + m(\xi-\zeta)\psi(\xi+\zeta) \\
&\qquad -\tfrac{1}{\rho T_0}\Omega_*(\xi-\zeta)\theta(\xi+\zeta)]\,dA\,d\zeta.
\end{aligned} \tag{1.1.54}$$

We perform integration by parts:

$$\begin{aligned}\int_0^\xi \ddot{u}_i(\xi-\zeta)u_i(\xi+\zeta)d\zeta = \\ = -u_i(\xi+\zeta)\dot{u}_i(\xi-\zeta)|_0^\xi + \int_0^\xi \dot{u}_i(\xi+\zeta)\dot{u}_i(\xi-\zeta)d\zeta = \\ = -u_i(2\xi)\dot{u}_i(0) + u_i(\xi)\dot{u}_i(\xi) + \int_0^\xi \dot{u}_i(\xi+\zeta)\dot{u}_i(\xi-\zeta)d\zeta.\end{aligned}$$

Analogically:

$$\begin{aligned}\int_0^\xi \ddot{\varphi}(\xi-\zeta)\varphi(\xi+\zeta)d\zeta = -\varphi(2\xi)\dot{\varphi}(0) + \varphi(\xi)\dot{\varphi}(\xi) + \int_0^\xi \dot{\varphi}(\xi+\zeta)\dot{\varphi}(\xi-\zeta)d\zeta, \\ \int_0^\xi \ddot{\psi}(\xi-\zeta)\psi(\xi+\zeta)d\zeta = -\psi(2\xi)\dot{\psi}(0) + \psi(\xi)\dot{\psi}(\xi) + \int_0^\xi \dot{\psi}(\xi+\zeta)\dot{\psi}(\xi-\zeta)d\zeta.\end{aligned}$$

Thus will be written:

$$\begin{aligned}\int_0^\xi F_{11}(\xi-\zeta,\xi+\zeta)\,d\zeta = \\ = \int_0^\xi \int_B [\rho F_i(\xi-\zeta)u_i(\xi+\zeta) + \rho M(\xi-\zeta)\varphi(\xi+\zeta) + \rho N(\xi-\zeta)\psi(\xi+\zeta) \\ -\tfrac{1}{\rho T_0}\omega(\xi-\zeta)\theta(\xi+\zeta)]\,dV\,d\zeta \\ -\rho\int_B(-u_i(2\xi)\dot{u}_i(0) + u_i(\xi)\dot{u}_i(\xi) + \int_0^\xi \dot{u}_i(\xi+\zeta)\dot{u}_i(\xi-\zeta)d\zeta)\,dV \\ -\kappa_1\int_B(-\varphi(2\xi)\dot{\varphi}(0) + \varphi(\xi)\dot{\varphi}(\xi) + \int_0^\xi \dot{\varphi}(\xi+\zeta)\dot{\varphi}(\xi-\zeta)d\zeta)\,dV \\ -\kappa_2\int_B(-\psi(2\xi)\dot{\psi}(0) + \psi(\xi)\dot{\psi}(\xi) + \int_0^\xi \dot{\psi}(\xi+\zeta)\dot{\psi}(\xi-\zeta)d\zeta)\,dV \\ -\tfrac{1}{\rho T_0}\int_0^\xi \int_B K_{ij}\theta_{*,i}(\xi-\zeta)\theta_{,j}(\xi+\zeta)\,dV\,d\zeta \\ +\int_0^\xi \int_{\partial B}[t_i(\xi-\zeta)u_i(\xi+\zeta) + \lambda(\xi-\zeta)\varphi(\xi+\zeta) + m(\xi-\zeta)\psi(\xi+\zeta) \\ -\tfrac{1}{\rho T_0}\Omega_*(\xi-\zeta)\theta(\xi+\zeta)]\,dA\,d\zeta.\end{aligned} \tag{1.1.55}$$

Based on the relations (1.1.53) and (1.1.55) the equality (1.1.51) becomes:

$$\begin{aligned}
&\int_0^\xi \int_B [\rho F_i(\xi+\zeta)u_i(\xi-\zeta) + \rho M(\xi+\zeta)\varphi(\xi-\zeta) + \rho N(\xi+\zeta)\psi(\xi-\zeta) \\
&\qquad -\tfrac{1}{\rho T_0}\omega(\xi+\zeta)\theta(\xi-\zeta)]\, dV\, d\zeta \\
&+\int_0^\xi \int_{\partial B} [t_i(\xi+\zeta)u_i(\xi-\zeta) + \lambda(\xi+\zeta)\varphi(\xi-\zeta) + m(\xi+\zeta)\psi(\xi-\zeta) \\
&\qquad -\tfrac{1}{\rho T_0}\Omega_*(\xi+\zeta)\theta(\xi-\zeta)]\, dA\, d\zeta \\
&-\tfrac{1}{\rho T_0}\int_0^\xi \int_B K_{ij}\theta_{*,i}(\xi+\zeta)\theta_{,j}(\xi-\zeta)\, dV\, d\zeta \\
&-\rho\int_B u_i(0)\dot{u}_i(2\xi)\, dV + \rho\int_B u_i(\xi)\dot{u}_i(\xi)\, dV - \rho\int_B (\int_0^\xi \dot{u}_i(\xi+\zeta)\dot{u}_i(\xi-\zeta)d\zeta)\, dV \\
&-\kappa_1\int_B \varphi(0)\dot{\varphi}(2\xi)\, dV + \kappa_1\int_B \varphi(\xi)\dot{\varphi}(\xi)\, dV - \kappa_1\int_B (\int_0^\xi \dot{\varphi}(\xi+\zeta)\dot{\varphi}(\xi-\zeta)d\zeta)\, dV \\
&-\kappa_2\int_B \psi(0)\dot{\psi}(2\xi)\, dV + \kappa_2\int_B \psi(\xi)\dot{\psi}(\xi)\, dV - \kappa_2\int_B (\int_0^\xi \dot{\psi}(\xi+\zeta)\dot{\psi}(\xi-\zeta)d\zeta)\, dV = \\
&= \int_0^\xi \int_B [\rho F_i(\xi-\zeta)u_i(\xi+\zeta) + \rho M(\xi-\zeta)\varphi(\xi+\zeta) + \rho N(\xi-\zeta)\psi(\xi+\zeta) \\
&\qquad -\tfrac{1}{\rho T_0}\omega(\xi-\zeta)\theta(\xi+\zeta)]\, dV\, d\zeta \\
&+\int_0^\xi \int_{\partial B} [t_i(\xi-\zeta)u_i(\xi+\zeta) + \lambda(\xi-\zeta)\varphi(\xi+\zeta) + m(\xi-\zeta)\psi(\xi+\zeta) \\
&\qquad -\tfrac{1}{\rho T_0}\Omega_*(\xi-\zeta)\theta(\xi+\zeta)]\, dA\, d\zeta \\
&-\tfrac{1}{\rho T_0}\int_0^\xi \int_B K_{ij}\theta_{*,i}(\xi-\zeta)\theta_{,j}(\xi+\zeta)\, dV\, d\zeta \\
&+\rho\int_B u_i(2\xi)\dot{u}_i(0)\, dV - \rho\int_B u_i(\xi)\dot{u}_i(\xi)\, dV - \rho\int_B (\int_0^\xi \dot{u}_i(\xi+\zeta)\dot{u}_i(\xi-\zeta)d\zeta)\, dV \\
&+\kappa_1\int_B \varphi(2\xi)\dot{\varphi}(0)\, dV - \kappa_1\int_B \varphi(\xi)\dot{\varphi}(\xi)\, dV - \kappa_1\int_B (\int_0^\xi \dot{\varphi}(\xi+\zeta)\dot{\varphi}(\xi-\zeta)d\zeta)\, dV \\
&+\kappa_2\int_B \psi(2\xi)\dot{\psi}(0)\, dV - \kappa_2\int_B \psi(\xi)\dot{\psi}(\xi)\, dV - \kappa_2\int_B (\int_0^\xi \dot{\psi}(\xi+\zeta)\dot{\psi}(\xi-\zeta)d\zeta)\, dV,
\end{aligned}$$

Hence, we may write the following relation:

$$
\begin{aligned}
2\rho\int\limits_B u_i(\xi)\dot{u}_i(\xi)\,dV + 2\kappa_1\int\limits_B \varphi(\xi)\dot{\varphi}(\xi)\,dV + 2\kappa_2\int\limits_B \psi(\xi)\dot{\psi}(\xi)\,dV \\
-\rho\int\limits_B (u_i(2\xi)\dot{u}_i(0) + \dot{u}_i(2\xi)u_i(0))\,dV \\
-\kappa_1\int\limits_B (\varphi(2\xi)\dot{\varphi}(0) + \dot{\varphi}(2\xi)\varphi(0))\,dV \\
-\kappa_2\int\limits_B (\psi(2\xi)\dot{\psi}(0) + \dot{\psi}(2\xi)\psi(0))\,dV = \\
= \int\limits_0^\xi\int\limits_B [\rho F_i(\xi-\zeta)u_i(\xi+\zeta) + \lambda(\xi-\zeta)\varphi(\xi+\zeta) + m(\xi-\zeta)\psi(\xi+\zeta) \\
-\tfrac{1}{\rho T_0}\omega(\xi-\zeta)\theta(\xi+\zeta)]\,dV\,d\zeta \\
-\int\limits_0^\xi\int\limits_B [\rho F_i(\xi+\zeta)u_i(\xi-\zeta) + \lambda(\xi+\zeta)\varphi(\xi-\zeta) + m(\xi+\zeta)\psi(\xi-\zeta) \\
-\tfrac{1}{\rho T_0}\omega(\xi+\zeta)\theta(\xi-\zeta)]\,dV\,d\zeta \\
+\int\limits_0^\xi\int\limits_{\partial B} [t_i(\xi-\zeta)u_i(\xi+\zeta) + \lambda(\xi-\zeta)\varphi(\xi+\zeta) + m(\xi-\zeta)\psi(\xi+\zeta) \\
-\tfrac{1}{\rho T_0}\Omega_*(\xi-\zeta)\theta(\xi+\zeta)]\,dA\,d\zeta \\
-\int\limits_0^\xi\int\limits_{\partial B} [t_i(\xi+\zeta)u_i(\xi-\zeta) + \lambda(\xi+\zeta)\varphi(\xi-\zeta) + m(\xi+\zeta)\psi(\xi-\zeta) \\
-\tfrac{1}{\rho T_0}\Omega_*(\xi+\zeta)\theta(\xi-\zeta)]\,dA\,d\zeta \\
+\tfrac{1}{\rho T_0}\int\limits_0^\xi\int\limits_B K_{ij}[\theta_{*,i}(\xi+\zeta)\theta_{,j}(\xi-\zeta) - \theta_{*,i}(\xi-\zeta)\theta_{,j}(\xi+\zeta)]\,dV\,d\zeta.
\end{aligned}
\tag{1.1.56}
$$

We notice that:

$$
\frac{d}{d\zeta}[\theta_{*,i}(\xi+\zeta)\theta_{*,j}(\xi-\zeta)] = \theta_{,i}(\xi+\zeta)\theta_{*,j}(\xi-\zeta) - \theta_{*,i}(\xi+\zeta)\theta_{,j}(\xi-\zeta),
$$

therefore the last term in (1.1.56) can be written:

$$
\begin{aligned}
\tfrac{1}{\rho T_0}\int\limits_0^\xi\int\limits_B K_{ij}[\theta_{*,i}(\xi+\zeta)\theta_{,j}(\xi-\zeta) - \theta_{*,i}(\xi-\zeta)\theta_{,j}(\xi+\zeta)]\,dV\,d\zeta = \\
= -\tfrac{1}{\rho T_0}\int\limits_0^\xi\int\limits_B K_{ij}[\theta_{,j}(\xi+\zeta)\theta_{*,i}(\xi-\zeta) - \theta_{*,i}(\xi+\zeta)\theta_{,j}(\xi-\zeta)]\,dV\,d\zeta = \\
= -\tfrac{1}{\rho T_0}\tfrac{d}{d\zeta}[\int\limits_0^\xi\int\limits_B K_{ij}\theta_{*,i}(\xi+\zeta)\theta_{*,j}(\xi-\zeta)\,dV\,d\zeta].
\end{aligned}
$$

In conclusion we can state the following lemma which represents a useful auxiliary result in deducing a new result of uniqueness for thermoelastic media with double porosity structure.

Lemma 1.1.2. *Based on the above, the following differential relationship occurs:*

$$\begin{aligned}
&\tfrac{d}{d\zeta}[\int\limits_B(\rho u_i(\xi)u_i(\xi)+\kappa_1\varphi(\xi)\varphi(\xi)+\kappa_2\psi(\xi)\psi(\xi))\,dV\\
&\qquad+\tfrac{1}{\rho T_0}\int\limits_0^\xi\int\limits_B K_{ij}\theta_{*,i}(\xi)\theta_{*,j}(\xi)\,dV\,d\zeta]\\
&\qquad-\int\limits_B[\rho(u_i(2\xi)\dot{u}_i(0)+\dot{u}_i(2\xi)u_i(0))+\kappa_1(\varphi(2\xi)\dot{\varphi}(0)\\
&\qquad+\dot{\varphi}(2\xi)\varphi(0))+\kappa_2(\psi(2\xi)\dot{\psi}(0)+\dot{\psi}(2\xi)\psi(0))]\,dV=\\
&=\int\limits_0^\xi\int\limits_B[\rho F_i(\xi-\zeta)u_i(\xi+\zeta)+\lambda(\xi-\zeta)\varphi(\xi+\zeta)+m(\xi-\zeta)\psi(\xi+\zeta)\\
&\qquad-\tfrac{1}{\rho T_0}\omega(\xi-\zeta)\theta(\xi+\zeta)]\,dV\,d\zeta\\
&-\int\limits_0^\xi\int\limits_B[\rho F_i(\xi+\zeta)u_i(\xi-\zeta)+\lambda(\xi+\zeta)\varphi(\xi-\zeta)+m(\xi+\zeta)\psi(\xi-\zeta)\\
&\qquad-\tfrac{1}{\rho T_0}\omega(\xi+\zeta)\theta(\xi-\zeta)]\,dV\,d\zeta\\
&+\int\limits_0^\xi\int\limits_{\partial B}[t_i(\xi-\zeta)u_i(\xi+\zeta)+\lambda(\xi-\zeta)\varphi(\xi+\zeta)+m(\xi-\zeta)\psi(\xi+\zeta)\\
&\qquad-\tfrac{1}{\rho T_0}\Omega_*(\xi-\zeta)\theta(\xi+\zeta)]\,dA\,d\zeta\\
&-\int\limits_0^\xi\int\limits_{\partial B}[t_i(\xi+\zeta)u_i(\xi-\zeta)+\lambda(\xi+\zeta)\varphi(\xi-\zeta)+m(\xi+\zeta)\psi(\xi-\zeta)\\
&\qquad-\tfrac{1}{\rho T_0}\Omega_*(\xi+\zeta)\theta(\xi-\zeta)]\,dA\,d\zeta.
\end{aligned}\tag{1.1.57}$$

Theorem 1.1.5. *If the thermal conductivity tensor K_{ij} is positive definite and the assumptions* (1.1.1) - (1.1.5) *are satisfied then the mixed problem consisting in* (1.1.4), (1.1.7), (1.1.8) *admits a unique solution.*

Proof. We will assume by contradiction that our mixed problem consisting in (1.1.4), (1.1.7), (1.1.8) admits two distinct solutions: $u_i^{(k)}$, $\varphi^{(k)}$, $\psi^{(k)}$, $\theta^{(k)}$, $t_{ij}^{(k)}$, $\sigma_i^{(k)}$, $\tau_i^{(k)}$, $p^{(k)}$, $r^{(k)}$, $\eta^{(k)}$, $q_i^{(k)}$, $k=1,2$. The difference between the two solutions will be marked as follows: $\hat{u}_i$, $\hat{\varphi}$, $\hat{\psi}$, $\hat{\theta}$, $\hat{t}_{ij}$, $\hat{\sigma}_i$, $\hat{\tau}_i$, $\hat{p}$, $\hat{r}$, $\hat{\eta}$, $\hat{q}_i$. Due to the linearity, the difference between the two solutions is also a solution of the problem corresponding to the null initial conditions and the null boundary conditions.

Given that the boundary conditions are null then relation (1.1.57) leads us to:

$$\begin{aligned}
&\tfrac{d}{d\xi}[\int\limits_B(\rho\hat{u}_i(\xi)\hat{u}_i(\xi)+\kappa_1\hat{\varphi}(\xi)\hat{\varphi}(\xi)+\kappa_2\hat{\psi}(\xi)\hat{\psi}(\xi))\,dV\\
&\qquad+\tfrac{1}{\rho T_0}\int\limits_0^\xi\int\limits_B K_{ij}\hat{\theta}_{*,i}(\xi)\hat{\theta}_{*,j}(\xi)\,dV\,d\zeta]=0.
\end{aligned}\tag{1.1.58}$$

From (1.1.58) we deduce:

$$\hat{u}_i(x,\xi)=0,\quad \hat{\varphi}(x,\xi)=0,\quad \hat{\psi}(x,\xi)=0,\quad \hat{\theta}_{*,i}(x,\xi)=0,\quad \forall(x,\xi)\in B\times[0,\infty).$$

If $\hat{\theta}_{*,i}(x,\xi)=0$, then $\hat{q}_{*i}(x,\xi)=0$, $\forall(x,\xi)\in B\times[0,\infty)$.

We consider (1.1.2) and we have $\hat{\dot{\eta}}(x,\xi) = 0$. Due to the null initial conditions we have $\hat{\eta}(x,\xi) = 0$ and the constitutive equations lead to the fact that $\hat{\theta}(x,\xi) = 0$, $\forall (x,\xi) \in B \times [0,\infty)$. □

1.2 Moore–Gibson–Thompson thermoelasticity in the context of double porous materials

In the last years the Moore – Gibson – Thompson (MGT) equations has drawn the attention of many researchers. Although initially, the MGT equation modeled the physical phenomena from fluid mechanics, [Thompson(1972)], in the last years it was approached under the thermoelasticity theory from the MGT perspective, where the heat transfer is governed by an integro-differential equation, [Conti(2020)]. The MGT thermoelasticity with two temperatures is studied in [Quintanilla(2020)]. Many scholars approached this theory from a theoretical point of view [Dell'Oro(2016)], [Dell'Oro(2017)], [LasieckaI(2015)], [Pellicer(2019)] and, also from a practical point of view [Pellicer(2019)], [Kaltenbacher(2011)], [Marchand(2012)], [Quintanilla(2019)], [Magana(2009)]. The domain of influence under the MGT thermoelasticity theory was studied recently, [Jangid(2021)], [Marin(2020a)]. Some papers deals with the linear elasticity theory for bodies with a dipolar structure [Marin(2020c)], [Marin(2020d)]. In this section it is considered the MGT theory in the context of materials with double porosity.

Therefore it is defined the mixt problem for MGT thermoelasticity with double porosity structure. The main obtained results are based on a reciprocity theorem for the anisotropic thermoelastic materials with double porosity that leads us in the determining of the uniqueness theorems for the solution of mixed problems for the materials with double porosity. The reciprocity theorem is a Betti type result that has the main goal to establish the connection between the external action systems and their thermoelastic states. In order to obtain the uniqueness results it was introduced a new form of energy equation.

1.2.1 Basic equations

The motion equations of a double porous material and the balance equations are given in (1.1.1).

The differential Moore-Gibson-Thompson (MGT) equation for thermoealsticity was obtained in [Quintanilla(2019)] for the relaxation parameter $\gamma > 0$ in the context of Maxwell and Cattaneo heat conduction:

$$\gamma \cdot c(x)\frac{d^3\theta}{dt^3} + c(x)\frac{d^2\theta}{dt^2} = \left(K_{ij}(x)\theta_{,i} + K^*_{ij}(x)\theta_{,i}\right)_{,j} \tag{1.2.1}$$

where K_{ij} is the conductivity rate tensor, θ is the temperature and c is the thermal capacity.

In order to have a mixed-initial boundary value problem, we have the initial conditions:

$$\theta(x,0)=\theta_0(x);\ \frac{d\theta}{dt}(x,0)=\theta_1(x);\ \frac{d^2\theta}{dt^2}(x,0)=\theta_2(x) \tag{1.2.2}$$

for all $x\in B$, where B is the three dimensional domain that is considered smooth enough in order to apply the divergence theorem.

The Dirichlet Boundary conditions are:

$$\theta(x,t)=0,(\forall)x\in\partial B,t>0 \tag{1.2.3}$$

Further, we consider the following assumptions:
a) the thermal capacity $c(x)$ is a positive function such as there is a positive constant $c_0>0:c(x)\geq c_0>0$
b) for every vector ζ_i there is a positive constant k^* such as:

$$K^*_{ij}\zeta_i\zeta_j\geq k^*\zeta_i\zeta_i \tag{1.2.a1}$$

c) for every vector ζ_i there is a positive constant $\tilde{k}$ such as

$$h_{ij}\zeta_i\zeta_j\geq \tilde{k}\zeta_i\zeta_i \tag{1.2.a2}$$

where $h_{ij}(x)=K_{ij}(x)-\gamma K^*_{ij}(x)$. d) for every vectr ζ_i there is a positive constant k^0 such as:

$$K_{ij}\zeta_i\zeta_j\geq k^0\zeta_i\zeta_i \tag{1.2.a3}$$

The deformations of the bodies with double porosity are given by the following variables: $u_i(x,t),\phi(x,t),\psi(x,t),\theta(x,t),(\forall)(x,t)\in B\times[0,\infty)$.

The energy function has the following quadratic form in the context of the linear thermoelasticity for materials with double porosity structure:

$$\begin{aligned}\mathcal{E}=&\frac{1}{2}C_{ijkl}u_{k,l}u_{i,j}+B_{ij}\phi u_{i,j}+D_{ij}\psi u_{i,j}+\\&+\frac{1}{2}\alpha_{ij}\phi_{,i}\phi_{,j}+b_{ij}\phi_{,i}\psi_{,j}+\frac{1}{2}\gamma_{ij}\psi_{,i}\psi_{,j}+\frac{1}{2}\alpha_1\phi^2+\\&+\alpha_3\phi\psi+\frac{1}{2}\alpha_2\psi^2-\frac{1}{2}c(\gamma\ddot{\theta}+\dot{\theta})^2+\frac{1}{2}K_{ij}\theta_{,i}\theta_{,j}-\\&-(\beta_{ij}u_{i,j}+a_1\phi+a_2\psi)(\gamma\ddot{\theta}+\dot{\theta})\end{aligned} \tag{1.2.4}$$

The constitutive ecuations for the bodies with double porosity in the context of

theMoore - Gibson - Thompson linear theromeasticity theory are:

$$\begin{aligned} t_{ij} =& C_{ijkl}u_{k,l} + B_{ij}\phi + D_{ij}\psi - \beta_{ij}(\gamma\ddot{\theta} + \dot{\theta}) \\ \sigma_{ij} =& \alpha_{ij}\phi_{,j} + b_{ij}\psi_{,j} \\ \tau_i =& b_{ij}\phi_{,j} + \gamma_{ij}\psi_{,j} \\ p =& - B_{ij}u_{i,j} - \alpha_1\phi - \alpha_3\psi + a_1(\gamma\ddot{\theta} + \dot{\theta}) \\ r =& - D_{ij}u_{i,j} - \alpha_3\phi - \alpha_2\psi + a_2(\gamma\ddot{\theta} + \dot{\theta}) \\ \eta =& \beta_{ij}u_{i,j} + a_1\phi + a_2\psi + c(\gamma\ddot{\theta} + \dot{\theta}) \\ q_i =& K_{ij}\theta_{,j} \end{aligned} \tag{1.2.5}$$

The relations (1.2.5) are obtained based on the quadratic form of internal energy (1.2.4) i.e.:

$$t_{ij} = \frac{\partial \mathcal{E}}{\partial u_{i,j}};\ \sigma_{ij} = \frac{\partial \mathcal{E}}{\partial \phi_{,i}};\ \tau_i = \frac{\partial \mathcal{E}}{\partial \psi_{,i}};\ \xi = -\frac{\partial \mathcal{E}}{\partial \phi};\ \zeta = -\frac{\partial \mathcal{E}}{\partial \psi};$$

$$\eta = -\frac{\partial \mathcal{E}}{\partial(\gamma\ddot{\theta} + \dot{\theta})};\ q_i = \frac{\partial \mathcal{E}}{\partial \theta_{,i}}.$$

The energy equation is given by (1.1.2). Taking into account the constitutive equation regarding the entropy $(1.2.5)_6$ and the flux equation $(1.2.5)_7$, the energy equation will have the following form:

$$\rho T_0 \left[\beta_{ij}\dot{u}_{i,j} + a_1\dot{\phi} + a_2\dot{\psi} + c(\gamma\dddot{\theta} + \ddot{\theta})\right] = (K_{ij}\theta_{,j})_{,i} + \rho\delta \tag{1.2.6}$$

In the context of MGT theory of thermoelasticity for materials with double porosity structure, it is necessary to insert the initial conditions for $t = 0$:

$$\begin{aligned} &u_i(x,0) = 0;\ \phi(x,0) = 0;\ \psi(x,0) = 0;\ \theta(x,0) = 0 \\ &\dot{u}_i(x,0) = 0;\ \dot{\phi}(x,0) = 0;\ \dot{\psi}(x,0) = 0;\ \dot{\theta}(x,0) = 0;\ \ddot{\theta}(x,0) = 0 \end{aligned} \tag{1.2.7}$$

The mixed problem for the MGT theory has the boundary conditions:

$$\begin{aligned} &u_i = u_i^* \text{ on } \partial\Omega_1 \times [0,t^*);\ t_i = t_i^* \text{ on } \partial\Omega_1^c \times [0,t^*) \\ &\phi = \phi^* \text{ on } \partial\Omega_2 \times [0,t^*);\ \lambda = \lambda^* \text{ on } \partial\Omega_2^c \times [0,t^*) \\ &\psi = \psi^* \text{ on } \partial\Omega_3 \times [0,t^*);\ m = \omega^* \text{ on } \partial\Omega_3^c \times [0,t^*) \\ &\theta = \theta^* \text{ on } \partial\Omega_4 \times [0,t^*);\ \nu = \Omega^* \text{ on } \partial\Omega_4^c \times [0,t^*) \end{aligned} \tag{1.2.8}$$

where $u_i^*, t_i^*, \phi^*, \psi^*, \omega^*, \theta^*, \Omega^*$ are prescribed functions for a specific moment of time t^* that can be finite or infinite.

The boundary of the domain B is divided in four surfaces ∂B_1, ∂B_2, ∂B_3, ∂B_4. The complement of the considered surface is noted by superscript index "c" such that: $\partial B_i \cap \partial B_i^c = \emptyset$ and $\partial B_i \cup \partial B_i^c = \partial B$, $\forall i = \overline{1,4}$.

The components of the surface force traction, surface couple and flux are expressed by (1.1.8').

In the context of MGT theory of thermoelasticity for materials with double porosity structure the mixed problem is formed from the equations (1.1.1), (1.1.2), (1.2.5) with initial conditions (1.2.7) and the boundary conditions (1.2.8).

The solution of the considered problem is the ordered array $(u_i, \phi, \psi, \theta)$ and it is represented by the effect of the external actions (E_A) on the system that are defined by the ordered array:

$$E_A = (F_i, M, N, \delta, u_i^*, \phi^*, \psi^*, \theta^*, t_i^*, \lambda^*, \omega^*, \Omega^*)$$

The thermoelastic state (T_S) generated by the external forces is defined by:

$$T_S = (u_i, \phi, \psi, \theta, t_{ij}, \sigma_i, \tau_i, p, r, q_i, \eta)$$

Further we will consider that on the double porous material act two different loading systems:

$$E_A^{(i)} = (F_i^{(i)}, \omega^{(i)}, N^{(i)}, \delta^{(i)}, u_i^{*(i)}, \phi^{*(i)}, \psi^{*(i)}, \theta^{*(i)}, t_i^{*(i)}, \lambda^{*(i)}, \omega^{*(i)}, \Omega^{*(i)}), i = \overline{1,2}$$

and for each loading system we have two thermoelastic states:

$$T_S^{(i)} = (u_i^{(i)}, \phi^{(i)}, \psi^{(i)}, \theta^{(i)}, t_{ij}^{(i)}, \sigma_i^{(i)}, \tau_i^{(i)}, p^{(i)}, r^{(i)}, q_i^{(i)}, \eta^{(i)}), i = \overline{1,2}$$

1.2.2 Reciprocity and uniqueness theorems

In this section we will enunciate some reciprocity theorems that are of Betti's type. These theorems are useful in order to determine a reciprocity relation between the external action systems and their corresponding thermoelastic states. Further we consider the convolution product $*$.

Theorem 1.2.1. *Let us consider the external action systems $E_A^{(i)}$ for two different types of loadings and their thermoelastic states $T_S^{(i)}$, respectively. The following*

reciprocity relation takes place:

$$\begin{aligned}
&\int_\Omega \rho(F_i^{(1)}*u_i^{(2)}-F_i^{(2)}*u_i^{(1)}+\omega^{(1)}*\phi^{(2)}-\omega^{(2)}*\phi^{(1)}+N^{(1)}*\psi^{(2)}-N^{(2)}*\phi^{(1)})dV-\\
&\quad-\int_{\partial\Omega_1^c}(t_i^{*(2)}*u_i^{(1)}-t_i^{*(1)}*u_i^{(2)})dA-\int_{\partial\Omega_1}(t_{ji}^{(2)}*u_i^{*(1)}-t_{ji}^{(1)}*u_i^{*(2)})n_jdA-\\
&\quad-\int_{\partial\Omega_2^c}(\lambda^{*(2)}*\phi^{(1)}-\lambda^{*(1)}*\phi^{(2)})dA-\int_{\partial\Omega_2}(\sigma_j^{(2)}*\phi^{*(1)}-\sigma_j^{(1)}*\phi^{*(2)})n_jdA-\\
&\quad-\int_{\partial\Omega_3^c}(\omega^{*(2)}*\psi^{(1)}-\omega^{*(1)}*\psi^{(2)})dA-\int_{\partial\Omega_3}(\tau_j^{(2)}*\psi^{*(1)}-\tau_j^{(1)}*\psi^{*(2)})n_jdA= \qquad (1.2.9)\\
&=\frac{1}{\rho T_0}\left\{\int_{\partial\Omega_4^c}\left[\Omega^{*(1)}*\left(\theta^{(2)}+\alpha\frac{\partial\theta^{(2)}}{dt}\right)-\Omega^{*(2)}*\left(\theta^{(1)}+\alpha\frac{\partial\theta^{(1)}}{dt}\right)\right]dA+\right.\\
&\quad+\int_{\partial\Omega_4}\left[q_i^{(1)}*\left(\theta^{*(2)}+\alpha\frac{\partial\theta^{*(2)}}{dt}\right)-q_i^{(2)}*\left(\theta^{*(1)}+\alpha\frac{\partial\theta^{*(1)}}{dt}\right)\right]n_idA+\\
&\quad+\int_{\partial\Omega}\left[q_i^{(2)}*\left(\theta_{,i}^{(1)}+\alpha\frac{\partial\theta_{,i}^{(1)}}{dt}\right)-q_i^{(1)}*\left(\theta_{,i}^{(2)}+\alpha\frac{\partial\theta_{,i}^{(2)}}{dt}\right)\right]dV+\\
&\quad\left.+\rho\int_{\partial\Omega}\left[\delta^{(1)}*\left(\theta^{(2)}+\alpha\frac{\partial\theta^{(2)}}{dt}\right)-\delta^{(2)}*\left(\theta^{(1)}+\alpha\frac{\partial\theta^{(1)}}{dt}\right)\right]dV\right\}
\end{aligned}$$

Proof.

In order to obtain the reciprocity relation of Betti type we will apply the Lapalce transform to the equations (1.1.1). Let us consider that the image through the Laplace transform of the original function $f(x,t)$ will be $\overline{f}(x,t)$. Therefore the governing equations for the double porous materials will have the following form:

$$\begin{aligned}
&\rho s^2\overline{u}_i^{(i)})=\overline{t}_{ji,j}^{(i)}+\rho\overline{F}_i^{(i)}\\
&\kappa_1 s^2\overline{\phi}^{(i)}=\overline{\sigma}_{j,j}^{(i)}+\overline{p}^{(i)}+\rho\overline{\omega}^{(i)}, \qquad i=\overline{1,2} \qquad (1.2.10)\\
&\kappa_2 s^2\overline{\psi}^{(i)}=\overline{\tau}_{j,j}^{(i)}+\overline{r}^{(i)}+\rho\overline{N}^{(i)}
\end{aligned}$$

The energy equation (1.2.6) through the Laplace transform will be:

$$\rho T_0\left[\beta_{ij}s\overline{u}_i^{(i)}+a_1s\overline{\phi}^{(i)}+a_2s\overline{\psi}^{(i)}+c(\gamma s^3\overline{\theta}^{(i)}+s^2\overline{\theta}^{(i)})\right]=K_{ij}\overline{\theta}_{,ij}^{(i)}+\rho\overline{\delta}^{(i)},i=\overline{1,2} \qquad (1.2.11)$$

The constitutive equations through the Laplace transform will have the following

form:

$$\begin{aligned}
\overline{t}_{ij}^{(i)} &= C_{ijkl}\overline{u}_{k,l}^{(i)} + B_{ij}\overline{\phi}^{(i)} + D_{ij}\overline{\psi}^{(i)} - \beta\left(\gamma s^2\overline{\theta}^{(i)} + s\overline{\theta}^{(i)}\right)\\
\overline{\sigma}_{ij}^{(i)}) &= \alpha_{ij}\overline{\phi}_{,j}^{(i)}) + b_{ij}\overline{\psi}_{,j}^{(i)}\\
\overline{\tau}_{i}^{(i)} &= b_{ij}\overline{\phi}_{,j}^{(i)} + \gamma_{ij}\overline{\psi}_{,j}^{(i)}\\
\overline{p}^{(i)} &= -B_{ij}\overline{u}_{i,j}^{(i)} - \alpha_1\overline{\phi}^{(i)} - \alpha_3\overline{\psi}^{(i)} + a_1\left(\gamma s^2\overline{\theta}^{(i)} + s\overline{\theta}^{(i)}\right)\\
\overline{r}^{(i)} &= -D_{ij}\overline{u}_{i,j}^{(i)} - \alpha_3\overline{\phi}^{(i)} - \alpha_2\overline{\psi}^{(i)} + a_2\left(\gamma s^2\overline{\theta}^{(i)} + s\overline{\theta}^{(i)}\right)\\
\overline{\eta}^{(i)} &= \beta_{ij}\overline{u}_{i,j}^{(i)} + a_1\overline{\phi}^{(i)} + a_2\overline{\psi}^{(i)} + c\left(\gamma s^2\overline{\theta}^{(i)} + s\overline{\theta}^{(i)}\right)\\
\overline{q}_{i}^{(i)} &= K_{ij}\overline{\theta}_{,j}^{(i)}
\end{aligned} \tag{1.2.12}$$

The boundary conditions (1.2.8) through the Laplace transform become:

$$\begin{aligned}
&\overline{u}_i = \overline{u}_i^{*(i)} \text{ on } \partial\Omega_1\times[0,t^*);\ \overline{t}_i = \overline{t}_i^{*(i)} \text{ on } \partial\Omega_1^c\times[0,t^*)\\
&\overline{\phi} = \overline{\phi}^{*(i)} \text{ on } \partial\Omega_2\times[0,t^*);\ \overline{\lambda} = \overline{\lambda}^{*(i)} \text{ on } \partial\Omega_2^c\times[0,t^*)\\
&\overline{\psi} = \overline{\psi}^{*(i)} \text{ on } \partial\Omega_3\times[0,t^*);\ \overline{m} = \overline{\omega}^{*(i)} \text{ on } \partial\Omega_3^c\times[0,t^*)\\
&\overline{\theta} = \overline{\theta}^{*(i)} \text{ on } \partial\Omega_4\times[0,t^*);\ \overline{\nu} = \overline{\Omega}^{*(i)} \text{ on } \partial\Omega_4^c\times[0,t^*)
\end{aligned} \tag{1.2.13}$$

Writing the equation $(1.2.10)_1$ for each loading and multiplying with $\overline{u}_i^{(2)}$ and $\overline{u}_i^{(1)}$, respectively, and after that subtract and integrate on the considered domain, we obtain:

$$\begin{aligned}
&\int_\Omega \rho\left(\overline{F}_i^{(1)}\overline{u}_i^{(2)} - \overline{F}_i^{(2)}\overline{u}_i^{(1)}\right)dV = \\
&\quad = \int_\Omega \left(\overline{t}_{ji}^{(2)}\overline{u}_i^{(1)} - \overline{t}_{ji}^{(1)}\overline{u}_i^{(2)}\right)_{,j} dV + \int_\Omega \left(\overline{t}_{ji}^{1)}\overline{u}_{i,j}^{(2)} - \overline{t}_{ji}^{(2)}\overline{u}_{i,j}^{(1)}\right)dV
\end{aligned} \tag{1.2.14}$$

In the first integral from the right side of (1.2.14) we apply the divergence theorem and in the second integral from the right side of (1.2.14) we will take into account the constitutive equations (1.2.12). Therefore the equation (1.2.14) will have the following form:

$$\begin{aligned}
&\int_\Omega \rho\left(\overline{F}_i^{(1)}\overline{u}_i^{(2)} - \overline{F}_i^{(2)}\overline{u}_i^{(1)}\right)dV = \\
&\quad = \int_{\partial\Omega^c} \left(\overline{t}_i^{*(2)}\overline{u}_i^{(1)} - \overline{t}_i^{*(1)}\overline{u}_i^{(2)}\right)dA + \int_{\partial\Omega_1}\left(\overline{t}_{ji}^{(2)}u_i^{*(1)} - \overline{t}_{ji}^{(1)}u_i^{*(2)}\right)n_j dA + \\
&\quad + \int_\Omega \Big[B_{ij}\left(\overline{\phi}^{(1)}\overline{u}_{i,j}^{(2)} - \overline{\phi}^{(1)}\overline{u}_{i,j}^{(2)}\right) + D_{ij}\left(\overline{\psi}^{(1)}\overline{u}_{i,j}^{(2)} - \overline{\psi}^{(1)}\overline{u}_{i,j}^{(2)}\right) - \\
&\qquad\qquad - \beta_{ij}s(1+\gamma s)\left(\overline{\theta}^{(1)}\overline{u}_{i,j}^{(2)} - \overline{\theta}^{(2)}\overline{u}_{i,j}^{(1)}\right)\Big]dV
\end{aligned} \tag{1.2.15}$$

Next we write the equation $(1.2.10)_2$ for the both loading systems and compute the subtractionafter each equation is multiply by $\overline{\phi}^{(2)}, \overline{\phi}^{(1)}$, respectively. Integrating on Ω we obtain:

$$\int\limits_{\Omega} \rho \left(\overline{\omega}^{(1)} \overline{\phi}^{(2)} - \overline{\omega}^{(2)} \overline{\phi}^{(1)} \right) dV = \tag{1.2.16}$$
$$\int\limits_{\Omega} \left(\overline{\sigma}_{j,j}^{(2)} \overline{\phi}^{(1)} - \overline{\sigma}_{j,j}^{(1)} \overline{\phi}^{(2)} \right) dV + \int\limits_{\Omega} \left(\overline{p}^{(2)} \overline{\phi}^{(1)} - \overline{p}^{(1)} \overline{\phi}^{(2)} \right) dV$$

In the first integral from the right side we apply the divergence theorem and for both integrals we take into account the constitutive equations. Therefore the relation (1.2.16) will have the following form:

$$\int\limits_{\Omega} \rho \left(\overline{\omega}^{(1)} \overline{\phi}^{(2)} - \overline{\omega}^{(2)} \overline{\phi}^{(1)} \right) dV = \int\limits_{\partial \Omega_2^c} \left(\overline{\lambda}^{*(2)} \overline{\phi}^{(1)} - \overline{\lambda}^{*(1)} \overline{\phi}^{(2)} \right) dA +$$
$$+ \int\limits_{\partial \Omega_2} \left(\overline{\sigma}_j^{(2)} \overline{\phi}^{*(1)} - \overline{\sigma}_j^{(1)} \overline{\phi}^{*(2)} \right) n_j dA + \int\limits_{\Omega} b_{ij} \left(\overline{\psi}_{,j}^{(1)} \overline{\phi}_{,j}^{(2)} - \overline{\psi}_{,j}^{(2)} \overline{\phi}_{,j}^{(1)} \right) dV - \tag{1.2.17}$$
$$- \int\limits_{\Omega} \Big[B_{ij} \left(\overline{u}_{i,j}^{(2)} \overline{\phi}^{(1)} - \overline{u}_{i,j}^{(1)} \overline{\phi}^{(2)} \right) + \alpha_3 \left(\overline{\psi}^{(2)} \overline{\phi}^{(1)} - \overline{\psi}^{(1)} \overline{\phi}^{(2)} \right) -$$
$$- a_1 s(\gamma s + 1) \left(\overline{\theta}^{(2)} \overline{\phi}^{(1)} - \overline{\theta}^{(1)} \overline{\phi}^{(2)} \right) \Big] dV$$

At last, we multiply the equations from $(1.2.10)_3$ with $\overline{\psi}^{(2)}$ and $\overline{\psi}^{(1)}$ written for each load of the system, making the subtraction and integrate on the considered domain. Now we have:

$$\int\limits_{\Omega} \rho \left(\overline{N}^{(1)} \overline{\psi}^{(2)} - \overline{N}^{(2)} \overline{\psi}^{(1)} \right) dV = \tag{1.2.18}$$
$$\int\limits_{\Omega} \left(\overline{\tau}_{j,j}^{(2)} \overline{\psi}^{(1)} - \overline{\tau}_{j,j}^{(1)} \overline{\psi}^{(2)} \right) dV + \int\limits_{\Omega} \left(\overline{r}^{(2)} \overline{\psi}^{(1)} - \overline{r}^{(1)} \overline{\psi}^{(2)} \right) dV$$

Using the divergence theorem and the constitutive equations and taking into account the boundary conditions (1.2.8) the relation (1.2.18) will have the form:

$$\int\limits_{\Omega} \rho \left(\overline{N}^{(1)} \overline{\psi}^{(2)} - \overline{N}^{(2)} \overline{\psi}^{(1)} \right) dV = \int\limits_{\partial \Omega_3^c} \left(\overline{\omega}^{*(2)} \overline{\psi}^{(1)} - \overline{\omega}^{*(1)} \overline{\psi}^{(2)} \right) dA +$$
$$+ \int\limits_{\partial \Omega_3} \left(\overline{\tau}_j^{(2)} \overline{\psi}^{*(1)} - \overline{\tau}_j^{(1)} \overline{\psi}^{*(2)} \right) n_j dA + \int\limits_{\Omega} b_{ij} \left(\overline{\phi}_{,j}^{(2)} \overline{\psi}_{,j}^{(1)} - \overline{\phi}_{,j}^{(1)} \overline{\psi}_{,j}^{(2)} \right) dV - \tag{1.2.19}$$
$$- \int\limits_{\Omega} \Big[D_{ij} \left(\overline{u}_{i,j}^{(2)} \overline{\psi}^{(1)} - \overline{u}_{i,j}^{(1)} \overline{\psi}^{(2)} \right) + \alpha_3 \left(\overline{\phi}^{(2)} \overline{\psi}^{(1)} - \overline{\phi}^{(1)} \overline{\psi}^{(2)} \right) -$$
$$- a_2 s(\gamma s + 1) \left(\overline{\theta}^{(2)} \overline{\psi}^{(1)} - \overline{\theta}^{(1)} \overline{\psi}^{(2)} \right) \Big] dV$$

Next we write the energy equation (1.2.11) for both loadings and we multiply them by $\overline{\theta}^{(2)}$ and $\overline{\theta}^{(1)}$, respectively and after that subtracting the relations and integrating on the domain Ω we have:

$$\begin{aligned}\int\limits_{\Omega}\Big[\beta_{ij}s\left(\overline{u}_{i,j}^{(1)}\overline{\theta}^{(2)}-\overline{u}_{i,j}^{(2)}\overline{\theta}^{(1)}\right)+a_1 s\left(\overline{\phi}^{(1)}\overline{\theta}^{(2)}-\overline{\phi}^{(2)}\overline{\theta}^{(1)}\right)+\\ +a_2 s\left(\overline{\psi}^{(1)}\overline{\theta}^{(2)}-\overline{\psi}^{(2)}\overline{\theta}^{(1)}\right)\Big]dV=\\ =\frac{1}{\rho T_0}\int\limits_{\Omega}K_{ij}\left(\overline{\theta}_{,ij}^{(1)}\overline{\theta}^{(2)}-\overline{\theta}_{,ij}^{(2)}\theta^{(1)}\right)dV+\frac{1}{T_0}\int\limits_{\Omega}\left(\overline{\delta}^{(1)}\overline{\theta}^{(2)}-\overline{\delta}^{(2)}\overline{\theta}^{(1)}\right)dV\end{aligned}\tag{1.2.20}$$

Using the divergence theorem and taking into account the boundary conditions, the relation (1.2.20) becomes:

$$\begin{aligned}\int\limits_{\Omega}\Big[\beta_{ij}s\left(\overline{u}_{i,j}^{(1)}\overline{\theta}^{(2)}-\overline{u}_{i,j}^{(2)}\overline{\theta}^{(1)}\right)+a_1 s\left(\overline{\phi}^{(1)}\overline{\theta}^{(2)}-\overline{\phi}^{(2)}\overline{\theta}^{(1)}\right)+\\ +a_2 s\left(\overline{\psi}^{(1)}\overline{\theta}^{(2)}-\overline{\psi}^{(2)}\overline{\theta}^{(1)}\right)\Big]dV=\\ =\frac{1}{\rho T_0}\int\limits_{\partial\Omega_4^c}\left(\overline{\theta}^{(2)}\overline{\Omega}^{*(1)}-\overline{\theta}^{(1)}\overline{\Omega}^{*(2)}\right)dA+\frac{1}{\rho T_0}\int\limits_{\partial\Omega_4}\left(\overline{\theta}^{*(2)}\overline{q}_i^{(1)}-\overline{\theta}^{*(1)}\overline{q}_i^{(2)}\right)n_i dA-\\ -\frac{1}{\rho T_0}\int\limits_{\Omega}\left(\overline{\theta}_{,i}^{(2)}\overline{q}_i^{(1)}-\overline{\theta}_{,i}^{(1)}\overline{q}_i^{(2)}\right)dV+\frac{1}{T_0}\int\limits_{\Omega}\left(\overline{\delta}^{(1)}\overline{\theta}^{(2)}-\overline{\delta}^{(2)}\overline{\theta}^{(1)}\right)dV\end{aligned}\tag{1.2.21}$$

We may observe that in the above equation (1.2.21) appear the terms from (1.2.15). (1.2.17) and (1.2.19), therefore the relation (1.2.21) will take the following form:

$$\begin{aligned}\int\limits_{\Omega}\Big[\rho\left(\overline{F}_i^{(1)}\overline{u}_i^{(2)}-\overline{F}_i^{(2)}\overline{u}_i^{(1)}\right)+\rho\left(\overline{\omega}^{(1)}\overline{\phi}^{(2)}-\overline{\omega}^{(2)}\overline{\phi}^{(1)}\right)+\rho\left(\overline{N}^{(1)}\overline{\psi}^{(2)}-\overline{N}^{(2)}\overline{\psi}^{(1)}\right)\Big]dV-\\ -\int\limits_{\partial\Omega_1^c}\left(\overline{t}_i^{*(2)}\overline{u}_i^{(1)}-\overline{t}_i^{*(1)}\overline{u}_i^{(2)}\right)dA-\int\limits_{\partial\Omega_1}\left(\overline{t}_{ji}^{(2)}\overline{u}_i^{*(1)}-\overline{t}_{ji}^{(1)}\overline{u}_i^{*(2)}\right)n_j dA-\\ -\int\limits_{\partial\Omega_2^c}\left(\overline{\lambda}^{*(2)}\overline{\phi}^{(1)}-\overline{\lambda}^{*(1)}\overline{\phi}^{(2)}\right)dA-\int\limits_{\partial\Omega_2}\left(\overline{\sigma}_j^{(2)}\overline{\phi}^{*(1)}-\overline{\sigma}_j^{(1)}\overline{\phi}^{*(2)}\right)n_j dA-\\ -\int\limits_{\partial\Omega_3^c}\left(\overline{\omega}^{*(2)}\overline{\psi}^{(1)}-\overline{\omega}^{*(1)}\overline{\psi}^{(2)}\right)dA-\int\limits_{\partial\Omega_3}\left(\overline{\tau}_j^{(2)}\overline{\psi}^{*(1)}-\overline{\tau}_j^{(1)}\overline{\psi}^{*(2)}\right)n_j dA=\\ =\frac{1+\gamma s}{\rho T_0}\left[\int\limits_{\partial\Omega_4^c}\left(\overline{\theta}^{(2)}\overline{\Omega}^{*(1)}-\overline{\theta}^{(1)}\overline{\Omega}^{*(2)}\right)dA+\int\limits_{\partial\Omega_4}\left(\overline{\theta}^{*(2)}\overline{q}_i^{*(1)}-\overline{\theta}^{*(1)}\overline{q}_i^{*(2)}\right)n_i dA+\right.\\ \left.+\int\limits_{\Omega}\left(\overline{\theta}_{,i}^{(1)}\overline{q}_i^{(2)}-\overline{\theta}_{,i}^{(2)}\overline{q}_i^{(1)}\right)dV+\int\limits_{\Omega}\rho\left(\overline{\delta}^{(1)}\overline{\theta}^{(2)}-\overline{\delta}^{(2)}\overline{\theta}^{(1)}\right)dV\right]\end{aligned}\tag{1.2.22}$$

In the relation (1.2.22) we apply the inverse Laplace transform $\mathcal{L}$ and the convolution product noted by $*$ is obtained. Thus we use:

$$\overline{F}_i^{(1)}\overline{u}_i^{(2)} = \mathcal{L}[F_i^{(1)}](s)\cdot\mathcal{L}[u_i^{(2)}](s) = F_i^{(1)} * u_i^{(2)}$$

$$s\overline{\theta}^{(2)}\Omega^{*(1)} = \mathcal{L}[\Omega^{*(1)}](s)\cdot\mathcal{L}\left[\frac{\partial\theta^{(2)}}{\partial t}\right](s) = \Omega^{*(1)} * \frac{\partial\theta^{(2)}}{\partial t}$$

The result from the theorem Th[1.2.1] is obtained. □

Based on the theory of Green and Lindsay, let us introduce the scalar function:

$$\Phi = T_0 + \dot{\theta} + \gamma\ddot{\theta} + \dot{\theta}\ddot{\theta} + \frac{1}{2}d\ddot{\theta}^2 \tag{1.2.23}$$

The energy function of Moore-Gibson-Thompson thermoelasticity will have the expression:

$$\mathbb{E} = E_i - \eta\Phi \tag{1.2.24}$$

where according to Biot, the generalized free energy function $\mathcal{E}$ is given by:

$$\mathcal{E} = E_i - \eta T_0 \tag{1.2.25}$$

where E_i is the internal energy. Taking into account the initial conditions of the MGT thermoelasticity from (1.2.7), the energy function $\mathbb{E}$ will have the following quadratic expression:

$$\begin{aligned}\mathbb{E}=&\frac{1}{2}C_{ijkl}u_{i,j}u_{k,l}+B_{ij}\phi u_{i,j}+D_{ij}\psi u_{i,j}+\frac{1}{2}\phi_{,i}\phi_{,j}+b_{ij}\phi_{,i}\psi_{,j}+\frac{1}{2}\gamma_{ij}\psi_{,i}\psi_{,j}+\\ &+\frac{1}{2}\alpha_1\phi^2+\alpha_3\phi\psi+\frac{1}{2}\alpha_2\psi^2+\frac{1}{2}K_{ij}\Theta_{,i}\theta_{,j}-A\dot{\theta}^2-B\dot{\theta}\ddot{\theta}+C\ddot{\theta}^2\end{aligned} \tag{1.2.26}$$

where: $A=\frac{3}{2}c,\ B=\frac{3}{2}c\gamma+b\mathcal{M}, C=\frac{3}{2}c\gamma^2+\frac{d}{2}\mathcal{M}$ and $\mathcal{M}=\beta_{ij}u_{i,j}+a_1\phi+a_2\psi$ The kinetic energy per mass unit is given by:

$$E_{\mathbb{K}}(t) = \frac{1}{2}\left[\rho\dot{u}_i(t)\dot{u}_i(t)+\kappa_1\dot{\phi}(t)\dot{\phi}(t)+\kappa_2\dot{\psi}(t)\dot{\psi}(t)\right] \tag{1.2.27}$$

Based on the relation of function of energy (1.2.26) and kinetic energy (1.2.27) we can enunciate the following theorem:

Theorem 1.2.2. *The variation of energy in the MGT thermoelasticity for double porous materials is expressed by:*

$$\begin{aligned}\frac{d}{dt}\int_\Omega(E_{\mathbb{K}}+\mathbb{E})dV=&\rho\int_\Omega\Big(F_i\dot{u}_i+M\dot{\phi}+N\dot{\psi}\Big)dV+\int_{\partial\Omega}\Big(t_{ji}\dot{u}_i+\sigma_j\dot{\phi}+\tau_j\dot{\psi}\Big)n_jdA+\\ &+\int_\Omega\left(q_i\dot{\theta}_{,j}+\frac{1}{\rho T_0}(q_{i,i}+\rho\delta)(\gamma\ddot{\theta}+\dot{\theta})\right)dV-\\ &-\int_\Omega\Big(\frac{2}{3}A(\gamma\ddot{\theta}+\dot{\theta})(\gamma\dddot{\theta}+\ddot{\theta})+(2A+B)\dot{\theta}\ddot{\theta}+B\ddot{\theta}^2+2C\ddot{\theta}\cdot\dddot{\theta}\Big)dV\end{aligned} \tag{1.2.28}$$

Proof. The variation of the kinetic energy in report with time is:

$$\dot{E}_{\mathbb{K}} = \rho\dot{u}_i(t)\ddot{u}_i(t) + \kappa_1\dot{\phi}(t)\ddot{\phi}(t) + \kappa_2\dot{\psi}(t)\ddot{\psi}(t) \tag{1.2.29}$$

The terms from (1.2.30) are obtained from the governing equations for the double porous bodies (1.1.1), multiplyed by $\dot{u}_i, \dot{\phi}$ and $\dot{\psi}$, respectively. Therefore, by integration on the B domain, using the divergence theorem and take into account the constitutive equations (1.2.5), the equation (1.2.30) takes the following form:

$$\begin{aligned}\int_\Omega \dot{E}_{\mathbb{K}}(t)dt = &\int_\Omega \rho(F_i\dot{u}_i + M\dot{\phi} + N\dot{\psi})dV + \int_{\partial\Omega}(t_{ji}\dot{u}_i + \sigma_j\dot{\phi} + \tau_j\dot{\psi})n_j dA\\ &- \int_\Omega \Big[B_{ij}u_{i,j}\dot{\phi} + \alpha_1\phi\dot{\phi} + \alpha_3\psi\dot{\phi} - a_1(\gamma\ddot{\theta} + \dot{\theta})\dot{\phi} +\\ &\quad + D_{ij}u_{i,j}\dot{\psi} + \alpha_3\phi\dot{\psi} + \alpha_2\psi\dot{\psi} - a_2(\gamma\ddot{\theta} + \dot{\theta})\dot{\psi} +\\ &\quad + C_{ijkl}u_{k,l}\dot{u}_{i,j} + B_{ij}\phi\dot{u}_{i,j} + D_{ij}\psi\dot{u}_{i,j} - \beta\dot{u}_{i,j}(\gamma\ddot{\theta} + \dot{\theta})\\ &\quad + \alpha_{ij}\phi_{,j}\dot{\phi}_{,j} + b_{ij}\psi_{,j}\dot{\phi}_{,j} + b_{ij}\phi_{,j}\dot{\psi}_{,j} + \gamma_{ij}\psi_{,j}\dot{\psi}_{,j}\Big]dV\end{aligned} \tag{1.2.30}$$

Integrating on the domain B the variation of the function of energy (1.2.26) in report with time we have:

$$\begin{aligned}\int_\Omega \dot{\mathbb{E}}(t)dV = &\int_\Omega \Big[C_{ijkl}u_{i,j}\dot{u}_{k,l} + B_{ij}\dot{\phi}u_{i,j} + B_{ij}\phi\dot{u}_{i,j} + D_{ij}\dot{\psi}u_{i,j} + D_{ij}\psi\dot{u}_{i,j} + \alpha_{ij}\phi_{,i}\dot{\phi}_{,j} +\\ &\quad + \alpha_3\phi\dot{\psi} + \alpha_3\dot{\phi}\psi + b_{ij}\dot{\phi}_{,i}\psi_{,j} + b_{ij}\phi_{,i}\dot{\psi}_{,j} + \gamma_{ij}\phi_{,i}\dot{\psi}_{,j} + \alpha_1\phi\dot{\phi} +\\ &\quad + \alpha_2\psi\dot{\psi} + K_{ij}\theta_{,i}\dot{\theta}_{,j} - 2A\dot{\theta}\ddot{\theta} - B\ddot{\theta}^2 - b\dot{\theta}\dddot{\theta} + 2C\ddot{\theta}\cdot\dddot{\theta}\Big]dV\end{aligned} \tag{1.2.31}$$

Taking into account the energy equation given in (1.2.6) we have:

$$\beta_{ij}\dot{u}_{i,j} + a_1\dot{\phi} + a_2\dot{\psi} = \frac{1}{\rho T_0}(q_{i,i} + \rho\delta) - c(\gamma\dddot{\theta} + \ddot{\theta})$$

Summing the relations (1.2.30) and (1.2.31) on the domain Ω we obtain the variation of the energy in the context of the MGT thermoelasticity for double porous materials. Therefore the result of the theorem Th[1.2.2] is obtained. □

Theorem 1.2.3. *If the energy function* $\mathbb{E}$ *from* (1.2.26) *is positive defined, then the considered mixte problem for double porous materials in the MGT thermoelasticity contexts admits only one solution.*

Proof. In order to prove the uniqueness of the solution of the mixed problem for double porous materials in the context of MGT thermoelasticity, we assume that the considered problem admits two solutions: $(u_{i1}, \phi_1, \psi_1, \theta_1)$ and $(u_{i2}, \phi_2, \psi_2, \theta_2)$.

For null loadings F_i, M and N and for zero boundary conditions: $u_i^* = 0, \phi^* = 0, \psi^* = 0, t_i^* = 0, \lambda^* = 0, \omega^* = 0, \Omega^* = 0$, the difference between these solutions $(u_{i1} - u_{i2}, \phi_1 - \phi_2, \psi_1 - \psi_2, \theta_1 - \theta_2)$ is also a solution of the mixed problem for double porous materials in the MGT thermoelasticity context.

Therefore, the energy equation (1.2.31) will have the following expression:

$$\int_\Omega (\dot{E}_{\mathbb{K}} + \dot{\mathbb{E}}) dV = -\int_\Omega \left(\frac{2}{3} A(\gamma \ddot{\theta} + \dot{\theta})(\gamma \dddot{\theta} + \ddot{\theta}) + (2A + B)\dot{\theta}\ddot{\theta} + B\ddot{\theta}^2 + 2C\ddot{\theta} \cdot \dddot{\theta} \right) dV \leq 0$$

Taking into account the null initial conditions for $t = 0$ from (1.2.7), we observe that the kinetic energy from (1.2.27) and the energy function from (1.2.26) are zero: $E_{\mathbb{K}} = 0$; $\mathbb{E} = 0$. Hence, their sum is also zero. Based on the above inequality, on the fact that the energy and the kinetic energy are positive defined, we may draw the conclusion that the difference between the considered solution is null. Therefore, the mixed problem with initial and boundary conditions for the double porous materials in the MGT thermoelasticity context is unique. □

1.3 Green-Lindsay thermoelasticity for double porous materials

In the last years many researchers have shown their interest into the theory of Green and Lindsay due to the fact that it takes into consideration also the temperature rate as a constitutive variable and it permits the propagation of the waves at finite speeds. This type of theory was approached from the point of view of classical thermoelasticity [Green(1972)], thermoviscoelasticity [Aouadi(2019)], thermoelastic solid [Nieto(2018)], thermoelasticity of dipolar bodies [Marin(2020b)]. Our study uses this theory in the context of double porous thermoelastic materials.

In this section the behaviour of a body with double porosity structure using Green-Lindsay theory is described. The main results represents Betti type result that establishes a reciprocity relation between two systems of external loadings. This reciprocity relation is useful in order to obtain the uniqueness results regarding the considered mixed with initial and boundary data problem in the context of double porous materials using the Green Lindsay function and the Biot's energy function.

1.3.1 Basic equations

The behavior of a body with a double porosity structure using Green-Lindsay thermoelasticity is described by the following variables: $u_i(t,x)$ the displacement components, $\varphi(t,x)$, $\psi(t,x)$ the fractional volume fields corresponding to the pores and cracks, respectively and $\theta(t,x)$ the temperature.

The internal energy denoted by Ψ depends on the deformation tensors. By adding the temperature and its derivative as an independent variable, is obtained the Helmholtz energy or the so-called free energy noted by ω, which depends on the internal energy Ψ, the temperature θ and the entropy η: $\omega = \Psi - \theta\eta$.

Based on the Green-Lindsay theory the heat flux components are exprssed by:

$$q_i = -\theta_0(b_i\dot{\theta} + K_{ij}\theta_{,j}). \tag{1.3.1}$$

Knowing that in the case of linear theory the temperature difference from some basic temperature is very small, θ_0 is a constant temperature.

A material with two porosities is govern by the motion equations and the balances of the equilibrated forces given in (1.1.1) and by the energy equation (1.1.2).

The constitutive equations are functions of the strain tensors and some constants

of materials in the context of Green - Lindsay theory are:

$$\begin{aligned}
&t_{ij} = C_{ijkl}u_{k,l} + B_{ij}\varphi + D_{ij}\psi - \beta_{ij}(\theta + \alpha\dot{\theta}) = \tfrac{\partial\omega}{\partial u_{i,j}},\\
&\sigma_i = a_{ij}\varphi_{,j} + b_{ij}\psi_{,j} = \tfrac{\partial\omega}{\partial\varphi_{,i}},\\
&\sigma_i = b_{ij}\varphi_{,j} + \delta_{ij}\psi_{,j} = \tfrac{\partial\omega}{\partial\psi_{,i}},\\
&p = -B_{ij}u_{i,j} - \alpha_1\varphi - \alpha_3\psi + \gamma_1(\theta + \alpha\dot{\theta}) = -\tfrac{\partial\omega}{\partial\varphi},\\
&r = -D_{ij}u_{i,j} - \alpha_3\varphi - \alpha_2\psi + \gamma_2(\theta + \alpha\dot{\theta}) = \tfrac{\partial\omega}{\partial\psi},\\
&\eta = \beta_{ij}u_{i,j} + \gamma_1\varphi + \gamma_2\psi + c(\theta + \alpha\dot{\theta}) = -\tfrac{\partial\omega}{\partial(\theta+\alpha\dot{\theta})},\\
&q_i = -\theta_0(b_i\dot{\theta} + K_{ij}\theta_{,j}) = \tfrac{\partial\omega}{\partial\theta_{,i}}.
\end{aligned} \tag{1.3.2}$$

Based on the above relations (1.3.2) further we will obtain the quadratic form of the Helmholtz energy:

$$\begin{aligned}
\omega = \tfrac{1}{2}C_{ijkl}u_{k,l}u_{i,j} + B_{ij}\varphi u_{i,j} + D_{ij}\psi u_{i,j} - \beta_{ij}u_{i,j}(\theta + \alpha\dot{\theta}) +\\
+\tfrac{1}{2}a_{ij}\varphi_{,i}\varphi_{,j} + b_{ij}\varphi_{,i}\psi_{,j} + \tfrac{1}{2}\delta_{ij}\psi_{,i}\psi_{,j} + \tfrac{1}{2}\alpha_1\varphi^2 + \tfrac{1}{2}\alpha_2\psi^2 +\\
+\alpha_3\varphi\psi - \gamma_1\varphi(\theta + \alpha\dot{\theta}) - \gamma_2\psi(\theta + \alpha\dot{\theta}) +\\
+\tfrac{1}{2}c(\theta + \alpha\dot{\theta})^2 + b_i\theta_0\dot{\theta}\theta_{,i} + \tfrac{1}{2}\theta_0K_{ij}\theta_{,i}\theta_{,j}.
\end{aligned} \tag{1.3.3}$$

We take into account (1.3.1) and $(1.3.2)_6$ then the energy equation becomes:

$$\rho\beta_{ij}\dot{u_{i,j}} + \rho\gamma_1\dot{\varphi} + \rho\gamma_2\dot{\psi} + \rho a\dot{\theta} + \rho c\alpha\ddot{\theta} + b_i\dot{\theta}_{,i} + K_{ij}\theta_{,ij} - \frac{\rho\delta}{\theta_0} = 0. \tag{1.3.4}$$

We consider a three dimensional space $B \subset \mathbb{R}^3$ that is filled up by the double porous body. The boundary of the considered domain is denoted by ∂B and the normal at the domain surface has the components n_i. Therefore we may define the expression of the surface couple (λ, m), the force traction (t_i) and also the flow (ν).

$$t_i = t_{ij}n_j, \quad \lambda = \sigma_i n_i, \quad m = \tau_i n_i, \quad \nu = q_i n_i. \tag{1.3.5}$$

The boundary conditions are:

$$\begin{aligned}
u_i = u_i^b \ \text{ on } \ \partial B_1 \times [0,\infty), \quad t_i = t_i^b \ \text{ on } \ \partial B_1^c \times [0,\infty),\\
\varphi = \varphi^b \ \text{ on } \ \partial B_2 \times [0,\infty), \quad \lambda = \lambda^b \ \text{ on } \ \partial B_2^c \times [0,\infty),\\
\psi = \psi^b \ \text{ on } \ \partial B_3 \times [0,\infty), \quad m = \omega^b \ \text{ on } \ \partial B_3^c \times [0,\infty),\\
\theta = \theta^b \ \text{ on } \ \partial B_4 \times [0,\infty), \quad \nu = \Omega^b \ \text{ on } \ \partial B_4^c \times [0,\infty),
\end{aligned} \tag{1.3.6}$$

where $u_i^b,\ \varphi^b,\ \psi^b,\ \theta^b,\ t_i^b,\ \lambda^b,\ \omega^b,\ \Omega^b$ are known functions. The boundary of the considered domain ∂B is divided into four subsurfaces noted by $B_i, i = \overline{1,4}$ with their complements $B_i^c, i = \overline{1,4}$ that fulfill the following conditions:

$$\partial B_i \cup B_i^c = \partial B, \quad \partial B_i \cap B_i^c = \Phi, \quad i = \overline{1,4}. \tag{1.3.7}$$

We consider that at the initial moment t_0 we have the initial conditions:

$$\begin{aligned} u_i(0,x) = \dot{u}_i(0,x) = 0, \quad \varphi(0,x) = \dot{\varphi}(0,x) = 0, \\ \psi(0,x) = \dot{\psi}(0,x) = 0, \quad \theta(0,x) = \dot{\theta}(0,x) = 0. \end{aligned} \tag{1.3.8}$$

The mixed data problem for bodies with double porosity consists of equations (1.1.1), (1.1.2), (1.3.2), with the initial conditions (1.3.8) and the boundary conditions (1.3.6).

The solution $(u_i, \varphi, \psi, \theta)$ of the problem with mixed data for bodies with double porosity is represented by the response of a system at the external actions. This system of external actions is defined by:

$$H = (F_i, M, N, \delta, u_i^b, \varphi^b, \psi^b, \theta^b, t_i^b, \lambda^b, \omega^b, \Omega^b).$$

and it generates a thermoelastic state defined by:

$$S = (u_i, \varphi, \psi, \theta, t_{ij}, \sigma_i, \tau_i, p, r, q_i, \eta).$$

The thermoelastic states corresponding to the two systems are:

$$S^{(a)} = (u_i^{(a)}, \varphi^{(a)}, \psi^{(a)}, \theta^{(a)}, \varepsilon_{ij}^{(a)}, \chi_{ij}^{(a)}, t_{ij}^{(a)}, \sigma_i^{(a)}, \tau_i^{(a)}, p^{(a)}, r^{(a)}, q_i^{(a)}, \eta^{(a)}), \quad a = 1, 2.$$

Let us consider two function m and n. The convolution product is defined as follows:

$$(m * n)(t,x) = \int_0^t m(t-\zeta, x)\, n(\zeta, x)\, d\zeta,$$

respectively,

$$(m * \hat{n})(t,x) = \int_0^t m(t-\zeta, x)\, \frac{\partial n}{\partial \zeta}(\zeta, x)\, d\zeta.$$

1.3.2 Main results

The following section contains the main results of the present study. Therefore the first theorem is a result of Betti type that establishes a reciprocity relation between the two systems of external loadings. This theorem is very useful in order to obtain the next uniqueness results regarding the mixted problem for the double porous materials using the Green-Lindsay function and also the energy function of Biot.

Theorem 1.3.1. *The following reciprocal relationship occures:*

$$
\begin{aligned}
&-\int_B \rho(F_i^{(1)} * \hat{u}_i^{(2)} - F_i^{(2)} * \hat{u}_i^{(1)})\, dV + \\
&+\int_B \rho(\omega^{(1)} * \hat{\varphi}^{(2)} - \omega^{(2)} * \hat{\varphi}^{(1)})\, dV + \int_B \rho(N^{(1)} * \hat{\psi}^{(2)} - N^{(2)} * \hat{\psi}^{(1)})\, dV + \\
&+\int_{\partial B_1} (t_{ij}^{(1)} * \hat{u}_i^{b(2)} - t_{ji}^{(2)} * \hat{u}_i^{b(1)}) n_j\, dA + \int_{\partial B_1^c} (t_i^{b(1)} * \hat{u}_i^{(2)} - t_i^{b(2)} * \hat{u}_i^{(1)})\, dA + \\
&+\int_{\partial B_2} (\sigma_j^{(1)} * \hat{\varphi}^{b(2)} - \sigma_j^{(2)} * \hat{\varphi}^{b(1)}) n_j\, dA + \int_{\partial B_2^c} (\lambda^{b(1)} * \hat{\varphi}^{(2)} - \lambda^{b(2)} * \hat{\varphi}^{(1)})\, dA + \\
&+\int_{\partial B_3} (\tau_j^{(1)} * \hat{\psi}^{b(2)} - \tau_j^{(2)} * \hat{\psi}^{b(1)}) n_j\, dA + \int_{\partial B_3^c} (\omega^{b(1)} * \hat{\psi}^{(2)} - \omega^{b(2)} * \hat{\psi}^{(1)})\, dA = \\
&= \tfrac{1}{\theta_0} \int_B \rho(\delta^{(1)} * \theta^{(2)} - \delta^{(2)} * \theta^{(1)})\, dV + \tfrac{\alpha}{\theta_0} \int_B \rho(\delta^{(1)} * \hat{\theta}^{(2)} - \delta^{(2)} * \hat{\theta}^{(1)})\, dV + \\
&+\tfrac{1}{\theta_0} \int_B (q_i^{(2)} * \theta_{,i}^{(1)} - q_i^{(1)} * \theta_{,i}^{(2)})\, dV + \tfrac{\alpha}{\theta_0} \int_B (q_i^{(2)} * \hat{\theta}_{,i}^{(1)} - q_i^{(1)} * \hat{\theta}_{,i}^{(2)})\, dV - \\
&-\tfrac{1}{\theta_0} \int_{\partial B_4} (q_i^{(2)} * \theta^{b(1)} - q_i^{(1)} * \theta^{b(2)}) n_i\, dA - \tfrac{\alpha}{\theta_0} \int_{\partial B_4} (q_i^{(2)} * \hat{\theta}^{b(1)} - q_i^{(1)} * \hat{\theta}^{b(2)}) n_i\, dA - \\
&-\tfrac{1}{\theta_0} \int_{\partial B_4^c} (\Omega^{b(2)} * \theta^{(1)} - \Omega^{b(1)} * \theta^{(2)})\, dA - \tfrac{\alpha}{\theta_0} \int_{\partial B_4^c} (\Omega^{b(2)} * \hat{\theta}^{(1)} - \Omega^{b(1)} * \hat{\theta}^{(2)})\, dA.
\end{aligned}
$$

Proof. We apply the Laplace transform to the equations (1.3.1), (1.1.1), (1.1.2) and (1.3.4):

$$L[f(t,x)](s) = \tilde{f}(s,x) \int_0^\infty f(t,x)\, e^{-st}\, dt.$$

We will use the derivation property of the original and take into account the null initial conditions (1.3.8):

$$
\begin{aligned}
&L[\ddot{u}_i(t,x)](s) = s^2 \tilde{u}_i(s,x) - s \cdot u_i(0,x) - \dot{u}_i(0,x) = s^2 \tilde{u}_i(s,x), \\
&L[\ddot{\varphi}(t,x)](s) = s^2 \tilde{\varphi}(s,x) - s \cdot \varphi(0,x) - \dot{\varphi}(0,x) = s^2 \tilde{\varphi}(s,x), \\
&L[\ddot{\psi}(t,x)](s) = s^2 \tilde{\psi}(s,x) - s \cdot \psi(0,x) - \dot{\psi}(0,x) = s^2 \tilde{\psi}(s,x).
\end{aligned}
$$

Thus the equations that govern the body with double porosity structure (1.1.1), (1.1.2) can be written:

$$
\begin{aligned}
&\rho s^2 \tilde{u}_i^{(a)} = \tilde{t}_{ji,j}^{(a)} + \rho \tilde{F}_i^{(a)}, \\
&\kappa_1 s^2 \tilde{\varphi}^{(a)} = \tilde{\sigma}_{j,j}^{(a)} + \tilde{p}^{(a)} + \rho \tilde{M}^{(a)}, \qquad a = 1, 2. \\
&\kappa_2 s^2 \tilde{\psi}^{(a)} = \tilde{\tau}_{j,j}^{(a)} + \tilde{r}^{(a)} + \rho \tilde{N}^{(a)}.
\end{aligned} \tag{1.3.9}
$$

The energy equation (1.3.4) through the Laplace transform will have the following form:

$$\rho \beta_{ij} s \tilde{u}_{i,j}^{(a)} + \rho \gamma_1 s \tilde{\varphi}^{(a)} + \rho \gamma_2 s \tilde{\psi}^{(a)} + \rho c \alpha s^2 \tilde{\theta}^{(a)} + b_i s \tilde{\theta}_{,i}^{(a)} + K_{ij} \tilde{\theta}_{,ij}^{(a)} - \frac{\rho \tilde{\delta}^{(a)}}{\theta_0} = 0. \tag{1.3.10}$$

The constitutive equations (1.3.2) through the Laplace transform become:

$$\begin{aligned}
\tilde{t}_{ij}^{(a)} &= C_{ijkl}\tilde{u}_{k,l}^{(a)} + B_{ij}\tilde{\varphi}^{(a)} + D_{ij}\tilde{\psi}^{(a)} - \beta_{ij}(\tilde{\theta}^{(a)} + \alpha s\tilde{\theta}^{(a)}),\\
\tilde{\sigma}_i^{(a)} &= a_{ij}\tilde{\varphi}_{,j}^{(a)} + b_{ij}\tilde{\psi}_{,j}^{(a)},\\
\tilde{\tau}_i^{(a)} &= b_{ij}\tilde{\varphi}_{,j}^{(a)} + \delta_{ij}\tilde{\psi}_{,j}^{(a)},\\
\tilde{p}^{(a)} &= -B_{ij}\tilde{u}_{i,j}^{(a)} - \alpha_1\tilde{\varphi}^{(a)} - \alpha_3\tilde{\psi}^{(a)} + \gamma_1(\tilde{\theta}^{(a)} + \alpha s\tilde{\theta}^{(a)}),\\
\tilde{r}^{(a)} &= -D_{ij}\tilde{u}_{i,j}^{(a)} - \alpha_3\tilde{\varphi}^{(a)} - \alpha_2\tilde{\psi}^{(a)} + \gamma_2(\tilde{\theta}^{(a)} + \alpha s\tilde{\theta}^{(a)}),\\
\tilde{\eta}^{(a)} &= \beta_{ij}\tilde{u}_{i,j}^{(a)} + \gamma_1\tilde{\varphi}^{(a)} + \gamma_2\tilde{\psi}^{(a)} + c(\tilde{\theta}^{(a)} + \alpha s\tilde{\theta}^{(a)}).
\end{aligned} \tag{1.3.11}$$

Applying the Laplace transform to the equation (1.3.1), the image of the heat flux is given by:

$$\tilde{q}_i^{(a)} = -\theta_0(b_i s\tilde{\theta}^{(a)} + K_{ij}\tilde{\theta}_{,j}^{(a)}), \quad a = 1, 2. \tag{1.3.12}$$

The image of the boundary conditions (1.3.6) through the Laplace transform will be:

$$\begin{aligned}
&\tilde{u}_i^{(a)} = \tilde{u}_i^{b(a)} \ \text{ on } \ \partial B_1 \times [0,\infty), \quad \tilde{t}_i = \tilde{t}_i^{b(a)} \ \text{ on } \ \partial B_1^c \times [0,\infty),\\
&\tilde{\varphi}^{(a)} = \tilde{\varphi}^{b(a)} \ \text{ on } \ \partial B_2 \times [0,\infty), \quad \tilde{\lambda} = \tilde{\lambda}^{b(a)} \ \text{ on } \ \partial B_2^c \times [0,\infty),\\
&\tilde{\psi}^{(a)} = \tilde{\psi}^{b(a)} \ \text{ on } \ \partial B_3 \times [0,\infty), \quad \tilde{m} = \tilde{m}^{b(a)} \ \text{ on } \ \partial B_3^c \times [0,\infty),\\
&\tilde{\theta}^{(a)} = \tilde{\theta}^{b(a)} \ \text{ on } \ \partial B_4 \times [0,\infty), \quad \tilde{\nu} = \tilde{\nu}^{b(a)} \ \text{ on } \ \partial B_4^c \times [0,\infty), \qquad a = 1, 2,
\end{aligned} \tag{1.3.13}$$

where with b higher index was noted the value on the boundary. The relation $(1.3.9)_1$ for the two systems of loads is written:

$$\begin{aligned}
\rho s^2\tilde{u}_i^{(1)}\tilde{u}_i^{(2)} &= \tilde{t}_{ji,j}^{(1)}\tilde{u}_i^{(2)} + \rho\tilde{F}_i^{(1)}\tilde{u}_i^{(2)},\\
\rho s^2\tilde{u}_i^{(2)}\tilde{u}_i^{(1)} &= \tilde{t}_{ji,j}^{(2)}\tilde{u}_i^{(1)} + \rho\tilde{F}_i^{(2)}\tilde{u}_i^{(1)}.
\end{aligned}$$

Performing the subtraction between the last two relations and integrating on B we have:

$$\int_B \rho(\tilde{F}_i^{(1)}\tilde{u}_i^{(2)} - \tilde{F}_i^{(2)}\tilde{u}_i^{(1)})\,dV = \int_B (\tilde{t}_{ji}^{(1)}\tilde{u}_i^{(2)} - \tilde{t}_{ji}^{(2)}\tilde{u}_i^{(1)})_{,j}\,dV + \int_B (\tilde{t}_{ji}^{(2)}\tilde{u}_{i,j}^{(1)} - \tilde{t}_{ji}^{(1)}\tilde{u}_{i,j}^{(2)})\,dV. \tag{1.3.14}$$

For the first integral of (1.3.14) we apply the divergence theorem: and for the second integral of (1.3.14) we take into account the constitutive equations (1.3.11):

$$\begin{aligned}
&\int_B (\tilde{t}_{ji}^{(2)}\tilde{u}_{i,j}^{(1)} - \tilde{t}_{ji}^{(1)}\tilde{u}_{i,j}^{(2)})\,dV =\\
&\quad = \int_B \Big[C_{ijkl}\tilde{u}_{k,l}^{(2)} + B_{ij}\tilde{\varphi}^{(2)} + D_{ij}\tilde{\psi}^{(2)} + \beta_{ij}(\tilde{\theta}^{(2)} + \alpha s\tilde{\theta}^{(2)})\Big]\cdot\tilde{u}_{i,j}^{(1)} -\\
&\qquad - \Big[C_{ijkl}\tilde{u}_{k,l}^{(1)} + B_{ij}\tilde{\varphi}^{(1)} + D_{ij}\tilde{\psi}^{(1)} + \beta_{ij}(\tilde{\theta}^{(1)} + \alpha s\tilde{\theta}^{(1)})\Big]\cdot\tilde{u}_{i,j}^{(2)}\,dV =\\
&\quad = \int_B [B_{ij}(\tilde{\varphi}^{(2)}\tilde{u}_{i,j}^{(1)} - \tilde{\varphi}^{(1)}\tilde{u}_{i,j}^{(2)}) + D_{i,j}(\tilde{\psi}^{(2)}\tilde{u}_{i,j}^{(1)} - \tilde{\psi}^{(1)}\tilde{u}_{i,j}^{(2)}) -\\
&\qquad - \beta_{ij}(\tilde{\theta}^{(2)} + \alpha s\tilde{\theta}^{(2)})\tilde{u}_{i,j}^{(1)} + \beta_{ij}(\tilde{\theta}^{(1)} + \alpha s\tilde{\theta}^{(1)})\tilde{u}_{i,j}^{(2)}]\,dV.
\end{aligned} \tag{1.3.15}$$

Therefore, the relationship (1.3.14) becomes:

$$\begin{aligned}\int_B \rho(\tilde{F}_i^{(1)}\tilde{u}_i^{(2)} - \tilde{F}_i^{(2)}\tilde{u}_i^{(1)})\,dV = \\ = \int_{\partial B_1} (\tilde{t}_{ji}^{(1)}\tilde{u}_i^{b(2)} - \tilde{t}_{ji}^{(2)}\tilde{u}_i^{b(1)})n_j\,dA + \int_{\partial B_1^c} (\tilde{t}_i^{b(1)}\tilde{u}_i^{(2)} - \tilde{t}_i^{b(2)}\tilde{u}_i^{(1)})\,dA + \\ + \int_B [B_{ij}(\tilde{\varphi}^{(2)}\tilde{u}_{i,j}^{(1)} - \tilde{\varphi}^{(1)}\tilde{u}_{i,j}^{(2)}) + D_{ij}(\tilde{\psi}^{(2)}\tilde{u}_{i,j}^{(1)} - \tilde{\psi}^{(1)}\tilde{u}_{i,j}^{(2)}) - \\ -\beta_{ij}(1+\alpha s)(\tilde{\theta}^{(2)}\tilde{u}_{i,j}^{(1)} - \tilde{\theta}^{(1)}\tilde{u}_{i,j}^{(2)})]\,dV.\end{aligned} \tag{1.3.16}$$

We will proceed in an analogous way for the relation $(1.3.9)_2$ for the two systems of loads. Performing the subtraction between the two obtained relations and integrating on B we have:

$$\begin{aligned}\int_B \rho(\tilde{M}^{(1)}\tilde{\varphi}^{(2)} - \tilde{M}^{(2)}\tilde{\varphi}^{(1)})\,dV = \\ = \int_B (\tilde{\sigma}_j^{(2)}\tilde{\varphi}^{(1)} - \tilde{\sigma}_j^{(1)}\tilde{\varphi}^{(2)})_{,j}\,dV + \int_B (\tilde{\sigma}_j^{(1)}\tilde{\varphi}_{,j}^{(2)} - \tilde{\sigma}_j^{(2)}\tilde{\varphi}_{,j}^{(1)})\,dV + \\ + \int_B (\tilde{p}^{(2)}\tilde{\varphi}^{(1)} - \tilde{p}^{(1)}\tilde{\varphi}^{(2)})\,dV.\end{aligned} \tag{1.3.17}$$

In the integrals from the relation (1.3.16) we apply the divergence theorem and we take into account the constitutive equations. Therefore the relation (1.3.17) will have the following form:

$$\begin{aligned}\int_B \rho(\tilde{M}^{(1)}\tilde{\varphi}^{(2)} - \tilde{M}^{(2)}\tilde{\varphi}^{(1)})\,dV = \\ = \int_{\partial B_2^c} (\tilde{\alpha}^{b(2)}\tilde{\varphi}^{(1)} - \tilde{\alpha}^{b(1)}\tilde{\varphi}^{(2)})\,dA + \int_{\partial B_2} (\tilde{\sigma}_j^{(2)}\tilde{\varphi}^{b(1)} - \tilde{\sigma}_j^{(1)}\tilde{\varphi}^{b(2)})n_j\,dA + \\ + \int_B b_{ij}(\tilde{\psi}_{,j}^{(1)}\tilde{\varphi}_{,j}^{(2)} - \tilde{\psi}_{,j}^{(2)}\tilde{\varphi}_{,j}^{(1)})\,dV + \int_B [-B_{ij}(\tilde{u}_{i,j}^{(2)}\tilde{\varphi}^{(1)} - \tilde{u}_{i,j}^{(1)}\tilde{\varphi}^{(2)}) - \\ -\alpha_3(\tilde{\psi}^{(2)}\tilde{\varphi}^{(1)} - \tilde{\psi}^{(1)}\tilde{\varphi}^{(2)}) + \gamma_1(1+\alpha s)(\tilde{\varphi}^{(1)}\tilde{\theta}^{(2)} - \tilde{\varphi}^{(2)}\tilde{\theta}^{(1)})]\,dV.\end{aligned} \tag{1.3.18}$$

For the third equation from (1.3.9) we perform the substraction between the relations of the two loading systems and by integration on B we obtain:

$$\begin{aligned}\int_B \rho(\tilde{N}^{(1)}\tilde{\psi}^{(2)} - \tilde{N}^{(2)}\tilde{\psi}^{(1)})\,dV = \\ = \int_B (\tilde{\tau}_j^{(2)}\tilde{\psi}^{(1)} - \tilde{\tau}_j^{(1)}\tilde{\psi}^{(2)})_{,j}\,dV + \int_B (\tilde{\tau}_j^{(1)}\tilde{\psi}_{,j}^{(2)} - \tilde{\tau}_j^{(2)}\tilde{\psi}_{,j}^{(1)})\,dV + \\ + \int_B (\tilde{r}^{(2)}\tilde{\psi}^{(1)} - \tilde{r}^{(1)}\tilde{\psi}^{(2)})\,dV.\end{aligned} \tag{1.3.19}$$

Using the divergence theorem and take into account the constitutive equations the

relation (1.3.19) becomes:

$$\begin{aligned}\int_B \rho(\tilde{L}^{(1)}\tilde{\psi}^{(2)} - \tilde{L}^{(2)}\tilde{\psi}^{(1)})\,dV = \\ = \int_{\partial B_3^c} (\tilde{\beta}^{b(2)}\tilde{\psi}^{(1)} - \tilde{\beta}^{b(1)}\tilde{\psi}^{(2)})\,dA + \int_{\partial B_3} (\tilde{\tau}_j^{(2)}\tilde{\psi}^{b(1)} - \tilde{\tau}_j^{(1)}\tilde{\psi}^{b(2)})n_j\,dA + \\ + \int_B b_{ij}(\tilde{\varphi}_{,j}^{(1)}\tilde{\psi}_{,j}^{(2)} - \tilde{\varphi}_{,j}^{(2)}\tilde{\psi}_{,j}^{(1)})\,dV + \int_B D_{ij}(\tilde{u}_{i,j}^{(1)}\tilde{\psi}^{(2)} - \tilde{u}_{i,j}^{(2)}\tilde{\psi}^{(1)}) + \\ + \alpha_3(\tilde{\varphi}^{(1)}\tilde{\psi}^{(2)} - \tilde{\varphi}^{(2)}\tilde{\psi}^{(1)}) + \gamma_2(1+\alpha s)(\tilde{\psi}^{(1)}\tilde{\theta}^{(2)} - \tilde{\psi}^{(2)}\tilde{\theta}^{(1)})\,dV.\end{aligned} \tag{1.3.20}$$

The last step into obtaining the results of the theorem Th[1.3.1] is to write the energy equation (1.3.10) for the two loads and to repeat the same procedure as above using the substraction of the two relations written for the both loading systems and by integration on B we obtain:

$$\begin{aligned}\int_B \rho\beta_{ij}s\left(\tilde{u}_{i,j}^{(1)}\tilde{\theta}^{(2)} - \tilde{u}_{i,j}^{(2)}\tilde{\theta}^{(1)}\right) + \rho\gamma_2 s\left(\tilde{\psi}^{(1)}\tilde{\theta}^{(2)} - \tilde{\psi}^{(2)}\tilde{\theta}^{(1)}\right) + \\ + \rho\gamma_1 s\left(\tilde{\varphi}^{(1)}\tilde{\theta}^{(2)} - \tilde{\varphi}^{(2)}\tilde{\theta}^{(1)}\right) + b_i s\left(\tilde{\theta}_{,i}^{(1)}\tilde{\theta}^{(2)} - \tilde{\theta}_{,i}^{(2)}\tilde{\theta}^{(1)}\right) + \\ + K_{ij}\left(\tilde{\theta}_{,ij}^{(1)}\tilde{\theta}^{(2)} - \tilde{\theta}_{,ij}^{(2)}\tilde{\theta}^{(1)}\right) - \frac{\rho}{\theta_0}\left(\tilde{\delta}^{(1)}\tilde{\theta}^{(2)} - \tilde{\delta}^{(2)}\tilde{\theta}^{(1)}\right)\,dV = 0.\end{aligned} \tag{1.3.21}$$

We apply the divergence theorem and take into account the boundary conditions (1.3.13) and the equation (1.3.12), the relation (1.3.21) becomes:

$$\begin{aligned}\int_B \rho\beta_{ij}s\left(\tilde{u}_{i,j}^{(1)}\tilde{\theta}^{(2)} - \tilde{u}_{i,j}^{(2)}\tilde{\theta}^{(1)}\right) + \rho\gamma_1 s\left(\tilde{\varphi}^{(1)}\tilde{\theta}^{(2)} - \tilde{\varphi}^{(2)}\tilde{\theta}^{(1)}\right) - \\ - \frac{\rho}{\theta_0}\left(\tilde{\delta}^{(1)}\tilde{\theta}^{(2)} - \tilde{\delta}^{(2)}\tilde{\theta}^{(1)}\right) + \rho\gamma_2 s\left(\tilde{\psi}^{(1)}\tilde{\theta}^{(2)} - \tilde{\psi}^{(2)}\tilde{\theta}^{(1)}\right)\,dV + \\ + \frac{1}{\theta_0}\int_{\partial B_4^c}\left(\tilde{\theta}^{(1)}\tilde{\nu}^{b(2)} - \tilde{\theta}^{(2)}\tilde{\nu}^{b(1)}\right)\,dA + \frac{1}{\theta_0}\int_{\partial B_4}\left(\tilde{\theta}^{b(1)}\tilde{q}_i^{(2)} - \tilde{\theta}^{b(2)}\tilde{q}_i^{(1)}\right)n_i\,dA - \\ - \frac{1}{\theta_0}\int_B\left(\tilde{\theta}_{,i}^{(1)}\tilde{q}_i^{(2)} - \tilde{\theta}_{,i}^{(2)}\tilde{q}_i^{(1)}\right)\,dV = 0.\end{aligned} \tag{1.3.22}$$

We notice that in (1.3.22) there are terms from (1.3.16), (1.3.18) and (1.3.20). Thus, from (1.3.16) we obtain:

$$\begin{aligned}\int_B \rho\beta_{ij}s\left(\tilde{\theta}^{(2)}\tilde{u}_{i,j}^{(1)} - \tilde{\theta}^{(1)}\tilde{u}_{i,j}^{(2)}\right)\,dV = \\ \Big[\int_{\partial B_1}\left(\tilde{t}_{ji}^{(1)}\tilde{u}_i^{b(2)} - \tilde{t}_{ji}^{(2)}\tilde{u}_i^{b(1)}\right)n_j\,dA + \int_{\partial B_1^c}\left(\tilde{t}_i^{b(1)}\tilde{u}_i^{(2)} - \tilde{t}_i^{b(2)}\tilde{u}_i^{(1)}\right)\,dA + \\ + \int_B\left[B_{ij}\left(\tilde{\varphi}^{(2)}\tilde{u}_{i,j}^{(1)} - \tilde{\varphi}^{(1)}\tilde{u}_{i,j}^{(2)}\right) + D_{ij}\left(\tilde{\psi}^{(2)}\tilde{u}_{i,j}^{(1)} - \tilde{\psi}^{(1)}\tilde{u}_{i,j}^{(2)}\right)\right]\,dV - \\ - \int_B \rho\left(\tilde{F}_i^{(1)}\tilde{u}_i^{(2)} - \tilde{F}_i^{(2)}\tilde{u}_i^{(1)}\right)\,dV\Big]\cdot\frac{\rho s}{1+\alpha s}.\end{aligned} \tag{1.3.23}$$

From (1.3.18) we obtain:

$$\begin{aligned}
&\int\limits_B \rho\gamma_1 s\left(\tilde{\varphi}^{(1)}\tilde{\theta}^{(2)}-\tilde{\varphi}^{(2)}\tilde{\theta}^{(1)}\right)\,dV=\\
&=[\int\limits_B \rho\left(\tilde{M}^{(1)}\tilde{\varphi}^{(2)}-\tilde{M}^{(2)}\tilde{\varphi}^{(1)}\right)\,dV-\int\limits_{\partial B_2^c}\left(\tilde{\lambda}^{b(2)}\tilde{\varphi}^{(1)}-\tilde{\lambda}^{b(1)}\tilde{\varphi}^{(2)}\right)\,dA-\\
&-\int\limits_{\partial B_2}\left(\tilde{\sigma}_j^{(2)}\tilde{\varphi}^{b(1)}-\tilde{\sigma}_j^{(1)}\tilde{\varphi}^{b(2)}\right)n_j\,dA-\int\limits_B b_{ij}\left(\tilde{\psi}_{,j}^{(1)}\tilde{\varphi}_{,j}^{(2)}-\tilde{\psi}_{,j}^{(2)}\tilde{\varphi}_{,j}^{(1)}\right)\,dV+\\
&+\int\limits_B\left[B_{ij}\left(\tilde{u}_{i,j}^{(2)}\tilde{\varphi}^{(1)}-\tilde{u}_{i,j}^{(1)}\tilde{\varphi}^{(2)}\right)+\alpha_3\left(\tilde{\psi}^{(2)}\tilde{\varphi}^{(1)}-\tilde{\psi}^{(1)}\tilde{\varphi}^{(2)}\right)\right]\,dV]\cdot\tfrac{\rho s}{1+\alpha s}.
\end{aligned}\tag{1.3.24}$$

From (1.3.20) we obtain:

$$\begin{aligned}
&\int\limits_B \rho\gamma_2 s\left(\tilde{\psi}^{(1)}\tilde{\theta}^{(2)}-\tilde{\psi}^{(2)}\tilde{\theta}^{(1)}\right)\,dV=\\
&=[\int\limits_B \rho\left(\tilde{N}^{(1)}\tilde{\psi}^{(2)}-\tilde{N}^{(2)}\tilde{\psi}^{(1)}\right)\,dV-\int\limits_{\partial B_3^c}\left(\tilde{m}^{b(2)}\tilde{\psi}^{(1)}-\tilde{m}^{b(1)}\tilde{\psi}^{(2)}\right)\,dA-\\
&-\int\limits_{\partial B_3}\left(\tilde{\tau}_j^{(2)}\tilde{\psi}^{b(1)}-\tilde{\tau}_j^{(1)}\tilde{\psi}^{b(2)}\right)n_j\,dA-\int\limits_B b_{ij}\left(\tilde{\varphi}_{,j}^{(1)}\tilde{\psi}_{,j}^{(2)}-\tilde{\varphi}_{,j}^{(2)}\tilde{\psi}_{,j}^{(1)}\right)\,dV-\\
&-\int\limits_B\left[D_{ij}\left(\tilde{u}_{i,j}^{(1)}\tilde{\psi}^{(2)}-\tilde{u}_{i,j}^{(2)}\tilde{\psi}^{(1)}\right)+\alpha_3\left(\tilde{\varphi}^{(1)}\tilde{\psi}^{(2)}-\tilde{\varphi}^{(2)}\tilde{\psi}^{(1)}\right)\right]\,dV]\cdot\tfrac{\rho s}{1+\alpha s}.
\end{aligned}\tag{1.3.25}$$

By replacing the relations (1.3.23)-(1.3.25) in the relation (1.3.22), we obtain:

$$\begin{aligned}
&\tfrac{\rho s}{1+\alpha s}\cdot[\int\limits_{\partial B_1}\left(\tilde{t}_{ij}^{(1)}\tilde{u}_i^{b(2)}-\tilde{t}_{ji}^{(2)}\tilde{u}_i^{b(1)}\right)n_j\,dA+\int\limits_{\partial B_1^c}\left(\tilde{t}_i^{b(1)}\tilde{u}_i^{(2)}-\tilde{t}_i^{b(2)}\tilde{u}_i^{(1)}\right)\,dA+\\
&+\int\limits_B\Big[B_{ij}\left(\tilde{\varphi}^{(2)}\tilde{u}_{i,j}^{(1)}-\tilde{\varphi}^{(1)}\tilde{u}_{i,j}^{(2)}\right)+D_{ij}\left(\tilde{\psi}^{(2)}\tilde{u}_{i,j}^{(1)}-\tilde{\psi}^{(1)}\tilde{u}_{i,j}^{(2)}\right)-\\
&-\rho\left(\tilde{F}_i^{(1)}\tilde{u}_i^{(2)}-\tilde{F}_i^{(2)}\tilde{u}_i^{(1)}\right)\Big]\,dV+\\
&+\int\limits_B\rho\left(\tilde{M}^{(1)}\tilde{\varphi}^{(2)}-\tilde{M}^{(2)}\tilde{\varphi}^{(1)}\right)\,dV-\int\limits_{\partial B_2^c}\left(\tilde{\lambda}^{b(2)}\tilde{\varphi}^{(1)}-\tilde{\lambda}^{b(1)}\tilde{\varphi}^{(2)}\right)\,dA-\\
&-\int\limits_{\partial B_2}\left(\tilde{\sigma}_j^{(2)}\tilde{\varphi}^{b(1)}-\tilde{\sigma}_j^{(1)}\tilde{\varphi}^{b(2)}\right)n_j\,dA-\int\limits_B b_{ij}\left(\tilde{\psi}_{,j}^{(1)}\tilde{\varphi}_{,j}^{(2)}-\tilde{\psi}_{,j}^{(2)}\tilde{\varphi}_{,j}^{(1)}\right)\,dV+\\
&+\int\limits_B\left[B_{ij}\left(\tilde{u}_{i,j}^{(2)}\tilde{\varphi}^{(1)}-\tilde{u}_{i,j}^{(1)}\tilde{\varphi}^{(2)}\right)+\alpha_3\left(\tilde{\psi}^{(2)}\tilde{\varphi}^{(1)}-\tilde{\psi}^{(1)}\tilde{\varphi}^{(2)}\right)\right]\,dV+\\
&+\int\limits_B\rho\left(\tilde{N}^{(1)}\tilde{\psi}^{(2)}-\tilde{N}^{(2)}\tilde{\psi}^{(1)}\right)\,dV-\int\limits_{\partial B_3^c}\left(\tilde{m}^{b(2)}\tilde{\psi}^{(1)}-\tilde{m}^{b(1)}\tilde{\psi}^{(2)}\right)\,dA-\\
&-\int\limits_{\partial B_3}\left(\tilde{\tau}_j^{(2)}\tilde{\psi}^{b(1)}-\tilde{\tau}_j^{(1)}\tilde{\psi}^{b(2)}\right)n_j\,dA-\int\limits_B b_{ij}\left(\tilde{\varphi}_{,j}^{(1)}\tilde{\psi}_{,j}^{(2)}-\tilde{\varphi}_{,j}^{(2)}\tilde{\psi}_{,j}^{(1)}\right)\,dV-\\
&-\int\limits_B\left[D_{ij}\left(\tilde{u}_{i,j}^{(1)}\tilde{\psi}^{(2)}-\tilde{u}_{i,j}^{(2)}\tilde{\psi}^{(1)}\right)+\alpha_3\left(\tilde{\varphi}^{(1)}\tilde{\psi}^{(2)}-\tilde{\varphi}^{(2)}\tilde{\psi}^{(1)}\right)\right]\,dV]=\\
&=\int\limits_B\tfrac{\rho}{\theta_0}\left(d\tilde{elta}^{(1)}\tilde{\theta}^{(2)}-d\tilde{elta}^{(2)}\tilde{\theta}^{(1)}\right)\,dV-\tfrac{1}{\theta_0}\int\limits_{\partial B_4^c}\left(\tilde{\theta}^{(1)}\tilde{\nu}^{b(2)}-\tilde{\theta}^{(2)}\tilde{\nu}^{b(1)}\right)\,dA-\\
&-\tfrac{1}{\theta_0}\int\limits_{\partial B_4}\left(\tilde{\theta}^{b(1)}\tilde{q}_i^{(2)}-\tilde{\theta}^{b(2)}\tilde{q}_i^{(1)}\right)n_i\,dA+\tfrac{1}{\theta_0}\int\limits_B\left(\tilde{\theta}_{,i}^{(1)}\tilde{q}_i^{(2)}-\tilde{\theta}_{,i}^{(2)}\tilde{q}_i^{(1)}\right)\,dV,
\end{aligned}$$

which leads to:

$$\begin{aligned}\rho s\cdot[-\int\limits_B \rho\left(\tilde F_i^{(1)}\tilde u_i^{(2)}-\tilde F_i^{(2)}\tilde u_i^{(1)}\right)\,dV+\int\limits_B \rho\left(\tilde M^{(1)}\tilde\varphi^{(2)}-\tilde M^{(2)}\tilde\varphi^{(1)}\right)\,dV+\\ +\int\limits_B \rho\left(\tilde N^{(1)}\tilde\psi^{(2)}-\tilde N^{(2)}\tilde\psi^{(1)}\right)\,dV+\\ +\int\limits_{\partial B_1}\left(\tilde t_{ij}^{(1)}\tilde u_i^{b(2)}-\tilde t_{ji}^{(2)}\tilde u_i^{b(1)}\right)n_j\,dA+\int\limits_{\partial B_1^c}\left(\tilde t_i^{b(1)}\tilde u_i^{(2)}-\tilde t_i^{b(2)}\tilde u_i^{(1)}\right)\,dA+\\ +\int\limits_{\partial B_2}\left(\tilde\sigma_j^{(1)}\tilde\varphi^{b(2)}-\tilde\sigma_j^{(2)}\tilde\varphi^{b(1)}\right)n_j\,dA+\int\limits_{\partial B_2^c}\left(\tilde\lambda^{b(1)}\tilde\varphi^{(2)}-\tilde\lambda^{b(2)}\tilde\varphi^{(1)}\right)\,dA+\\ +\int\limits_{\partial B_3}\left(\tilde\tau_j^{(1)}\tilde\psi^{b(2)}-\tilde\tau_j^{(2)}\tilde\psi^{b(1)}\right)n_j\,dA+\int\limits_{\partial B_3^c}\left(\tilde m^{b(1)}\tilde\psi^{(2)}-\tilde m^{b(2)}\tilde\psi^{(1)}\right)\,dA]=\\ =(1+\alpha s)\cdot\tfrac{1}{\theta_0}[\int\limits_B \rho\left(\tilde\delta^{(1)}\tilde\theta^{(2)}-\tilde\delta^{(2)}\tilde\theta^{(1)}\right)\,dV+\int\limits_B\left(\tilde\theta_{,i}^{(1)}\tilde q_i^{(2)}-\tilde\theta_{,i}^{(2)}\tilde q_i^{(1)}\right)\,dV-\\ -\int\limits_{\partial B_4}\left(\tilde\theta^{b(1)}\tilde q_i^{(2)}-\tilde\theta^{b(2)}\tilde q_i^{(1)}\right)n_i\,dA-\int\limits_{\partial B_4^c}\left(\tilde\theta^{(1)}\tilde\nu^{b(2)}-\tilde\theta^{(2)}\tilde\nu^{b(1)}\right)\,dA].\end{aligned}\tag{1.3.26}$$

We will apply the inverse Laplace transform to the relation (1.3.26) and we will take into account the convolution product. We will also take into account:

$$s\tilde F_i^{(1)}\tilde u_i^{(2)}=\tilde F_i^{(1)}\cdot s\cdot\tilde u_i^{(2)}=L\left[F_i^{(1)}\right]\cdot L\left[\tfrac{\partial u_i^{(2)}}{\partial t}\right]=F_i^{(1)}*\hat u_i^{(2)},$$

where $\hat u_i^{(2)}=\frac{\partial u_i^{(2)}}{\partial t}$. The result of Theorem Th[1.3.1] is obtained immediately. □

In order to obtain a uniqueness result for the mixed problem with initial values and boundary values considered above, we will use the generalized free energy function, ω, proposed by Biot as follows:

$$\omega=\Psi-\eta\theta_0,\tag{1.3.27}$$

which leads to the fact that the internal energy, Ψ, has the following expression:

$$\Psi=\omega+\eta\theta_0.$$

Green and Lindsay introduce the scalar function

$$\phi=\theta_0+\theta+\alpha\dot\theta+\beta\theta\dot\theta+\frac{1}{2}\gamma\dot\theta^2,$$

and the exprssion of the energy function is:

$$\xi=\Psi-\eta\phi=\omega+\eta\theta_0-\eta\theta_0-\eta\theta-\eta\alpha\dot\theta-\eta\beta\theta\dot\theta-\frac{1}{2}\eta\gamma\dot\theta^2.\tag{1.3.28}$$

Taking into account the constitutive equations The energy function can be written in the following form:

$$\begin{aligned}\xi\ &=\tfrac{1}{2}C_{ijkl}u_{k,l}u_{i,j}+B_{ij}\varphi u_{i,j}+D_{ij}\psi u_{i,j}+\tfrac{1}{2}a_{ij}\varphi_{,i}\varphi_{,j}+b_{ij}\varphi_{,i}\psi_{,j}+\\ &+\tfrac{1}{2}\delta_{ij}\psi_{,i}\psi_{,j}+\tfrac{1}{2}\alpha_1\varphi^2+\tfrac{1}{2}\alpha_2\psi^2+\alpha_3\varphi\psi+b_i\theta_0\dot\theta\theta_{,i}+\tfrac{1}{2}\theta_0K_{ij}\theta_{,i}\theta_{,j}-\\ &-a(\theta+\alpha\dot\theta)-\tfrac{c}{2}\theta^2-e\theta\dot\theta-f\dot\theta^2-c\beta\theta^2\dot\theta-c\alpha\beta\theta\dot\theta^2-\tfrac{1}{2}c\gamma\theta\dot\theta^2-\tfrac{1}{2}c\alpha\gamma\dot\theta^3,\end{aligned}\tag{1.3.29}$$

where:

$$\begin{aligned}
a &= 2(\beta_{ij}u_{i,j} + \gamma_1\varphi + \gamma_2\psi),\\
e &= (\beta_{ij}u_{i,j} + \gamma_1\varphi + \gamma_2\psi)\beta + c\alpha = \tfrac{a\beta}{2} + c\alpha,\\
f &= (\beta_{ij}u_{i,j} + \gamma_1\varphi + \gamma_2\psi)\tfrac{\gamma}{2} + \tfrac{c\alpha^2}{2} = \tfrac{a\gamma}{4} + \tfrac{c\alpha^2}{2}.
\end{aligned}$$

Taking into account the initial conditions, the quadratic form of the energy function is obtained according to Biot:

$$\begin{aligned}
\omega = \tfrac{1}{2}C_{ijkl}u_{k,l}u_{i,j} + B_{ij}\varphi u_{i,j} + D_{ij}\psi u_{i,j} + \tfrac{1}{2}a_{ij}\varphi_{,i}\varphi_{,j} + b_{ij}\varphi_{,i}\psi_{,j} +\\
+\tfrac{1}{2}\delta_{ij}\psi_{,i}\psi_{,j} + \tfrac{1}{2}\alpha_1\varphi^2 + \tfrac{1}{2}\alpha_2\psi^2 + \alpha_3\varphi\psi + b_i\theta_0\dot{\theta}\theta_{,i} + \tfrac{1}{2}\theta_0 K_{ij}\theta_{,i}\theta_{,j} +\\
+\tfrac{1}{2}c\theta^2 + c\alpha\theta\dot{\theta} + \tfrac{\alpha^2 c}{2}\dot{\theta}^2.
\end{aligned} \tag{1.3.30}$$

Theorem 1.3.2. *The energy equation in the context of Green Lindsay thermoelasticity for double porosity bodies has the following form:*

$$\begin{aligned}
\tfrac{d}{dt}\int\limits_B (\xi_c + \omega)\ dV =\\
= \rho\int\limits_B \left(F_i\dot{u}_i + M\dot{\varphi} + N\dot{\psi} + \tfrac{h}{\theta_0}\left(\theta + \alpha\dot{\theta}\right)\right)\ dV +\\
+\int\limits_{\partial B}\left(t_{ji}\dot{u}_i + \sigma_j\dot{\varphi} + \tau_j\dot{\psi}\right)n_i\ dA +\\
+\tfrac{1}{\rho}\int\limits_{\partial B}\left[\tfrac{q_i}{\theta_0}\left(\theta + \alpha\dot{\theta}\right) + q_i\dot{\theta}\right]n_i\ dA + \int\limits_{\partial B} b_i\theta_0\theta\ddot{\theta}n_i\ dA.
\end{aligned} \tag{1.3.31}$$

Proof. We consider the kinetic energy of the body with double porosity

$$\xi_c = \frac{1}{2}\rho\left[\dot{u}_i(t)\right]^2 + \frac{1}{2}\kappa_1\left[\dot{\varphi}(t)\right]^2 + \frac{1}{2}\kappa_2\left[\dot{\psi}(t)\right]^2, \tag{1.3.32}$$

whose derivative in relation to time is:

$$\frac{d\xi_c}{dt} = \rho\dot{u}_i(t)\ddot{u}_i(t) + \kappa_1\dot{\varphi}(t)\ddot{\varphi}(t) + \kappa_2\dot{\psi}(t)\ddot{\psi}(t). \tag{1.3.33}$$

Multiplying by $\dot{u}_i(t), \dot{\phi}(t)$ and $\dot{\psi}(t)$ the equations (1.1.1) and $(1.1.2)_1$, respectively, we have:

$$\begin{aligned}
\rho\ddot{u}_i\dot{u}_i &= t_{ji,j}\dot{u}_i + \rho F_i\dot{u}_i,\\
\kappa_1\ddot{\varphi}\dot{\varphi} &= \sigma_{j,j}\dot{\varphi} + p\dot{\varphi} + \rho M\dot{\varphi},\\
\kappa_2\ddot{\psi}\dot{\psi} &= \tau_{j,j}\dot{\psi} + r\dot{\psi} + \rho N\dot{\psi}.
\end{aligned} \tag{1.3.34}$$

We replace (1.3.33) in (1.3.34) and we have:

$$\begin{aligned}
\tfrac{d\xi_c}{dt} = t_{ji,j}\dot{u}_i + \rho F_i\dot{u}_i + \sigma_{j,j}\dot{\varphi} + p\dot{\varphi} + \rho M\dot{\varphi} + \tau_{j,j}\dot{\psi} + r\dot{\psi} + \rho N\dot{\psi} =\\
= \rho F_i\dot{u}_i + \rho M\dot{\varphi} + \rho N\dot{\psi} + p\dot{\varphi} + r\dot{\psi} + (t_{ji}\dot{u}_i)_{,j} - t_{ji}\dot{u}_{i,j} +\\
+(\sigma_j\dot{\varphi})_{,j} - \sigma_j\dot{\varphi}_{,j} + (\tau_j\dot{\psi})_{,j} - \tau_j\dot{\psi}_{,j}.
\end{aligned} \tag{1.3.35}$$

We will integrate (1.3.35) on the domain B and apply the divergence theorem:

$$\begin{aligned}\frac{d}{dt}\int\limits_B \xi_c(t)\,dV = \int\limits_B \left(\rho F_i\dot{u}_i + \rho G\dot{\varphi} + \rho L\dot{\psi} + p\dot{\varphi} + r\dot{\psi}\right)\,dV - \\ - \int\limits_B \left(t_{ji}\dot{u}_{i,j} + \sigma_j\dot{\varphi}_{,j} + \tau_j\dot{\psi}_{,j}\right)\,dV + \\ + \int\limits_{\partial B} t_{ji}\dot{u}_i n_i\,dA + \int\limits_{\partial B}\sigma_j\dot{\varphi}n_i\,dA + \int\limits_{\partial B}\tau_j\dot{\psi}n_i\,dA = \\ = \int\limits_B \left(\rho F_i\dot{u}_i + \rho G\dot{\varphi} + \rho L\dot{\psi}\right)\,dV + \\ + \int\limits_B [-B_{ij}u_{i,j}\dot{\varphi} - \alpha_1\varphi\dot{\varphi} - \alpha_3\psi\dot{\varphi} + \gamma_1\left(\theta + \alpha\dot{\theta}\right)\dot{\varphi} - \\ - D_{ij}u_{i,j}\dot{\psi} - \alpha_3\varphi\dot{\psi} - \alpha_2\psi\dot{\psi} + \gamma_2\left(\theta + \alpha\dot{\theta}\right)\dot{\psi} - \\ - C_{ijkl}u_{k,l}\dot{u}_{i,j} - B_{ij}\varphi\dot{u}_{i,j} - D_{ij}\psi\dot{u}_{i,j} + \beta_{ij}\left(\theta + \alpha\dot{\theta}\right)\dot{u}_{i,j} - \\ - a_{ij}\varphi_{,j}\dot{\varphi}_{,j} - b_{ij}\psi_{,j}\dot{\varphi}_{,j} - b_{ij}\varphi_{,j}\dot{\psi}_{,j} - \delta_{ij}\psi_{,j}\dot{\varphi}_{,j}]\,dV + \\ + \int\limits_{\partial B} t_{ji}\dot{u}_i n_i\,dA + \int\limits_{\partial B}\sigma_j\dot{\varphi}n_i\,dA + \int\limits_{\partial B}\tau_j\dot{\psi}n_i\,dA.\end{aligned} \tag{1.3.36}$$

We derive (1.3.30) in relation to time:

$$\begin{aligned}\frac{d}{dt}\omega = C_{ijkl}u_{k,l}\dot{u}_{i,j} + B_{ij}\varphi\dot{u}_{i,j} + B_{ij}\dot{\varphi}u_{i,j} + D_{ij}\dot{\psi}u_{i,j} + D_{ij}\psi\dot{u}_{i,j} + \\ + a_{ij}\varphi_{,i}\dot{\varphi}_{,j} + b_{ij}\dot{\varphi}_{,i}\psi_{,j} + \delta_{ij}\psi_{,i}\dot{\psi}_{,j} + \alpha_1\varphi\dot{\varphi} + \alpha_2\psi\dot{\psi} + \alpha_3\varphi\dot{\psi} + \\ + b_i\theta_0\ddot{\theta}\theta_{,i} + b_i\theta_0\dot{\theta}\dot{\theta}_{,i} + \theta_0 K_{ij}\theta_{,i}\dot{\theta}_{,j} + c\theta\dot{\theta} + c\alpha\dot{\theta}^2 + c\alpha\theta\ddot{\theta} + c\alpha^2\dot{\theta}\ddot{\theta}.\end{aligned} \tag{1.3.37}$$

We will add (1.3.36) to (1.3.37) and we obtain:

$$\begin{aligned}\frac{d}{dt}\int\limits_B (\xi_c + \omega)\,dV = \int\limits_B \left(\rho F_i\dot{u}_i + \rho M\dot{\varphi} + \rho N\dot{\psi}\right)\,dV + \\ + \int\limits_B \left(\gamma_1\dot{\varphi} + \gamma_2\dot{\psi} + \beta_{ij}\dot{u}_{i,j}\right)\left(\theta + \alpha\dot{\theta}\right)\,dV + \\ + \int\limits_B b_i\theta_0\ddot{\theta}\theta_{,i} + b_i\theta_0\dot{\theta}\dot{\theta}_{,i} + \theta_0 K_{ij}\theta_{,i}\dot{\theta}_{,j} + c\theta\dot{\theta} + c\alpha\dot{\theta}^2 + c\alpha\theta\ddot{\theta} + c\alpha^2\dot{\theta}\ddot{\theta}\,dV + \\ + \int\limits_{\partial B} t_{ji}\dot{u}_i n_i\,dA + \int\limits_{\partial B}\sigma_j\dot{\varphi}n_i\,dA + \int\limits_{\partial B}\tau_j\dot{\psi}n_i\,dA.\end{aligned} \tag{1.3.38}$$

We take into account (1.3.1) and we obtain:

$$\theta_0\left(b_i\dot{\theta} + K_{ij}\theta_{,i}\right)\dot{\theta}_{,j} = -q_i\dot{\theta}_{,j}. \tag{1.3.39}$$

From (1.3.4) we obtain:

$$\beta_{ij}\dot{u}_{i,j} + \gamma_1\dot{\varphi} + \gamma_2\dot{\psi} = \frac{h}{\theta_0} - c\dot{\theta} - c\alpha\ddot{\theta} - \frac{1}{\rho}b_i\dot{\theta}_{,i} - \frac{1}{\rho}K_{ij}\theta_{,ij}. \tag{1.3.40}$$

From the above relations (1.3.38)-(1.3.40) we have:

$$\begin{aligned}\frac{d}{dt}\int\limits_B (\xi_c + \omega)\,dV = \rho\int\limits_B \left(F_i\dot{u}_i + M\dot{\varphi} + N\dot{\psi} + \tfrac{h}{\theta_0}\left(\theta + \alpha\dot{\theta}\right)\right)\,dV + \\ + \int\limits_{\partial B}\left(t_{ji}\dot{u}_i + \sigma_j\dot{\varphi} + \tau_j\dot{\psi}\right)n_i\,dA + \tfrac{1}{\rho}\int\limits_{\partial B}\tfrac{q_i}{\theta_0}\left(\theta + \alpha\dot{\theta}\right)n_i\,dA + \\ + \int\limits_{\partial B} b_i\theta_0\ddot{\theta}\theta n_i\,dA + \int\limits_{\partial B} q_i\dot{\theta}n_i\,dA.\end{aligned} \tag{1.3.41}$$

□

Theorem 1.3.3. *The mixed problem for double porous bodies admits a unique solution if the energy function of Biot, ω, from* (1.3.27) *is positively defined.*

Proof. We consider that the mixed problem admits two solutions: $S_1 = (u_i^{(1)}, \varphi^{(1)}, \psi^{(1)}, \theta^{(1)})$ and $S_2 = (u_i^{(2)}, \varphi^{(2)}, \psi^{(2)}, \theta^{(2)})$.

The difference between the two solutions is also a solution of the mixed problem for double porous bodies: $S_1 = (u_i^{(1)} - u_i^{(2)}, \varphi^{(1)} - \varphi^{(2)}, \psi^{(1)} - \psi^{(2)}, \theta^{(1)} - \theta^{(2)})$.

We notice that this difference leads to zero loads: $F_i \equiv 0$, $M \equiv 0$, $N \equiv 0$.

If we take into account the zero conditions on the boundary then the energy equation (1.3.41) is reduced to:

$$\frac{d}{dt}\int\limits_B (\xi_c + \omega)\ dV = \int\limits_{\partial B} \left(\frac{q_i}{\rho\theta_0}\left(\theta + \alpha\dot{\theta}\right) + \frac{q_i}{\rho}\dot{\theta} + b_i\theta_0\theta\ddot{\theta}n_i \right)\ dA.$$

We take into account (1.3.1) and we have: $\frac{d}{dt}\int\limits_B (\xi_c + \omega)\ dV \leq 0$ for $\forall t \geq 0$.

If we take into account the initial conditions (1.3.8) at the moment $t = 0$ we have: $\xi_c = \omega = 0$.

But as ξ_c and ω are positively defined it follows that $\xi_c = \omega = 0, \forall t \geq 0$.

From this we deduce that the difference S is zero, so the problem admits a unique solution.

□

Chapter 2

Advanced Numerical Methods in Nonlinear Dynamical Systems

2.1 Fractional Features of a Double Pendulum System

In real world we face many forms of motion (e.g, periodic, quasiperiodic, and chaotic). Some physical systems undergo only one form of these motions, while other systems can have more than one form of motion. Two important physical systems appear in real world problems: pendulums, and oscillators. In classical mechanics texts, one can find many interesting examples about pendulums, oscillators, and other systems for example, one can refer to the classical texts [Landau(1976)], [Hand(1995)], [Marion(1988)],[Fowles(2005)].

These systems (e.g, pendulum or oscillators) can be investigated by two classical methods: The first method depends on vector concepts (i.e, forces acting on the system) and is mainly known as Newtonian Mechanics, while the second method depends on scalar concepts (i.e, kinetic and potential energies of the system) and it is known as Lagrangian and Hamiltonian mechanics. In classical mechanics, the second approach is preferred and used widely to study different physical systems even if they look complicated when trying to solve them using Newtonian mechanics. For more details about the two approaches those who are interested can refer to classical mechanics texts, and we recommend readers to refer to references[Landau(1976)], [Hand(1995)],[Marion(1988)],[Fowles(2005)].

The importance of fractional derivatives was argued by many researchers, these having applications in different branches of engineering: bioengineering [Magin(2006)], in the study of the behavior of materials with viscoelastic structure

[Bagley(1991)], [Koeller(1984)], [Koeller(1986)], [Skaar(1988)], in the study of optimal control
[Oustaloup(2000)], [Xue(2002)], [Manabe(2003)], [Monje(2004)], chemical and electrochemical processes [Ichise(1971)], [Sun(1984)], chaos theory [Hartley(1995)], etc. The fractional calculus can be approached using the Laplace and Fourier transforms, Taylor series or numerical analysis. In the last years the fractional differential equations kept the attention of researchers that used more frequent the fractional calculus Riemann - Liouville or Caputo [Li(2007)], [Li(2009)], [Liand(2009)], [Qian(2010)], [Li(2010)], [Miller(1993)].

In the last years the numerical fractional calculus was approached by many researchers, for example one can refer to [Baleanu(2011)], [Baleanu(2020)] and reference therein. In these works [Alqahtani(2019)], [Shatanawi(2020)] one can see that many significant and important physical systems have been studied numerically in fractional sense. For a Caputo Atangana Baleanu fractional differential equation the existence and uniqueness were studied in [Alqahtani(2019)] and some applications on Caputo nonlinear fractional differential equations were investigated in [Shatanawi(2020)].

Many recent efforts have been paid on studying fractional calculus specially when dealing with differential equations using many techniques. Among these techniques one can find fixed-point theorem [Karapınar(2019a)], [A(2019)], [Afshari(2015)], Quasi- metric spaces [Karapınar(2019b)], the existence–uniqueness theorem [Adiguzel(2020)], and Hybrid contractions [Alqahtani(2019)]. As one can notice fractional calculus prove its importance of using it in many branches in solving different systems using different techniques, and we believe that this branch of mathematics will be of more advantages in future in all branches of mathematics and science.

This section is structured as follows. We realized a short presentation of the basic notions regarding fractional calculus and we presented the classical description of a double pendulum accompanied by the classical Euler-Lagrange equations (CELE). Further are obtained the fractional Euler - Lagrange equations (FELE) and the system of fractional Hamiltonian equations for the considered double pendulum, using the Caputo's derivatives. The nonlinear fractional system of differential equations is numerically implemented using the Euler technique in order to discretize the convolution integrals. For different values of fractional derivatives was analyzed the behavior of the double pendulum using Maple software.

Let us consider a function $f : [a, b] \in R$ that is time dependent. The left Caputo

fractional derivative is defined as:

$$ {}_a^C D_t^\alpha f(t) = \frac{1}{\Gamma(n-\alpha)} \int_a^t f^{(n)}(\xi)(t-\xi)^{n-1-\alpha} d\xi. \tag{2.1.1} $$

The right Caputo fractional derivative is defined as:

$$ {}_t^C D_b^\alpha f(t) = \frac{1}{\Gamma(n-\alpha)} \int_t^b (-1)^n f^{(n)}(\xi)(t-\xi)^{n-1-\alpha} d\xi, \tag{2.1.2} $$

where $\Gamma(\circ)$ represents the Gamma function and $\alpha \in (n-a, n)$ is the fractional derivative order.

For the case when $n = 1$ and $\alpha \in (0, 1)$ the left and right Caputo fractional derivatives are expressed by the following relations:

$$ {}_a^C D_t^\alpha f(t) = \frac{1}{\Gamma(1-\alpha)} \int_a^t f^{'}(\xi)(t-\xi)^{-\alpha} d\xi, \tag{2.1.3} $$

$$ {}_t^C D_b^\alpha f(t) = -\frac{1}{\Gamma(1-\alpha)} \int_t^b (-1) f^{'}(\xi)(t-\xi)^{-\alpha} d\xi. \tag{2.1.4} $$

Let us consider $f(t)$ an integrable function, then the Riemann-Liouville integral is defined by:

$$ {}_a^{RL} I_t^\beta = \frac{1}{\Gamma(\beta)} \int_a^t f(\xi)(t-\xi)^{\beta-1} d\xi, \quad (\forall)\beta > 0. \tag{2.1.5} $$

It is obvious that the Caputo derivative is:

$$ {}_a^C D_t^\alpha f(t) =_a^{RL} I_t^{1-\alpha} f'(t). \tag{2.1.6} $$

The integral operators associated with the definition (2.1.3) and (2.1.4) are:

$$ {}_a^C I_t^\alpha = \frac{1}{\Gamma(\alpha)} \int_a^t f(\xi)(t-\xi)^{\alpha-1} d\xi \tag{2.1.7} $$

$$ {}_t^C I_b^\alpha = -\frac{1}{\Gamma(\alpha)} \int_t^b f(\xi)(t-\xi)^{\alpha-1} d\xi. \tag{2.1.8} $$

Between the differential and integral operators, the following relations hold:

$$ {}_a^C I_t^\alpha ({}_a^C D_t^\alpha f(t)) = f(t) - f(a); \tag{2.1.9} $$

$$ {}_t^C I_b^\alpha ({}_t^C D_b^\alpha f(t)) = f(t) - f(b). \tag{2.1.10} $$

Caputo's formula for the Laplace transform of the Caputo derivative is given by the following relation:

$$ \int_0^\infty e^{-st} \left({}_0^C D_t^\alpha f(t)\right) dt = s^\alpha F(s) - \sum_{k=0}^{n-1} s^{\alpha-k-1} f^{(k)}(0), n-1 < \alpha \leq n. \tag{2.1.11} $$

The physical interpretations of dynamical systems are more facile by using the Laplace transform of the Caputo's derivative with initial values of integer-order derivatives. For the Caputo's derivative we have the following property:

$$ {}_a^C D_t^\alpha \left({}_a^C D_t^p f(t)\right) = {}_a^C D_t^p \left({}_a^C D_t^\alpha f(t)\right) = {}_a^C D_t^{\alpha+p} f(t), p = 0, 1, 2, \ldots, n-1 < \alpha < n. \tag{2.1.12} $$

2.1.1 Classical Description of the general case

A double pendulum is a system consisting of two simple pendulums connected to each other as shown in Figure[2.1] below. As it is clear, the system consists of two masses ω_1 and ω_2 attached by light rods with lengths (b_1 , b_2). In this example we need

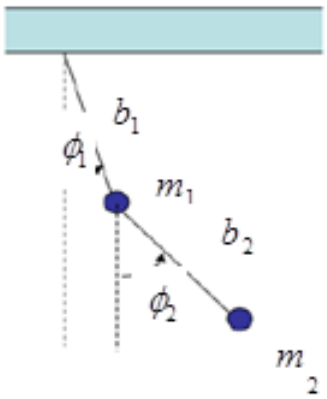

Figure 2.1: The double pendulum system

just two generalized coordinates to describe the motion (φ_1 , φ_2), and this is due to the fact that the length of each rod remains constant. Therefore, the kinetic and potential energies of the system respectively read:

$$T = \frac{1}{2}\left(\omega_1+\omega_2\right) b_1^2\dot{\varphi}_1^2 + \frac{1}{2}\omega_2 b_2^2\dot{\varphi}_2^2 + \omega_2 b_1 b_2 \cos\left(\varphi_1-\varphi_2\right)\dot{\varphi}_1\dot{\varphi}_2, \tag{2.1.13}$$

$$V = -\left(\omega_1+\omega_2\right) g b_1 \cos\varphi_1 - \omega_2 g b_2 \cos\varphi_2. \tag{2.1.14}$$

Consequently, the classical Lagrangian $L_c = T - V$ takes the form:

$$\begin{aligned} L_c \;&= \tfrac{1}{2}\left(\omega_1+\omega_2\right) b_1^2\dot{\varphi}_1^2(t) + \tfrac{1}{2}\omega_2 b_2^2\dot{\varphi}_2^2(t) + \omega_2 b_1 b_2 \cos\left(\varphi_1(t)-\varphi_2(t)\right)\dot{\varphi}_1\dot{\varphi}_2(t) \\ &\quad + \left(\omega_1+\omega_2\right) g b_1 \cos\varphi_1 + \omega_2 g b_2 \cos\varphi_2. \end{aligned} \tag{2.1.15}$$

Now, applying the relation

$$\frac{\partial L_c}{\partial \varphi_i} - \frac{d}{dt}\frac{\partial L_c}{\partial \dot{\varphi}_i} = 0$$

to Eq. (2.1.15) for both ($\varphi_1(t)$, $\varphi_2(t)$) one get respectively the following two Classical Euler- Lagrange equations (CELE):

$$\begin{aligned} &\left(\omega_1+\omega_2\right) b_1\ddot{\varphi}_1(t) + \omega_2 b_2\ddot{\varphi}_2(t)\cos\left(\varphi_1(t)-\varphi_2(t)\right) + \\ &+\omega_2 b_2\dot{\varphi}_1^2(t)\sin\left(\varphi_1(t)-\varphi_2(t)\right) + \left(\omega_1+\omega_2\right) g\sin\varphi_1(t) = 0, \end{aligned} \tag{2.1.16}$$

$$b_2\ddot{\varphi}_2 + b_1\ddot{\varphi}_1\cos\left(\varphi_1-\varphi_2\right) - b_1\dot{\varphi}_1^2\sin\left(\varphi_1-\varphi_2\right) + g\sin\varphi_2 = 0. \tag{2.1.17}$$

The classical Hamiltonian equation of motion is:

$$\begin{aligned} \mathrm{H}_1(t) &= \tfrac{\partial L_c}{\partial\dot{\phi}_1(t)} = \left(\omega_1+\omega_2\right) b_1^2\dot{\phi}_1(t) + \omega_2 b_1 b_2\cos(\phi_1(t)-\phi_2(t))\dot{\phi}_2(t) \\ \mathrm{H}_2(t) &= \tfrac{\partial L_c}{\partial\dot{\phi}_2(t)} = \omega_2 b_2^2\dot{\phi}_2(t) + \omega_2 b_1 b_2\cos(\phi_1(t)-\phi_2(t))\dot{\phi}_1. \end{aligned} \tag{2.1.18}$$

The classical Hamilton function is:

$$\begin{aligned} \mathrm{H}(t) \;&= \dot{\phi}_1(t)\mathrm{H}_1(t) + \dot{\phi}_2(t)\mathrm{H}_2(t) - L_c(t) = \\ &= \tfrac{\left(\omega_1+\omega_2\right) b_1^2\dot{\phi}_1^2(t) + \omega_2 b_2^2\dot{\phi}_2^2(t)}{2} + \omega_2 b_1 b_2\cos(\phi_1(t)-\phi_2(t))\dot{\phi}_1\dot{\phi}_2 - \\ &\quad -\left(\omega_1+\omega_2\right) g b_1\cos\phi_1(t) - \omega_2 g b_2\cos\phi_2(t). \end{aligned} \tag{2.1.19}$$

2.1.2 Fractional Description for General Case

Equation (2.1.15) can be written in the fractional form using Caputo's fractional derivative as:

$$\begin{aligned} L_F \;&= \tfrac{\left(\omega_1+\omega_2\right) b_1^2\left({}_a^C D_t^\alpha\varphi_1(t)\right)^2 + \omega_2 b_2^2\left({}_a^C D_t^\alpha\varphi_2(t)\right)^2}{2} + \\ &\quad +\omega_2 b_1 b_2\cos\left(\varphi_1(t)-\varphi_2(t)\right) {}_a^C D_t^\alpha\varphi_1(t)\, {}_a^C D_t^\alpha\varphi_2(t) + \\ &\quad + \left(\omega_1+\omega_2\right) g b_1\cos\varphi_1(t) + \omega_2 g b_2\cos\varphi_2(t). \end{aligned} \tag{2.1.20}$$

The fractional Euler- Lagrange equations (FELE's) can be obtained by plugging the equation (2.1.20) and the following relation

$$\frac{\partial L_F}{\partial \varphi_i(t)} +_t^C D_b^\alpha \left(\frac{\partial L_F}{\partial {}_a^C D_t^\alpha \varphi_i(t)} \right) +_a^C D_t^\alpha \left(\frac{\partial L_F}{\partial {}_t^C D_b^\alpha \varphi_i(t)} \right) = 0,$$

for both $\varphi_1(t)$, and $\varphi_2(t)$. Consequently, we obtain:

$$\begin{aligned} &{}_t^C D_b^\alpha \left((\omega_1+\omega_2)\, b_1^2 \left({}_a^C D_t^\alpha \varphi_1(t) \right) + \omega_2 b_1 b_2 \cos\left(\varphi_1(t)-\varphi_2(t)\right) \left({}_a^C D_t^\alpha \varphi_2(t) \right) \right) \\ &= \omega_2 b_1 b_2 \sin\left(\varphi_1(t)-\varphi_2(t)\right) \left({}_a^C D_t^\alpha \varphi_1(t) \right) \left({}_a^C D_t^\alpha \varphi_2(t) \right) + (\omega_1+\omega_2)\, g b_1 \sin\varphi_1(t), \end{aligned} \tag{2.1.21}$$

$$\begin{aligned} &{}_t^C D_b^\alpha \left(\omega_2 b_2^2 \left({}_a^C D_t^\alpha \varphi_2(t) \right) + \omega_2 b_1 b_2 \cos\left(\varphi_1(t)-\varphi_2(t)\right) \left({}_a^C D_t^\alpha \varphi_1(t) \right) \right) \\ &= \omega_2 g b_2 \sin\varphi_2(t) - \omega_2 b_1 b_2 \sin\left(\varphi_1(t)-\varphi_2(t)\right) \left({}_a^C D_t^\alpha \varphi_1(t) \right) \left({}_a^C D_t^\alpha \varphi_2(t) \right). \end{aligned} \tag{2.1.22}$$

As $\alpha \to 1$, the FELE's (2.1.21), (2.1.22) are reduced to the CELE's (2.1.16), (2.1.17). The fractional Hamiltonian function is given by the following relation:

$$\begin{aligned} \mathrm{H}_f(t) \;&= \mathrm{H}_{1,1}(t) \left({}_a^C D_t^\alpha \phi_1(t) \right) + \mathrm{H}_{1,2}(t) \left({}_t^C D_b^\alpha \phi_1(t) \right) + \\ &+ \mathrm{H}_{2,1}(t) \left({}_a^C D_t^\alpha \phi_2(t) \right) + \mathrm{H}_{2,2}(t) \left({}_t^C D_b^\alpha \phi_2(t) \right) - L_f(t), \end{aligned} \tag{2.1.23}$$

where $\mathrm{H}_{i,j}(t), i,j = 1,2$ are the generalized momentuum:

$$\mathrm{H}_{i,1}(t) = \frac{\partial L_f(t)}{\partial ({}_a^C D_t^\alpha \phi_i(t))}, \qquad \mathrm{H}_{i,2}(t) = \frac{\partial L_f(t)}{\partial \left({}_t^C D_b^\alpha \phi_i(t) \right)}, \qquad i = 1,2. \tag{2.1.24}$$

Therefore, we have:

$$\begin{aligned} &\mathrm{H}_{1,1}(t) = (\omega_1+\omega_2) b_1^2 \left({}_a^C D_t^\alpha \phi_1(t) \right) + \omega_2 b_1 b_2 \cos(\phi_1(t)-\phi_2(t)) \left({}_a^C D_t^\alpha \phi_2(t) \right) \\ &\mathrm{H}_{2,1}(t) = \omega_2 b_2^2 \left({}_a^C D_t^\alpha \phi_2(t) \right) + \omega_2 b_1 b_2 \cos(\phi_1(t)-\phi_2(t)) \left({}_a^C D_t^\alpha \phi_1(t) \right) \\ &\mathrm{H}_{1,2}(t) = H_{2,2}(t) = 0. \end{aligned} \tag{2.1.25}$$

In consequence, we will obtain the fractional Hamilton function:

$$\begin{aligned} \mathrm{H}_f(t) \;&= \tfrac{1}{2}(\omega_1+\omega_2) b_1^2 \left({}_a^C D_t^\alpha \phi_1(t) \right)^2 + \tfrac{1}{2}\omega_2 b_2^2 \left({}_a^C D_t^\alpha \phi_2(t) \right)^2 + \\ &+ \omega_2 b_1 b_2 \cos(\phi_1(t)-\phi_2(t)) \left({}_a^C D_t^\alpha \phi_1(t) \right) \left({}_a^C D_t^\alpha \phi_2(t) \right) - \\ &- (\omega_1+\omega_2) g b_1 \cos\phi_1(t) - \omega_2 g b_2 \cos\phi_2(t). \end{aligned} \tag{2.1.26}$$

The equations of motion for the fractional Hamiltonian are:

$$\frac{\partial H_f(t)}{\partial \phi_i(t)} =_t^C D_b^\alpha \left(\frac{\partial L_f(t)}{\partial ({}_a^C D_t^\alpha \phi_i(t))} \right) + a^C D_t^\alpha \left(\frac{\partial L_f(t)}{\partial \left({}_t^C D_b^\alpha \phi_i(t) \right)} \right), i = 1,2. \tag{2.1.27}$$

The above equations lead us to the following system:

$$\begin{cases} -\omega_2 b_1 b_2 \sin(\phi_1(t)-\phi_2(t)) \left({}_a^C D_t^\alpha \phi_1(t) \right) \left({}_a^C D_t^\alpha \phi_2(t) \right) + (\omega_1+\omega_2) g b_1 \sin\phi_1(t) = \\ = (\omega_1+\omega_2) b_{1t}^{2C} D_b^\alpha \left({}_a^C D_t^\alpha \phi_1(t) \right) + \omega_2 b_1 b_{2t}^C D_b^\alpha \left(\cos(\phi_1(t)-\phi_2(t)) \left({}_a^C D_t^\alpha \phi_2(t) \right) \right) \\ \omega_2 b_1 b_2 \sin(\phi_1(t)-\phi_2(t)) \left({}_a^C D_t^\alpha \phi_1(t) \right) \left({}_a^C D_t^\alpha \phi_2(t) \right) + \omega_2 g b_2 \sin\phi_2(t) = \\ = \omega_2 b_{2t}^{2C} D_b^\alpha \left({}_a^C D_t^\alpha \phi_2(t) \right) + \omega_2 b_1 b_{2t}^C D_b^\alpha \left(\cos(\phi_1(t)-\phi_2(t)) {}_a^C D_t^\alpha \phi_1(t) \right). \end{cases} \tag{2.1.28}$$

We will consider the case when $\phi_1(t) \approx \phi_2(t)$. This approach leads us to have $\sin(\phi_1(t) - \phi_2(t)) \approx 0$ and $\cos(\phi_1(t) - \phi_2(t)) \approx 1$. In this situation we have the following fractional Hamiltonian equations (FHE):

$$\begin{array}{l} (\omega_1+\omega_2)b_{1t}^{2C}D_b^{\alpha}\left({}_a^CD_t^{\alpha}\phi_1(t)\right)+\omega_2 b_1 b_{2t}{}^CD_b^{\alpha}\left({}_a^CD_t^{\alpha}\phi_2(t)\right)=(\omega_1+\omega_2)gb_1\sin\phi_1(t) \\ \omega_2 b_1 b_{2t}{}^CD_b^{\alpha}\left({}_a^CD_t^{\alpha}\phi_1(t)\right)+\omega_2 b_{2t}^{2C}D_b^{\alpha}\left({}_a^CD_t^{\alpha}\phi_2(t)\right)=\omega_2 gb_2\sin\phi_2(t) \end{array} . \tag{2.1.29}$$

2.1.3 Numerical method

We want to reduce the nonlinear system above to a simplified system that can be implemented numerically. Based on this idea the above system can be written in the following form:

$$\left\{\begin{array}{l} {}_a^CD_t^{\alpha}\phi_1(t)=y_1(t) \\ {}_a^CD_t^{\alpha}\phi_2(t)=y_2(t) \\ {}_t^CD_b^{\alpha}y_1(t)=\frac{(\omega_1+\omega_2)g}{\omega_1 b_1}\sin\phi_1(t)-\frac{\omega_2 g}{\omega_1 b_1}\sin\phi_2(t) \\ {}_t^CD_b^{\alpha}y_2(t)=-\frac{(\omega_1+\omega_2)g}{\omega_1 b_2}\sin\phi_1(t)+\frac{(\omega_1+\omega_2)g}{\omega_1 b_2}\sin\phi_2(t) \end{array}\right. . \tag{2.1.30}$$

Let us consider the approximations $\sin\phi_1(t) \approx \phi_1(t)$ and $\sin\phi_2(t) \approx \phi_2(t)$. We obtain the following fractional order system:

$$\left\{\begin{array}{l} {}_a^CD_t^{\alpha}\phi_1(t)=y_1(t) \\ {}_a^CD_t^{\alpha}\phi_2(t)=y_2(t) \\ {}_t^CD_b^{\alpha}y_1(t)=\frac{(\omega_1+\omega_2)g}{\omega_1 b_1}\phi_1(t)-\frac{\omega_2 g}{\omega_1 b_1}\phi_2(t) \\ {}_t^CD_b^{\alpha}y_2(t)=-\frac{(\omega_1+\omega_2)g}{\omega_1 b_2}\phi_1(t)+\frac{(\omega_1+\omega_2)g}{\omega_1 b_2}\phi_2(t) \end{array}\right. . \tag{2.1.31}$$

Taking into account the relations (2.1.7)-(2.1.10), by applying the integral operators on the system (2.1.31) we have:

$$\left\{\begin{array}{l} \phi_1(t)-\phi_1(a)=\frac{1}{\Gamma(\alpha)}\int\limits_a^t y_1(\xi)(t-\xi)^{\alpha-1}d\xi \\ \phi_2(t)-\phi_2(a)=\frac{1}{\Gamma(\alpha)}\int\limits_a^t y_2(\xi)(t-\xi)^{\alpha-1}d\xi \\ y_1(t)-y_1(b)=-\frac{(\omega_1+\omega_2)g}{\omega_1 b_1\Gamma(\alpha)}\int\limits_t^b \phi_1(\xi)(t-\xi)^{\alpha-1}d\xi+\frac{\omega_2 g}{\omega_1 b_1\Gamma(\alpha)}\int\limits_t^b \phi_2(\xi)(t-\xi)^{\alpha-1}d\xi \\ y_2(t)-y_2(b)=\frac{(\omega_1+\omega_2)g}{\omega_1 b_2\Gamma(\alpha)}\int\limits_t^b \phi_1(\xi)(t-\xi)^{\alpha-1}d\tau-\frac{(\omega_1+\omega_2)g}{\omega_1 b_2\Gamma(\alpha)}\int\limits_t^b \phi_1(\xi)(t-\xi)^{\alpha-1}d\xi \end{array}\right. \tag{2.1.32}$$

We want to apply the Euler method in order to discretize the convolution integrals. In the range $[l_1, l_2] = [a, b]$ let us consider the time step $h = \frac{l_2-l_1}{n} = \frac{b-a}{n}$, where $n \in \mathbb{N}$ is arbitrary. In the matrices formulation we express the numerical approximation of

$\phi_i(t_j)$ by $\phi_{i,j}(t_j)$ and $y_i(t_j)$ by $y_{i,j}(t_j)$, where $t_j = a + jh, 0 \leq j \leq n$ represents the time at iteration j. Therefore, the convolution integrals can be approximated by:

$$\frac{1}{\Gamma(\alpha)} \int_a^t f(\xi)(t-\xi)^{\alpha-1} d\xi \approx h^\alpha A_{n,\alpha} \begin{pmatrix} f_{1,0} \\ \dots \\ f_{1,n} \end{pmatrix},$$

where

$$A_{n,\alpha} = \begin{pmatrix} a_{0,\alpha} & 0 & \dots & 0 & 0 \\ a_{1,\alpha} & a_{0,\alpha} & \dots & 0 & 0 \\ \dots & \dots & \dots & \dots & \dots \\ a_{n-1,\alpha} & a_{n-2,\alpha} & \dots & a_{1,\alpha} & a_{0,\alpha} \end{pmatrix},$$

and the recurrence formula is given by:

$$a_{0,\alpha} = 1, \qquad a_{j,n} = \frac{j+\alpha-1}{j} a_{j-1,\alpha}, j = \overline{1,n}.$$

Therefore, the system (2.1.32) can be written in the approximation matrix form with the fractional Euler method:

$$\begin{cases} \Phi_1 = \Phi_{1,a} + h^\alpha A_{n,\alpha} Y_1 \\ \Phi_2 = \Phi_{2,a} + h^\alpha A_{n,\alpha} Y_2 \\ Y_1 = Y_{1,b} + \frac{(\omega_1+\omega_2)g}{\omega_1 b_1} h^\alpha A_{n,\alpha} \Phi_1 - \frac{\omega_2 g}{\omega_1 b_1} h^\alpha A_{n,\alpha} \Phi_2 \\ Y_2 = Y_{2,b} - \frac{(\omega_1+\omega_2)g}{\omega_1 b_2} h^\alpha A_{n,\alpha} \Phi_1 + \frac{(\omega_1+\omega_2)g}{\omega_1 b_2} h^\alpha A_{n,\alpha} \Phi_2 \end{cases}. \tag{2.1.33}$$

Here we have:

$$\Phi_i = \begin{pmatrix} \phi_{i,0} \\ \dots \\ \phi_{i,n} \end{pmatrix}, Y_i = \begin{pmatrix} y_{i,0} \\ \dots \\ y_{i,n} \end{pmatrix}, \Phi_{i,a} = \begin{pmatrix} \phi_{i,a} \\ \dots \\ \phi_{i,a} \end{pmatrix}, Y_{i,b} = \begin{pmatrix} y_{i,b} \\ \dots \\ y_{i,b} \end{pmatrix}, i = 1, 2.$$

Rearranging the system (2.1.33) we obtain:

$$\begin{cases} \Phi_1 - h^\alpha A_{n,\alpha} Y_1 = \Phi_{1,a} \\ \Phi_2 - h^\alpha A_{n,\alpha} Y_2 = \Phi_{2,a} \\ Y_1 - \frac{(\omega_1+\omega_2)g}{\omega_1 b_1} h^\alpha A_{n,\alpha} \Phi_1 + \frac{\omega_2 g}{\omega_1 b_1} h^\alpha A_{n,\alpha} \Phi_2 = Y_{1,b} \\ Y_2 + \frac{(\omega_1+\omega_2)g}{\omega_1 b_2} h^\alpha A_{n,\alpha} \Phi_1 - \frac{(\omega_1+\omega_2)g}{\omega_1 b_2} h^\alpha A_{n,\alpha} \Phi_2 = Y_{2,b} \end{cases}. \tag{2.1.34}$$

The following system of linear algebraic equations is obtained:

$$\begin{pmatrix} I_n & O_n & -h^{\alpha}A_{n,\alpha} & O_n \\ O_n & I_n & O_n & -h^{\alpha}A_{n,\alpha} \\ -\frac{(\omega_1+\omega_2)g}{\omega_1 b_1}h^{\alpha}A_{n,\alpha} & \frac{\omega_2 g}{\omega_1 b_1}h^{\alpha}A_{n,\alpha} & I_n & O_n \\ \frac{(\omega_1+\omega_2)g}{\omega_1 b_2}h^{\alpha}A_{n,\alpha} & -\frac{(\omega_1+\omega_2)g}{\omega_1 b_2}h^{\alpha}A_{n,\alpha} & O_n & I_n \end{pmatrix} \begin{pmatrix} \Phi_1 \\ \Phi_2 \\ Y_1 \\ Y_2 \end{pmatrix} = \\ = \begin{pmatrix} \Phi_{1,a} \\ \Phi_{2,a} \\ Y_{1,b} \\ Y_{2,b} \end{pmatrix}. \tag{2.1.35}$$

The above system can be easily implemented by a linear solver.

First of all, for simplicity we consider the following parameters ($\omega_1 = \omega_2 = 1$), and ($b_1 = b_2 = 1$) with ($g = 9.81m/s^2$) . Further, we aim to solve the FHEs given in the Equation (2.1.29) for some specified initial conditions.

2.1.4 Simulation results

Below, we analyze the dynamical behavior of the FELEs (FHEs) of motion for the double pendulum system expressed by (2.1.21)-(2.1.22) or (2.1.29) by considering the following values of the fractional order $\alpha = 0.2, \quad 0.4 \quad , 0.5, \quad 0.6, \quad 0.8, \quad 1.0$, where is important to mention that we will use the algorithms of [Yezhi(2013)], the system of equations (2.1.30) for the mentioned above initial conditions returned us the following graphics.

To do this task we consider the following five specified initial conditions for our double pendulum system under consideration.

Case 1: $\varphi_1 = 0.1rad, \dot{\varphi}_1 = 0, \varphi_2 = 0.1rad, \text{and} \dot{\varphi}_2 = 0$

Case 2: $\varphi_1 = 0.1rad, \dot{\varphi}_1 = 0, \phi_2 = 0.8rad, \text{and} \dot{\varphi}_2 = 0$

Case 3: $\varphi_1 = 0.1rad, \dot{\varphi}_1 = 0, \varphi_2 = 1.5rad, \text{and} \dot{\varphi}_2 = 0$

Case 4: $\varphi_1 = 0.1rad, \dot{\varphi}_1 = 0, \varphi_2 = 3.1rad, \text{and} \dot{\varphi}_2 = 0$

Case 5: $\varphi_1 = 1.5rad, \dot{\varphi}_1 = 0, \varphi_2 = 3.1rad, \text{and} \dot{\varphi}_2 = 0$

In Figures [2.2-2.7] the simulation results are plotted for the ELEs in both fractional and classical cases. As it is clear the Figure[2.2] represents cases 1- 5 for the value of $\alpha = 0.2$. While the Figure[2.3] shows the five initial conditions mentioned above for the value of $\alpha = 0.4$, and in Figure[2.4] the initial conditions where plotted for $\alpha = 0.5$. Furthermore, in Figures [2.5-2.7] we predicted the

dynamical behavior of the five initial conditions listed above for the following values of $\alpha = 0.6, 0, 8$, and 1.0 respectively.

The numerical solution of the FELEs reveals, for different values of α different behaviors Figure[2.2-2.7]. In the last figure Figure[2.7] the solution of the CELEs when α goes to 1 is represented. This approves that the fractional calculus offers a flexible model, which is capable of extracting hidden features of the studied physical system, features which are unavailable using the ordinary time-derivatives.

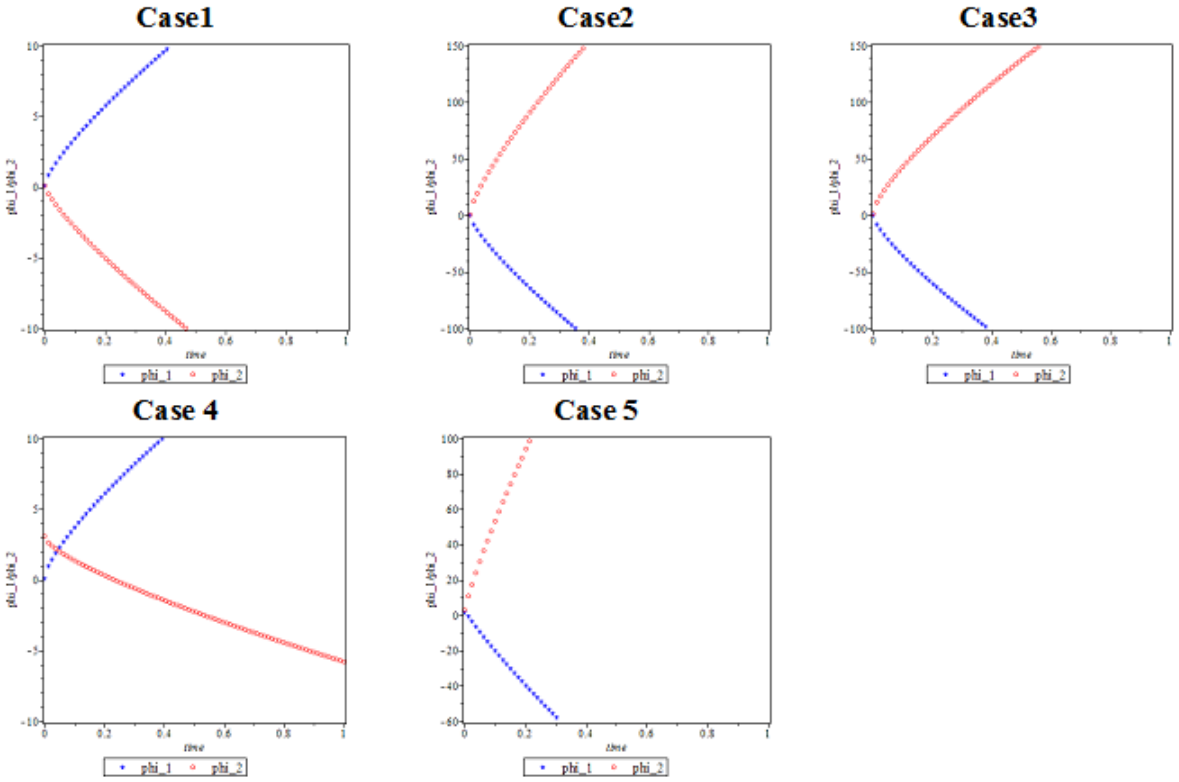

Figure 2.2: The behavior of the solution for $\alpha = 0.2$ in the FELE equations

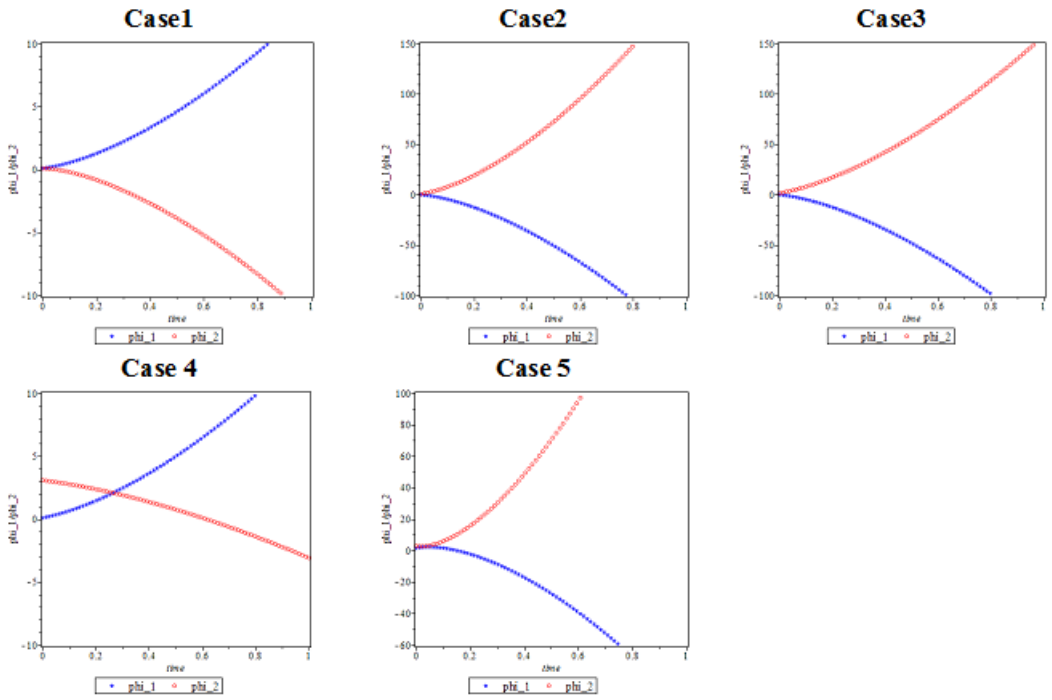

Figure 2.3: The behavior of the solution for $\alpha = 0.4$ in the FELE equations

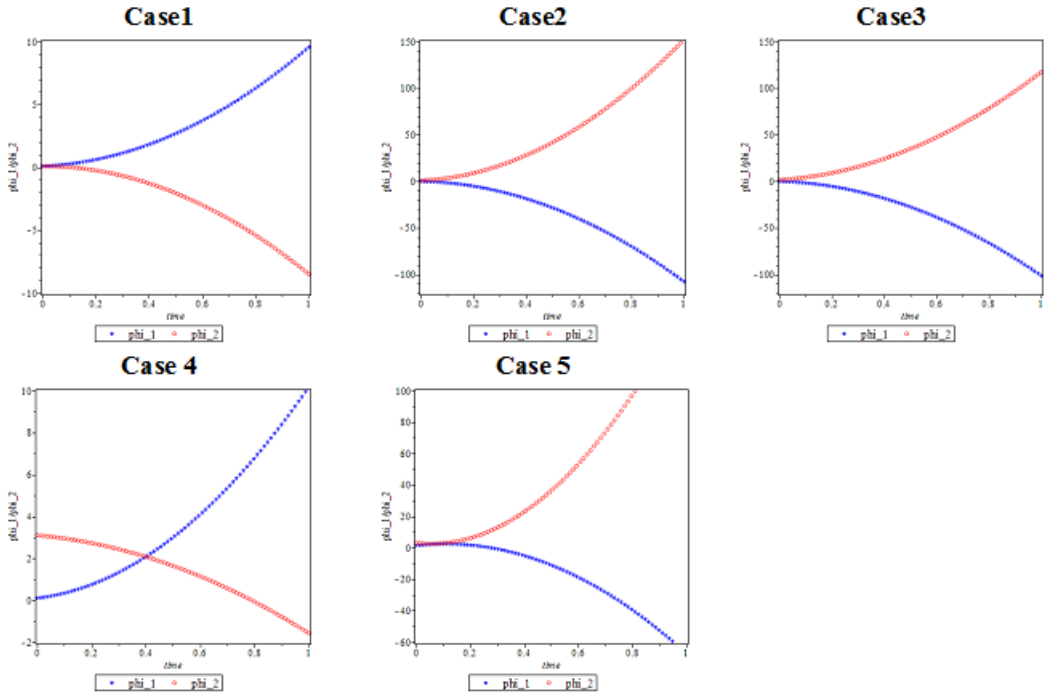

Figure 2.4: The behavior of the solution for $\alpha = 0.5$ in the FELE equations

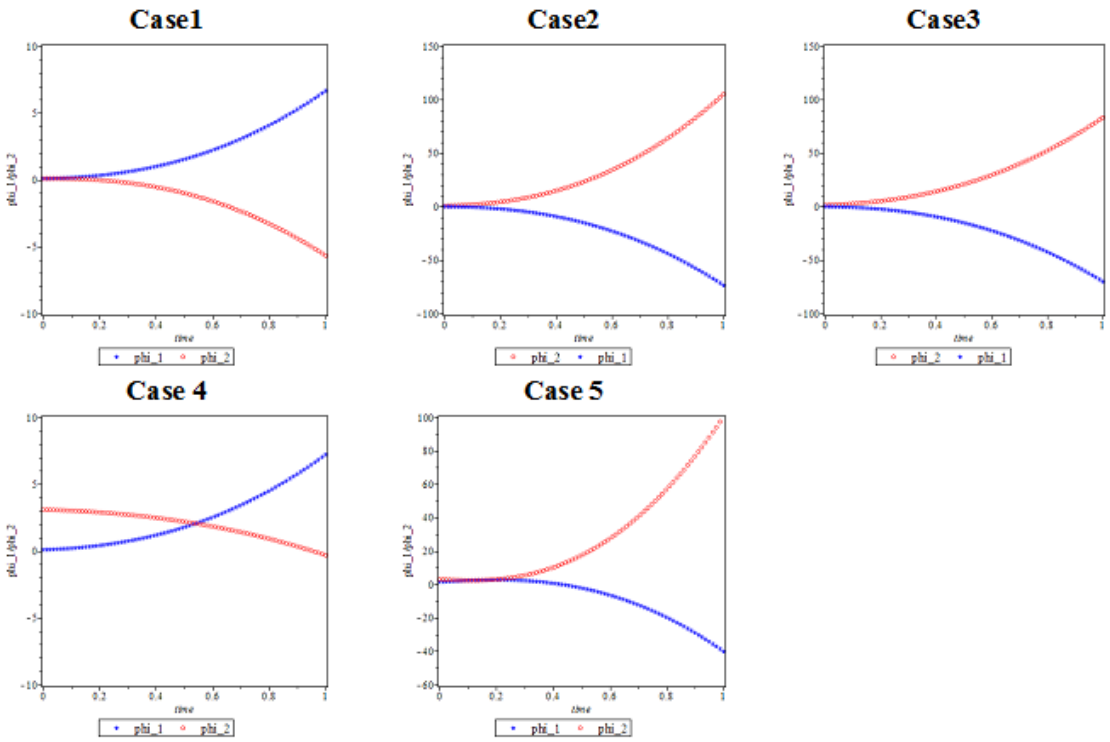

Figure 2.5: The behavior of the solution for $\alpha = 0.6$ in the FELE equations

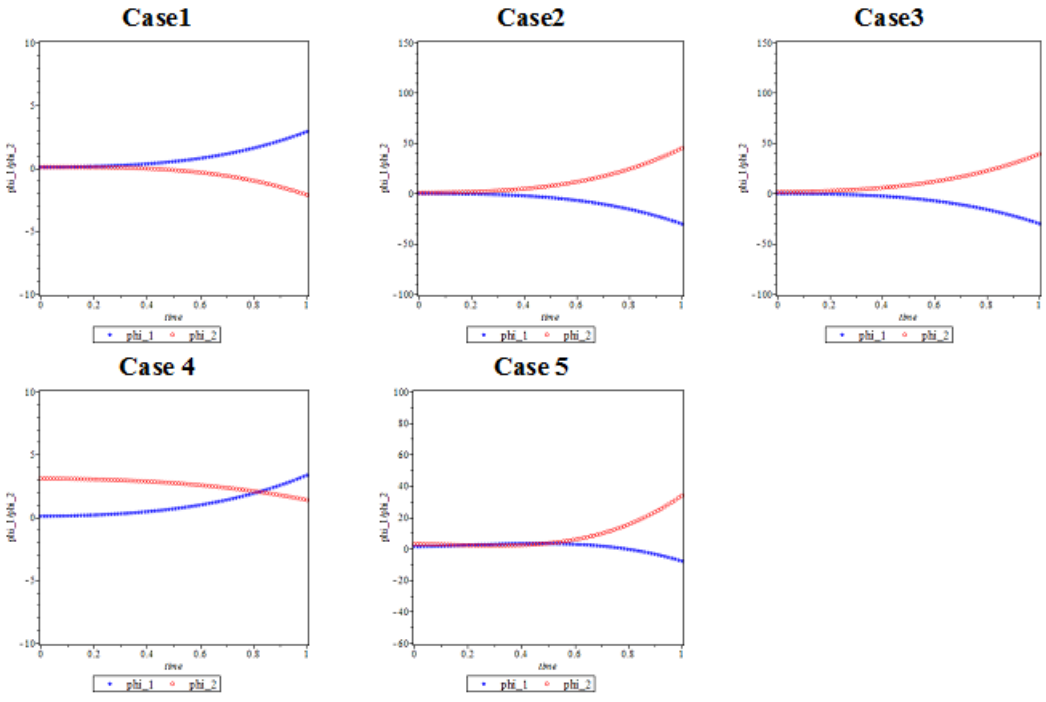

Figure 2.6: The behavior of the solution for $\alpha = 0.8$ in the FELE equations

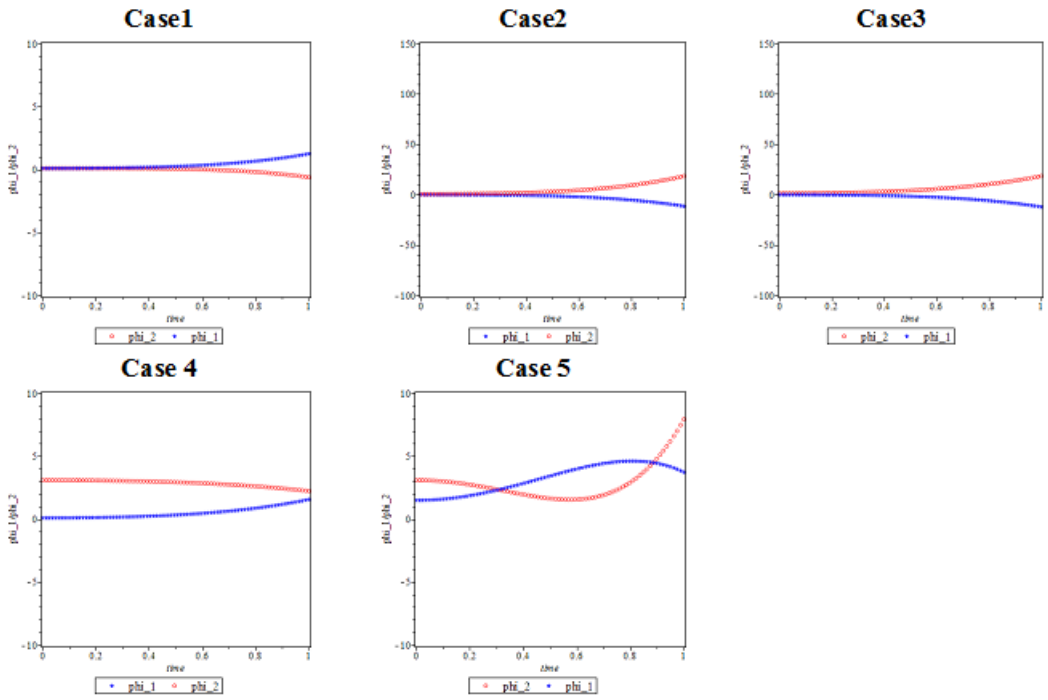

Figure 2.7: The behavior of the solution for $\alpha = 1.0$ in the FELE equations

This work considered the importance of the derivatives and integrals in fractional form to study the motion of an important physical system called double pendulum. We built the Lagrangian equation in both classical and fractional form and derived the FELEs. After that we derived the fractional Hamiltonian equation, and derived the FHEs using the fractional Caputo's fractional derivatives. Then, for solving the previous obtained fractional equations, the nonlinear fractional system of differential equations is numerically implemented using the Euler method in order to discretize the convolution integrals. For different values of fractional derivatives was analyzed the behavior of the double pendulum using Maple software. Simulation results proved that the behavior of the FELEs (FHEs) gives an excellent and efficient results for the dynamical behavior of the system. Moreover, the related classical solution was recovered as $\alpha \to 1$.

Therefore, the new fractional operators are able to present more accurate and flexible models for real-world dynamical systems.

2.2 Numerical Study of the Motion of a heavy bead sliding on a rotating wire

Differential equations (DE's) play an important role in many branches of physics such as: classical mechanics [Hand(1995)], [Marion(1988)],[Fowles(2005)], electromagnetic theory [Griffiths(1999)], quantum mechanics [Griffiths(2005)], fluid mechanics [Bansal(2017)], etc.

In classical mechanics, we deal with ordinary differential equation (ODE's) either when using Newtonian mechanics, or when applying Lagrangian mechanics in studying many physical systems. The Lagrangian mechanics enables us to solve a variety of physical examples due to the fact that writing the Lagrangian depends only on scalar quantities (kinetic energy and potential energy). One can refer to some classical texts to show how Lagrangian can be built [Hand(1995)], [Fowles(2005)]. As a result of building the Lagrange equation of any system DE's (called Euler- Lagrange equations) are obtained, and these equations have to be solved analytically or in some cases due to difficulties we seek numerical solutions [Khalilia(2018)].

Many numerical methods and techniques have been considered in solving DE's [Rheinboldt(1995)],[Potra(2007)], [Atkinson(2008)], [Butcher(2008)]. Techniques and methods used in numerical analysis are powerful because they help scientists in solving many kinds of differential equations without seeking for their analytical solutions.

A physical description for the system is listed where Euler- Lagrange equation has been obtained and the numerical method, and simulation results with discussion are presented. In section 4 we close the present work by a conclusion.

2.2.1 Description of the Physical System

Consider a heavy ball slipping on a rotating wire, with angular frequency ω, as discussed in a well-known text in analytical mechanics [Hand(1995)]. The present system deals with a ball slipping without resistance on a thin wire revolving around a vertical axis by a mechanical external agent at a constant angular frequency ω as shown in Figure[2.8] below.

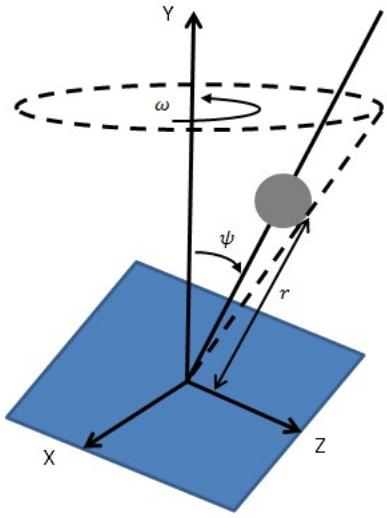

Figure 2.8: Heavy ball sliding on a rotating wire

The wire deviated away from the vertical axis by an angle ψ . The ball is forced to move on the wire, and to define its motion we need just one variable which is r (i.e., the distance from origin). It is important to mentioned that the importance of this example comes from the fact that the kinetic energy in this case depends on both the dynamical variable and on its derivative, instead of on the time derivative alone.

The kinetic energy and the potential energy of the ball respectively read:

$$T = \frac{1}{2}m\left(\dot{r}^2 + r^2\omega^2\sin^2\psi\right) \tag{2.2.1}$$

$$V = mgr\cos\psi \tag{2.2.2}$$

As a result, the classical Lagrangian takes the form

$$L = T - V = \frac{1}{2}m\left(\dot{r}^2 + r^2\omega^2\sin^2\psi\right) - mgr\cos\psi \tag{2.2.3}$$

The classical Euler-Lagrange equation (CELE) can be derived using

$$\frac{\partial L}{\partial r} - \frac{d}{dt}\frac{\partial L}{\partial \dot{r}} = 0 \tag{2.2.4}$$

In view of (2.2.3)-(2.2.4), the CELE reads:

$$\ddot{r} = r\omega^2\sin^2\psi - g\cos\psi \tag{2.2.5}$$

The last equation obtained is a non- homogenous second order linear differential equation. We aim to solve this equation in the next section numerically for some given initial conditions.

2.2.2 Analytic Solution of the Problem

In this section we obtained the analytical solution for the motion of equation (2.2.5), the canonical system of Hamilton and Poisson parenthesis are deduced, the reader can refer to [Taraphdar(2017)], [Arnold(1989)], [José(1998)] for more details. Let us consider the differential equation of second degree non-homogeneous:

$$\ddot{r} - r\omega^2 \sin^2 \psi = -g \cos \psi \tag{2.2.6}$$

The general solution of (2.2.6) is:

$$r = r_o + r_p = C_1 e^{\omega \sin \psi \cdot t} + C_2 e^{-\omega \sin \psi \cdot t} + \frac{g}{\omega^2} \frac{\cos \psi}{\sin^2 \psi} \tag{2.2.7}$$

Taking into consideration the initial conditions $r(0) = 5$ and $\dot{r}(0) = 0$ we obtain that $C_1 = C_2 = \frac{5}{2} - \frac{g}{2\omega^2} \frac{\cos \psi}{\sin^2 \psi}$ and the solution of (2.2.6) will be

$$r(t) = \left(\frac{5}{2} - \frac{g}{2\omega^2} \frac{\cos \psi}{\sin^2 \psi} \right) \left(e^{\omega \sin \psi \cdot t} + e^{-\omega \sin \psi \cdot t} \right) + \frac{g}{\omega^2} \frac{\cos \psi}{\sin^2 \psi} \tag{2.2.8}$$

Next, we want to deduce the canonical system of Hamilton in order to obtain the Poisson parenthesis.

We note by $p = \frac{\partial L}{\partial \dot{r}}$ where $p = p(t, r, \dot{r})$ is the generalized impulse. Let us introduce the Hamilton function:

$$H = p\dot{r} - L \Leftrightarrow H = p\dot{r} - \frac{1}{2} m \left(\dot{r}^2 + r^2 \omega^2 \sin^2 \psi \right) + mgr \cos \psi \tag{2.2.9}$$

The Hamilton system will be:

$$\begin{cases} \dot{r} = \frac{\partial H}{\partial p} \\ \dot{p} = -\frac{\partial H}{\partial r} = mr\omega^2 \sin^2 \psi - mg \cos \psi \end{cases} \tag{2.2.10}$$

Based on the above system we may obtain the Poisson parenthesis. The symmetric system attached to the Hamilton system is:

$$\frac{dr}{\frac{\partial H}{\partial p}} = \frac{dp}{-\frac{\partial H}{\partial r}} \tag{2.2.11}$$

Let $F(t, r, p) = C$ be a prime integral of the symmetric system (2.2.11) such that $\frac{dF}{dt} = 0$. In this case we obtain the following equation:

$$\frac{\partial F}{\partial t} + \frac{\partial F}{\partial r} \dot{r} + \frac{\partial F}{\partial p} \dot{p} = 0 \tag{2.2.12}$$

Taking into account the Hamilton system we have:

$$\frac{\partial F}{\partial t} + (F, H) = 0 \tag{2.2.13}$$

where

$$(F, H) = \frac{\partial F}{\partial r} \frac{\partial H}{\partial p} - \frac{\partial F}{\partial p} \frac{\partial H}{\partial r} \tag{2.2.14}$$

is the Poisson parenthesis.

2.2.3 Numerical Method and Simulation Results

The `dsolve` command can be used to solve ordinary differential equations (ODE), such as first-order ODE's and high-order ODE's via MATLAB framework.

In this subsection, we propose the numerical solution for (2.2.5) using `diff(s,n)`, `dsolve\left('eq','cond1','var'\right)` , and loop structure. We consider some initial conditions, and the numerical solutions for these particular conditions have been obtained, and one has to note that in all figures obtained x_1 refers to r .

Here we consider the following initial condition $r(0) = 5$, and $\dot{r}(0) = 0$ for the following three different angles $\psi = \frac{\pi}{6}$, $\frac{\pi}{4}$, and $\frac{\pi}{2}$, and for the following three different angular speeds $\omega = 1$, 2 , and 3 . The obtained results that are shown in Figure[2.9].

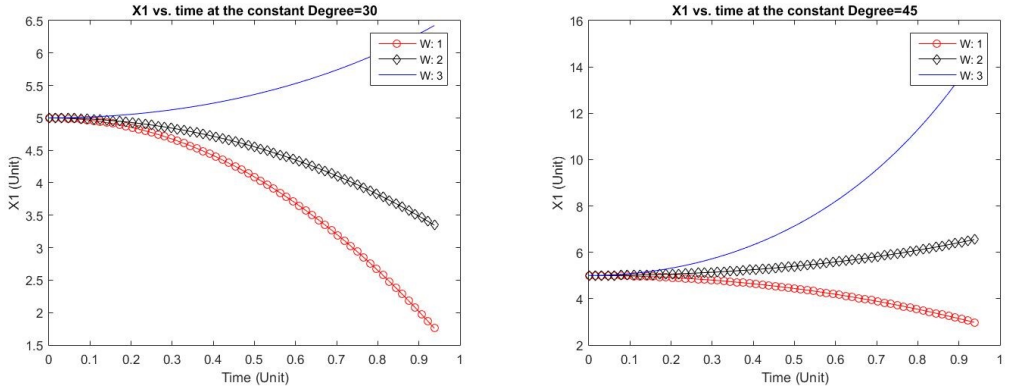

(a)

(b)

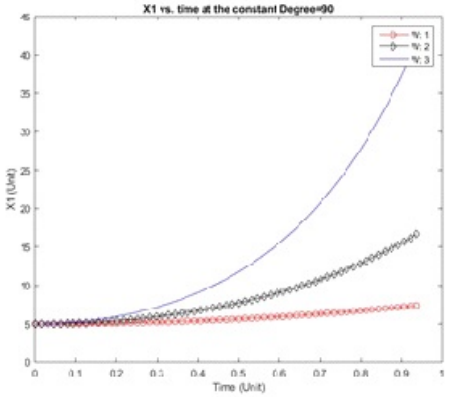

(c)

Figure 2.9: (a)The behaviour of distance against time for $\psi = \frac{\pi}{6}$ and $\omega = 1, 2$ and 3; (b)The behaviour of distance against time for $\psi = \frac{\pi}{4}$ and $\omega = 1, 2$ and 3; (c) The behaviour of distance against time for $\psi = \frac{\pi}{2}$ and $\omega = 1, 2$ and 3;

In Figure[2.9] shown above the behaviour of the distance against time is presented for different angular speed $\omega = 1, 2, 3$ where in each case we consider a specific angle, for example in Figure[2.9(a)] $\psi = \frac{\pi}{6}$, while $\psi = \frac{\pi}{4}$ in Figure[2.9(b)], and finally, we consider $\psi = \frac{\pi}{2}$ in Figure[2.9(c)]. On the other hand, in Figure[2.10] below we show the behavior of distance against time for different angles $\psi = \frac{\pi}{6}, \frac{\pi}{4}, \frac{\pi}{2}$ where in each case we consider a specific angular speed $\omega = 1$ for Figure[2.10(a)], $\omega = 2$ for Figure[2.10(b)], and in Figure[2.10(c)] $\omega = 3$.

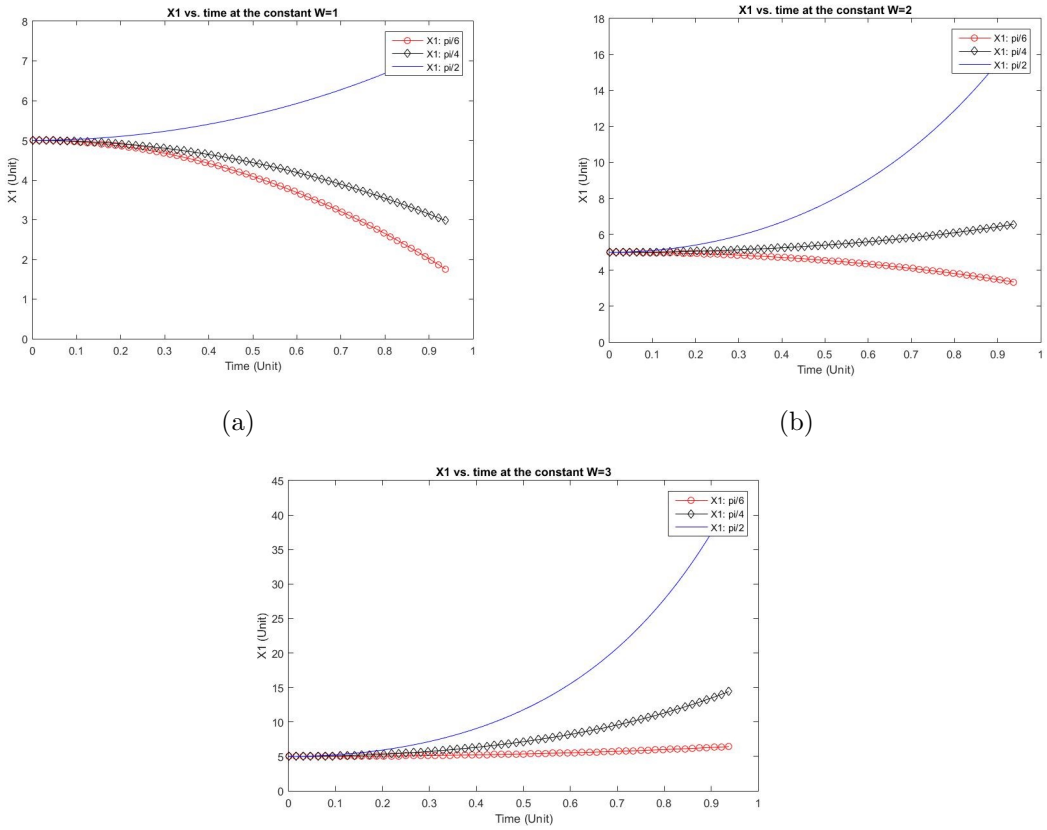

(a) (b)

(c)

Figure 2.10: (a)The behaviour of distance against time for $\omega = 1$ and $\psi = \frac{\pi}{6}, \frac{\pi}{4}, \frac{\pi}{2}$; (b)The behaviour of distance against time for $\omega = 2$ and $\psi = \frac{\pi}{6}, \frac{\pi}{4}, \frac{\pi}{2}$; (c) The behaviour of distance against time for $\omega = 3$ and $\psi = \frac{\pi}{6}, \frac{\pi}{4}, \frac{\pi}{2}$;

In all figures obtained above it is clear that the distance $r(t) = x_1(t)$ increases in all considered cases for the special case when $\psi = \frac{\pi}{2}$. This is due to the fact that in this case the wire rotates about the vertical axis in a horizontal plane, so the particle will move away from the origin (the right direction is considered to be positive). For other chosen angles sometimes the heavy bead moves away from origin and sometimes moving towards the origin depending on the value of the angular speed ω at which

the wire is rotating.

The `ode45` code has been successfully applied to find a truthful numerical solution for the motion of a ball sliding on a rotating wire. The position of the bead is depicted for the time period $[0, 1]$. We examine the motion for different values of angle ψ and for different values of angular speed ω .

It is clear from the figures that when angle $\psi = \frac{\pi}{2}$, the heavy ball moves away from the origin (to the right) in all considered cases because in this case the wire rotates on a horizontal plane, while for other angles considered the motion depends on the angular speed ω considered.

Furthermore, we believe that this method is effective for predicting analytical solutions in many branches of science and engineering problems.

2.3 Mathematical and numerical approach for telegrapher equation

Telegraph equation is a linear partial differential equation that describes the current (voltage) on an electrical transmission line with both time and distance. This equation is used to describe and study many physical and biological phenomena such as: the study of dispersive wave propagation, electric signal in a transmission line, pulsating blood flow in arteries, random motion of bugs along a hedge and many others. For more details about these phenomena and others one can refer to [Bohme(1987)], [Mohanty(2001)], [Dehghan(2010)], [Pascal(1986)].

The telegraph equations are due to Oliver Heaviside [Heaviside(1899)] who developed the transmission line model. This model demonstrates that the electromagnetic waves can be reflected on the wire, and that appear wave patterns along the transmission line. The telegraph equations are in terms of voltage and current for a section of a transmission media and that are applicable in several fields such as wave propagation [Weston(1993)], random walk theory [Banasiak(1998)], signal analysis [Jordan(1999)] and etc.
Nowadays communication system plays a significant key role in the society. They use transmission media for transferring the information carrying signal from one point to another point. For example, in guided medium the signal is transferred through the coaxial cable or transmission line [Srivastava(2013)]. Among the devices used in communication systems telegraph, and telephone in addition to too many other devices.
On the other hand, scientists always seeking for an analytical solution for differential equations. In undergraduate level students always studying many useful courses that enables them to solve differential equations analytically. Unfortunately many differential equations cannot be solved analytically, therefore numerical techniques have to be used. In literature one can find many useful numerical techniques that can be used for this purpose such as: Differential Transformation Method (DTM) [Abazari(2011)], Reduced Differential Transformation Method (RDTM) [Abazari(2012)], [Keskin(2010)], [Keskin(2009)] , Adomian Decomposition Method (ADM) [Nhawu(2016)], and many other methods.
In this section we aimed to solve analytically and numerically the so- called telegraph equation. The rest of this work is organized as follows: a mathematical derivation for the telegraph equation is presented and the analytical solution is obtained. In the end of this study we present the numerical solution of the system.

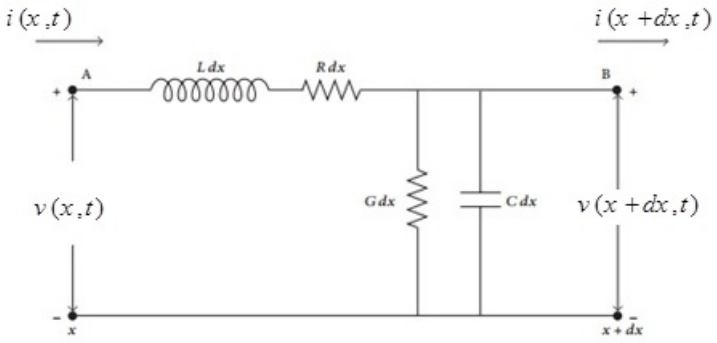

Figure 2.11: Schematic diagram of telegraphic transmission line with leakage

A mathematical derivation for the telegraph equation in terms of voltage and current for a section of a transmission line has been formulated. Let us consider an infinitesimal piece of telegraph cable wire as an electrical circuit shown in Figure[2.11] below.

Further assume that the cable is imperfectly insulated so that there are both capacitance and current leakage to ground. Suppose x is the distance from sending end of the cable; $v(x,t)$ is the voltage at any point and any time, on the cable; $i(x+dx,t)$ is the current at any point and any time, on the cable; R denotes the resistance of the cable; C denotes the capacitance to the ground; L denotes the inductance of the cable; G denotes the conductance to the ground.

According to Ohm's law, the voltage across the resistor (R), the inductor (L), and the capacitor (C) respectively read:

$$v = iR. \tag{2.3.1}$$

$$v = L\frac{di}{dt} \tag{2.3.2}$$

$$v = \frac{1}{C}\int idt \tag{2.3.3}$$

From Figure[2.11] above $v_B = v_A - (v_R + v_L)$. So, combining Eqs. (2.3.1)-(2.3.3) together one can write:

$$v(x+dx,t) - v(x,t) = -[Rdx]i - [Ldx]\frac{\partial i}{\partial t} \tag{2.3.4}$$

Now taking $dx \to 0$ and differentiating (2.3.4) partially with respect to x then, we have

$$\frac{\partial v(x,t)}{\partial x} = -Ri - L\frac{\partial i}{\partial t}. \tag{2.3.5}$$

In a similar way the current $i_B$can be written as:

$$i(x+dx,t) = i(x,t) - [Gdx]v - i_C dx. \tag{2.3.6}$$

where $i_C = C\frac{\partial v}{\partial t}$.

Again, differentiating (2.3.4) with respect to $t$and $i_C$with respect to $x$one got:

$$c^2\frac{\partial^2 i}{\partial x^2} = \frac{\partial^2 i}{\partial t^2} + (n+m)\frac{\partial i}{\partial t} + (nm)i. \tag{2.3.7}$$

where $n = \frac{G}{C}$, $m = \frac{R}{L}$, and $c^2 = \frac{1}{LC}$

The last equation is known as a one-dimensional hyperbolic second-order telegraph equations.

There is an easy solution in the case where the resistance per unit length of the wire, and the conductance of the insulation separating the outgoing and returning wires, are small. So let's say R is small compared with $\sqrt{L/C}$, and G is small compared with $\sqrt{C/L}$, $\sqrt{L/C}$has the same dimensions as resistance, and is known as the *characteristic impedance* of the line. If we put R and G equal to zero in (2.3.7), so that we have an ideal lossless cable, and the transmission of the potential is governed by its inductance and capacitance per unit length alone, the equation becomes simply

$$c^2\frac{\partial^2 i}{\partial x^2} = \frac{\partial^2 i}{\partial t^2}. \tag{2.3.8}$$

2.3.1 Analytical solution of the system

In order to obtain a solution for the (2.3.8), we consider the following initial conditions

$$i(0,t) = f(x), \qquad \frac{\partial i}{\partial t}(x,0) = g(x). \tag{2.3.9}$$

and the null boundary conditions

$$i(0,t) = 0; \qquad i(1,t) = 0. \tag{2.3.10}$$

We will search for a solution for (2.3.8) having the separable form:

$$i(x,t) = X(x)\cdot T(t). \tag{2.3.11}$$

Therefore we (2.3.8) reads:

$$c^2 X''(x)T(t) = X(x)T''(t). \tag{2.3.12}$$

That is equivalent with:

$$\frac{T''(t)}{c^2 T(t)} = \frac{X''(x)}{X(x)} = -p^2. \tag{2.3.13}$$

Thus we have $x-$dependent differential equation of second order:

$$X''(x) + p^2 X(x) = 0. \tag{2.3.14}$$

with the conditions:

$$X(0) = X(1) = 0. \tag{2.3.15}$$

According to the rules used in solving DE's [Tenenbaum(1985)], [Coddington(1989)], [Bear(1999)], the characteristic equation has the complex roots: $\lambda_{1,2} = \pm pi$ and as a result the solution will be:

$$X(x) = C_1 \cos(px) + C_2 \sin(px). \tag{2.3.16}$$

Using the considered initial conditions we have:

$$X(0) = C_1 = 0. \tag{2.3.17}$$

$$X(1) = C_2 \sin p = 0 \Rightarrow \sin p = 0 \Rightarrow p = k\pi, k \in \mathbf{N}. \tag{2.3.18}$$

Therefore we have the solution:

$$X_k(x) = \sin(k\pi x), k \in \mathbf{N}. \tag{2.3.19}$$

The second differential equation ($t-$dependent) is:

$$T''(t) + c^2 p^2 T(t) = 0. \tag{2.3.20}$$

Again referring to the rules used in solving DE's [Tenenbaum(1985)], [Coddington(1989)], [Bear(1999)], the characteristic equation has the complex roots: $\lambda_{1,2} = \pm cpi = \pm ck\pi i$, and as a result the its solution takes the form:

$$T_k(t) = a_k \cos(kc\pi t) + b_k \sin(kc\pi t), k \in \mathbf{N}. \tag{2.3.21}$$

Thus the solution of (2.3.8) is:

$$i_k(x,t) = [a_k \cos(kc\pi t) + b_k \sin(kc\pi t)] \cdot \sin(k\pi x). \tag{2.3.22}$$

and the form of the general solution will be:

$$i(x,t) = \sum_{k=1}^{\infty} [a_k \cos(kc\pi t) + b_k \sin(kc\pi t)] \cdot \sin(k\pi x). \tag{2.3.23}$$

Finally in order to obtain a_k, and b_k we use the initial conditions defined in Eq. (2.3.9) and taking into account the Fourier series [Seeley(2006)], [Dyke(2014)], [Lasser(1996)] we have:

$$i(x,0) = \sum_{k=1}^{\infty} a_k \sin(k\pi x) = f(x) \Rightarrow a_k = 2\int_0^1 f(x) \sin(k\pi x) dx. \tag{2.3.24}$$

$$\frac{\partial i}{\partial t}(x,0)=\sum_{k=1}^{\infty}b_k(kc\pi)\sin(n\pi x)=g(x)\Rightarrow b_k=\frac{2}{kc\pi}\int_0^1 g(x)\sin kpixdx. \quad (2.3.25)$$

Now in order to obtain a solution for the (2.3.7), with the initial and boundary conditions (2.3.9), (2.3.10), we have the form:

$$\frac{X''}{X}=\frac{T''}{c^2T}+\frac{n+m}{c^2}\frac{T'}{T}+\frac{nm}{c^2}=-p^2. \quad (2.3.26)$$

with the solution:

$$X_k(x)=\sin(k\pi x). \quad (2.3.27)$$

and the second differential equation:

$$T''+(n+m)T'+(nm+p^2)T=0. \quad (2.3.28)$$

with the discriminant of characteristic equation: $\Delta=(n-m)^2-4k^2\pi^2=-a^2$ and the complex roots $\lambda_{1,2}=-\frac{n+m}{2}\pm i\frac{a}{2}$. Thus the solution will be:

$$T(t)=e^{-\frac{n+m}{2}t}\left[a_k\cos\left(\frac{a}{2}t\right)+b_k\sin\left(\frac{a}{2}t\right)\right]. \quad (2.3.29)$$

Therefore

$$i_k(x,t)=e^{-\frac{n+m}{2}t}\left[a_k\cos\left(\frac{a}{2}t\right)+b_k\sin\left(\frac{a}{2}t\right)\right]\cdot\sin(k\pi x). \quad (2.3.30)$$

and the general solution for telegrapher's equation (2.3.7) is:

$$i(x,t)=e^{-\frac{n+m}{2}t}\sum_{k=1}^{\infty}\left[a_k\cos\left(\frac{a}{2}t\right)+b_k\sin\left(\frac{a}{2}t\right)\right]\cdot\sin(k\pi x). \quad (2.3.31)$$

with

$$a_k=2\int_0^1 f(x)\sin(k\pi x)dx. \quad (2.3.32)$$

$$b_k=-\frac{8}{a(n+m)}\int_0^1 g(x)\sin(k\pi x)dx. \quad (2.3.33)$$

2.3.2 Numerical Method

We approached the evolution in time of the intensity of the current that passes through the transmission line of the telegrapher. For a better accuracy we realized a parallel using the numerical analysis between equation (2.3.7) and equation (2.3.8). In our study we have considered six cases that are encountered in the real life for the boundary conditions. The evolution of the current's intensity is considered for different values of time: t=0.2; t=0.4; t=0.6; t=0.8 and t=1. With star symbol is represented the variation of i(x,t) from equation (2.3.7) and with continuous line is represented the variation of i(x,t) from equation (2.3.8).

Typical order-or-magnitude values for a telephone cable might be about $C = 5 \cdot 10^{-11} F\omega^{-1}$, and $L = 5 \cdot 10^{-7} H\omega^{-1}$, giving a speed of about $2 \cdot 10^{8} ms^{-1}$or about $\frac{2}{3}$ of the speed of light in vacuum . If we require to solve the general case Eq. (2.3.7) we have to choose R so that it is comparable in size to $\sqrt{L/C}$, and G so that it comparable in size to $\sqrt{C/L}$.

We can consider the following boundary conditions enumerated below in five cases. The evolution in time of the intensity of the current that passes through the transmission line of the telegrapher has been plotted against time for the five cases considered in Sec. 5, as shown in Figure[2.12-2.15], respectively. In first case we can observe Figure[2.12] that the intensity of the current varies assymetric for equation (2.3.7) and for the equation (2.3.8) we can observe tat the behavior of amplitude is symmetric. The intensity in case of equation (2.3.7) is dissipating. While for the second case we observe Figure[2.13] that the signal given by the equation (2.3.8) is amplified and for the equation (2.3.7) the signal is dissipating.

Case One:

$i(x,0) = \sin x$, $\frac{\partial i(x,0)}{\partial t} = -\sin x$,$i(0,t) = 0$, and $i(1,t) = 0$

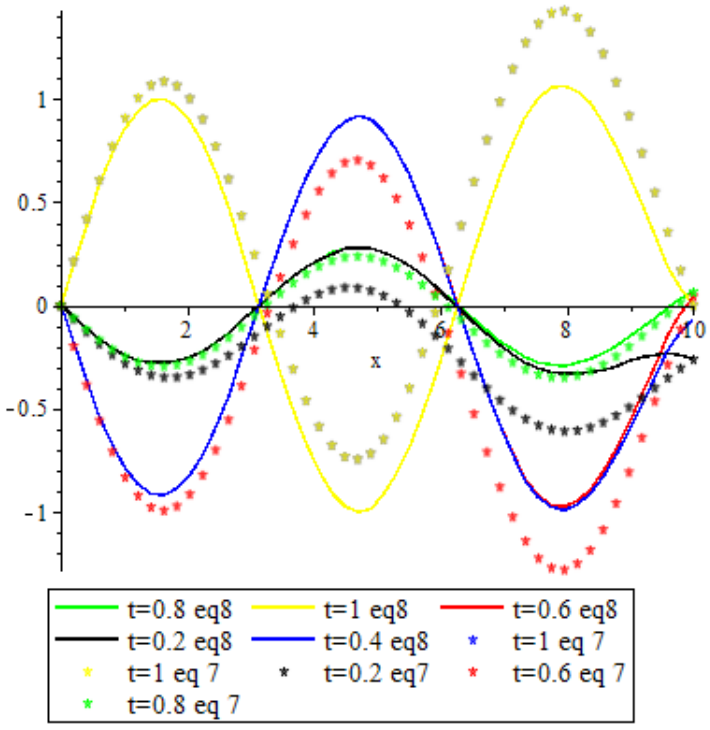

Figure 2.12: Comparision between (2.3.7) and (2.3.8) for the first considered case

Case Two:

$i(x,0) = \sinh x$, $\frac{\partial i(x,0)}{\partial t} = -\cosh x$,$i(0,t) = 0$, and $i(1,t) = 0$

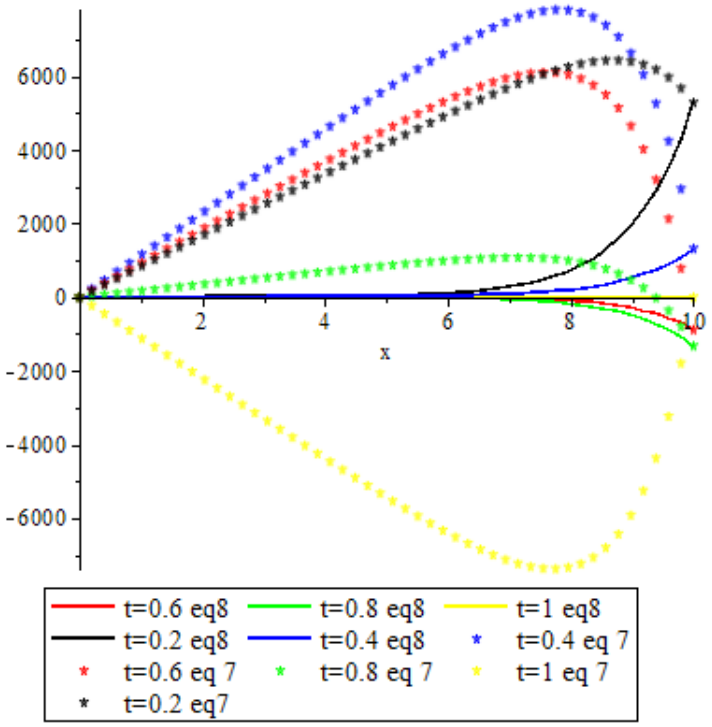

Figure 2.13: Comparision between (2.3.7) and (2.3.8) for the second considered case

Case Three:

$i(x,0) = e^x, \frac{\partial i(x,0)}{\partial t} = -e^x, i(0,t) = 0$, and $i(1,t) = 0$

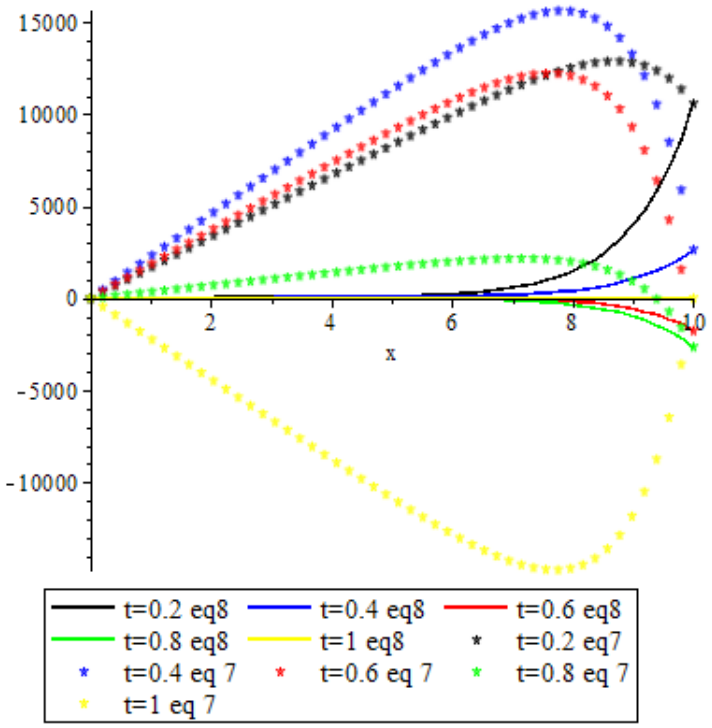

Figure 2.14: Comparision between (2.3.7) and (2.3.8) for the third considered case

Case Four:

$i(x,0) = \sinh x$, $\frac{\partial i(x,0)}{\partial t} = -2\sinh(x)$,$i(0,t) = 0$, and $i(1,t) = e^{-2t}\sinh(1)$

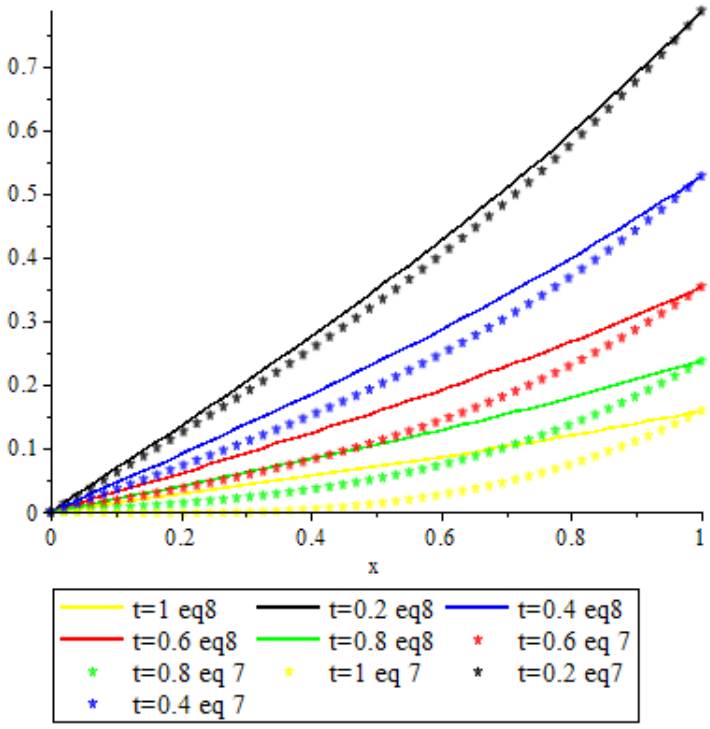

Figure 2.15: Comparision between (2.3.7) and (2.3.8) for the fourth considered case

For the third case we observe Figure[2.14] that the signal has a similar behavior as the second case, but the values of current's intensity ar considerable bigger than in previous case. The current's intensity in the fourth case has a sharper growth for (2.3.8) in contrast to (2.3.7). After x=1 the ratio is changed as it is clear from Figure[2.15].

Figure[2.12] shows that the current intensity behaves in nearly sinusoidal way for equation (2.3.8) while it is not behaving sinusoidally for equation (2.3.7). Figure[2.13], and Figure[2.14] show that the current intensity for equation (2.3.7) is higher that that of equation (2.3.8) for the same time and there is no similarity between the behaviors of them. Finally, it is clear from Figure[2.15] that the current intensity for equation (2.3.8) is always higher than that of equation (2.3.7) and the two behaviors are nearly similar to each other.

2.4 Numerical aspects of two coupled harmonic oscillators

The stability of two dynamical systems using Lyapunov function was studied by Bala in [Bala(2009)]. The structural influence of the forces of the stability of dynamical systems using Hurwitz criterion and also Lyapunov function was studied in [Lupu(2009)]. The motion equations of a one-dimensional finite element having a general three-dimensional motion together the body using the Lagrang'es equations are established in [Vlase(2019)]. Similar techniques in order to obtain some theoretical and experimental results can be encountered in papers [Lupu(1993b)], [Lupu(1993a)], [Groza(2018)].

Simulink is an environment of Matlab Software that is used for the simulation of dynamical systems and also for the model-based design of embedded systems. With Simulink the considered systems can be designed, simulated and implemented based on a set of block libraries. Different types of continuous, discrete and mixed-signal systems (e.g. communications, controls, signal/video/image processing) are simulated and tested with Simulink, [Xue(2013)] [Klee(2011)], [Chaturvedi(2010)], [Beucher(2006)], [Halvorsen]. When the mathematical models contain differential or algebraic equations then the behavior of the systems could be explained from the point of view of scientific principles based on the parameters or variables that influence the models over time.

This section deals with a two coupled harmonic oscillators known in literature as a symmetric linear triatomic molecule. The contribution of authors consists in the analysis of the behavior of the system from a mathematical and also a numerical point of view. The solution of the considered system is obtained analytic by using the Laplace transform and the numerical analysis is considered for two modes of oscillations: symmetric and asymmetric using Simulink environment from MATLAB software.

A description for the system is presented, a Lagrange equation is obtained and the Euler- Lagrange equations are derived. The mathematical solution is given using the Laplace transform. This study ends with the numerical techniques that are discussed for the two considered cases (anti-symmetric and mixed symmetric).

Therefore, we are going to investigate a two coupled oscillators. To start, we consider a two coupled harmonic oscillators of three masses connected linearly by two springs each of stiffness k. The masses at the ends are identical m, while the mass at the center is differ M as indicated in Figure[2.16] below. This system is known in literature as a symmetric linear triatomic molecule e.g, CO_2.

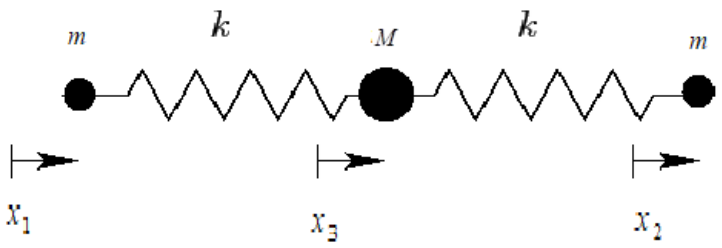

Figure 2.16: A two coupled harmonic oscillators

The kinetic energy T, and potential energy V of the system respectively are:

$$T = \frac{1}{2}\omega_1 \dot{x}_1^2 + \frac{1}{2}\omega_2 \dot{x}_2^2 + \frac{1}{2}\omega_3 \dot{x}_3^2 \tag{2.4.1}$$

$$V = \frac{1}{2}k\left(x_3 - x_1\right)^2 + \frac{1}{2}k\left(x_2 - x_3\right)^2 \tag{2.4.2}$$

As a result the classical Lagrangian reads:

$$L = T - V;$$

$$L = \frac{1}{2}\omega_1 \dot{x}_1^2 + \frac{1}{2}\omega_2 \dot{x}_2^2 + \frac{1}{2}\omega_3 \dot{x}_3^2 - \frac{1}{2}k\left(x_3 - x_1\right)^2 - \frac{1}{2}k\left(x_2 - x_3\right)^2 \tag{2.4.3}$$

Now, in order to obtain the classical Euler- Lagrange Equations (CELE's) we use the relation $\frac{\partial L}{\partial x_i} - \frac{d}{dt}\frac{\partial L}{\partial \dot{x}_i} = 0$. With $i = 1, 2, 3$

So for $x_1, \quad x_2, \quad and \quad x_3$ we have

$$\ddot{x}_1 = \Omega^2\left(x_3 - x_1\right) \tag{2.4.4}$$

$$\ddot{x}_2 = \Omega^2\left(x_3 - x_2\right) \tag{2.4.5}$$

$$r\ddot{x}_3 = \Omega^2\left(x_1 + x_2 - 2x_3\right) \tag{2.4.6}$$

where $r = \frac{M}{m}$, and $\Omega = \sqrt{\frac{k}{m}}$

It is clear from (2.4.3) that we have 3 degrees of freedom. We can reduce this to 2 degrees of freedom by considering only oscillatory modes of motion (i.e., neglecting translational modes), this can be achieved by demanding that the center of mass of the system remains stationary. Thus, we require that:

$$m(x_1 + x_2) + Mx_3 = 0 \tag{2.4.7}$$

The above equation can be rearranged to give:

$$x_3 = -\frac{m}{M}\left(x_1 + x_2\right) \tag{2.4.8}$$

On the other hand

$$\ddot{x}_3 = -\frac{m}{M}\left(\ddot{x}_1 + \ddot{x}_2\right) \tag{2.4.9}$$

Now, eliminating x_3 from (2.2.4)-(2.4.6) we yield respectively:

$$r\ddot{x}_1 = -\Omega^2\left((1+r)x_1 + x_2\right) \tag{2.4.10}$$

$$r\ddot{x}_2 = -\Omega^2\left((1+r)x_2 + x_1\right) \tag{2.4.11}$$

$$\ddot{x}_1 + \ddot{x}_2 = \left(1+\frac{2}{r}\right)\Omega^2 x_1 + \left(1+\frac{2}{r}\right)\Omega^2 x_2 \tag{2.4.12}$$

Note here that (2.4.12) is just the sum of (2.4.10) and (2.4.11).

We aim to solve (2.4.10), (2.4.11) numerically for some initial conditions.

2.4.1 Mathematical solution

We will solve analytic the system formed by (2.4.10) and (2.4.11) using the Laplace transform. Therefore the mentioned system can be written in the simplified form:

$$\begin{cases} \ddot{x}_1 = ax_1 + bx_2 \\ \ddot{x}_2 = bx_1 + ax_2 \end{cases} \tag{2.4.13}$$

where $a = -\frac{\Omega^2(1+r)}{r}$ and $b = -\frac{\Omega^2}{r}$.
In a general case we will consider the following initial conditions:

$$\begin{aligned} x_1(0) = \alpha_0;\ \dot{x}_1(0) = \alpha_1; \\ x_2(0) = \alpha_2;\ \dot{x}_2(0) = \alpha_3; \end{aligned} \tag{2.4.14}$$

Using the property of original derivation of the Laplace transform the system (2.4.13) will have the following form:

$$\begin{cases} (s^2-a)X_1(s) - bX_2(s) = s\alpha_0 + \alpha_1 \\ -bX_1(s) + (s^2-a)X_2(s) = s\alpha_2 + \alpha_3 \end{cases} \tag{2.4.15}$$

Solving the above system we will obtain the images through the Laplace transform:

$$X_1(s) = \frac{s^3\alpha_0 + s^2\alpha_1 + s(b\alpha_2 - a\alpha_0) + b\alpha_3 - a\alpha_1}{[s^2+\xi^2][s^2+\zeta^2]} \tag{2.4.16}$$

respectively,

$$X_2(s) = \frac{s^3\alpha_2 + s^2\alpha_3 + s(b\alpha_0 - a\alpha_2) + b\alpha_1 - a\alpha_3}{[s^2+\xi^2][s^2+\zeta^2]} \tag{2.4.17}$$

where $\xi^2 = -a - b = \frac{\Omega^2}{r}(2+r)$; $\zeta^2 = -a + b = \Omega^2$. Using the inverse method of Mellin Fourier for Laplace transform we will deduce the originals:

$$x_1(t) = A_1\cos(\zeta t) + \frac{B_1}{\zeta}\sin(\zeta t) + C_1\cos(\xi t) + \frac{D_1}{\xi}\sin(\xi t) \tag{2.4.18}$$

where $A_1 = \frac{\alpha_0-\alpha_2}{2};\ B_1 = \frac{\alpha_1-\alpha_3}{2};\ C_1 = \frac{\alpha_2+\alpha_0}{2};\ D_1 = \frac{\alpha_1+\alpha_3}{2}$, respectively

$$x_2(t) = A_2\cos(\zeta t) + \frac{B_2}{\zeta}\sin(\zeta t) + C_2\cos(\xi t) + \frac{D_2}{\xi}\sin(\xi t) \tag{2.4.19}$$

where $A_2 = \frac{\alpha_2-\alpha_0}{2};\ B_2 = \frac{\alpha_3-\alpha_1}{2};\ C_1 = \frac{\alpha_2+\alpha_0}{2};\ D_1 = \frac{\alpha_1+\alpha_3}{2}$.

We observe that $A_1 = -A_2, B_1 = -B_2, C_1 = C_2, D_1 = D_2$.

2.4.2 Numerical solution

The system presented in our work has two modes of oscillations. The first mode of oscillation occurred when $x_1(0) = -x_2(0)$, and $x_3(0) = 0$. This mode of oscillation is known in literature as symmetric (breathing) mode. In this mode of oscillation, the two end atoms move in opposite direction whilst the central atom remains stationary.

The second mode in our system is the asymmetric mode in which $x_1(0) = x_2(0)$, and $x_3(0) = \frac{-2}{r}x_1(0) = \frac{-2}{r}x_2(0)$. In this mode of oscillation the two end atoms move in the same direction whilst the central atom moves in the opposite direction.

Below, we aim to study the above two modes numerically for two cases of coupled oscillators. In the first case (i.e., case I) we consider $r = \frac{M}{m} = 1.50$, with the following values of angular frequencies $\Omega = \sqrt{\frac{k}{m}} = 0.50$, 1.50, and 1.50, while for the second case(i.e., case II) with the following values of angular frequencies $\Omega = \sqrt{\frac{k}{m}} = 0.50$, 1.50, and 1.50.

Therefore, our system of differential equations will have the following form

$$\begin{cases} x_1'' = ax_1 + bx_2 \\ x_2'' = bx_1 + ax_2 \\ x_3'' = c\,(x_1 + x_2) \end{cases} \tag{2.4.20}$$

where $a = -\frac{\Omega^2(1+r)}{r}, b = -\frac{\Omega^2}{r}, c = \frac{\Omega^2(2+r)}{r}$. The numerical analysis is realized using the Simulink environment from Matlab. The Simulink scheme of the system (2.4.13) is:

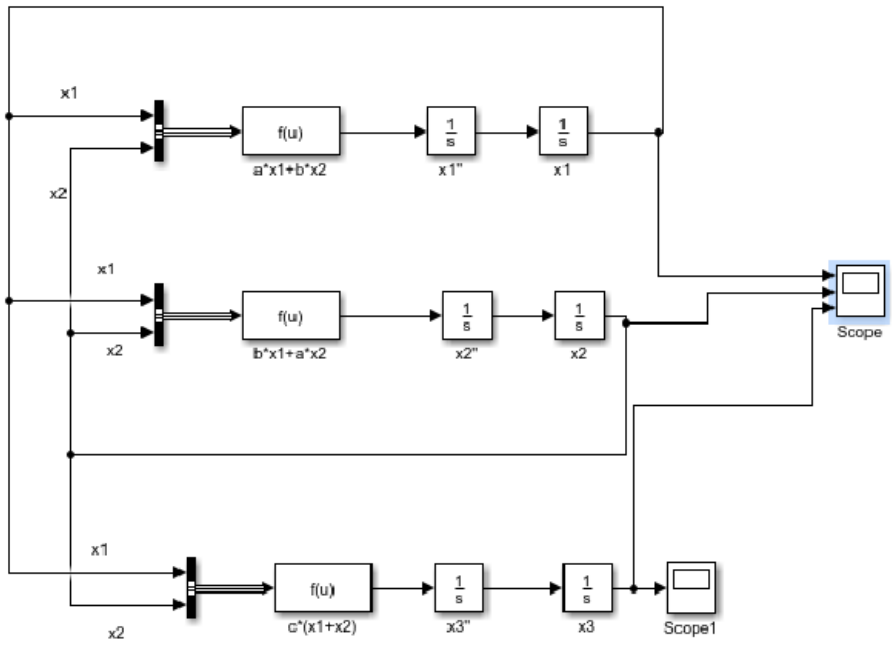

Figure 2.17: The Simulink scheme for the system (2.4.13)using the Fcn block from the block library User Defined Functions

The symmetric mode

For this mode of oscillation let us assume that $x_1(0) = -x_2(0) = 1$, and $x_3(0) = 0$, while $\dot{x}_1(0) = \dot{x}_2(0) = \dot{x}_3(0) = 0$.

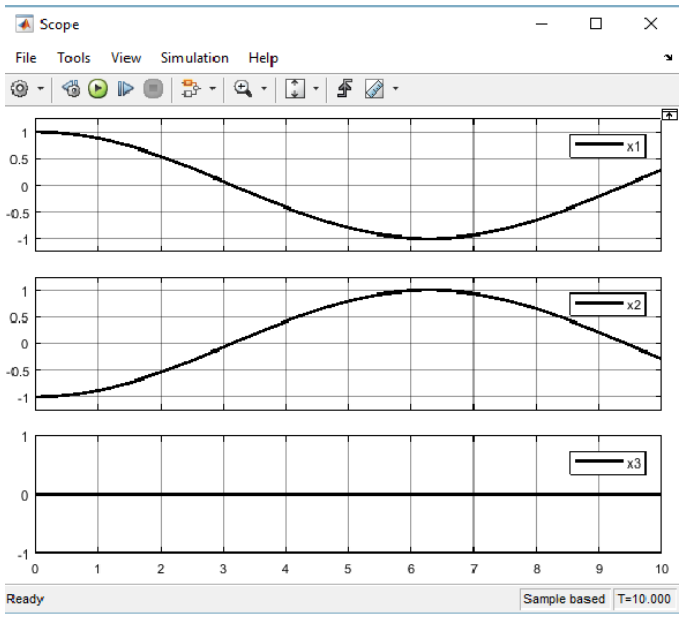

Figure 2.18: The behavior of the solutions of the system (2.4.13) in the case when r=1.5 and $\Omega = \sqrt{\frac{k}{m}} = 0.50$

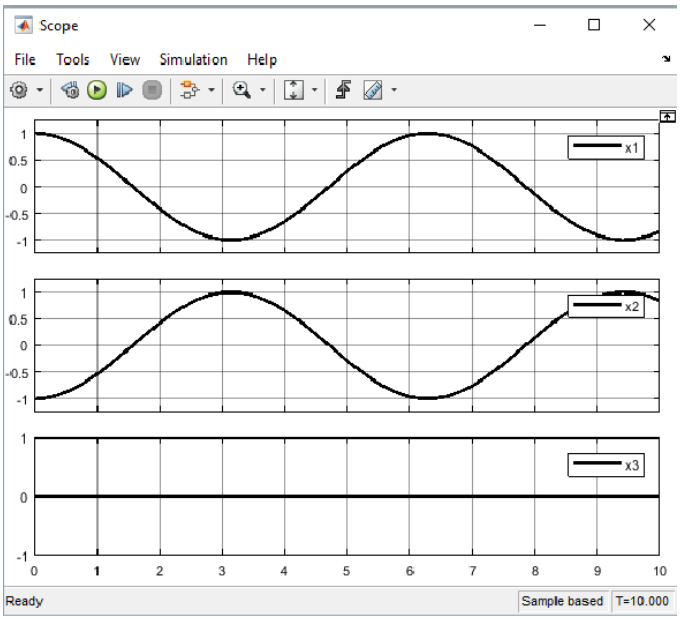

Figure 2.19: The behavior of the solutions of the system (13) in the case when r=1.5 and $\Omega = 1.0$

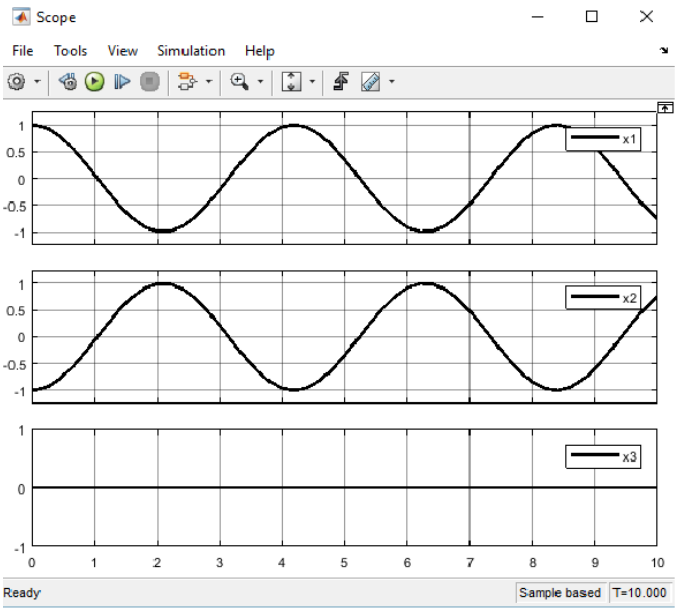

Figure 2.20: The behavior of the solutions of the system (2.4.13) in the case when r=1.5 and $\Omega = 1.5$

The asymmetric mode

For this mode $x_1(0) = x_2(0) = 1$, and $x_3(0) = \frac{-2}{r}x_1(0) = \frac{-2}{r}x_2(0) = \frac{-2}{r}$. While $\dot{x}_1(0) = \dot{x}_2(0) = \dot{x}_3(0) = 0$.

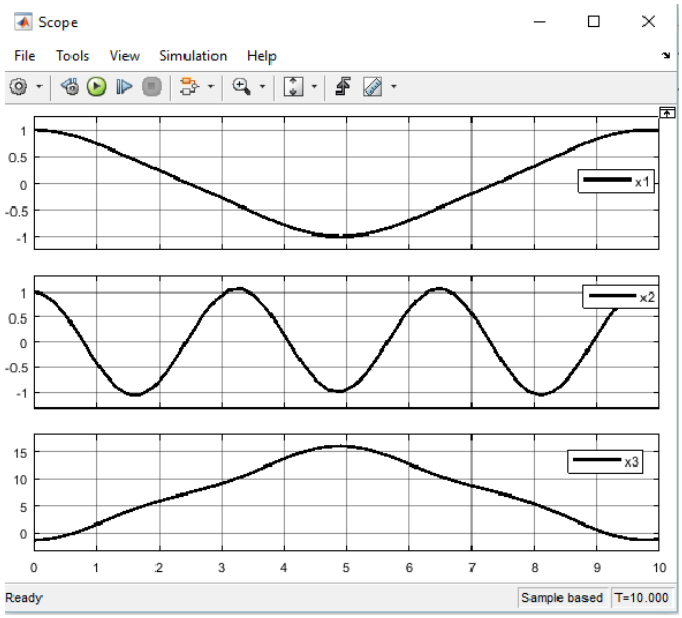

Figure 2.21: The behavior of the solutions of the system (2.4.13) in the case when r=1.5 and $\Omega = \sqrt{\frac{k}{m}} = 0.50$

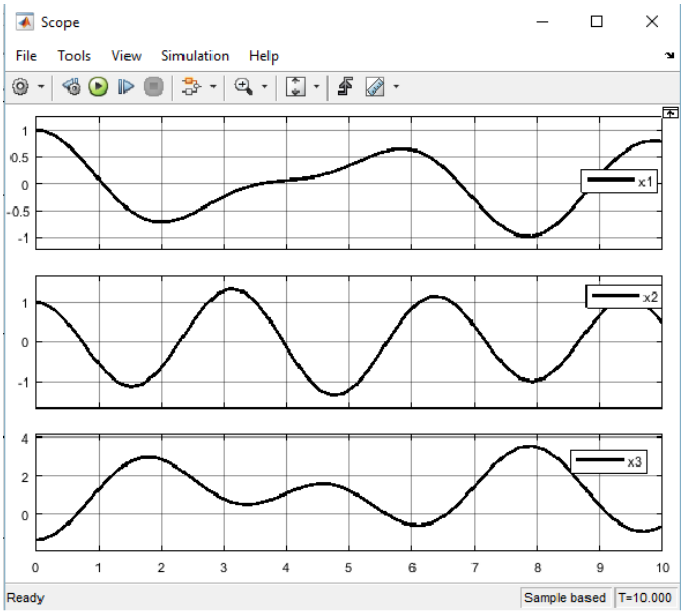

Figure 2.22: The behavior of the solutions of the system (2.4.13) in the case when r=1.5 and $\Omega = 1.5$

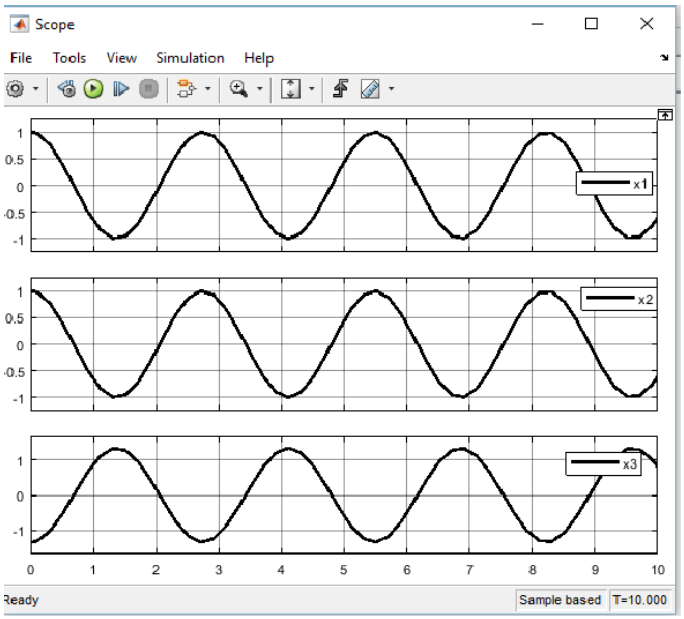

Figure 2.23: The behavior of the solutions of the system (2.4.13) in the case when r=1.5 and $\Omega = 1.5$

We investigated numerically the behaviour of a famous physical system called a linear two coupled oscillators. This interesting system is a symmetric linear system, with carbon dioxide CO_2 being a good example. Firstly, the symmetric mode, where the behaviour of the system has been presented in Figure[2.18-2.20]. Secondly, the asymmetric, where the behaviour of the system has been showed in Figure[2.21-2.23].

The numerical analysis of the system (2.4.13) is realized using the Simulink environment, part of MATLAB software. Due to the fact that the differential equations from (2.4.13) are of second degree we used two integrator blocks that are continuous-time integration of the input signal with initial conditions of internal type in order to obtain the behaviour of the solutions. To simplify the Simulink scheme, the expressions of those three equations are inserted in three different function blocks. The scheme is realized based on the loop diagrams, therefore in front of the function blocks we included a bus creator that creates a bus signal from its inputs.

Figures[2.18-2.20] show the behaviour of the solutions of the system represented by (2.4.13) for different values of Ω . It is clear from these figures that the particle at the center remains at rest as we assumed previously, while the position of mass 1 behaves in the opposite direction to that of particle 2. This is why we call this mode symmetric. Also the resulting motion of masses 1, and 2 is oscillatory motion but with 180^o out of phase with each other.

In Figure[2.21-2.23], the behaviour of the solutions of the system represented by (2.4.13) for different values of Ω has been showed. For this asymmetric mode it is clear from Figure[2.21-2.23] that the behaviour of the solution of the system (2.4.13) depends on the value of Ω. For example, Figure[2.23] shows that we have oscillatory motion for the three masses but as clear mass 3 with 180^o out of phase with the other two masses.

Chapter 3

Innovative Modeling Approaches in Nanomaterials and Biomass Analysis

3.1 Microscopic Hamiltonian and chaotic behavior for Barium Titanate nanoparticles revealed by photonic tunneling model

Ferroelectricity is the ability that possess certain class of materials by having an impulsive electric polarization that can reverse under the effect of an applied outward electric field [Werner(1957)], [Lines(1979)]. J. Valasek during the investigations of the dielectric properties of Rochelle salt discovered in 1921 this phenomenon [Valasek(1920)]. It is difficult to say exactly in a single sentence what a ferroelectric is. Usually, they are viewed as materials that sustain a dielectric polarization when exposed to an electric field. Ferroelectrics are widely used because of their properties. These applications include hysteresis which is used in nonvolatile memories; a high permittivity used for capacitors engineering. These phenomena are also found in devices with resonant waves of radio frequency filters, sensors, or actuators, presenting high piezoelectric effects. Other properties are their high pyroelectric coefficients commonly used for the development of infra-red detectors [Kasap(2006)]. Their electro-optical effects are found in optical switches, and another important characteristic is given by the abnormal resistivity coefficients. [Kasap(2006)].

In recent years, research based on ferroelectric nanoparticles have been approached both in the field of materials technology as well as in medicine or biology. For

material technology, ferroelectrics has been used in multilayered capacitors and nanocomposites [Haertling(1999)] and in liquid crystals for display and non-display applications [Reznikov(2003)]. In biology they are used as proliferation agents for cells and tissues cultures[Ciofani(2011)], [Ciofani(2012)]. Screening for genetic diseases or cancer has an important role in the early identification of infected tissues, thus the use of ferroelectric nanoparticles in the field of medical imaging of deep tissue in vitro and in vivo represents a real success. [Barranco(2012)] .

In ordinary materials, the polarization field is proportional to the applied electric field whereas in ferroelectric, it is a nonlinear function of the electric field then, making the ferroelectrics been nonlinear materials. Therefore, they are subject to many nonlinear phenomena. The physical phenomenon in which the physical behavior of a system cannot be correlated with the effect it generates is represented by nonlinearity. The response as well as the stimulus of such a system represent the physical parameters that are not proportional. This nonlinearity is obviously found in natural systems, their behavior being independent of their size (atom vs universe) or their type of motion (classical vs relativistic) [Lam(1997)]. In recent years, scientific studies have focused on chaos theory. The etymology of the term comes from the Greek language, which implies an unformed, disordered world. This expression can resemble a gaping chasm (a precipice). [Moon(1992)]. From a scientific point of view, the non-linear state of a natural system is given by its non-periodic oscillatory characteristic.[Aoki(2001)].

In this section, we derive the extended Hamiltonian from the photonic tunneling model which Je Huan Koo and Kwang-Sei Lee proposed by studying ferroelectricity and antiferromagnetism in multiferroic materials [Koo(2017)]. Recently, they carried out their studies by using the second quantization formalism for calculation of an impulsive polarization of ferroelectrics [Koo(2019)]. Due to nonlinear and complex media of the ferroelectrics, they display numerous types of nonlinear behaviors. We investigate the possibility of complex chaotic vibrations propagating in **Barium Titanate Nanoparticles** using derivation of semiquantal dynamics via the Ehrenfest theorem.

3.1.1 Extended Hamiltonian microscopic model of Barium Titanate

Photon field couplings are formed between many-body electrons. In our study we will focus on photons whose finite mass is made up of interacting electrons. The photon field correlations of the electrons are the propagators of ferroelectric ordering due

to frequent virtual absorption and emission of photons by electrons. It is revealed by many authors that multiferroics, spin glasses and polar glasses are assumed as composed of electron clusters. That is why they may be looked as finite block spins [Fischer(1991)], [Binder(1986)], [Edwards(1975)], [Kim(2016)], [Lee(2016)].

The effective Hamiltonian associated to Barium Titanate ferroelectric ordering can be characterized as an ensemble of effective photons for finite sized block spins in a tunneling potential of a double well assumption as follows:

$$\widehat{H} = \frac{\hat{P}^2}{2mN} + \frac{1}{2}k^2\left(\hat{x}^4 - 2x_0^2\hat{x}^2 + x_0^4\right), \quad k = Nm\omega^2 \tag{3.1.1}$$

where $\hat{P}$ is the photon's momentum and $\hat{x}$ is the photon's position. The mass of the electron -photon is m, N represents the average number of electro-photons in a finite standard block spin and ω represents the tunneling frequency for a double well potential appropriate to the KDP-type crystals. The repulsion between the core ion-ion of neighboring atoms leads to obtaining a periodic potential relative to the lattice site

Further, based on Ehrenfest's theorem [Pattanayak(1992)], we will use the method of derivation of semi-quantal dynamics due to the fact that its approach is closer to the formulations of non-equilibrium static mechanics. Thus, the dynamics obtained is similar to the TDVP technique. Let us consider the motion of an effective photon for finite sized block spins in a one-dimensional time-independent tunneling potential. Its Hamiltonian will be $\widehat{H} = \frac{\hat{P}^2}{2mN} + V(\hat{x})$ where by $\widehat{\mathcal{O}}$ are represented the operators. The centroid of a wave group representing the effective photon has the movement equations as follows:

$$\frac{d}{dt} < \hat{x} > = < \hat{p} >, \quad \frac{d}{dt} < \hat{p} > = \ - < \frac{\partial V\left(\hat{x}\right)}{\partial \hat{x}} >, \tag{3.1.2}$$

where the <> indicate expectation values. In general, the centroid deviates from the classical trajectory. Using the following identity, we will expand the equations around the centroid:

$$F\left(\hat{u}\right) > = \ \frac{1}{n!} < \hat{U}^n > F^{(n)}, \quad n \geq 0 \quad where\ F^{(n)} = \frac{\partial^n F}{\hat{U}^n}|_{<\hat{u}>} \ \ and\ \hat{U} = \ \hat{u} - < \hat{u} > . \tag{3.1.3}$$

Using the index summation convention and taking into account the commutativity property of the operators, we will be able to generate an infinite number of equations corresponding to an infinite Hilbert space for the considered problem. The assumption that the wave group is a squeezed coherent state renders the space finite will lead us

to the following relations:

$$< \hat{X}^{2m} > = \frac{(2m)!\mu^m}{m!2^m}, \quad < \hat{X}^{2m+1} > = 0,$$
$$4\mu < \hat{P}^2 > = \mathrm{h}^2 + \alpha^2 and < \hat{X}\hat{P} + \hat{X}\hat{P} > = \alpha \tag{3.1.4}$$

We can see that the above relations are similar to the generalized Gaussian wave functions [Cooper(1986)], [Kovner(1989)], [Klauder(1985)], [Zhang(1990)], [Tsue(1992)] . This assumption is precisely that of the TDVP: The wave group is confined to a given subspace. In addition, we introduce the change of variables $\mu = \rho^2$ *et* $\alpha = 2\rho\xi$.

However, the explicit form of the dynamics equation from the photonic tunneling model in ferroelectrics yields as follow

$$\frac{dx}{dt} = \frac{p}{mN}, \tag{a}$$
$$\frac{dp}{dt} = 2k^2x_0^2x - 2k^2x^3 - 6k^2x\ \rho^2 \tag{b}$$
$$\frac{d\rho}{dt} = \xi \tag{c}$$
$$\frac{d\xi}{dt} = \frac{1}{4\rho^3} + \rho\left(2k^2x_0^2 - 6k^2x^2\right) - 6k^2\rho^3. \tag{d}$$
$$\tag{3.1.5}$$

The dynamics reduced of x and p are written for $< \hat{x} >, < \hat{p} >$ and are exactly those derived from the action principle [27]. The above equations are the Ehrenfest theorem ones we have set $\mathrm{h} = 1$. Due to the nonlinearity of the equations, we expect the system to have a chaotic behavior, the trajectories being both regular and irregular. it is worth noting that our equations are coupled, thus highlighting the connection between classical and quantum interactions. At $\mathrm{h} \to 0$ classical limit, only the first two equations remain, confirming that the fluctuation variables are responsible for quantum effects. Besides, the associated Hamiltonian is

$$H_{ext} = \frac{P^2}{2} + \frac{\xi^2}{2} + V_{ext}(x,\rho), \tag{a}$$
$$V_{ext}(x,\rho) = \frac{1}{2}k^2\left(x^4 - 2x_0^2x^2 + x_0^4\right) + \frac{1}{8\rho^2} + k^2\rho^2\left(3x^2 - x_0^2\right) + \frac{3}{4}k^2\rho^4 \tag{b}$$
$$\tag{3.1.6}$$

In the above equations the subscript *ext* is used in order to express the "extended" Hamiltonian and potential, respectively. This approach is very interesting, offering an explicit way of presenting the gradient system, and for a simplistic visualization of the semiquantal space, the extended potential is used. In this way, before the detailed numerical analysis, we can have an overview of the semiquantitative dynamics.

3.1.2 Numerical Simulations and discussions

In this section, the numerical analysis of equations (a) is addressed using the Runge-Kutta numerical integration method of the 4th order. The numerical interpretation was made on several sets of values for the parameter k and different initial conditions. The results of the numerical analysis are obtained for the value $x_0 = 10$ when the quantum effects are small, but obviously they cannot be neglected.

For the different parameters, k, the periodicity of the system is determined, thus highlighting the shape of the effective photon trajectories. Figure[3.1] shows the irregular chaotic movement for the case where the tunnelling frequency admits low values.

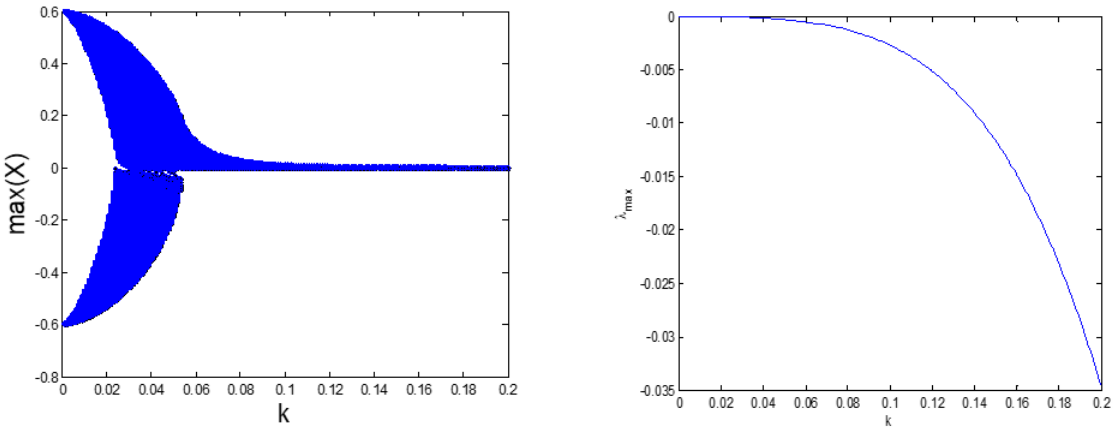

Figure 3.1: Poincare sections in the plane (ξ, x). We set parameters as $k = 0.22$; $x_0 = 10$; $m = 0.00278$; with the initial conditions (0.3; 0.3; 0.01; 0.01).

In order to determine the qualitative changes in the system dynamics when changing the values of parameter k as well as the type of bifurcation and their nature, we performed simulations by varying parameter k from 0 to 0.2. The Fig. 2 represents the evolution of the x -coordinate as a function of the parameter k.

- For $k < 0.05$ the system contains no stable fix point and then becomes chaotic. The state of the system changes completely. The trajectory always revolves around the attractor and the calculated coordinates are then arbitrary. A change in behavior occurs from $k = 0.05$.The equilibrium point is no longer a stable point, and the system stabilizes at one of the two points fixes.

For $k > 0.05$ the trajectory converges towards the equilibrium point. The system is stable around this equilibrium point.Bifurcation is the event in which the qualitative property of attractor of a dynamical system is changed as a control parameter of the system is varied.

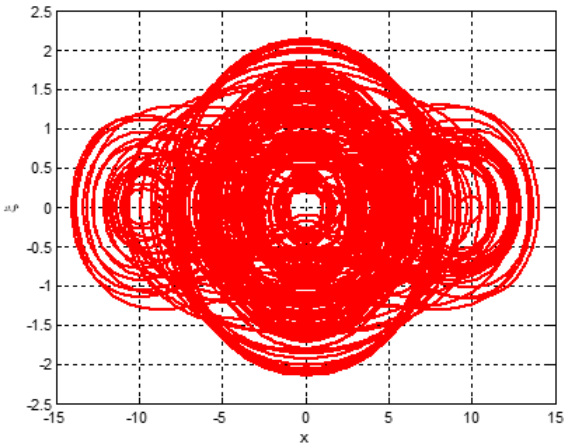

Figure 3.2: Dynamics with respect to the bifurcation diagram for $x_0 = 10$ under the effect of the tunneling frequency ω and the maximal Lyapunov exponent for the set of equations (a) versus the parameter k with the initial conditions (0.3; 0.6; 0.1; 0.1).

During the evolution of the system as a function of parameter k, the behavior of the system undergoes two qualitative changes:

The calculation of the Lyapunov exponent is done from a numerical simulation and the logarithmic difference between the evolutions of the state variables of the system, the results obtained are represented by the Figure[3.2]. From Figure[3.2] analysis, the Lyapunov exponent estimated is positive when the parameter k is below 0.05, a positive exponent implies the divergence of neighboring trajectories, i.e. for these values of the system parameters, and we have a chaotic behavior. In addition, the Lyapunov exponent is negative when the parameter k is over 0.05 that is to say the system is stable in this domain.

Therefore, we derive an extended Hamiltonian photon correlation concept for multiferroics from conventional theories of pseudo-spin formalism and proton tunneling model. Because of the fact that ferroelectrics are nonlinear and complex media; their phenomena originate from spontaneous photon-phonon correlations to induce numerous kind of nonlinear behaviors. Order-disorder nature of phase transitions propagates in Barium Titanate ferroelectric through this study. In conclusion, chaotic regions and periodic regions exhibited by photon correlations are

of course in certain correspondence with bifurcation diagram and Lyapunov exponent as shown in Figure[3.2].

3.2 Indirect evaluation of the porosity of waste wood briquettes by assessing their surface quality

Biomass, like agricultural straws and grasses, wood chips and sawdust, is an attractive feedstock because of its renewability, abundance and positive environmental impact. Biomass is difficult to handle, transport, store and utilize in its original form due to the high moisture content, irregular shape and sizes and low bulk density. Densification can produce products with uniform shape and sizes that can be more easily handled and thereby reduce cost associated with transportation, handling and storage [Karunanithy(2012)],[Chaney(2010)], [Mani(2005)]. Conventional processes for biomass densification can be classified into baling, pelletizing, extrusion, and briquetting. Among them, pelletizing and briquetting are the most common processes used for biomass densification for solid fuel applications. During briquetting the biomass particles self-bond to form a briquette due to the thermoplastic flow. The briquettes' densities generally range from 900 to 1300 kg/m^3 [Tumuluru(2010)]. The five basic categories of biomass materials include: virgin wood, energy crops, agricultural residues, food wastes, industrial wastes and co-products [Al-Hamamre(2017)]. Biomass from wood originated from forest residues or as waste from wood industries is one of the most universal renewable sources of energy [Križan(2014)], [Grover(1996)].

Usta [Usta(2003)] defines wood as a cellular/porous material composed of cell wall substance and cavities containing air and extractives. Without cavities and intercellular spaces the density of the cell wall substance is constant for all timbers (1530 kg/m^3 on an oven-dry mass and volume basis). However, wood is not comprised of 100% cell wall substance because it contains air pockets in the cell lumens. Therefore, the amount of cell wall substance (K) is a function of wood density, d (K = d/1530). The void volume (porosity, P) is defined in relation to the cell wall substance (P = 1-K).

Siau [Siau(1995)] regarded wood cells as a rectangular model of square cross section with unit overall dimensions Figure[3.3(a)]. All cells are equally sized and the ends of the cells are neglected. The cell lumen has also a square cross section. The model refers to cells at oven-dry conditions, where the lumen has only dead air. A more general model of wood cells that considers the wood moisture content is described by Siau [Siau(1995)] and also by Hunt et al. [Hunt(2008)], where the bound water is added as a surrounding area to the outside of the squared cell cross section having the side equal to unity Figure[3.3(b)].

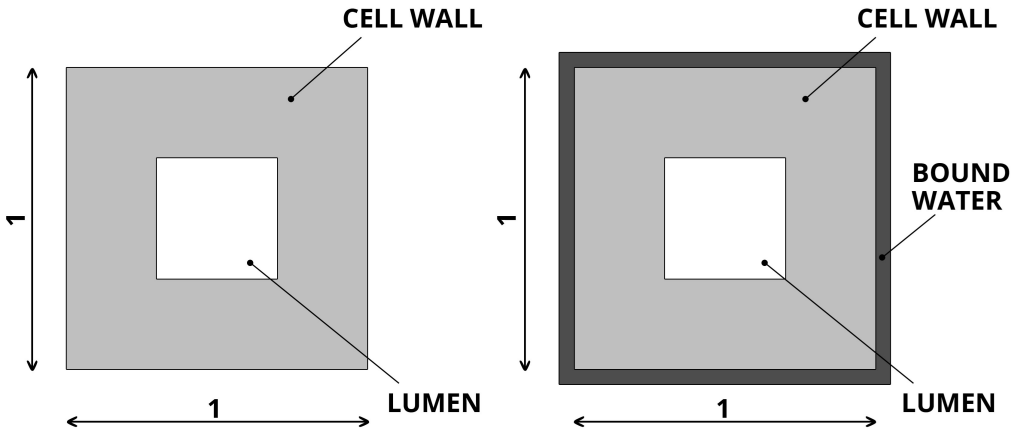

Figure 3.3: Wood cell model (cross section): (a)left side - oven-dry conditions, (b)right side - wet conditions

Porosity is one of the physical properties of wood and wood briquettes, as well, combustion analysis, heat and mass transfer processes during combustion stages, determination of effective thermal conductivity or other related properties, such as density or durability [Hunt(2008)], [Ragland(1991)], [Saptoadi(2008)], [Dunlap(1914)].

Wood porosity can be determined by application of pycnometric methods, displacement of various liquids and mercury intrusion porosimetry [Dunlap(1914)], [Moura(2002)], [Plötze(2011)]. However, wood has a different configuration than wood briquettes and can be submitted to different methods of porosity measurement. Mercury porosimetry and gas pycnometry are usually used to estimate the pore size distribution and porosity of wood. According to Moura et al. [Moura(2002)], the mercury porosimetry is suitable to evaluate the porosity of wood, pulp and paper, being a valuable tool to anticipate properties like surface roughness, air permeance or coating distribution. A limitation of the porosimeter that the authors have used is that voids with diameters below about 0.007 μm are not detected.

Brewer et al. [Brewer(2014)] have calculated the porosity of biochar by means of skeletal density, determined by helium pycnometry and envelope density, by using an envelope density analyzer. Additional methods were required since some macro-voids were inaccessible to helium gas.

Newer research [Huang(2017)] applied computed tomography (CT) and backscattered electron (BSE) imaging methods to investigate and quantify the porosity of wood (bamboo cross section). The authors of the research compared different methods

of porosity measurement, such as mercury intrusion porosimetry, gas pycnometry, microscopy image processing and computed tomography, and evaluated the strengths and the limitations of each method. Considering the strengths and limitations of the existing porosity measurement techniques, they decided to simultaneously use two methods, SEM and CT scanning methods, in order to investigate the porosity distribution as function of orientation within bamboo wood.

In contrast, there are reported only few methods for briquettes or pellets porosity measurement, both bulk and individual porosity. The individual porosity (also called porosity index) of briquettes made of coal and corn cob in different ratios, with binder, was determined by Ikelle and Ivoms [Ikelle(2014)] based on the amount of water each sample is able to absorb. The porosity index was calculated as the ratio of the mass of water absorbed to the mass of the sample immersed in the water. The authors did not describe very well the measurements they performed and question marks can arise regarding briquettes water absorption, whether all voids were filled or not with water after immersion, as well as regarding the risk of swelling occurrence. The bulk porosity or macro-porosity is specific to cylindrical wood pellets and it is determined, for example, by using the method of stereometric measurements [Igathinathane(2010)], [Guo(2012)].

A correlation between surface and volume (bulk) characteristics was reported by Suliman et al. [Suliman(2017)]. They described the relationships existing between porosity and surface functionality of different wood biochars and soil water retention characteristics. One of their conclusions was that the capability of biochar to retain soil water is a function of the combination of its porosity and surface functionality, i.e. generation of oxygenated functional groups on the surface.

Since porosity is important for the analysis of briquettes combustion, it would be interesting to see if this property can be indirectly evaluated by another method, such as by measuring some roughness parameters of the briquette surface in connection with briquette density. It can be assumed, based on previous studies, that both porosity [Usta(2003)] and roughness parameters [Gurau(2004)] are properties depending on wood density.

Therefore, this paper examined correlations between the following properties: porosity and density of briquettes, surface roughness parameters and density of briquettes, as well as surface roughness and porosity of briquettes. Porosity and density were determined by using three different methods.

3.2.1 Material, methods and equipment

The briquettes used for this research were obtained from beech and spruce chips, in uncontrolled proportions, originated as waste material from secondary wood processing in the faculty workshop. The wood chips were compressed using a MB4 GOLDMARK type hydraulic briquetting press with the main characteristics indicated in Table 1.

Table 1. Characteristics of the briquetting press

Press power	4 kW
Pressure	15 MPa
Maximum capacity	40 kg/h
Diameter of briquette	40 mm
Length of briquette	30-75 mm
Maximum moisture content	17 %
Tank diameter	800 mm
Press dimensions (LxHxW)	1200x980x1300 mm

The mixture of chips was compressed without binders. Cylindrical briquettes with uniform circular cross section and different lengths were obtained.

vcd Roughness parameters

Ten briquettes were randomly taken from the press container and stored in a controlled environment (22±1 ^{o}C temperature and 40±2 % RH). Firstly, they were subjected to roughness measurements. The measurements were performed by using a MarSurf XT20 instrument manufactured by MAHR Gottingen GMBH, endowed with a scanning head MFW 250 with tracing arm in the range of ±500 μm and a stylus with 2 μm tip radius and 90∘ tip angle, which measured the briquettes lengthwise at a speed of 0.5 mm/s and at a low scanning force of 0.7 mN. The instrument had MARWIN XR20 software installed for processing the measured data.

The briquettes were scanned on tracing lengths of 15 mm. Four profiles were scanned for each specimen, at every 90^o angle of the briquette cross-section, so that a total of 40 profiles were available for further evaluation of parameters. The lateral measuring resolution was 5 μm and the instrument provided a vertical resolution of 50 nm.

First, the software removed the form error and after that, the waviness. The roughness profiles were obtained by filtering each profile by using a robust filter RGRF (Robust Gaussian Regression Filter) contained in ISO 16610-31 [ISO(2010)]. The cut-off used

was 2.5 mm as recommended in previous research of Gurau [Gurau(2004)]. This filter was tested and found useful for wood surfaces.

After generating the roughness profiles, *Ra*, representing the arithmetic mean deviation of the assessed profile irregularities, was calculated on sampling lengths according to ISO 4287 [24]. Other calculated parameters were the material ratio curve (Abbot curve) parameters *Rpk*, *Rk* and *Rvk* from ISO 13565-2 [ISO(1996)]. *Rk* is the depth of the roughness core profile, *Rpk* is the average height of the protruding peaks above the roughness core profile and *Rvk* represents the average depth of the profile valleys projecting through the roughness core profile. *Rvk* may be especially sensitive to species' anatomical valleys or to various gaps caused during the briquettes pressing process. *Rpk* is a measure of fuzziness protruding above the core roughness. The sum *Rk*+*Rpk*+*Rvk* was also determined for comparisons, because of the cumulative effect on surface roughness and together with *Rvk* should be sensitive to variations in briquette density (and porosity).

For each briquette and roughness parameter, a mean value and the standard deviation were calculated and included in a table.

Briquettes density

For evaluating the briquettes density, two stereometric methods and a liquid displacement method were applied. The reason for applying different methods was to evaluate the best correlation of density with both porosity and roughness parameters. The first stereometric method (St1) was based on the measurement of the length and diameter of each briquette and on calculating the volume of a cylinder as regular geometrical shape. Two lengths (at right angle of each other) and three diameters (at each end and in the middle) of each briquette were measured using a digital pocket caliper (ULTRA, 0.01 mm accuracy). The average values and the volume were then calculated. The briquettes were weighed by using a KERN-EW 3000 g technical balance (0.01 g accuracy). The density was calculated as the ratio of mass to briquette volume.

The second stereometric method (St2) consisted in estimating the cross-section area of each briquette by the use of a paper sheet of known area density (80 g/m^2), as described in [Rabier(2006)]. The briquette was placed on the paper, its contour was drawn on the paper and the cross-section surface was accurately cut. The piece of paper was then weighed and its surface was calculated from the mass and the area density of the paper. The paper surface approximating the cross-section of the briquette was multiplied by the average length of the briquette and the volume of the briquette was thus obtained. Again, the density was calculated as the ratio of mass

to briquette volume.

After that, the briquettes were oven dried at 103±2^{o}C to constant mass in order to determine the moisture content. The moisture content was calculated based on wet and oven-dry briquette masses (SR EN 13183-1-2003/AC-2004 [ISO(2003)]). Finally, the oven-dry briquettes' dimensions were measured again by using the two stereometric methods described before. Oven-dry and wet briquettes densities were calculated based on relations (3.2.1) and (3.2.2):

$$\rho_{\mathrm{OD}} = \frac{\omega_{\mathrm{OD}}}{V_{\mathrm{OD}}} \tag{3.2.1}$$

$$\rho = \frac{\omega_{br.}}{V_{br.}} \tag{3.2.2}$$

where: ρ_{OD}(kg/m^3) andρ(kg/m^3) are the densities of the oven-dry and wet briquettes, m_{OD} (kg) and $m_{br.}$ (kg) are the oven-dry and wet briquettes' masses, V_{OD} (m^3) and $V_{br.}$ (m^3) are the oven-dry and wet briquettes' volumes. Wet briquettes are denoted as those briquettes which have the moisture content in equilibrium with the relative humidity of the surrounding air, that is, equilibrium moisture content (EMC).

The volume of oven-dry and wet briquettes by the liquid displacement method was estimated by immersion (Im) of each briquette in toluene ($C_6H_5CH_3$), having the density equal to 865.5 kg/m^3 at 20 ^{o}C. The change of the toluene density with slight environmental temperature changes was neglected. The volume of the briquette was obtained from the mass of the volume of toluene that was displaced while immersing the briquette in the liquid. Firstly, a Berzelius glass beaker was filled with toluene to a fixed volume Figure[3.4(a)]. The beaker with toluene was weighed. Then, the briquette was placed in a metallic (copper) cage that was submerged in the Berzelius glass beaker with known mass of toluene. The part of the liquid that exceeded the fixed initial volume was removed. The cage was fixed by means of a wire on a glass rod placed on the glass top Figure[3.4(b)]. The volume of the briquette was calculated from the density of toluene and the difference in the masses of toluene before and after briquette immersion. The density of the briquettes was evaluated by using this method, following Figure[3.4(b)] and the equations indicated below:

$$V_l = V_{l_1} + V_{br.} + V_{cage} \tag{3.2.3}$$

where: V_l (m^3) is a fixed volume of liquid (toluene) in the glass beaker, V_{l1} (m^3) is the volume of the liquid in the glass beaker when the briquette and cage were immersed (the part of the liquid that exceeded the initial volume was removed), $V_{br.}$ (m^3) is the volume of the briquette, V_{cage} (m^3) is the volume of the cage.

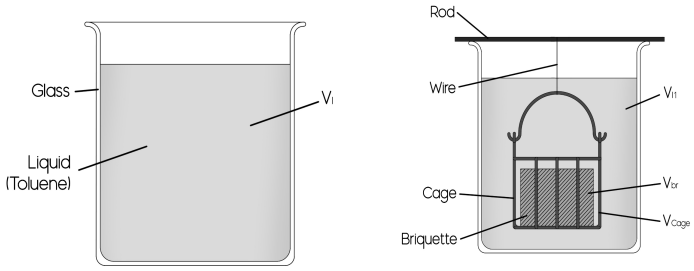

Figure 3.4: Briquette volume determination by using the liquid displacement method: (a) left side- before briquette immersion, (b) right side - after briquette immersion

If rearranging the terms of Eq. (3.2.3), the volume of the briquette becomes:

$$V_{br.} = V_l - V_{l_1} - V_{cage} \tag{3.2.4}$$

Eq. (3.2.4) can also be written in terms of masses and liquid density (ρ_l), as:

$$V_{br.} = \frac{\omega_l - \omega_{l_1}}{\rho_l} - V_{cage} \tag{3.2.5}$$

and the expression of the briquette's density is therefore:

$$\rho = \frac{\omega_{br.}}{\frac{\omega_l - \omega_{l_1}}{\rho_l} - V_{cage}} \tag{3.2.6}$$

The terms m_l (kg) and m_{l1} (kg) refer to the masses of liquid corresponding to the volumes V_l and V_{l1}.

Briquettes are porous materials. During immersion, a part of the pores (voids developed during chips compression) is filled with liquid. For evaluating possible errors, the mass of the liquid, briquette and cage was firstly measured, as indicated in Figure[3.4(b)], and afterwards, separately, the masses of the liquid (M_{l1}), that of the briquette filled with liquid ($m_{\ w.br.}$) and that of the cage (m_{cage}).

The total mass is:

$$M = \omega_{l_1} + \omega_{w.br.} + \omega_{cage} \tag{3.2.7}$$

and the sum of the individual masses is:

$$M' = \omega_{l_1} + \omega_{w.br.} + \omega_{cage} \tag{3.2.8}$$

During the successive measurements of masses, some toluene may evaporate and thus, m_{l1} may be different from M_{l1}. The difference

$$M - M' = \omega_{l_1} - \omega_{l_1} = \Delta \tag{3.2.9}$$

represents the error that occurs during mass measurements. The errors that were calculated for all briquettes are very small, below 1 g. The ratio Δ/ω_{l_1} was also evaluated and it is lower than 0.2%, showing that there were not important liquid mass losses during the experiment. The liquid that fills a part of the pores does not influence the briquette's volume determination by the liquid displacement method. Corrections in calculating the density were made for slight equilibrium moisture content changes. The volume of the cage was also determined by using the liquid displacement method and it was calculated from the following relations:

$$V_l = V_{l_2} + V_{cage} \tag{3.2.10}$$

or

$$V_{cage} = V_l - V_{l_2} = \frac{\omega_l - \omega_{l_2}}{\rho_l} \tag{3.2.11}$$

where: V_{l2} (m^3) is the volume of the liquid existing in the glass beaker when the cage was immersed and m_{l2} (kg) is the corresponding mass Figure[3.5].

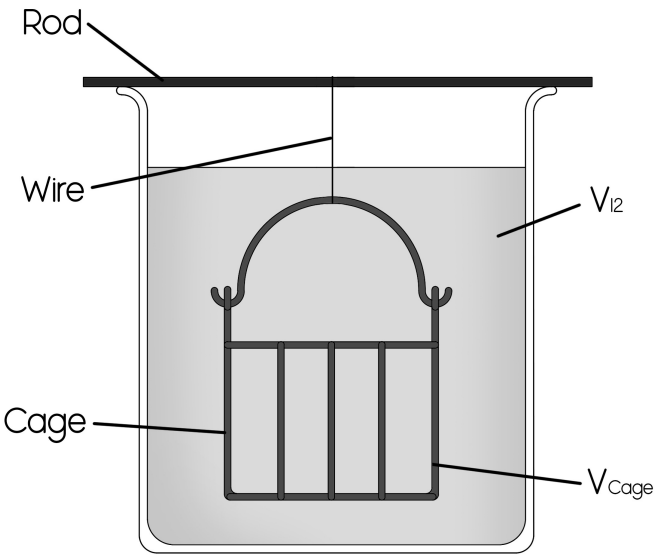

Figure 3.5: Determination of the cage volume by using the liquid displacement method

Briquettes porosity

Further on, the briquettes' porosity was calculated by using three methods. One method is very often mentioned in literature, for example in [Plötze(2011)], [Hunt(2008)], [Huang(2017)], and the other two are in accordance with the recommendations of two publications, Siau [Siau(1995)] and Hunt et al. [Hunt(2008)], as presented below.

The first method that was applied in this paper is similar to relations reported by different authors. Plötze and Niemz [Plötze(2011)] calculated the oven-dry porosity (n) of different wood types from the oven-dry density ρ and the solid cell wall density (ρ_s), as$n = 1 - \frac{\rho}{\rho_s}$.

Hunt et al. [Hunt(2008)] determined the oven-dry wood cell porosity (P_d) from the oven-dry density (ρ_{OD}), the density of the cell wall (ρ_{cw}) and the density of air (ρ_{air}), by using the following equations:

$$\rho_{\mathrm{OD}} = \rho_{cw}\,(1 - P_d) + \rho_{air} P_d \tag{3.2.12}$$

and

$$P_d = \frac{\rho_{cw} - \rho_{\mathrm{OD}}}{\rho_{cw} - \rho_{air}} \tag{3.2.13}$$

They assumed that with the increase of the moisture content, the wood cell lumen size remains the same, because the moisture content (bound water) is added as an outside layer to the cell wall Figure[3.3(b)]. Even so, they calculated a wet porosity, as it will be later described within the third method, since the cross-section side of the cell wall increases with an increase in moisture content (the dimensional change because of the increase in moisture content is added to the outside of the cell wall dimension).

Similarly with Hunt et al., Huang et al. [Huang(2017)] calculated the porosity of oven-dried bamboo wood (ϕ) from the bulk density (ρ_{bulk}) (this includes wood substance and cavities) and skeletal density (ρ_s) (this excludes wood cavities), as:

$$\rho_{bulk} = \rho_s\,(1 - \phi) + \rho_{air}\phi \tag{3.2.14}$$

Even if different notations are used, the oven-dry porosity has according to the aforementioned authors a similar expression that takes into account or not the density of air. Since the density of air is around 1 kg/m^3, it can be neglected.

A second method, calculating the wood porosity in wet conditions, is based on Siau's equation, as indicated in [Siau(1995)], which is:

$$P = 1 - \frac{\omega_{\mathrm{OD}}}{1000\ V_{br.}}(0.653 + 0.01M) \tag{3.2.15}$$

where: P is the porosity or the fractional void volume of wood, $0.653{\times}10^{-3}$ (m^3/kg) is the specific volume of the wood substance, M (%) is wood moisture content.

Eq. (3.2.15) was obtained by subtracting the cell wall volume fraction ($V\%_{cw}$) and moisture volume fraction ($V\%_M$) from unity:

$$P = 1 - V\%_{cw} - V\%_M \tag{3.2.16}$$

Similar to wood composition, made of dried cellular walls, plus the bound water, plus the lumens filled with air, one can consider a similar situation in case of briquettes and Eq. (3.2.16) can be considered valid for wood briquettes as well.

The third method used for wood porosity calculation, which was proposed by Hunt et al. [Hunt(2008)], is based on dry cell porosity and moisture content. The oven-dry density of the cell was expressed in Eq. (3.2.12) in terms of cell wall density, density of air and oven-dry porosity, and the dry porosity was defined in Eq. (3.2.13). The oven-dry cell wall density $\rho_{cw} = 1530$ kg/m^3 used in calculating the dry porosity (3.2.13) is based on its determination by water displacement, as described by Siau in [Siau(1995)]. The density of air at 20^{o}C is $\rho_{air} = 1.18$ kg/m^3(Çengel and Boles 1998)[Cengel(1998)] .

Wet porosity is obtained by the same authors from:

$$P = \frac{(1 - V\%_{bw})\, P_d}{1 - V\%_{bw} P_d} \tag{3.2.17}$$

where: $V\%_{bw}$ is the bound water volume fraction.

The bound water volume fraction is calculated with respect to the wood moisture content, according to Eqs. (3.2.18) and (3.2.19), [Hunt(2008)]:

$$M = \frac{V\%_{bw}\rho_{bw}}{\rho_{cw}\,(1 - V\%_{bw})} \tag{3.2.18}$$

or

$$V\%_{bw} = \frac{\rho_{cw} M}{\rho_{cw} M + \rho_{bw}} \tag{3.2.19}$$

where: ρ_{bw} is the bound water density. It was considered that $\rho_{bw} = 1115$ kg/m^{3}for bound water volume fraction calculation [Siau(1995)]. The equations above, developed by Hunt et al. [Hunt(2008)] for wood, were used in calculating the effective thermal conductivity of wood briquettes with the moisture content ranging from 0% to the equilibrium moisture content [Sova(2018)]. Again, the wood cell is the structural component of both wood and wood briquettes, showing the validity of the method in the case of briquettes.

The first method of porosity calculation, mentioned above, was referring only to the calculation of porosity characteristic to the dry conditions. However, in order to be able to compare it to the second and third methods (for wet conditions), it was considered appropriate to develop a modified equation to be valid for the calculation of porosity in wet conditions. As such, considering Eqs. (3.2.12) and (3.2.13), similar equations can be written for the density and wet porosity of wood cells. The density can be expressed as:

$$\rho = \rho_{cw_M}\,(1 - P) + \rho_{air} P \tag{3.2.20}$$

where: $\rho_{cw_M}$is the density of the cell wall with bound water.

The density of the cell wall with bound water can be obtained from the rule of mixtures:

$$\rho_{cw_M} = \rho_{cw}\,(1 - V\%_{bw}) + \rho_{bw} V\%_{bw} \tag{3.2.21}$$

The mass of a wood cell that consists of the cell wall, bound water and air in the lumen is:

$$m = \omega_{cw} + \omega_{bw} + \omega_{air} \tag{3.2.22}$$

where m_{cw} is the mass of the cell wall, m_{bw} is the mass of the bound water, m_{air} is the mass of the air in the lumen of the wood cell. By replacing the masses by corresponding volumes and densities, the following equation can be written:

$$\rho \cdot V = \rho_{cw} V_{cw} + \rho_{bw} V_{bw} + \rho_{air} V_{air} \tag{3.2.23}$$

If dividing each term of (3.2.23) by V,(3.2.24) becomes:

$$rho = \frac{\rho_{cw} V_{cw} + \rho_{bw} V_{bw}}{V} + \rho_{air} P \tag{3.2.24}$$

By definition, the porosity is:

$$\frac{V_{air}}{V} = P \tag{3.2.25}$$

Also, the following relations can be written:

$$V = V_{cw_M} + V_{air} \tag{3.2.26}$$

$$V_{cw_M} = V_{cw} + V_{bw} \tag{3.2.27}$$

and

$$\frac{V_{cw_M}}{V} = 1 - P \tag{3.2.28}$$

where: V_{cwM} is the volume of the cell wall with bound water.

The cell wall and bound water volume fractions are expressed as:

$$\frac{V_{cw}}{V_{cw_M}} = 1 - V\%_{bw} \tag{3.2.29}$$

$$\frac{V_{bw}}{V_{cw_M}} = V\%_{bw} \tag{3.2.30}$$

Considering Eqs. (3.2.26)-(3.2.30), Eq. (3.2.24) becomes:

$$P = \frac{\rho - \rho_{cw}\left(1 - V\%_{bw}\right) - \rho_{bw} V\%_{bw}}{\rho_{air} - \rho_{cw}\left(1 - V\%_{bw}\right) - \rho_{bw} V\%_{bw}} \tag{3.2.31}$$

But, from the rule of mixtures:

$$\rho_{cw_M} = \rho_{cw}\left(1 - V\%_{bw}\right) + \rho_{bw} V\%_{bw} \tag{3.2.32}$$

By replacing (3.2.32) in Eq. (3.2.31), Eq. (3.2.24) is therefore:

$$P = \frac{\rho_{cw_M} - \rho}{\rho_{cw_M} - \rho_{air}} \tag{3.2.33}$$

The wet porosity is obtained from Eq. (3.2.20), as follows:

$$P = \frac{\rho_{cw_M} - \rho}{\rho_{cw_M} - \rho_{air}} \tag{3.2.34}$$

The new developed equation (3.2.20), based on the first method, was applied in this research, in order to calculate the wet porosity of briquettes. It was named in the porosity analysis as "general relation".

Having the porosity calculated according to the three methods presented above, as well as briquettes' density, correlations were examined in the paper between: porosity and briquette density, surface roughness data and briquette density, as well as surface roughness and porosity of briquettes.

The largest mean density difference was encountered between the first and the second stereometric method, while the second stereometric method and the liquid displacement method (Im) showed statistically similar values, as tested by ANOVA single factor, for a confidence level $p<0.05$. However, regression analysis of density data has shown a weak correlation between individual density values calculated with St2 and liquid displacement method (R^2=0.469) and a better correlation with St1 method (R^2=0.7). Rabier et al. [Rabier(2006)] have also obtained a high variability of the density of different types of briquettes, especially for the stereometric methods. They explained the variability due to the intrinsic physical properties of the briquettes, such as the surface roughness. They noticed that stereometric methods led to more variable results compared to immersion methods. Also, from the statistical results they concluded that the two stereometric methods cannot be regarded as equivalent, which is in agreement with our findings.

Slight differences in briquettes moisture content can have also an influence on density variability. The relationship between individual porosity and density of

briquettes at EMC is shown in Figure[3.6, 3.7, 3.8]. All figures indicate, as expected, the decrease of the porosity with an increase in density. This is in agreement with the results obtained for wood, as indicated by [Usta(2003)] and [Plötze(2011)]. There was a strong correlation between the porosity determined according to Siau's and the general relation methods and density, regardless the measurement method. According to the method described by Hunt et al. for the determination of the porosity, the density measurement method has an influence on the porosity results. While porosity determined by Hunt's et al. method showed high correlation with density for St1 and St2 methods (0.976 and 0.939, respectively), this decreased to 0.5016 for the liquid displacement method Figure[3.8]. This result shows that determination of porosity with Hunt's et al. method is less reliable when density is measured by using the liquid displacement method. The regression analysis has revealed a weaker correlation of porosity data from Hunt's et al. equation with porosity calculated with the other two relations, when density was determined by immersion.

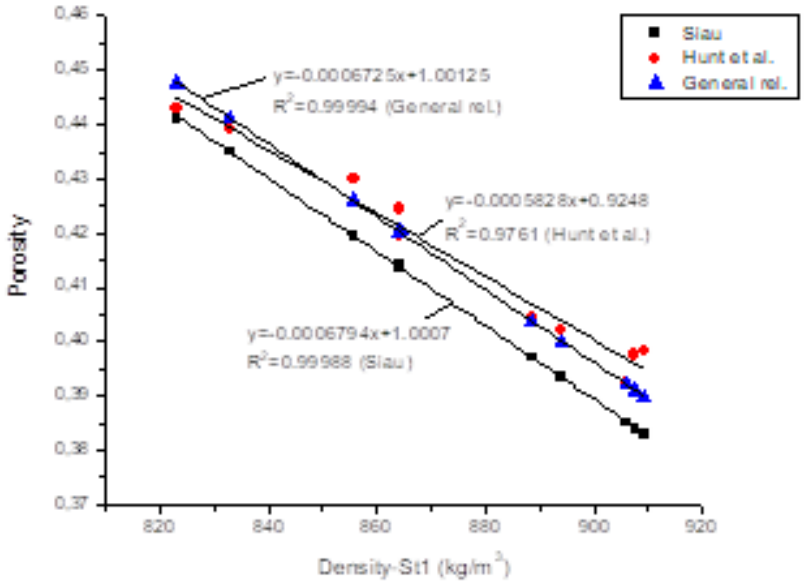

Figure 3.6: Porosity of briquettes as a function of the density obtained from the first stereometric method (St1)

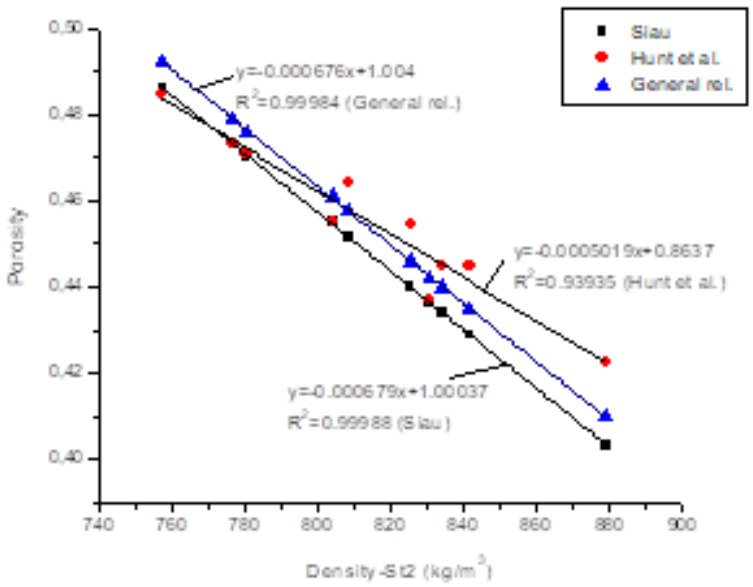

Figure 3.7: Porosity of briquettes as a function of the density obtained from the second stereometric method (St2)

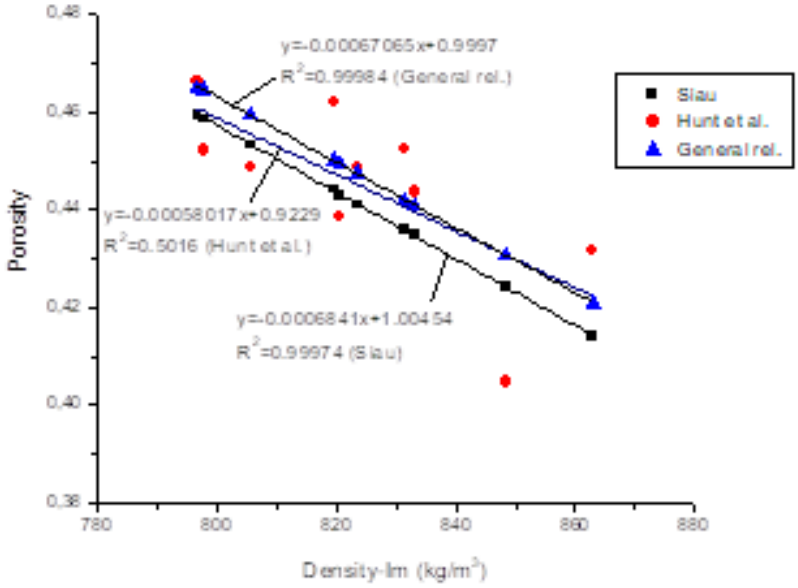

Figure 3.8: Porosity of briquettes as a function of the density obtained from the liquid displacement method (Im)

From a first analysis of the roughness parameters results, they showed a high variability and a weak inverse correlation with density. This may be a result of

variable local density of the briquettes on their circumference. The measured profiles were taken so that two profiles corresponded to the densest generatrix and the other two on the softest generatrix, after a visual assessment. Given the high density variation, it was considered that the selection of measuring lines for each briquette can have an influence on the assessment of its overall roughness. In former studies on sanded solid wood, the density was found in an inverse relationship with surface roughness [Gurau(2004)]. It was reasonable to expect that density of briquettes might have a similar relation with their surface roughness. In order to come to an answer, a mathematical procedure was applied, which selects means of roughness parameters from combinations of three profiles from the measured data. As such, although 4 profiles were measured, resulting in one mean value of the four profiles (1,2,3,4), the calculations took into consideration more means taken from groups/combinations of 3 profiles, which were further checked for their best correlation with density and indirectly with porosity, respectively. For example, the combinations were means of profiles: 1+2+3; 1+2+4; 2+3+4 and 1+3+4. The more measurements are performed, more means are available and the better the chance of a more reliable approximation of the surface quality.

The mathematical procedure is looking to find a linear regression roughness parameters – density, with negative slope and maximum coefficient of determination. For the ten briquettes there were ten densities and four different average roughness parameters (the four means mentioned before) per briquette, that is, a matrix with ten rows and four columns. For the matrix, the following function is considered$f : \{l_1, l_2, ..., l_{10}\} \rightarrow \{c_1, c_2, c_3, c_4\}$, where $l_i,\ i = 1...10$represent the matrix rows and c_j, $j = 1...4$are the matrix columns. The total number of possible combinations is$4^{10} = 1048576$, as stated in the following theorem: the total number of functions $f : D \rightarrow E$ is $N = |E|^{|D|}$, where D and E are finite sets [30]. The algorithm implemented in Python programming language contains a procedure of conversion of a number from the 10^{th} base into the 2^{nd} base. It is necessary to mention that in Python the indices of arrays start from zero. If an element from the first column of the matrix is selected, the iteration is zero; if an element from the second column is selected, its index is one; if an element from the third column is selected, its index is two and if an element from the fourth column is selected, the index is three. The algorithm does not allow selecting two elements from the same row. Another procedure used in Python, called padding, prepends zeroes to the values obtained in the 4^{th} base. Another procedure, called padding, used in Python, is those that concatenates the obtained values in the 4^{th} base: {0,1,2,3} arranged on the tenth positions such that in the end the array S_i, i=1..10 could be read in order to calculation of the sum.

In order to analyze the correlations of density with roughness, as well as of porosity with roughness, the Regression analysis tool was used. This performs linear regression analysis by using the "least squares" method to fit a line through a set of observations. This function analyzes how, for example briquette surface roughness is affected by the values of briquette density or porosity. High correlations indicate a strong dependence of the two properties.

The roughness parameters values decreased with an increase in density. Figure[]3.9] shows an example of correlation of roughness parameters and density of briquettes obtained by using the St2 method. From the regression analysis it can be concluded that the correlations were reasonable in the case of the first stereometric density measurement method; however, significantly stronger correlations were obtained for the second stereometric density measurement method. This was observed especially in what regards the correlation of the parameter $Rk+Rpk+Rvk$ and density, where the coefficient of determination was 0.911. The correlations were statistically not significant when the liquid displacement method was applied. This shows that the selection of the density measurement method has an important influence on the roughness parameters.

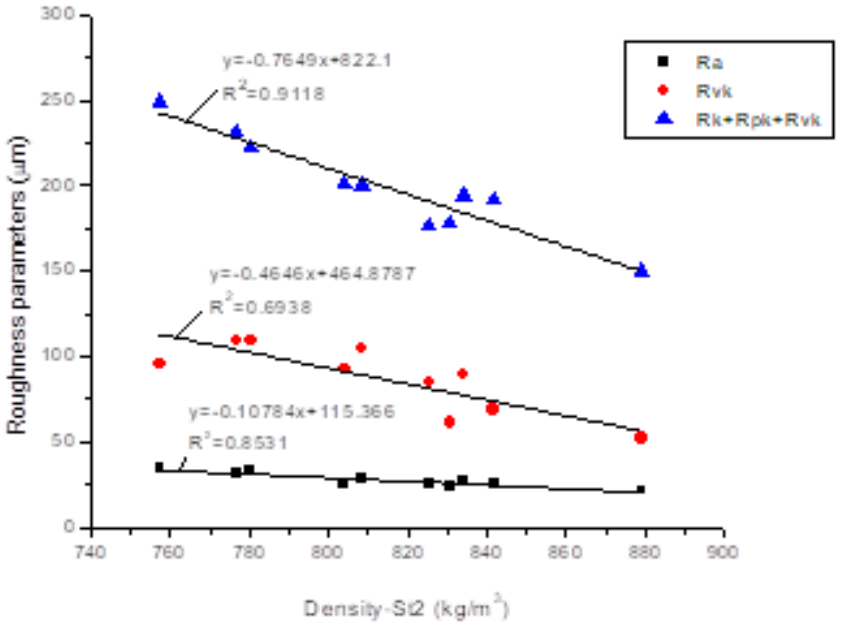

Figure 3.9: The roughness parameters of briquettes as a function of the density obained from the second stereometric method (St2)

In case of density measured by the St1 method, the porosity determined with all three relations, has shown a similar moderate positive correlation with briquettes

roughness, (R^2>0.5), statistically significant for a confidence level p<0.05.

However, when the density was calculated with the St2 method, the porosity determined with all three methods, has shown strong positive correlations with briquettes roughness. The correlations were almost similar between the three methods and were statistically significant for a confidence level p<0.05. Very good correlations were met by all three roughness parameters measured, but were best for *Rk+Rpk+Rvk*. The coefficient of determination R^2 was greater than 0.9 for porosity determined by Siau and general relation methods and the roughness composed parameter *Rk+Rpk+Rvk* (see Fig.8). The correlation of the porosity with *Ra* did not differ considerably with respect to the method of porosity calculation. The correlation of the porosity with *Rvk* was weaker in comparison with the other two parameters, but was better when Hunt's et al. method of porosity calculation was applied.

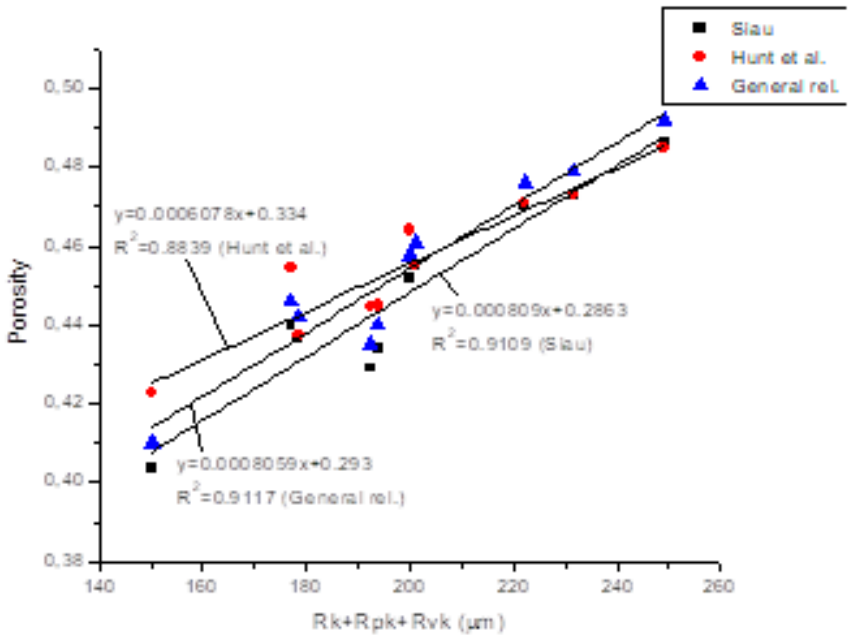

Figure 3.10: Porosity of briquettes (St2) as a function of (*Rk+Rpk+Rvk*) roughness parameter

Among the three porosity relations, only relation of Hunt et al. determined a weak positive correlation with surface roughness, for a confidence level p<0.05, when density was obtained by immersion, while the other porosity relations produced no correlation with surface roughness.

If the porosity of briquettes is to be estimated by measurements of surface roughness, the best correlation can be obtained when measuring the roughness

parameters *Rk+Rpk+Rvk*, followed closely by *Ra*. Very strong correlations with roughness were obtained for porosity calculated with all three relations, but when density was determined by St2 method. The findings are encouraging for providing an alternative method to estimate the briquette porosity based on measured surface roughness.

Correlations were analyzed between porosity and density, three roughness parameters and density, and porosity and roughness parameters of briquettes. Porosity had a strong negative correlation with density when it was calculated from Siau's equation or by using the general equation, regardless the method of density determination. The correlation was weaker if the method proposed by Hunt et al. was used and when the density was determined by the liquid displacement method. Strong negative correlations were obtained for the roughness parameters and density, if the density was determined according to the second stereometric method, while no correlation was found when the liquid displacement method was used. Very strong positive correlations porosity-surface roughness, were obtained for porosity calculated with all three relations, when density was determined by the second stereometric method. If the porosity of briquettes is to be estimated by measurements of surface roughness, the recommended parameter is *Rk+Rpk+Rvk*. Further work is required to verify if those initial results remain consistent and repeatable for other briquettes from different batches and for other combination of wood species.

Chapter 4

(B-ii) The evolution and development plans for career development

I am Associate Professor at Transilvania University of Brașov (2016 - present) and I stand out as a leading academic figure with dual expertise in both Mechanical Engineering and Mathematics. My groundbreaking contributions to Fluid Mechanics and Continuum Mechanics highlight my interdisciplinary approach and dedication to advancing knowledge in these critical fields.

4.1 Educational Background

My academic journey began with a Bachelor's degree in Mathematics, which I earned in 2001. This foundation in analytical and problem-solving skills sparked my passion for applying mathematical principles to real-world challenges, leading me to pursue a PhD in Mechanical Engineering. I completed my PhD in 2010, focusing on complex engineering systems. My doctoral thesis made significant contributions to the field, demonstrating my ability to merge mathematical rigor with engineering applications.

In 2014-2015, I further expanded my research scope through a postdoctoral fellowship, where I specialized in the modeling and simulation of bio-dynamical systems. This experience allowed me to bridge the gap between engineering and biological systems, highlighting my interdisciplinary approach to research. The work I conducted during this fellowship underscored my capability to address complex, multifaceted problems by applying my mathematical expertise to the emerging field of bio-dynamical systems.

In my pursuit of continuous academic growth, I earned a second PhD in Mathematics in 2019. This achievement solidified my commitment to advancing my knowledge and expertise in mathematical sciences, reinforcing my role as a researcher who effectively applies mathematical theories to solve intricate engineering challenges.

Throughout my career, I have authored 25 papers indexed in the Web of Science (WOS), with my research receiving considerable attention in the scientific community. I am proud to have 117 citations in WOS, with 99 of these being independent of self-citation, reflecting the impact and relevance of my work. Between 2020 and 2023, I published 7 influential papers, further establishing myself as a thought leader in my field.

My research is deeply interdisciplinary, combining the precision of mathematics with the practical demands of engineering. I am particularly proud of my work in the modeling and simulation of bio-dynamical systems, where I have introduced innovative approaches with practical significance. My contributions have not only advanced theoretical understanding but have also provided valuable insights with real-world applications in engineering and technology.

First Ph.D. in Mechanical Engineering (Fluid Mechanics) (July, 2010)

My first doctoral thesis in Mechanical Engineering centered on Fluid Mechanics with the title: *Analytical and Numerical Methods for Solving Problems of Dynamical Systems Applied in the Simulation of Some Components of the Hydraulic Systems*, supervisor Prof. Dr. Eng. Mat. Adrian Postelnicu, a field crucial for various engineering applications such as aerodynamics, hydrodynamics, and energy systems. My research focused on understanding fluid behavior under different conditions, which has practical implications for industries ranging from automotive to aerospace and environmental engineering.

Research Contributions:

- **Advanced Computational Fluid Dynamics (CFD)**: I developed models to simulate fluid flow in complex systems, enhancing the predictive capabilities of CFD tools.
- **Turbulence Modeling:** My work on turbulence modeling provided new insights into the behavior of fluids in turbulent states, contributing to improved designs in engineering systems that rely on fluid dynamics.
- **Energy Systems:** I explored the optimization of fluid flow in energy systems, leading to more efficient designs and operations of turbines, compressors, and other critical components.

Second Ph.D. in Mathematics (Continuum Mechanics) (February, 2019)

My second Ph.D. in Mathematics focused on Continuum Mechanics, with the title: Mixt Problems With Boundary And Initial Data For Generalized Continua, supervisor Prof. dr. habil. Marin Marin, which extends the principles of mechanics to thermoelastic porous materials. My research in this area involved the mathematical modeling of material behavior, which is essential for understanding how materials deform, flow, and respond to external forces.

Research Contributions:

- **Material Deformation:** My work in Continuum Mechanics provided a deeper understanding of how materials behave under various stress and strain conditions, contributing to advancements in material science.
- **Nonlinear Dynamics:** My exploration of nonlinear dynamics within continuum systems has applications in predicting complex behaviors in both natural and engineered systems.
- **Mathematical Modeling:** I developed mathematical models that describe the behavior of materials at both macroscopic and microscopic levels, bridging the gap between theoretical predictions and real-world applications.

4.2 Career Evolution

Administrative managing at The Faculty of Mathematics and Computer Science

My role as Vice-Dean (2016-2019, 2023-2024) of the Faculty of Mathematics and Computer Science exemplifies my leadership and strategic vision. As Vice-Dean, I was responsible for overseeing the faculty's academic programs, research initiatives, and administrative functions.

Coordinator of study programs

As the Coordinator of the Bachelor Program in Mathematics (2022 - present), I have has been instrumental in shaping the program's direction and ensuring its relevance in a rapidly changing educational landscape. My responsibilities include curriculum design, program assessment, and student engagement. I have led efforts

to redesign the mathematics curriculum, incorporating modern mathematical theories and applications. My focus on providing students with a strong foundation in both theoretical and applied mathematics prepares graduates for diverse career paths. I prioritize student engagement, encouraging active participation in research projects, mathematical competitions, and extracurricular activities. My approach has fostered a vibrant and dynamic learning environment that inspires students to excel.

My role as the Coordinator of the Mathematics Teacher Conversion Program (2013 - 2024) highlights my dedication to improving mathematics education at all levels. This program is designed to provide teachers with the skills and knowledge necessary to teach mathematics effectively.I have developed a comprehensive curriculum that addresses the specific needs of teachers seeking to enhance their mathematical expertise. The program covers advanced mathematical concepts, pedagogical strategies, and classroom management techniques.

Academic achievements

My career evolution is a testament to my ability to integrate engineering and mathematical principles. I joined Transilvania University of Brașov as an Assistant Professor (2004), where my interdisciplinary expertise has been pivotal in shaping the curriculum and research initiatives within my colleagues.

Teaching and Mentorship

As an educator, I am committed to fostering a dynamic learning environment. My courses in Fluid Mechanics, Continuum Mechanics, and Applied Mathematics are designed to challenge students and encourage critical thinking. I haves played a significant role in mentoring students, guiding them in research projects that explore the intersections of engineering and mathematics.

Research Impact

My research has been widely recognized for its impact on both academia and industry. I have published numerous papers in prestigious journals, presenting my findings at international conferences and workshops. My ability to translate complex mathematical concepts into practical engineering solutions has made my a

sought-after collaborator for interdisciplinary research projects.

Key Achievements

- **Interdisciplinary Research:** I have successfully bridged the gap between mathematics and engineering, leading to innovative solutions that address real-world challenges.
- **Collaborative Projects:** My collaborative efforts with international researchers have resulted in groundbreaking studies that explore new frontiers in fluid and continuum mechanics.

4.3 Professional Development Plans

My future career development plans are focused on expanding my research, enhancing educational practices, and engaging with the global academic community. My vision includes:

1. **Advanced Research Initiatives:** I plan to explore emerging areas such as biofluid mechanics and smart materials, which promise to open new avenues for innovation.
2. **Interdisciplinary Collaborations:** I aim to strengthen my partnerships with experts from diverse fields, fostering interdisciplinary research that addresses complex, multifaceted problems.
3. **Educational Innovation:** I am committed to integrating cutting-edge technologies into my teaching, such as virtual simulations and computational tools, to provide students with immersive learning experiences.
4. **International Engagement:** I plan to participate actively in international forums, contributing to the global discourse on engineering and mathematics and building collaborations with leading institutions worldwide.
5. **Community Outreach:** I am passionate about using my expertise to inspire future generations. I plan to engage in outreach programs that promote STEM education and encourage young students to pursue careers in applied mathematics.

As I continue to advance in my academic career, my focus will be on further developing my role as a PhD supervisor in the fields of Mathematics, particularly within the domains of Continuum Mechanics and Dynamical Systems. My experience and research achievements to date have provided me with a strong foundation to mentor and guide the next generation of researchers. I am committed to fostering an environment of academic excellence and innovation, where my students can thrive and make significant contributions to these critical areas of mathematics.

In the field of Continuum Mechanics, my future research will delve deeper into the complexities of thermoelastic materials with double porosity, exploring new theoretical frameworks and mathematical models that can better describe the behaviors of such materials under various conditions. I aim to lead research projects that push the boundaries of our understanding in this area, encouraging my PhD students to engage in cutting-edge research that integrates advanced mathematical techniques with practical engineering applications. Through collaborative efforts, we will explore the stability, uniqueness, and dynamic responses of complex material systems, contributing to both theoretical advancements and practical innovations.

In the domain of Dynamical Systems, I will focus on the development of new numerical methods and their application to real-world problems. My goal is to supervise research that not only explores the mathematical underpinnings of dynamical systems but also applies these findings to solve complex, interdisciplinary problems. This could include further exploration of fractional calculus in dynamical systems, as well as the use of advanced computational tools such as MATLAB and Maple to simulate and analyze the behavior of these systems. By involving my students in these projects, I aim to equip them with the skills and knowledge needed to excel in both academic and industrial settings.

My involvement in scientific projects will be a cornerstone of my further career development. I plan to actively seek out and participate in collaborative research initiatives, both nationally and internationally, that align with my areas of expertise. These projects will provide valuable opportunities for my PhD students to engage with the broader scientific community, gain exposure to diverse research methodologies, and contribute to impactful, high-profile research. I am particularly interested in projects that explore the intersection of mathematics, engineering, and applied sciences, where the innovative application of mathematical principles can lead to significant advancements in technology and industry.

As a PhD supervisor, I will emphasize the importance of interdisciplinary research, encouraging my students to think beyond traditional boundaries and to

apply their mathematical knowledge to a wide range of scientific challenges. By fostering a collaborative, inclusive, and innovative research environment, I aim to develop a new generation of mathematicians who are not only skilled in theoretical research but are also capable of driving scientific and technological progress.

In conclusion, my further career development as a PhD supervisor will be centered on advancing research in Continuum Mechanics and Dynamical Systems, mentoring students to achieve excellence in these fields, and actively participating in scientific projects that contribute to the advancement of knowledge and technology. I am committed to building a strong, vibrant research community that will continue to make meaningful contributions to the field of Mathematics and its applications.

4.4 Further research

4.4.1 A qualitative analysis on the double porous thermoelastic bodies with microtemperature

Regarding thermoelastic bodies with double porosity structure and microtemperature, [Florea(2019a)], demonstrates that, in the situation where double porous temperature and microtemperature are the dissipation mechanisms, the only solution that disappears after a finite period of time is the null solution. In the last years, many researchers focused on the thermoelastic materials with microtemperature, [Aouadi(2018)], [Bazarra(2019a)], [Ieşan(2018a)], [Ieşan(2018b)], [Jaiani(2016)], [Pamplona(2012)], [Quintanilla(2011)].

The mixed boundary value problem with initial data for different types of media to obtain the corresponding constitutive laws, using similar methods as in the classical elasticity were approached for dipolar bodies with voids, [Codarcea(2019)], [Codarcea(2020)]. Uniqueness theorems in the dynamical theory of anisotropic bodies with microstructure and microtemperatures were proven by Ieşn, [Ieşan(2007)]. The theory of the semigroup of operators is used by researchers for different media from continuum mechanics, [Bazarra(2021)].

We will consider the mixed problem of a body with double porosity. In order to prove the existence of the solution we transform the considered problem into a Cauchy problem. Due to the fact that the number of equations and conditions is very large, the theory of contractions for a semigroup into a particular Hilbert space is considered. The unicity of the solution is proven using the results of the Lumer-Phillips and Hille-Yosida theorems, [Yosida(1980)], that represent the base of the semigroups strong continuous in order to obtain new conditions necessary and

sufficient for a linear operator from the Banach space to generate a semigroup of contraction. The continuous dependence for the solution of the mixed problem will be deduced. The notion regarding the thermal displacement was introduced by Green and Naghdi in 1991, [Green(1885)], by the variable denoted ω that depends on the temperature variation θ, between two states of the body: ξ_0 that is the initial time and the moment of the reference configuration when the body achieves the absolute temperature T_0:

$$\omega(x,\xi) = \int_{\xi_0}^{\xi} \theta(x,s)ds, \tag{4.4.1}$$

where $\theta(x,\xi) = \Theta(x,\xi) - T_0$. Also, the microthermal displacement is noted by the variable Ω_i that depends on the variation of microtemperatures $\mathcal{T}_i$ between two states of the body:

$$\Omega_i(x,\xi) = \int_{\xi_0}^{\xi} \mathcal{T}_i(x,s)ds, \tag{4.4.2}$$

where $\mathcal{T}_i(x,\xi) = \Theta_i(x,\xi) - T_{0i}$.

The equations that govern the behavior of an anisotropic thermoelastic body with two porosities and microtemperatures are the equation of motion and the balances of the equilibrated forces (1.1.1).

The energy equations taking into account the microtemperatures:

$$\begin{aligned} \rho\dot{\eta} &= q_{j,j} + \rho\delta, \\ \rho\dot{\eta}_i &= q_{ji,j} + \rho\delta_i. \end{aligned} \tag{4.4.3}$$

In the equations above the behavior of a thermoelastic body with microtemperature is expressed by means of variables $(u_i, \varphi, \psi, \omega, \Omega_i)$ where:
- u_i are the displacement vector components,
- φ, ψ are fractional volume fields corresponding to the pores and the cracks,
- ω, Ω_i are the new variables regarding the microtemperature.

Due to the fact that this study is realized in the context of linear thermoelesticity we will define the internal energy as a quadratic form, positively definite:

$$\begin{aligned} W = \tfrac{1}{2}M_{ijkl}u_{i,j}u_{k,l} + N_{ij}u_{i,j}\varphi + P_{ij}u_{i,j}\psi + R_{ij}\Omega_{i,j}\varphi + S_{ij}\Omega_{i,j}\psi + \tfrac{1}{2}a_1\varphi^2 \\ + \tfrac{1}{2}a_2\psi^2 + a_3\varphi\psi + a_{ijkl}u_{i,j}\Omega_{k,l} + A_{ij}\varphi_{,i}\psi_{,j} + b_{ij}\varphi_{,i}\omega_{,j} + c_{ij}\psi_{,i}\omega_{,j} \\ + \tfrac{1}{2}d_{ij}\omega_{,i}\omega_{,j} + \tfrac{1}{2}e_{ijkl}\Omega_{i,j}\Omega_{k,l} + \tfrac{1}{2}B_{ij}\varphi_{,i}\varphi_{,j} + \tfrac{1}{2}C_{ij}\psi_{,i}\psi_{,j}. \end{aligned} \tag{4.4.4}$$

For future research, the study of mixed initial-boundary value problems in thermoelastic materials with double porosity and microtemperature effects presents a rich area for further investigation. Building on the framework established by converting the problem into a Cauchy-type problem, future research could explore more generalized conditions or alternative materials to extend the applicability of the findings. The use of contraction semigroup theory within a specific Hilbert space could be further refined or adapted to other complex systems, potentially leading to new insights into the behavior of such materials under different conditions. Additionally, exploring the implications of the Lax-Milgram theorem and the Lumer-Phillips corollary in different contexts could provide a deeper understanding of the existence and uniqueness of solutions. Finally, the continuous dependence of the solution on the mixed initial-boundary conditions suggests a pathway for experimental validation and potential real-world applications, where the robustness of the solution could be tested against varying parameters and initial conditions. This line of inquiry could significantly advance the theoretical foundations and practical applications of thermoelasticity in materials with complex internal structures.

4.4.2 Pendulum between two springs using MS- DTM

Solving nonlinear systems is a critical area of research with numerous applications across science and engineering. Perturbation methods, the Adomian Decomposition Method, and the Multi-Step Differential Transformation Method offer powerful analytical tools, each with its strengths and limitations. Advances in hybrid methods and computational techniques continue to expand the capabilities and applicability of these methods, paving the way for solving increasingly complex nonlinear problems. As technology evolves, integrating these methods with emerging fields such as machine learning and quantum computing will further enhance their potential and impact.

The Multi-Step Differential Transformation Method (Ms-DTM) plays a vital role in solving nonlinear systems due to its enhanced accuracy, adaptability, and efficiency. Its ability to handle complex nonlinearities, stiff equations, and large domains with improved convergence and accuracy makes it a powerful tool for researchers and practitioners alike. With its broad range of applications and potential for integration with emerging technologies, Ms-DTM continues to be a valuable method in the advancement of science and engineering, [Eslami(2012)], [Arikoglu(2007a)].

Ms-DTM improves upon the standard Differential Transformation Method (DTM) by implementing a multi-step approach that enhances convergence, especially for

complex and stiff problems. This makes it more suitable for solving nonlinear systems where traditional methods may struggle to converge. By dividing the problem domain into multiple sub-intervals, Ms-DTM allows for more accurate approximation of solutions. This step-wise approach ensures that local errors are minimized and corrections are applied throughout the interval, leading to a highly precise solution [Arikoglu(2006a)].

In engineering, Ms-DTM is used for modeling and analyzing dynamic systems, such as fluid dynamics, heat transfer, and structural mechanics. Its accuracy and adaptability make it suitable for designing and optimizing engineering solutions. Researchers use Ms-DTM in fields like physics and chemistry to solve differential equations that describe phenomena such as wave propagation, chemical kinetics, and quantum mechanics. The method is also applied in biology for modeling population dynamics, ecological interactions, and the spread of diseases, where systems are often highly nonlinear and complex [Arikoglu(2007b)].

For the system described in the Figure[4.1] below, we want to determine the equation of motion (EOM) of a pendulum that is coupled to two springs with linear stiffnesses (κ_1, κ_2), respectively. The pendulum shown in Figure[4.1] has a length (ℓ) and a small bob mass (m) attached to its lower end, while the upper end is attached to a mass ($\mathcal{M}$) that is connected to two springs with linear stiffnesses.

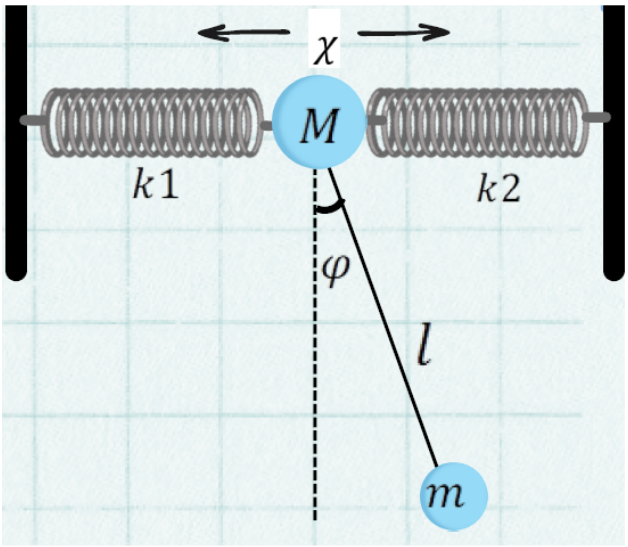

Figure 4.1: A simple pendulum between two springs

Further, we aim to derive the Euler- Lagrange Equations of motion (ELE's); known also as equations of motion (EOM's). So, our first step will be constructing the Lagrangian ($\mathcal{L}$) which is defined as:

$$\mathcal{L} = \mathcal{T} - \mathcal{V}. \tag{4.4.5}$$

where $\mathcal{T}$, and $\mathcal{V}$ represent the kinetic and potential energies of the system respectively. The kinetic energy ($\mathcal{T}$) of m and $\mathcal{M}$ can easily be shown that:

$$\mathcal{T} = \frac{1}{2}\mathcal{M}\dot{\chi}^2 + \frac{1}{2}m\dot{\chi}^2 + \frac{1}{2}m\ell^2\dot{\phi}^2 + m\ell\dot{\phi}\dot{\chi}\cos\phi. \tag{4.4.6}$$

While the potential energy ($\mathcal{V}$) of the system consisting from two parts: the gravitational potential energy ($\mathcal{V}_g$), and the potential energy due to the two springs ($\mathcal{V}_s$). So, we can write:

$$\mathcal{V} = \mathcal{V}_g + \mathcal{V}_s = -mg\ell\cos\phi + \frac{1}{2}\kappa_1\chi^2 + \frac{1}{2}\kappa_2\chi^2. \tag{4.4.7}$$

Based on [Hatami(2015)] , [Zhou(1986)], let us consider the following nonlinear differential equation:

$$f(t, y, y', y'', \cdots, y^{(n)}) = 0. \tag{4.4.8}$$

with the initial conditions

$$y^{(k)} = d_k, \quad k = \overline{0, n-1}. \tag{4.4.9}$$

The function $y(t)$ is an analytical function in the domain $D \subset \mathbb{R}$. This function can be represented by the power series with the center in t_0.

The differential transformation of the derivative of k degree of the function $y(t)$ is defined by [Odibat(2010)]

$$Y(k) = \frac{1}{k!}\left(\frac{d^k y(t)}{dt^k}\right)_{t=t_0}, (\forall t \in D). \tag{4.4.10}$$

where $y(t)$ is the original function and $Y(k)$ is the transformed function. The inverse transformation of the image $Y(k)$ is:

$$y(t) = \sum_{k=0}^{N} Y(k)(t-t_0)^k, (\forall) t \in [t_a, t_b] \subset D. \tag{4.4.11}$$

that can be written into the following form

$$y(t) = \sum_{k=0}^{\infty} \frac{(t-t_0)^k}{k!}\left(\frac{d^k y(t)}{dt^k}\right)_{t=t_0}, (\forall) t \in D. \tag{4.4.12}$$

here, N represents the necessary number of terms in order that the power series be convergent. This implies the concept that the differential transformation is obtained from the expand of the Taylor series.

The differential transformation is a linear operator, therefore if the original function is given in the following form $f(t) = \alpha g(t) + \beta h(t)$ where $\alpha, \beta \in \mathbb{R}$ then the transformation function will be:

$$F(k) = \alpha G(k) + \beta H(k). \tag{4.4.13}$$

This property is verified with both methods: differential transformation method (DTM) or multistep differential transformation method (MS-DTM).

The differential transformation of the derivatives of n degree is given by the following equations:

$$f(t)=\frac{du(t)}{dt}\Leftrightarrow F(k)=(k+1)U(k+1). \tag{4.4.14}$$

$$f(t)=\frac{d^m u(t)}{dt^m}\Leftrightarrow F(k)=(k+1)(k+2)\dots(k+m)U(k+m). \tag{4.4.15}$$

The solution of the differential equation (4.4.8) can be written on sub-ranges in the following form:

$$y_j(t)=\sum_{k=0}^{N} Y_j(k)(t-t_j)^k, t\in[t_j,t_{j+1}], j=1,2,3,\dots,M. \tag{4.4.16}$$

where M is the numbers of sub-ranges having equal lengths with the step $p=\frac{t_b-t_a}{M}, t_1=t_a, t_{M+1}=t_b$.

The general solution of the nonlinear differential equation (4.4.8) using the MS-DTM method can be written in the following form:

$$y(t)=\begin{cases} y_1(t)=\sum\limits_{k=0}^{N} Y_1(k)(t-t_a)^k, t\in[t_a,t_2] \\ y_2(t)=\sum\limits_{k=0}^{N} Y_2(k)(t-t_2)^k, t\in[t_2,t_3] \\ y_3(t)=\sum\limits_{k=0}^{N} Y_3(k)(t-t_3)^k, t\in[t_3,t_4] \\ \dots \\ y_{M-1}(t)=\sum\limits_{k=0}^{N} Y_{M-1}(k)(t-t_{M-1})^k, t\in[t_{M-1},t_M] \\ y_M(t)=\sum\limits_{k=0}^{N} Y_M(k)(t-t_M)^k, t\in[t_M,t_b] \end{cases}. \tag{4.4.17}$$

with the initial conditions:

$$y_j^{(r)}(t-t_j)=\begin{cases} y_1^{(r)}(t-t_a)=Y(r) \\ y_2^{(r)}(t-t_2)=y_1^{(r)}(t_2) \\ y_3^{(r)}(t-t_3)=y_2^{(r)}(t_3) \\ \dots \\ y_{M-1}^{(r)}(t-t_{M-1})=y_{M-2}^{(r)}(t_{M-1}) \\ y_M^{(r)}(t-t_M)=y_{M-1}^{(r)}(t_M) \end{cases}. \tag{4.4.18}$$

For future research, the study of a pendulum suspended between two horizontal springs offers a promising avenue for further exploration of the system's complex dynamics. The mathematical framework established through the derivation of the Lagrangian and the resulting equations of motion provides a solid foundation for

continued analysis. Future work could expand on this by exploring the efficacy of alternative numerical methods, potentially refining or challenging the findings related to the multi-step differential transformation approach when compared to the Runge-Kutta technique. Additionally, more in-depth simulations under varied initial conditions and system parameters could yield further insights into the nonlinear behavior and stability of such systems. Moreover, the potential for real-world applications in similar mechanical configurations warrants additional experimental validation and optimization studies. This continued research could significantly contribute to both theoretical advancements and practical innovations in the field of coupled mechanical systems.

Bibliography

[A(2019)] Abdeljawad, T., Agarwal, R.P., Karapınar, E., Kumari, P.S., Solutions of the Nonlinear Integral Equation and Fractional Differential Equation Using the Technique of a Fixed Point with a Numerical Experiment in Extended b-Metric Space, *Symmetry*, **11**: 686, 2019.

[Abazari(2011)] Abazari, R., Ganji, M., Extended two-dimensional DTM and its application on nonlinear PDEs with proportional delay, *International Journal of Computer Mathematics*, **88(8)**: 1749-1762, 2011.

[Abazari(2012)] Abazari, R., Abazari, M., Numerical simulation of generalized Hirota-Satsuma coupled KdV equation by RDTM and comparison with DTM, *Communications in Nonlinear Science and Numerical Simulation*, **17(2)**: 619-629, 2012.

[Adiguzel(2020)] Adiguzel, R.S., Aksoy, U., Karapinar, E., Erhan, I.M., On the solution of a boundary value problem associated with a fractional differential equation, *Mathematical Methods in the Applied Sciences*, **2020**: 1-12, 2020.

[Adomian(1984)] Adomian, G. , A review of the decomposition method in applied mathematics, *Journal of Mathematical Analysis and Applications*, **135(2)**: 501-544, 1984.

[Afshari(2015)] Afshari, H., Kalantari, S., Karapinar, E., Solution of fractional differential equations via coupled fixed point, *Electronic Journal of Differential Equations*, **286**: 1-12, 2015.

[Al-Hamamre(2017)] Al-Hamamre, Z., Saidan, M., Hararah, M., Rawajfeh, K., Alkhasawneh, H.E., Al-Shannag, M., Wastes and biomass materials as sustainable-renewable energy resources for Jordan, *Renewable and Sustainable Energy Reviews*, **67**: 295-314, 2017

[Alqahtani(2019)] Alqahtani, B., Fulga, A., Jarad, F., Karapinar, E. , Nonlinear F -contractions on b -metric spaces and differential equations in the frame of

fractional derivatives with Mittag-Leffler kernel, *Chaos, Solitons and Fractals*, **128**: 349-354, 2019.

[Alqahtani(2019)] Alqahtani, B., Aydi, H., Karapınar, E., Rakocevic, V., Solution for Volterra Fractional Integral Equations by Hybrid Contractions, *Mathematics*, **7**: 694, 2019.

[Amrani(2008)] Amrani, D., Paradis, P. and Beaudin, M, Approximation expressions for the large-angle period of a simple pendulum revisited, *Rev. Mex. Fis. E*, **54**: 59-64, 2008.

[Aoki(2001)] Aoki, K., Nonlinear Dynamics and Chaos in Semiconductors, *IOP Publishing Ltd*, London, 2001.

[Aouadi(2018)] Aouadi, M, Ciarletta, M, Passarella, F, Thermoelastic theory with microtemperatures and dissipative thermodynamics, *J Thermal Stress*, **41**: 522-542, 2018

[Aouadi(2019)] Aouadi, M., Campo, M., Copetti, M.I.M., Fernández, J.R., Analysis of a multidimensional thermoviscoelastic contact problem under the Green–Lindsay theory, *J. Comput. Appl. Math.*, **1**: 224–246, 2019.

[Arikoglu(2006a)] Arikoglu, A., Ozkol, I., Multi-Step Differential Transform Method and Application to Nonlinear Problems, *International Journal for Numerical Methods in Engineering*, **67(12)**: 1912-1929, 2006.

[Arikoglu(2006b)] Arikoglu, A., Ozkol, I., Application of Multi-Step Differential Transform Method for Solving Strongly Nonlinear Oscillatory Systems, *Journal of Sound and Vibration*, **309(3-5)**: 452-459, 2006.

[Arikoglu(2007a)] Arikoglu, A., Ozkol, I., Multi-Step Differential Transform Method for Solving Nonlinear Differential Equations, *Chaos, Solitons & Fractals*, **34(5)**: 1473-1481, 2007.

[Arikoglu(2007b)] Arikoglu, A., Ozkol, I., Multi-Step Differential Transformation Method for Complex Boundary Value Problems: Applications in Engineering and Sciences, *Applied Mathematics and Computation*, **189(2)**: 992-1001, 2007.

[Arnold(1989)] Arnold, V.I., Mathematical Methods of Classical Mechanics, *Springer*, 1989.

[Asad(2024)] Asad, A.A., Asad, J., Power series approach to nonlinear oscillators, *Journal of Low Frequency Noise, Vibration and Active Control*. **43(1)**: 220-238, 2024.

[Atkinson(2008)] Atkinson, K., Han, W., Stewart, D. Numerical Solution of Ordinary Differential Equations., *A John Wiley and sons, Inc. Publication*, 2008.

[Attaway(2009)] Attaway, S. , Matlab: A Practical Introduction to Programming and Problem Solving, *College of Engineering, Boston University*, 2009.

[Bagley(1991)] Bagley, R.L., Calico, R.A., Fractional order state equations for the control of viscoelastically damped structures, *J. Guid. Control Dyn.*, **14(2)**: 304–311, 1991.

[Bai(1994)] Bai, M. , Roegiers, J.C. ,Fluid flow and heat flow in deformable fractured porous media, *Internat. J. Engrg. Sci.*, **32**: 1615–1633, 1994.

[Baker(2005)] Baker, G.L., Blackburn, J.A., The Pendulum: A Case Study in Physics, *Oxford University Press*, 2005.

[Bala(2009)] Bala, D., Geometric Methods In Study Of The Stability Of Some Dynamical Systems, *An. St. Univ. Ovidius Constanta*, **17(3)**, 27-35, 2009.

[Baleanu(2011)] Baleanu, D., Petras, I., Asad, J.H., Pilar Velasco, M., Fractional Pais-Uhlenbeck Oscillator, *Int J Theor Phys*, **51**: 1253–1258, 2012.

[Baleanu(2012)] Baleanu, D., Asad, J.H., Petras, I., Elagan, S., Bilgen, A., Fractional Euler-Lagrange Equation Of Caldirola-Kanai Oscillator, *Romanian Reports In Physics*, **64**: 1171–1177, 2012.

[Baleanu(2018a)] Baleanu, D., Asad, J.H., Jajarmi, A., New Aspects Of The Motion Of A Particle In A Circular Cavity, *Proc.Of The Romanian Academy, Series A*, **19(2)**: 143–149, 2018.

[Baleanu(2018b)] Baleanu, D., Asad, J.H., Jajarmi, A. , The Fractional Model Of Spring Pendulum: New Features Within Different Kernels, *Proc. Of The Rom. Acad., Series A*, **19(3)**: 447–454, 2018.

[Baleanu(2019a)] Baleanu, D., Jajarmi, A., Asad, J.H., Classical And Fractional Aspects Of Two Coupled Pendulums. Romanian Reports In Physics, **71(1)**, 103, 2019.

[Baleanu(2019b)] Baleanu, D., Sajjadi, S.S., Jajarmi, A., Asad, J.H., New Features Of The Fractional Euler-Lagrange Equations For A Physical System Within Non-Singular Derivative Operator, *Eur. Phys. J. Plus*, **134:** 181, 2019.

[Baleanu(2020)] Baleanu,D., Jajarmi, A., Sajjadi, S.S., Asad, J.H., The Fractional Features Of A Harmonic Oscillator With Position-Dependent Mass. *Commun. Theor. Phys.*, **72:** 055002, 2020.

[Banasiak(1998)] Banasiak, J., Mika, J.R., Singular perturbed telegraph equations with applications in the random walk theory, *J. Appl. Math. Stoch. Anal.*, **11**: 9-28, 1998.

[Bansal(2017)] Bansal, R. K., Fluid Mechanics, *Laxmi Publications*, 2017.

[Barbu(2020)] Barbu, L., Nicolescu, A. E., An overdetermined problem for a class of anisotropic equations in a cylindrical domain, *Math. Method. Appl. Sci.*, **43(9)**: 6117-6125, 2020.

[Barenblatt(1960a)] Barenblatt, G. I., Zheltov, I., Kochina, I. N., Basic concept in the theory of seepage of homogeneous liquids in fissured rocks, *J. Appl. Math. Mech.*, **24**: 1286–1303, 1960.

[Barenblatt(1960b)] Barenblatt, G.I., Zheltov, I.P., On the basic equations of seepage of homogeneous liquids in fissured rock, *Akad Nauk SSSR (English translation.)*, **132**: 545-548, 1960.

[Barenblatt(1963)] Barenblatt, G. I., On certain boundary-value-problems for the equations of seepage of liquid in fissured rocks, *Prikl. Mat. Mekh.*, **27**: 513–518, 1963.

[Barranco(2012)] Barranco, A. P., Advances in Ferroelectrics, *InTech*, 2012.

[Bateman(1932)] Bateman, H., Partial Differential Equations of Mathematical Physics, *Cambridge University Press, 1st edition*, 1932.

[Bazarra(2019a)] Bazarra, N., Campo, M., Fernández, J.R., A thermoelastic problem with diffusion, microtemperatures, and microconcentrations, *Acta Mech*, **230**: 31-48, 2019.

[Bazarra(2019b)] Bazarra, N., Fernández, J.R., Leseduarte, M.C., Magaña, A., Quintanilla, R., On the thermoelasticity with two porosities: asymptotic behaviour, *Math. Mech. Solids*, **24(9)**: 2713-2725, 2019.

[Bazarra(2021)] Bazarra, N., Fernández, J.R., Quintanilla, R., Lord-Shulman thermoelasticity with microtemperatures, *Appl Math Optim*, **84**: 1667-1685, 2021.

[Bear(1999)] Bear, H.S., Differential Equations: A Concise Course, *Dover Publications; Revised ed. edition*, 1999.

[Beléndez(2009)] Beléndez, A., Rodes, J.J., Beléndez, T., Hernández, A, Approximation for the large-angle simple pendulum period, Eur. J. Phys., 30, 25–28. (2009).

[Beléndez(2010)] Beléndez, A., Francés, J., Ortuño, M., Gallego, S., Bernabeu, J.G., Higher accurate approximate solutions for the simple pendulum in terms of elementary functions, *Eur. J. Phys.*, **31**: 65–70, 2010.

[Berryman(2000)] Berryman, J.G., Wang, H.F., Elastic wave propagation and attenuation in a double porosity dual permeability medium, *Int J Rock Mech Min Sci.*, **37**: 63-78, 2000.

[Beucher(2006)] Beucher, O., Weeks, M., Introduction to MATLAB and SIMULINK, A Project Approach, *Third Edition - Engineering, Infinity Science Press LLC Hingham, Massachusetts New Delhi*, 2006.

[Binder(1986)] Binder, K., Young, A. P., Spin glasses: Experimental facts, theoretical concepts, and open questions, *Rev. Mod. Phys.* **58**: 801, 1986.

[Biot(1941)] Biot, M.A., General theory of three-dimensional consolidation, *J. Appl. Phys.*, **12**: 155-164, 1941.

[Bohme(1987)] Bohme, G., Non-Newtonian fluid mechanics, *New York: North-Holland*, 1987.

[Brewer(2014)] Brewer, C.E., Chuang, V.J., Masiello, C.A., Gonnermann, H., Gao, X., Dugan, B., Driver, L.E., Panzacchi, P., Zygourakis, K., Davies, C.A., New approaches to measuring biochar density and porosity, *Biomass and Bioenergy*, **66**: 176-185, 2014.

[Butcher(2008)] Butcher, J.C., Numerical Methods for Ordinary Differential Equations, *2nd edition. John Wiley & sons Ltd.*, 2008.

[Casas(2005)] Casas, P., Quintanilla, R., Exponential decay in one-dimensional porous-thermoelasticity, *Mech Res Commun*, **32**: 652-658, 2005.

[Cengel(1998)] Cengel, Y.A., Boles, M.A., Thermodynamics. An engineering approach, *3rd edition. McGraw-Hill, New York*, 1998.

[Chaney(2010)] Chaney, J., Combustion characteristics of biomass briquettes, *PhD thesis, University of Nottingham*, 2010.

[Chaturvedi(2010)] Chaturvedi, D.K., Modeling and Simulation of Systems Using MATLAB and Simulink, *CRC Press Taylor & Francis Group,* 2010.

[Chirita(2013)] Chirita, S., Ciareltta, M., D'Apice, C., On the theory of thermoelasticity with microtemperatures, *J Math Anal Appl*, **397**: 349-361, 2013.

[Ciofani(2011)] Ciofani, G. , Ricotti, L. , Mattoli, V. , Preparation, characterization and in vitro testing of poly(lactic-co-glycolic) acid/barium titanate nanoparticle composites for enhanced cellular proliferation, *Biomedical Microdevices*, **13**: 255-266, 2011.

[Ciofani(2012)] Ciofani, G., et al., Applications of Piezoelectricity in Nanomedicine in Piezoelectric Nanomaterials for Biomedical Applications, *Springer Berlin Heidelberg*, 213-238, 2012.

[Codarcea(2019)] Codarcea-Munteanu, L., Marin M., A study on the thermoelasticity of three-phase-lag dipolar materials with voids, *Bound Value Probl*, **137**, 2019.

[Codarcea(2020)] Codarcea-Munteanu, L., Marin, M., Influence of geometric equations in mixed problem of porous micromorphic bodies with microtemperature, *Mathematics*, **8(8)**: 1386, 2020.

[Coddington(1989)] Coddington, E.A., An Introduction to Ordinary Differential Equations, *Dover Publications. Unabridged edition*, 1989.

[Conti(2020)] Conti, M., Pata, V., Quintanilla, R., Thermoelasticity of Moore–Gibson–Thompson type with history dependence in the temperature, *Asymptotic Analysis*, **120(1-2)**: 1-21, 2020.

[Cooper(1986)] Cooper, F., Pi, S.Y., Stancioff, P.N., Quantum dynamics in a time-dependent variational approximation, *Phys. Rev. D*, **34**: 3831, 1986.

[Cowin(1983)] Cowin, S.C., Nunziato, J.W., Linear elastic materials with voids, *J. Elast.*, **13**: 125-147, 1983.

[Cowin(1999)] Cowin, S.C., Bone poroelasticity, *J Biomech.*, **32**: 217-238, 1999.

[Dehghan(2010)] Dehghan, M., Ghesmati, A., Solution of the second order one-dimensional hyperbolic telegraph equation by using the dual reciprocity boundary integral equation (DRBIE) method, *Eng. Anal. Boundary Elem.*, **34 (1)**: 51–59, 2010.

[Dell'Oro(2016)] Dell'Oro, F., Lasiecka, I., Pata, V.: The Moore-Gibson-Thompson equation with memory in the critical case, *J Differ Equ.*, **261(7)**: 4188-4222, 2016.

[Dell'Oro(2017)] Dell'Oro, F., Pata, V., On the Moore-Gibson-Thompson equation and its relation to linear viscoelasticity, *Appl Math Optim.*, **76**: 641-655, 2017.

[Duan(2011)] Duan, J.S., The Adomian decomposition method for nonlinear differential equations, *Computers & Mathematics with Applications*, **61(5)**: 1655-1661, 2011.

[Dunlap(1914)] Dunlap, F., Density of wood substance and porosity of wood, *Journal of Agricultural Research*, **6**: 423-428, 1914.

[Dyke(2014)] Dyke, P., An Introduction to Laplace Transforms and Fourier Series, 2^{nd} *edition. Springer*, 2014.

[Edwards(1975)] Edwards, S.F.E, Anderson, P.W., Theory of spin glasses, *J. Phys. F*, **5**: 965, 1975.

[El-Shahed(2008)] El-Shahed, M., Application of differential transform method to non-linear oscillatory systems, *Communications in Nonlinear Science and Numerical Simulation*, **13(8)**: 1714-1720, 2008.

[Emin(2020)] Emin, A. N., Florea, O.A., Craciun, E.M., Some uniqueness results for thermoelastic materials with double porosity structure, *Continuum Mech. Thermodyn*, **33**: 1083–1106, 2021.

[Emin(2023)] Emin, A.M., Florea, O., Green-Lindsay thermoelasticity for double porous materials, *Analele ştiinţifice ale Universităţii Ovidius Constanţa. Seria Matematică,* **31(1)**: 97-113, 2023.

[Erturk(2021)] Erturk, V.S., Asad, J., Jarrar, R., Shanak, H., Khalilia, H., The kinematics behaviour of coupled pendulum using differential transformation method, *Results in Physics*, **26**: 104325, 2021.

[Eslami(2012)] Eslami, M., Khalili, M., A New Application of the Multi-Step Differential Transformation Method for Solving Nonlinear Systems, *Applied Mathematical Modelling*, **36(10)**: 4941-4948, 2012.

[Fischer(1991)] Fischer, K.H., Hertz, J.A., Spin Glasses, *Cambridge University Press, New York*, 1991.

[Florea(2017)] Florea, O., Spatial behavior in thermoelastodynamics with double porosity structure, *Int J Appl Mech*, **9(07)**: 1750097, 2017.

[Florea(2019a)] Florea, O., The backward in time problem of double porosity material with microtemperature, *Symmetry*, **11(4)**: 552, 2019.

[Florea(2019b)] Florea, O., Harmonic vibrations in thermoelastic dynamics with double porosity structure, *Math. Mech. Solids*, **24(8)**: 2410–2424, 2019.

[Florea(2021a)] Florea, O.A., Bobe, A., Moore–Gibson–Thompson thermoelasticity in the context of double porous materials, *Continuum Mech. Thermodyn.*, **33**:2243–2252, 2021.

[Florea(2021b)] Florea, O., Baleanu, D., Asad., J., Fractional Features of a Double Pendulum System, *Dynamic Systems and Applications*, **30(2)**: 305-319, 2021.

[Fowles(2005)] Fowles, G.R, Cassiday, G.L, Analytical Mechanics, *7th edn. Thomson Brooks/Cole*, 2005.

[Fulcher(1976)] Fulcher, L.P., Davis, B.F., Theoretical and experimental study of the motion of the simple pendulum, *Am. J. Phys*, **44**: 51–55, 1976.

[Gilat(2011)] Gilat, A., Matlab an Introduction with Applications Fourth Edition, *Ohio University*, 2011.

[Gitman(2007)] Gitman, D.M., Kupriyanov, V.G., Canonical quantization of so-called non-Lagrangian systems, *European Physical Journal*, **50(3)**: 691–700, 2007.

[Godwe(2019)] Godwe, E., Mibaile, J., Gambo, B., Dokac, S.Y., Kofane, T.C., *Chinese Journal of Physics*, **60**: 379, 2019.

[Goldstein(1980)] Goldstein, H., Poole, C.P., Safko J.L., Classical Mechanics, *3rd edn. Addison Wesley*, 1980.

[Green(1885)] Green, A.E., Naghdi, P.M., A re-examination of the basic postulates of thermomechanics, *Proc R Soc, Math Phys Eng Sci,* **432(1885)**: 171-194, 1991.

[Green(1972)] Green, A.E, Lindsay, K.A., Thermoelasticity, *J. Elast.*, **2:** 1–7, 1972.

[Green(1992)] Green, A.E, Naghdi, P.M., On undamped heat waves in an elastic solid, *J Therm Stresses*, **15(2)**: 253-264, 1992.

[Green(1993)] Green, A.E., Naghdi, P.M., Thermoelasticity without energy dissipation, *J Elast*, **31(3)**: 189-208, 1993.

[Greiner(2010)] Greiner, W., Classical Mechanics, Systems of Particles and Hamiltonian Dynamics, *Springer-Verlag Berlin Heidelberg*, 2010.

[Grewal(2014)] Grewal, B. S., Higher Engineering Mathematics, *Khanna publication, New Delhi*, 2014.

[Griffiths(1999)] Griffiths, D.J., Introduction to electrodynamics, *Upper Saddle River, N.J.: Prentice Hall*, 1999.

[Griffiths(2005)] Griffiths, D.J. , Introduction to quantum mechanics, *Upper Saddle River, N.J.: Prentice Hall*, 2005.

[Grover(1996)] Grover, P.D., Mishra, S.K., Biomass briquetting: technology and practices, *Food and Agriculture Organization of the United Nations, Bangkok, Thailand*, 1996.

[Groza(2018)] Groza, G., Mitu, A.M., Pop, N., Sireteanu, T., Transverse vibrations analysis of a beam with degrading hysteretic behavior by using Euler-Bernoulli beam model, *An. St. Univ. Ovidius Constanta, seria Matematica*, **26(1)**: 125 - 139, 2018.

[Guo(2012)] Guo, W., Lim, C.J., Bi,X., Sokhansanj, S., Melin, S., Determination of effective thermal conductivity and specific heat capacity of wood pellets, *Fuel* , **103**: 347–355, 2012.

[Gurau(2004)] Gurau, L., The roughness of sanded wood surfaces, *Doctoral thesis, Forest Products Research Centre, Buckinghamshire Chilterns University College, Brunel University*, 2004.

[Haertling(1999)] Haertling, G.H., Ferroelectric Ceramics: History and Technology, *Journal of the American Ceramic Society*, **82**: 797-818, 1999.

[Halvorsen] Halvorsen, H.P., Introduction to Simulink, Faculty of Technology, Norway, http://www.academia.edu/9207393/Introduction_to_Simulink

[Hand(1995)] Hand, L.N., Finch, J.D., Analytical Mechanics, *Cambridge University Pres*, 1988.

[Hartley(1995)] Hartley, T.T, Lorenzo, C.F., Qammar, H.K., Chaos in a fractional order Chua's system, *IEEE Trans Circuits Syst: Part I: Fund Theory Appl*, **42(8)**: 485–490, 1995.

[Hatami(2015)] Hatami, M., Ghasemi, S.E., Sahebi, S.A.R., Mosayebidorcheh, S., Ganji, D.D., Hatami, J., Investigation of third-grade non-Newtonian blood flow in arterie under periodic body acceleration using multi-step differential transformation method, *Appl. Math. Mech. Engl. Ed*, **36(11)**: 1449-1458, 2015.

[Heaviside(1899)] Heaviside, O., Electromagnetic theory, *Chelsea Publishing Company, New York,* **Vol-2**, 1899.

[Hopf(1948)] Hopf, L., Introduction to the Differential Equations of Physics, *Dover; Notations, Name inked on Fep edition*, 1948.

[Houcque(2007)] Houcque, D., Robert, R., Applications of MATLAB: Ordinary Difierential Equations (ODE), *McCormick School of Engineering and Applied Science - Northwestern University*, 2007.

[Huang(2017)] Huang, P., Chang, W.S., Ansell, M.P., John, C.Y.M., Shea, A., Porosity estimation of Phyllostachys edulis (Moso bamboo) by computed tomography and backscattered electron imaging, *Wood Science and Technology*, **51**: 11-27, 2017.

[Hunt(2008)] Hunt, J.F., Gu, H., Lebow, P.K., Theoretical thermal conductivity equation for uniform density wood cells, *Wood and Fiber Science*, **40(2)**: 167-180, 2008.

[Ichise(1971)] Ichise, M., Nagayanagi, Y., Kojima, T., An analog simulation of non-integer order transfer functions for analysis of electrode processes, *J Electroanal Chem Interfacial Electrochem*, **33(2)**: 253-265, 1971.

[Ieşan(1985)] Iesan, D., Some theorems in the theory of elastic materials with voids, *J. Elast.*, **15**: 215-224, 1985.

[Ieşan(1986)] Iesan, D., A theory of thermoelastic materials with voids, *Acta Mechanica*, **60**: 67-89, 1986.

[Ieşan(2000)] Ieşan, D., Quintanilla, R., On a theory of thermoelasticity with microtemperatures, *J Therm Stresses*, **23**: 199-215, 2000.

[Ieşan(2007)] Ieşan, D., Thermoelasticity of bodies with microstructure and microtemperatures, *Int J Solids Struct*, **44(25-26)**: 8648-8662, 2007.

[Ieşan(2009)] Ieşan, D., Quintanilla, R., On thermoelastic bodies with inner structure and microtemperatures, *J Math Anal Appl*, **354(1)**: 12-23, 2009.

[Ieşan(2014)] Ieşan, D., Quintanilla, R., On a theory of thermoelastic materials with a double porosity structure, *J Therm Stresses*, **37(9)**: 1017–1036, 2014.

[Ieşan(2018a)] Ieşan, D., On a theory of thermoelasticity without energy dissipation for solids with microtemperatures, *ZAMM - Z Angew Math Mech*, **98(6)**: 870-885, 2018.

[Ieşan(2018b)] Ieşan, D., Quintanilla, R., Qualitative properties in strain gradient thermoelasticity with microtemperatures, *Math Mech Solids*, **23(2)**: 240-258, 2018.

[Igathinathane(2010)] Igathinathane, C., Tumuluru, J.S., Sokhansanj, S., Bi, X., Lim, C.J., Melin, S., Mohammad, E. , Simple and inexpensive method of wood pellets macro-porosity measurement, *Bioresource Technology*, **101**: 6528-6537, 2010.

[Ikelle(2014)] Ikelle, I.I., Ivoms, O.S.P., Determination of the heating ability of coal and corn cob briquettes, *IOSR Journal of Applied Chemistry*, **7(2)**: 77-82, 2014.

[ISO(1996)] *ISO 13565-2 (1996) + Cor 1 (1998)* Geometrical product specifications (GPS) – Surface texture: Profile method. Surfaces having stratified functional properties. Part 2: Height characterisation using the linear material ratio curve.

[ISO(1997)] *ISO 4287 (1997) + Amd1 (2009)* Geometrical product specifications (GPS). Surface texture. Profile method. Terms. Definitions and surface texture parameters.

[ISO(2003)] *SR EN 13183-1 (2003)/AC (2004)* Wood. Moisture content of a piece of timber. Determination by the drying method.

[ISO(2010)] *ISO/TS 16610-31*, Geometrical product specification (GPS) – Filtration. Part 31: Robust profile filters. Gaussian regression filters, (2010).

[Jaiani(2016)] Jaiani, G., Bitsadze, L., On basic problems for elastic prismatic shells with microtemperatures, *ZAMM - Z Angew Math Mech*, **96(9)**: 1082-1088, 2016.

[Jajarmi(2019)] Jajarmi, A., Baleanu, D., Sajjadi, S.S., Asad, J.H., A New Feature Of The Fractional Euler-Lagrange Equations For A Coupled Oscillator Using A Nonsingular Operator Approach, *Front. Phys.*, **7:** 196, 2019.

[Jangid(2021)] Jangid, K., Mukhopadhyay, S., A domain of influence theorem under MGT thermoelasticity theory, *Mathematics and Mechanics of Solids*, **26(2)**: 285-295, 2021.

[Jordan(1999)] Jordan, P.M. J, Puri, A., Digital signal propagation in dispersive media, *J. Appl. Phys.*, **85**: 1273- 1283, 1999.

[José(1998)] José, J. V., Saletan, E.J., Classical Dynamics: A Contemporary Approach, *Cambridge University Press,* 1998.

[Kalbaugh(2017)] Kalbaugh, D.V., Differential Equations for Engineers, *The Essentials. 1st Edition*, 2017.

[Kaltenbacher(2011)] Kaltenbacher, B., Lasiecka, I., Marchand, R., Wellposedness and exponential decay rates for the Moore-Gibson-Thompson equation arising in high intensity ultrasound, *Control Cybern.*, **40**: 971–988, 2011.

[Kansal(2018)] Kansal, T., Generalized theory of thermoelastic diffusion with double porosity, *Arch. Mech.*, **70(3)**: 241-268, 2018.

[Karapınar(2019a)] Karapınar, E., Abdeljawad, T., Jarad, F., Applying new fixed point theorems on fractional and ordinary differential equations, *Adv Differ Equ*, **2019**: 421, 2019.

[Karapınar(2019b)] Karapınar, E., Fulga, A., Rashid, M., Shahid, L., Aydi, H., Large Contractions on Quasi-Metric Spaces with an Application to Nonlinear Fractional Differential Equations, *Mathematics*, **7:** 444, 2019.

[Karunanithy(2012)] Karunanithy, C., Wang, Y., Muthukumarappan, K., Pugalendhi, S., Physiochemical characterization of briquettes made from different feedstocks, *Biotechnology Research International*, 1-12, 2012.

[Kasap(2006)] Kasap, S., Capper, P., Springer Handbook of Electronic and Photonic Materials, *Springer Science Business Media*, 2006.

[Keskin(2009)] Keskin, Y., Oturanc, G., Reduced differential transform method for partial differential equations, *International Journal of Nonlinear Sciences and Numerical Simulation*, **10(6)**: 741–749, 2009.

[Keskin(2010)] Keskin, Y., Oturanc, G., Reduced differential transform method for solving linear and nonlinear wave equations, *Iranian Journal of Science and Technology A*, **34(2)**: 113–122, 2010.

[Khalili(2003)] Khalili, N., Selvadurai, A.P.S., A fully coupled constitutive model for thermo-hydro-mechanical analysis in elastic media with double porosity, *Geophys Res Lett*, **30(24)**: 2268, 2003.

[Khalilia(2018)] Khalilia, H., Jarrar, R., Asad, J., Numerical Study of Motion of a Spherical Particle in a Rotating Parabola Using Lagrangian, *Journal of the Serbian Society for Computational Mechanics*, **12(1)**: 44-51, 2018.

[Kim(2016)] Kim, Y. K., Koo, J. H., Lee, K.S., Finite pseudo block spin model of ferroelectrics, *Ferroelectrics*, **494**: 110-116, 2016.

[Klauder(1985)] Klauder, J., Skagerstam, B.S., Coherent States: Applications in Physics and Mathematical Physics, *World Scientific*, 1985.

[Klee(2011)] Klee, H., Allen, R., Simulation of Dynamic Systems with MATLAB® and Simulink, *CRC Press Taylor & Francis Group*, 2011.

[Knops(1971)] Knops, R.J., Payne, L.E., Growth estimates for solutions of evolutionary equations in Hilbert space with applications to elastodynamics, *Arch Ration Mech Anal*, **41**: 363–398, 1971).

[Knops(2014)] Knops, R.J., Quintanilla, R., Continuous data dependence in linear theories of thermoelastodynamics. Part I: classical theories. Basics and logarithmic convexity, in: *Hetnarski RB, editor. Encyclopedia of thermal stresses. Dordrecht: Springer,* 2014.

[Koeller(1984)] Koeller, R.C., Application of fractional calculus to the theory of viscoelasticity, *J Appl Mech*, **51(2)**: 299-307, 1984.

[Koeller(1986)] Koeller, R.C., Polynomial operators, Stieltjes convolution, and fractional calculus in hereditary mechanics, *Acta Mechanica*, **58(3-4)**: 251–264, 1986.

[Koo(2017)] Koo, J. H., Lee, K.S., Ferroelectricity and antiferromagnetism in multiferroic materials explained by photonic tunneling model, *Ferroelectrics Letters Section*, **44(1-3)**: 42-48, 2017.

[Koo(2019)] Koo, J. H., Lee, K.S., Spontaneous polarization by photon tunneling model in ferroelectrics, *Ferroelectrics*, **540**: 4-9, 2019.

[Kovner(1989)] Kovner, A., Rosenstein, B., Covariant Gaussian approximation. I. Formalism, *Phys. Rev. D*, **39**: 2332, 1989.

[Kreyszig(2006)] Kreyszig, E., Advance Engineering Mathematics. 9^{th} *Edition. Wiley eastern Pvt. Ltd. (India)*, 2006.

[Križan(2014)] Križan, P., The densification of wood waste, *De Gruyter Open Ltd., Warsaw/Berlin*, 2014.

[Kumar(2016a)] Kumar, R., Vohra, R., Gorla, M.G., Reflection of plane waves in thermoelastic medium with double porosity, *Multidiscip Model Mater Struct*, **12(4)**: 748-778, 2016.

[Kumar(2016b)] Kumar, R., Vohra, R., Gorla, M.G., Some considerations of fundamental solution in micropolar thermoelastic materials with double porosity, *Arch. Mech.*, **68(4)**: 263–284, 2016.

[Kumar(2017)] Kumar, R., Vohra, R., Effect of hall current in thermoelastic materials with double porosity structure, *Int J Appl Mech Eng*, **22(2)**: 303-319, 2017.

[Kumar(2019)] Kumar, R., Vohra, R., Forced vibrations of a thermoelastic double porous microbeam subjected to a movine load, *J Theor Appl Mech*, **57(1)**: 155-166, 2019.

[Lam(1997)] Lam, L., Introduction to nonlinear Physics, *Springer-velag, New York*, 1997.

[Landau(1976)] Landau, L.D., Lifshitzl, E.M., Mechanics, *Vol. 1, Butterworth-Heinemann*, 1976.

[LasieckaI(2015)] Lasiecka ,I., Wang, X., Moore-Gibson-Thompson equation with memory, part II: general decay of energy, *J Differ Equ.* **259**: 7610–7635, 2015.

[Lasser(1996)] Lasser, R., Introduction to Fourier Series, *Marcel Dekker, Inc.*, 1996.

[Lee(2016)] Lee, K.S., Koo, J.H. , Lee, C.E., Finite block pseudo-spin approach of proton glass, *Solid State Commun.* , **240**: 10-14, 2016.

[Li(2007)] Li, C.P., Deng, W.H., Remarks on fractional derivatives, *Appl Math Comput*, **187(2)**: 777–784, 2007.

[Li(2009)] Li, C.P., Dao, X.H., Guo, P., Fractional derivatives in complex plane, *Nonlinear Anal-Theor*, **71(5-6)**: 1857–1869, 2009.

[Li(2010)] Li, C.P., Gong, Z.Q., Qian, D.L., Chen, Y.Q., On the bound of the Lyapunov exponents for the fractional differential systems, *Chaos*, **20(1)**: 013127, 2010.

[Liand(2009)] Liand, C.P., Zhao, Z.G., Asymptotical stability analysis of linear fractional differential systems, *J Shanghai Univ (Engl Ed)*, **13(3)**: 197–206, 2009.

[Lines(1979)] Lines, M. ,Glass, A., Principles and Applications of Ferroelectrics and Related Materials, *Clarendon Press, Oxford*, 1979.

[Lord(1967)] Lord, H.W., Shulman, Y., A generalized dynamical theory of thermoelasticity, *J. Mech. Phys. Solids.*, **15**: 299-309, 1967.

[Lupu(1993a)] Lupu, G. , Rabaea, A., Craciun, E.M., *Theoretical Aspects Concerning Vibrations of Elastical Technological Systems*, *An. St. Univ. Ovidius Constanta, seria Matematica,* **1**: 133-139, 1993.

[Lupu(1993b)] Lupu, G., Craciun, E.M., Suliman, E., An Extension of Equilibrum Problem for the Plane Simple Pendulum, *An. St. Univ. Ovidius Constanta,seria Matematica*, **1**: 141-145, 1993.

[Lupu(2009)] Lupu, M., Florea, O., Lupu, C., The structural influence of the forces of the stability of dynamical systems, *An. St. Univ. Ovidius Constanta*, **17(3)**: 159 - 169, 2009.

[Magana(2009)] Magana, A., Quintanilla, R., Uniqueness and growth of solutions in two-temperature generalized thermoelastic theories, *Math Mech Solids.* **14**: 622–634, 2009.

[Magin(2006)] Magin, R.L., Fractional Calculus in Bioengineering, *Begell House, Connecticut,* 2006.

[Maleknejad(2009)] Maleknejad, K., Beheshtian, E., Multi-step differential transform method for solving a class of nonlinear optimal control problems, *Communications in Nonlinear Science and Numerical Simulation*, **14(8)**: 3126-3136, 2009.

[Manabe(2003)] Manabe, S., Early development of fractional order control, *Proc. of the ASME International Design Engineering Technical Conference* DETC2003/VIB-48370, 2003.

[Mani(2005)] Mani, S., A systems analysis of biomass densification process, *PhD thesis, University of British Columbia,* 2005.

[Marchand(2012)] Marchand, R., McDevitt, T., Triggiani, R., An abstract semigroup approach to the third order Moore-Gibson-Thompson partial differential equation arising in high-intensity ultrasound: structural decomposition, spectral analysis, exponential stability, *Math Meth Appl Sci.*, **35**: 1896–1929, 2012.

[Marin(2017a)] Marin, M., Baleanu, D., Vlase, S., Effect of microtemperatures for micropolar thermoelastic bodies, *Struct Eng Mech,* **61(3)**: 381-387, 2017.

[Marin(2017b)] Marin, M., Baleanu, D., Carstea, C., A uniqueness result for final boundary value problem of microstretch bodies, *J. Nonlinear Sci. Appl.,* **10**: 1908-1918, 2017.

[Marin(2017c)] Marin, M., Craciun, E.M., Uniqueness results for a boundary value problem in dipolar thermoelasticity to model composite materials, *Comp Part B Eng.*, **126**: 27-37, 2017.

[Marin(2019)] Marin, M., Ochsner, A., Radulescu, V., A polynomial way to control the decay of solutions for dipolar bodies, *Continuum Mech. Thermodyn.*, **31**, 331–340, 2019.

[Marin(2020a)] Marin , M., Othman, M.I.A., Seadawy, A.R., Carstea, C., A domain of influence in the Moore–Gibson–Thompson theory of dipolar bodies, *Journal of Taibah University for Science*, **14(1)**: 653-660, 2020.

[Marin(2020b)] Marin, M., Craciun, E.M., Pop, N., Some Results in Green–Lindsay Thermoelasticity of Bodies with Dipolar Structure, *Mathematics*, **8**: 497, 2020.

[Marin(2020c)] Marin, M., Ochsner, A., Craciun, E.M., A generalization of the Saint-Venant's principle for an elastic body with dipolar structure, *Continuum Mech. Thermodyn.*, **32**: 269-27, 2020.

[Marin(2020d)] Marin, M., Ochsner, A., Craciun, E.M., A generalization of the Gurtin's variational principle in thermoelasticity without energy dissipation of dipolar bodies, *Continuum Mech. Thermodyn.*, **32**: 1685-1694,2020.

[Marin(2020e)] Marin, M., Ochsner, A., Taus, D., On structural stability for an elastic body with voids having dipolar structure, *Continuum Mech. Thermodyn.*, **32**: 147–160, 2020.

[Marion(1988)] Marion, J.B, Thornton, S.T., Classical Dynamics of Particles and Systems, 3rd ed., *Harcourt Brace Jovanovich,* 1988.

[Marion(2003)] Marion, J.B., Thornton, S.T., Classical Dynamics of Particles and Systems, 5th Edition, *Brooks Cole*, 2003.

[Martínez-Pérez(2018)] Martínez-Pérez, N.E., Ramírez, C., On the Lagrangian description of dissipative systems, *Journal of Mathematical Physics*, **59 (3)**: 032904, 2018.

[Masters(2000)] Masters, I., Pao, W.K.S., Lewis, R.W., Coupling temperature to a double-porosity model of deformable porous media, *Int. J. Numer. Methods Eng.*, **49**: 421–38, 2000.

[Matthews(2005)] Matthews, M.R., Gauld, C.F., Stinner, A., The pendulum: scientific, historical, philosophical and educational perspectives, *Berlin: Springer Science & Business Media,* 2005.

[Miller(1993)] Miller, K.S., Ross, B., An introduction to the fractional calculus and fractional differential equations, *Wiley, New York,* 1993.

[Mohanty(2001)] Mohanty, R.K., Jain, M.K., An unconditionally stable alternating direction implicit scheme for the two space dimensional linear hyperbolic equation, *Numer. Methods Partial Differ. Equ.*, **17(6)**: 684–688, 2001.

[Monje(2004)] Monje, C.A., Calderon, J.A., Vinagre, B.M., Chen, Y.O., Feliu, V., On fractional PIλ controllers: some tuning rules for robustness to plant uncertainties, *Nonlinear Dyn*, **38:** 369–381, 2004.

[Moon(1992)] Moon, F.C., Chaotic Vibrations - An Introduction for Applied Scientists and Engineers *John Wiley & Sons, New York*, 1987; Chaotic and Fractal Dynamics -An Introduction for Applied Scientists and Engineers *John Wiley & Sons, New York*, 1992.

[Moura(2002)] Moura, M.J., Ferreira, P.J., Figueiredo, M.M., The use of mercury intrusion porosimetry to the characterization of eucalyptus wood, pulp and paper, *Iberoamerican congress on pulp and paper research*, 2002.

[Nhawu(2016)] Nhawu, G., Mafuta, P., Mushanyu, J., The Adomian Decomposition Method For Numerical Solution Offirst-Order Differential Equations, *J. Math. Comput. Sci.*, **6(3):** 307-314,2016.

[Nieto(2018)] Nieto, M., Rivera, J.E.M., Naso, M.G., Quintanilla, R., Qualitative results for a mixture of Green–Lindsay thermoelastic solids, *Chaotic Mod. Simul.*, **3**: 285–294, 2018.

[Odibat(2010)] Odibat, Z.M., Bertelle, C., Aziz-Alaoui, M.A., Duchamp, G.H.E., A multi-step differential transforms method and application to non-chaotic or chaotic systems, *Computers & Mathematics with Applications,* **59(4):** 1462–1472, 2010.

[Oustaloup(2000)] Oustaloup, A., Levron, F., Mathieu, B., Nanot, F.M., Frequency-band complex noninteger differentiator: Characterization and synthesis, *IEEE Trans Circ Syst I*, **47(1):** 25–39, 2000.

[Pamplona(2012)] Pamplona, P.X., Muñoz-Rivera, J.E., Quintanilla, R., Analyticity in porous-thermoelasticity with microtemperatures, *J Math Anal Appl*, **394(2)**: 645-655, 2012.

[Pascal(1986)] Pascal, H., Pressure wave propagation in a fluid flowing through a porous medium and problems related to interpretation of Stoneley's wave attenuation in acoustical well logging, *Int J Eng Sci*, **24**: 1553–1570, 1986.

[Pattanayak(1992)] Pattanayak, A.K., Schieve, W.C., *Physical Review Letters,* **72**: 2855 1994; *Physical Review Letters*, **46**: 1821, 1992.

[Pellicer(2019)] Pellicer, M., Sola-Morales, J., Optimal scalar products in the Moore-Gibson-Thompson equation, *Evol Equat Contr Theor.*, **8**: 203-220, 2019.

[Pesce(2007)] Pesce, C.P., The Application of Lagrange Equations to Mechanical Systems With Mass Explicitly Dependent on Position, *Journal of Applied Mechanics*, **70**: 751- 756, 2007.

[Plötze(2011)] Plötze, M., Niemz, P., Porosity and pore size distribution of different wood types as determined by mercury intrusion porosimetry, *European Journal of Wood and Wood Products*, **69(4)**: 649-657, 2011.

[Potra(2007)] Potra, F.A, Yen, J., Implicit Numerical Integration for Euler-Lagrange Equations via Tangent Space Parameterization, *Mechanics of Structures and Machines*, **19(1)**: 77-98, 2007.

[Prasad(2013)] Prasad, R., Das, S., Mukhopadhyay, S., Boundary integral equation formulation for coupled thermoelasticity with three phase-lags, *Mathematics and Mechanics of Solids*, **18(1)**: 44-58, 2013.

[Qian(2010)] Qian, D.L., Li, C.P., Agarwal, R.P., Wong, P.J.Y., Stability analysis of fractional differential system with Riemann-Liouville derivative, *Math Comput Model*, **52(5-6)**: 862–874, 2010.

[Quintanilla(2011)] Quintanilla, R., On the growth and continuous dependence in thermoelasticity with microtemperatures, *J Therm Stress*, **34(9)**: 911-922, 2011.

[Quintanilla(2019)] Quintanilla, R. Moore-Gibson-Thompson thermoelasticity, *Math Mech Solids.*, **24**: 4020-4031, 2019.

[Quintanilla(2020)] Quintanilla, R., Moore-Gibson-Thompson thermoelasticity with two temperatures, *Applications in Engineering Science*, **1**: 100006, 2020.

[Rabier(2006)] Rabier, F., Temmerman, M., Böhm, T., Hartmann, H., Jensen, P.D., Rathbauer, J., Carrasco, J., Fernández, M., Particle density determination of pellets and briquettes, *Biomass and Bioenergy*, **30**: 954-963, 2006.

[Ragland(1991)] Ragland, K.W., Aerts,D.J., Baker, A.J., Properties of wood for combustion analysis, *Bioresource Technology*, **37**: 161-168, 1991.

[Reznikov(2003)] Reznikov, Y., et al., Ferroelectric nematic suspension, *Applied Physics Letters* **82**: 1917, 2003.

[Rheinboldt(1995)] Rheinboldt, W.C., Performance Analysis of Some Methods for Solving Euler-Lagrange Equations, *Appl. Math. Lett.*, **8(1)**: 77-82, 1995.

[Saptoadi(2008)] Saptoadi, H., The best biobriquette dimension and its particle size, *Asian Journal on Energy & Environment*, **9(3- 4)**: 161-175, 2008.

[Scarpetta(2014)] Scarpetta, E., Svanadze, M., Zampoli, V., Fundamental solutions in the theory of thermoelasticity for solids with double porosity, *J. Therm. Stresses*, **37(6)**: 727–748, 2014.

[Seeley(2006)] Seeley, R.T., Introduction to Fourier series and Integrals, *Dover Publications*, 2006.

[Shatanawi(2020)] Shatanawi, W., Karapinar, E., Aydi, H., Fulga, A., Wardowski type contractions with applications on Caputo type nonlinear fractional differential equations, *U.P.B. Sci. Bull., Series A*, **82(2)**: 157–170, 2020.

[Sherrington(1975)] Sherrington, D., Kirkpatrick, S., Solvable Model of a Spin-Glass, Phys. Rev. Lett. **35**: 1972, 1975.

[Siau(1995)] Siau, J.F., Wood: influence of moisture on physical properties, *Virginia Polytechnic Institute and State University*, 1995.

[Skaar(1988)] Skaar, S.B., Michel, A.N., Miller, R.K., Stability of viscoelastic control systems, *IEEE Trans Automatic Control*, **33(4)**: 348–357, 1988.

[Smullyan(2010)] Smullyan, R.M., Fitting, M., Set theory and the continuum problem, *Dover Publications, New York,* 2010.

[Sova(2018)] Sova, D., Porojan, M., Bedelean, B., Huminic, G., Effective thermal conductivity models applied to wood briquettes, *Int. J. Therm. Sci.*, **124**: 1–12, 2018.

[Srivastava(2013)] Srivastava, V.K., Awasthi, M.K., Chaurasia, R. K., Tamsir, M., The Telegraph Equation and Its Solution by Reduced Differential Transform Method, *Modelling and Simulation in Engineering*, **2013**: 746351, 2013

[Straughan(2013)] Straughan, B., Stability and Uniqueness in Double Porosity Elasticity, *Int. J. Eng. Sci.*, **65**: 1-8, 2013.

[Suliman(2017)] Suliman, W., Harsh, J.B., Abu-Lail, N.I., Fortuna, A.M., Dallmeyer, I., Garcia-Pérez, M., The role of biochar porosity and surface functionality in augmenting hydrologic properties of a sandy soil, *Science of the Total Environment*, **574**: 139-147, 2017.

[Sun(1984)] Sun, H.H., Onaral, B., Tsao, Y., Application of positive reality principle to metal electrode linear polarization phenomena, *IEEE Trans Biomed Eng*, **31(10)**: 664–674, 1984.

[Svanadze(2004)] Svanadze, M., Fundamental solutions of the equations of the theory of thermoelasticity with microtemperatures, *J Therm Stress*, **27(2)**: 151-170, 2004.

[Svanadze(2005)] Svanadze, M., *Fundamental solution in the theory of consolidation with double porosity, J. Mech. Behav. Mat.*, **16**: 123-130, 2005.

[Svanadze(2010)] Svanadze, M., Dynamical problems of the theory of elasticity for solids with double porosity, *Proc. Appl. Math. & Mech.*, **10**: 309-310, 2010.

[Svanadze(2012)] Svanadze, M., Plane waves and boundary value problems in the theory of elasticity for solids with double porosity, *Acta Appl. Math.*, **122**: 461-470, 2012.

[Svanadze(2013)] Svanadze, M., Scalia, A., Mathematical problems in the coupled linear theory of bone poroelasticity, *Comput. Math. Appl.*, **662**: 1554–1566, 2013.

[Svanadze(2014a)] Svanadze, M., On the theory of viscoelasticity for materials with double porosity, *Discr. Cont. Dyn. Sys. – Series B.*, **19**: 2335-2352, 2014.

[Svanadze(2014b)] Svanadze, M., Uniqueness theorems in the theory of thermoelasticity for solids with double porosity, *Meccanica*, **49**: 2099–2108, 2014.

[Svanadze(2015)] Svanadze, M., External boundary value problems of steady vibrations in the theory of rigid bodies with a double porosity structure, *Proc. Appl.Math. & Mech.*, **15**: 365–366, 2015.

[Svanadze(2016)] Svanadze, M., Plane waves and problems of steady vibrations in the theory of viscoelastic-ity for Kelvin–Voigt materials with double porosity, *Arch. Mech.* **68**: 441-458, 2016.

[Svanadze(2017)] Svanadze, M., Boundary value problems of steady vibrations in the theory of thermoelasticity for materials with a double porosity structure, *Arch. Mech.*, **69**: 347-370, 2017.

[Svanadze(2020)] Svanadze, M., Steady vibration problems in the coupled linear theory of porous elastic solids, *Math. Mech. Solids*, **25**: 768–790, 2020.

[Svanadze(2021)] Svanadze, M., Potential method in the coupled theory of elastic double-porosity materials, *Acta Mechanica*, **232**: 2307–2329, 2021.

[Taraphdar(2017)] Taraphdar, C., Hamilton's Canonical Equations for a Classical System with Velocity Dependent Potential Energy- a Mathematical Study, *Global Journal of Mathematical Sciences: Theory and Practical,* 9(2): 133-138, 2017.

[Tenenbaum(1963)] Tenenbaum, M., Pollard, H., Ordinary Differential Equations, *Dover Publications, INC., New York*, 1963.

[Tenenbaum(1985)] Tenenbaum, M., Pollard, H., Ordinary Differential Equations, *Dover Publications; Revised ed. Edition*, 1985.

[Thompson(1972)] Thompson, P.A., Compressible-fluid dynamics, *McGraw-Hill. New York*, 1972.

[Tsue(1992)] Tsue, Y., Maslov Phase as Geometric Phase in the Time-Dependent Variational Approach with Squeezed Coherent States, *Prog. Theor. Phys.*, **88(5)**: 911-932, 1992.

[Tumuluru(2010)] Tumuluru, J.S., Wright, C.T., Kenny, K.L., Hess, J.R., A review on biomass densification technologies for energy application, *U.S. Department of Energy*, 3-20, 2010.

[Usta(2003)] Usta, I., Comparative study of wood density by specific amount of void volume (porosity), *Turkish Journal of Agriculture & Forestry*, **27**: 1-6, 2003.

[Valasek(1920)] Valasek, S.J., Piezo-Electric and Allied Phenomena in Rochelle Salt, *Phys. Rev.*, **17**: 475, 1921.

[Vlase(2019)] Vlase, S., Marin, M., Ochsner, A., Scutaru, M.L, Motion equation for a flexible one-dimensional element used in the dynamical analysis of a multibody system, *Continuum Mechanics and Thermodynamics*, **31(3)**: 715-724, 2019.

[Wazwaz(2011)] Wazwaz, A.M., A First Course in the Adomian Decomposition Method, *World Scientific Publishing*, 2011.

[Werner(1957)] Werner, K., Ferroelectrics and Antiferroeletrics, *Solid State Physics*, **4**: 1-197, 1957.

[Weston(1993)] Weston, V.H., He, S., Wave splitting of the telegraph equation in and its application to inverse scattering, *Inverse Problems*, **9**: 789-812, 1993.

[Wilson(1982)] Wilson, R., Aifantis, E., On the theory of consolidation with double porosity, *Int. J. Eng. Sci.*, **20**: 1009–1035, 1982.

[Xu(1994)] Xu, Z., Cheung, Y. K., Averaging method using generalized harmonic functions for strongly non-linear oscillators, *Journal of Sound and Vibration*, **174**: 563-576, 1994.

[Xue(2002)] Xue, D., Chen, Y.O., A comparative introduction of four fractional order controllers, *Proc. 4th IEEE World Congress on Intelligent Control and Automation (WCICA02)*, **4**: 3228–3235, 2002.

[Xue(2013)] Xue, D.D., Chen, Y., System Simulation Techniques with MATLAB and Simulink, *Wiley*, 2013.

[Yezhi(2013)] Yezhi, L., Yinping, L., Zhibin, L., Symbolic computation of analytic approximate solutions for nonlinear fractional differential equations, *Mendeley Data*, 2013.

[Yosida(1980)] Yosida, K., Functional Analysis, *6st Ed, Springer-Verlag, Berlin*, 1980.

[Yuste(1990)] Yuste, S.B., Bejarano, J.D., Improvement of a Krylov- Bogolubov method that uses Jacobi elliptic functions., *Journal of Sound and Vibration*, **139**: 151-163, 1990

[Zhang(1990)] Zhang, W.M. , Feng, D.H., Gilmore, R., Coherent States: Theory and Some Applications, *Rev. Mod. Phys.* **62**: 867-924, 1990.

[Zhou(1986)] Zhou, J.K., Differential Transformation Method and Its Application for Electrical Circuits, *Hauzhang University Press, Wuhan*, 1986